~~PHYSICAL FACTORS AFFECTING~~ THE FLOW OF GASES AND LIQUIDS THROUGH SWOLLEN AND UNSWOLLEN SOFTWOOD

A thesis presented in part fulfilment of
the requirements for the degree of
Doctor of Philosophy
of the
University of London

by
William Clive Barton Banks DIC

Department of Botany
Imperial College of Science and Technology
London SW7

December 1974

ABSTRACT

Fluid movement through wood is important in several technological processes. For example, it is necessary to dry felled timber before it is suitable for use as a constructional material. Drying involves fluid movement by both diffusion and mass flow processes. For use in certain situations it is desirable to impregnate timber with liquids (eg wood preservatives and fire retardants) in order to improve the technical properties of the material. Such impregnation processes are almost entirely controlled by mass flow mechanisms.

This study was undertaken to investigate the physical factors affecting fluid transport through conifer wood (softwood).

Flow longitudinally is strongly influenced by the structure of the cell to cell connections (bordered pits). Species selected for the study were chosen:-

1 to be commercially important
2 to exhibit several types of bordered pit structure.

Gas flow at the rates investigated was found to be within the 'viscous with slip' régime. Because of the complexity of the capillary structure of softwood it was found to be difficult to separate total flow into the 'viscous' and 'slip' components.

Liquid flow appeared to be mainly laminar, but with an indication of some turbulence at higher flow rates. Analysis suggested that the turbulent component is associated with flow across the membrane of the bordered pit. Some irreversible permeability decrease was observed as the magnitude of the applied pressure gradient was increased. This must result from either pore blocking by the shifting of cell debris or to pore structural deformation in response to applied forces.

Swelling of the cell wall by the sorption of various polar molecules (water and the lower aliphatic alcohols) caused marked decrease in permeability. In the case of air dried wood this decrease amounted to about 70%, for swelling from the shrunken to the fully water swollen state.

During impregnation, surface, as well as viscous and inertial forces, affect rate of penetration. Under some conditions these forces may dominate. Their effect may be minimised by the use of low surface tension liquids.

Hence, optimum penetration should be attained by adoption of the following criteria:-

1 Wood should be in the unswollen state prior to impregnation.
2 The impregnant should not cause cell wall swelling.
3 The impregnant should be of low viscosity and surface tension.

INDEX

		Page
Title page		i
Abstract		ii
Index		iv
Part 1 - INTRODUCTION		1
1.1	Processes involving fluid flow in wood	1
1.2	Softwood structure and fluid transport	2
1.3	Physics of fluid flow	7
1.3.1	Laminar flow	7
1.3.2	Turbulent flow	9
1.3.3	Molecular flow	10
1.3.4	Flow in short tubes	12
1.4	Flow through porous media	13
1.5	Flow in wood	17
1.5.1	Liquid flow through softwood	17
1.5.2	Gas flow through softwood	23
1.5.3	Softwood structural features affecting gas flow	28
1.6	Effect of swelling on permeability	32
1.7	Scope of the present work	32
Part 2 - BORDERED PIT STRUCTURE		34
2.1	Structural variation in bordered pit membranes - selection of test species	34
2.2	Pit aspiration	37
Part 3 - SCANNING REFLECTION ELECTRON MICROSCOPIC STUDY OF TEST SPECIES		39
3.1	Objectives of the study	39
3.2	Specimen preparation and examination technique	39
3.3	Pit membrane structure of test species	40
3.3.1	*Abies grandis* sapwood	41
3.3.2	*Picea abies* sapwood	44
3.3.3	*Tsuga heterophylla* sapwood	44
3.3.4	*Cedrus deodara* sapwood	44
3.3.5	*Araucaria angustifolia* sapwood	47

		Page
3.3.6	Heartwood of test species	47
3.3.7	Pit membrane pore sizes	47
Part 4 - GAS FLOW PERMEABILITY		50
4.1	Objectives	50
4.2	Apparatus and experimental technique	50
4.3	Gas flow results	57
4.4	Mathematical analysis of data	59
4.5	Calculation of specimen viscous permeability constant from gas flow data	64
4.6	Pore size estimation from gas permeability data	66
4.7	Limitations of the gas flow technique	71
4.7.1	Uncertainty associated with the numerical analysis	71
4.7.2	Oversimplification of the flow path model	72
4.7.3	Effect of flow path model oversimplification on estimation of viscous permeability constant	76
4.7.4	Effect of flow path model oversimplification on pore size estimation	86
4.8	Gas flow permeability - summary	89
Part 5 - FLOW OF INERT (NON SWELLING) LIQUIDS THROUGH DRY SOFTWOOD		91
5.1	Objectives	91
5.2	Apparatus and experimental technique	91
5.3	Non-swelling liquid flow results and discussion	97
5.3.1	Viscous permeability to non-swelling liquid	97
5.3.2	Effect of magnitude of pressure differential on rate of flow	101
5.3.3	Effect of viscous force on permeability	108
5.4	Non swelling liquid flow - summary	116

		Page
Part 6 - LIQUID FLOW THROUGH SWOLLEN SOFTWOOD		117
6.1	Swelling of wood	117
6.2	Objectives	119
6.3	Hexane flow through water swollen wood	120
6.3.1	Specimen preparation	120
6.3.1.1	Cutting and drying of air dried specimens	120
6.3.1.2	Cutting and drying of solvent dried specimens	123
6.3.1.3	Adjustment of specimen moisture content	123
6.3.1.4	Impregnation with hexane	124
6.3.2	Flow measurement	124
6.3.3	Swelling measurement	125
6.3.4	Results and discussion	129
6.3.4.1	Hexane flow through moist 'air dried' wood	129
6.3.4.2	Hexane flow through solvent dried wood	133
6.3.4.3	Swelling due to moisture sorption	135
6.4	Swelling liquid flow through dry wood	136
6.4.1	Specimen preparation	136
6.4.1.1	Cutting and conditioning of specimens	136
6.4.2	Impregnation and flow measurement	137
6.4.3	Measurement of swelling caused by sorption of test liquids	138
6.4.4	Results and discussion	140
6.4.4.1	Permeability measurement	140
6.4.4.2	Swelling measurement	144
6.5	Liquid flow through green wood	145
6.5.1	Specimen preparation	145
6.5.2	Flow measurement	146
6.5.3	Measurement of dimensional change due to liquid exchange	146
6.5.4	Results and discussion	147
6.5.4.1	Permeability measurement	147
6.5.4.2	Dimensional change	151

		Page
6.6	The relationship between permeability and swelling	152
6.6.1	The effect of swelling on the permeability of air dried wood	153
6.6.2	The effect of swelling on the permeability of 'solvent exchange' dried wood	157
6.6.3	The effect of dimension change on the permeability of green wood	159
6.6.4	Mechanism of permeability decrease caused by swelling	161
6.6.4.1	Effect of cell wall swelling on pit structure	167
6.6.5	Liquid flow through swollen softwood - summary	175
Part 7 - GENERAL DISCUSSION		177
7.1	The relationship between permeability to gases and inert liquids	177
7.2	Pore size measurement	182
7.3	Permeability of non-swollen and swollen wood	186
7.3.1	Effect of atmospheric conditions	187
7.3.2	Impregnation with various liquids	187
7.4	Relationship between permeability and rate of penetration	188
7.4.1	Effect of pore blockage	189
7.4.2	Effect of surface forces	189
Part 8 - CONCLUSIONS AND SUGGESTIONS FOR FURTHER WORK		194
8.1	Gas flow permeability measurement	194
8.2	Pore size estimation	194
8.3	Non swelling liquid flow	195
8.4	Effect of swelling on permeability	195
8.4.1	De-aspiration of pit membranes	196

		Page
8.5	The relationship between gas and liquid flow	197
8.6	Penetration of wood by liquids	197
ACKNOWLEDGEMENTS		199
Appendix 1	Data tables	200
Appendix 2	Analysis of specific mass flow/mean gas pressure relationship	210
References		214

Part 1 INTRODUCTION

1.1 PROCESSES INVOLVING FLUID FLOW IN WOOD

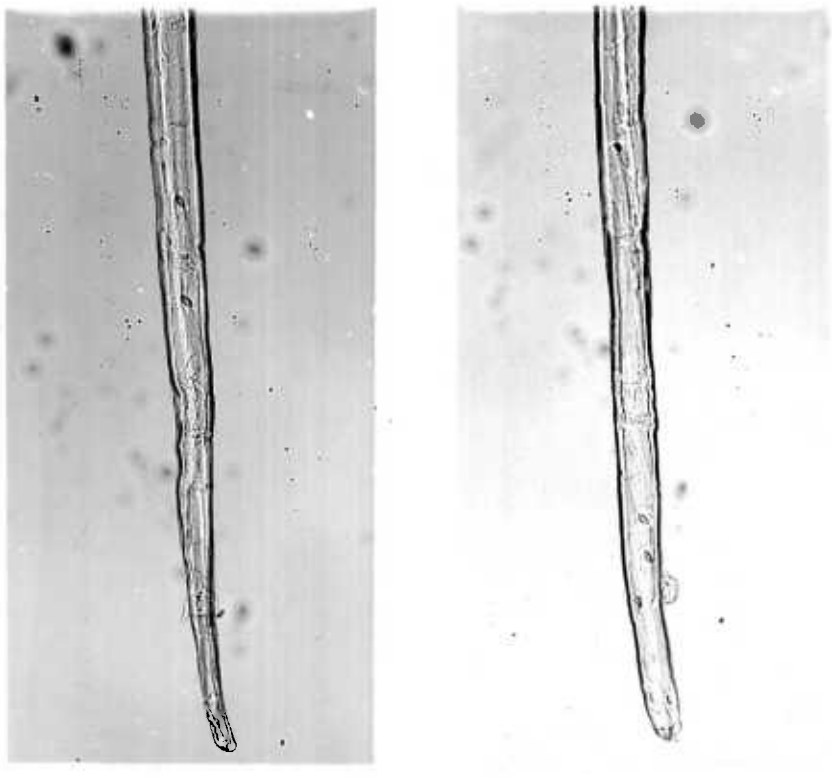
For most purposes it is necessary to dry timber from the high moisture content associated with the living tree and with freshly felled logs (sometimes in excess of 100 per cent expressed on a dry wood basis) to levels suitable for various end uses (generally less than 20 per cent). Drying from higher moisture contents involves some mass flow of water along the capillary network, although molecular diffusion also plays an important part in the process. Thus, fluid movement is important in the processing of practically all timber for use as an industrial material. For many applications, wood is subjected to further processing involving liquid flow. This may include impregnation of wood chips with pulping chemicals as part of the paper-making process, impregnation of wood and wood products with fungicidal and insecticidal liquids and treatment with fire-retardant salts.

Thus it may be appreciated that an understanding of the mechanisms of fluid flow in wood is important technically as well as interesting academically. In the past when timber supplies were abundant, preferred species could be obtained suited to the process to be applied to them. For example, permeable species were readily available for use where a liquid impregnation treatment was required. Currently, however, timber is in relatively short supply and it is often necessary to use species less suited to impregnation with fluids. In this situation there is perhaps a greater need to gain a deeper understanding of flow mechanisms, so that process variables may be optimised and possibly novel processes developed.

1.2 SOFTWOOD STRUCTURE AND FLUID TRANSPORT

Softwoods or gymnosperms are structurally relatively simple, about 92 to 95 per cent of their bulk volume being comprised of a single type of cell - the longitudinal tracheid.

Of the remaining volume, up to about one per cent may be comprised of longitudinal resin canals (these cells are absent as a regular feature in some species) and 5 to 8 per cent of ray tissue. Individual rays may be homocellular, containing either ray parenchyma or ray tracheid cells exclusively, or heterocellular, containing both these types of cell, together with radial resin canals. Longitudinal tracheids are relatively long, tubular cells with closed ends. In the tangential plane the ends of the cells taper sharply, whilst, seen in radial view, they are blunt ended (Figure 1.1).



(a) (b)

Fig 1.1 LONGITUDINAL TRACHEID: (a) tangential plane; (b) radial plane

Cell length varies with species and, to a smaller extent, within a species. In general, however, longitudinal tracheids vary in length from about 2 to about 5 mm. Tracheid cross-section varies from rectangular to hexagonal. Tangential breadth of tracheids covers the range about 20 to 60 micron for most species whilst, radially, breadth is much more variable and dependent, to a large extent, on the period of formation of the cell. The radial breadth of cells formed early in a growing season (early wood) is similar in magnitude to the tangential dimension whilst, in late wood, radial breadth may be only 10 to 20 per cent of the tangential dimension (Figure 1.2). Apart from differences in overall cell dimensions, it is clear from Figure 1.2 that late wood cell

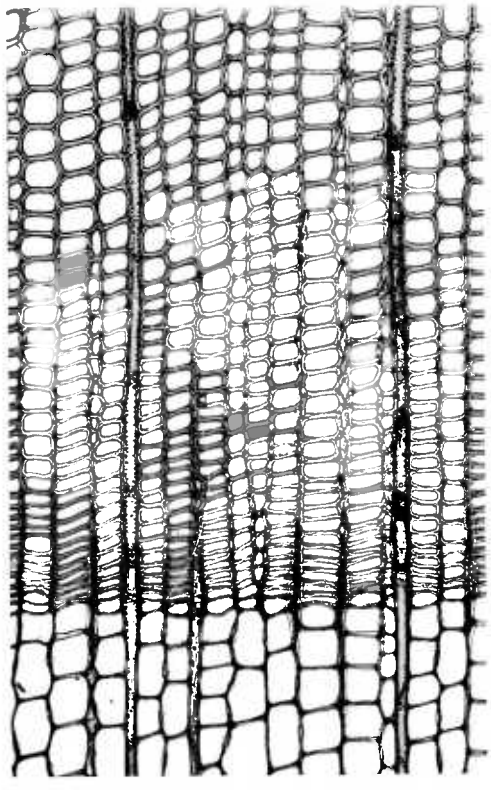


Fig 1.2 SOFTWOOD (*Abies grandis*) transverse section showing late wood (narrow) and early wood (wide) cells

walls are considerably thicker than those in early wood. Thus early wood cell spaces (or lumina) apparently offer much easier passage for fluid conduction than do those of late wood.

Adjacent longitudinal tracheids overlap one another over about a third of their length on the average, and interconnection between them is by way of bordered pits. These, valve-like structures occur abundantly in early wood (up to about 90 pits per early wood tracheid are reported by Phillips (1933) who examined a number of softwoods), and less abundantly in late wood tracheids.

Bordered pit structure is shown diagrammatically in Figure 1.3 below. It can be seen that communication from tracheid to tracheid is provided by the pit apertures and the porous part of the pit membrane, called the margo. Structure of bordered pits is discussed in more detail in Part 2.

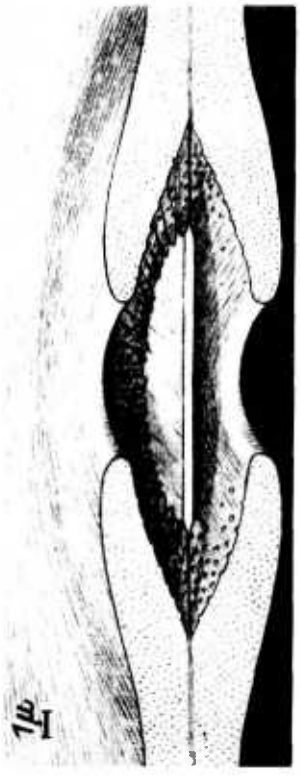


Fig 1.3 DIAGRAM OF 'b' PIT SECTION (AFTER LIESE, 1952)

As stated above, rays may contain three types of cell:-

i ray parenchyma

ii ray tracheid

iii resin canal

Ray parenchyma cells are 'building-brick' shaped, their long axes running parallel to the radius of the tree stem. The length of ray parenchyma cells varies from about 0.2 to 0.5 mm, cross-section dimensions being of the order of 10 by 50 microns. Communication between adjacent parenchyma cells radially, tangentially and longitudinally is by way of so called simple pits. These are discrete zones in adjacent cell walls free of secondary thickening, so that in these zones cells are separated only by a membrane consisting of the primary wall. Similar interconnection occurs between parenchyma and longitudinal tracheids, in this case, however, a border is formed on the tracheid side of the pit, so that it appears and is termed 'half-bordered'. The area of the membrane of individual pits varies with species. At the smaller end of the range pit membrane area in *Abies* and *Picea* spp is about 10 μm^2, whilst the area of half bordered pit membranes in certain *Pinus* species may be as large as 500 μm^2.

Ray tracheids are aligned similarly and are dimensionally similar to parenchyma cells. They are connected to one another and to longitudinal tracheids by bordered pits, similar in structure to but considerably smaller than those interconnecting longitudinal tracheids. Pits between ray tracheids and ray parenchyma are of the half-bordered type.

Resin canals, either longitudinal or radial, are not true wood elements, but cell spaces between rows of resin secreting parenchyma cells. The canals which are usually quite heavily laden with resin are of diameter in the region of 50 to 200 μm, and they may attain length up to several millimetres. They are usually quite effectively blocked with resin and are therefore unlikely to conduct fluid over large distances.

It is seen, therefore, that the cellular spaces of wood cells form a continuous and complex system of interconnected pores. Several workers have investigated which parts of the pore system are important for longitudinal fluid conduction. It was originally believed that tracheids were totally sealed against mass liquid flow and that transport of water (in the living tree) from cell to cell occurred by diffusion (Tiemann, 1910). In felled timber, Tiemann believed conduction was by way of cell wall cracks developing during seasoning. It was shown, however, by Bailey (1913) that such cracks developed infrequently and that the major flow path from tracheid to tracheid was by way of naturally occurring perforations in the pit membrane. Using techniques involving microscopic examination of blocks impregnated with molten wax and with aqueous dye solutions, Buro and Buro (1959) demonstrated that the tracheid/bordered pit system forms the principal longitudinal flow paths in both early wood and late wood of Scots pine (*Pinus sylvestris*). It was suggested by Buro and Buro, however, that ray cells may also contribute to longitudinal transport, where principal flow paths are blocked. In an investigation of Australian species using electron microscopic techniques, Wardrop and Davies (1961) report similar findings for the penetration of *Pinus radiata* by copper sulphate solution. Also using electron-microscopic techniques, Côté and Krahmer (1962) found that bordered pits of dry, white pine (*Pinus strobus*) were permeable to Indian ink particles. Membranes of ray parenchyma half bordered pits, however, were found to resist penetration by the particles, although the evidence suggested that these membranes allowed slow penetration of the clear solvent, possibly by a diffusion mechanism.

To avoid redistribution effects occurring during drying, Erickson and Balatinecz (1964) impregnated Douglas fir specimens with styrene monomer, which was subsequently polymerised *in situ*. Using this technique these workers, in general agreement with the foregoing, found bordered pits to be the principal longitudinal flow path from tracheid to tracheid. Similar results can be inferred from the data of

Behr, Sachs, Kukachka and Blew (1969) who examined specimens from six American softwood species after pressure impregnation with a solution of pentachlorophenol in an aromatic oil and with creosote.

The evidence produced by all these workers suggests strongly that longitudinal flow in softwoods is principally by way of the tracheid/bordered pit system. It is likely, however, that other routes (eg ray cells and pits) may contribute to some extent.

1.3 PHYSICS OF FLUID FLOW

Fluid transport through capillaries or porous media may occur in several régimes. For both liquids and gases, flow may be laminar or turbulent whilst, for gases, a proportion of transport may occur by molecular diffusion processes (slip and Knudsen flow).

1.3.1 LAMINAR FLOW

Laminar flow is the term used to describe flow through a capillary or around an immersed body where the resistance to flow is essentially due to shearing forces. Under these conditions it has been shown that liquid flow through a capillary is governed by the following equation:-

$$Q = \frac{\pi r^4 \Delta P}{8 \eta \ell} \qquad \text{Equation 1.1}$$

where Q = Volume rate of flow
r = Capillary radius
ΔP = Pressure drop across capillary
ℓ = capillary length
η = fluid viscosity

This well known equation was derived in the mid-19th century independently by Hagen, a German engineer interested in water conduction through brass pipes, and Poiseuille, a French scientist studying the laws governing blood flow through veins.

Its derivation is discussed in basic texts of fluid mechanics (eg Daugherty and Franzini, 1965).

An essentially similar equation applies to the flow of gases, but in this case it is necessary to take account of the expansion of gas which takes place along the pressure gradient. For gas flow, therefore, the following equation applies:-

$$Q = \frac{\pi r^4 \Delta P \, \overline{P}}{8\eta \ell \, P_o} \qquad \text{Equation 1.2}$$

where $\overline{P}$ = mean gas pressure within capillary

P_o = pressure of gas at 'volume flow rate' measuring point.

From equations 1.1 and 1.2 it is clear that rate of flow 'Q' is directly proportional to pressure gradient causing flow ($\Delta P/\ell$). This relationship, which is a useful characteristic of laminar flow, has been extensively investigated and verified experimentally.

Whilst pipe flow theory is useful in many fluid transport situations, it is often more convenient to use a treatment based on the movement of fluid past an immersed body. Laminar flow in this régime is described by Stokes' law and is dealt with in detail in standard texts of fluid mechanics (see, for example, Daugherty and Franzini, 1965).

Stokes' law is expressed in the following equation:

$$F_D = 3\pi\eta u D \qquad \text{Equation 1.3}$$

where F_D = viscous drag imposed by sphere immersed in fluid stream

u = linear velocity of fluid stream relative to immersed body

D = diameter of sphere

From equation 1.3 it is clear that whilst flow is laminar the resistance to flow or 'drag' offered by a sphere of diameter

'D' is directly proportional to velocity 'u'.

1.3.2 TURBULENT FLOW

It has been shown (Reynolds, 1883) that as rate of fluid flow in a pipe is increased, a point is reached where flow ceases to be laminar. At this point, the streamlines become disturbed and eddies form. This type of flow is called 'turbulent'. In turbulent flow, the principal forces resisting transport are inertial rather than shearing. The complexity of turbulent flow has so far proved beyond any mathematical treatment analogous to the Hagen-Poiseuille treatment for laminar flow. Experimental work has shown, however, that turbulent flow through tubes is characterised by the relationship:-

$$Q \propto (\Delta P)^{\frac{1}{2}} \qquad \text{Equation 1.4}$$

where Q = volume rate of flow

ΔP = pressure drop across tube

Furthermore, the work of Reynolds demonstrated that for straight tubes of circular cross-section, the shift from laminar to turbulent flow depends upon the ratio of inertial to viscous flow resisting forces. This dimensionless quantity is called the Reynolds number (Nr) and is calculated according to the following equation:-

$$Nr = \frac{\rho \ell e' u}{\eta} \qquad \text{Equation 1.5}$$

where u = fluid linear velocity

ρ = fluid density

η = fluid viscosity

The linear dimension "$\ell e'$" in equation 1.5 may be any length that has significance in determining flow resistance. For flow in pipes it is conventional to take "$\ell e'$" as the pipe diameter. The Reynolds number at which change from laminar to turbulent flow occurs is called the 'Critical Reynolds

number' and is symbolised 'Nrc'. For straight pipes of circular section, Nrc ∿ 2000. Small deviations from the simple 'straight pipe of circular section' geometry cause considerable reduction in the value of Nrc. It has been shown, indeed, that even small degrees of curvature in the pipe greatly reduces this value (Comolet 1949, Topakoglu 1951).

For fluid transport past immersed bodies deviation from the linear relationship between drag (F_D) and liquid velocity (u) occurs at very low values of Reynolds number. For flow around a sphere, deviation from Stokes' law (equation 1.3) occurs at Reynolds number equal to about 0.5. In this type of system as with tube flow the critical Reynolds number is sensitive to shape. For example, flow around a long cylinder remains laminar to Reynolds number equal to one. Classical experiments in this field were conducted by Prandtl (1923) but the subject is dealt with in most fluid mechanic texts - for example that of Daugherty and Franzini (1965), suggested earlier.

From the foregoing it will be appreciated that, except for very simple geometries, it is impossible to predict mode of flow without experiment. However, systems involving the flow of various fluids through a common porous specimen are dynamically similar for constant 'Nr'. That is, if the mode of flow of liquid 'a' at a given value of 'Nr' is known, then flow of another liquid 'b' will be in the same mode at the same 'Nr' value.

1.3.3 MOLECULAR FLOW

It has been shown by Kundt and Warburg (1875) that the Hagen-Poiseuille law does not completely describe the flow of gases through capillaries. These workers showed that as gas pressure is reduced, so that the mean free path 'λ' becomes an appreciable fraction of the capillary diameter, flow rate under the influence of a pressure gradient exceeds that predicted by the Hagen-Poiseuille law. It is believed

that this extra component of flow is due to a significant proportion of specular collisions occurring between molecules and tube wall, in addition to the intermolecular collisions responsible for viscous forces in gases according to kinetic theory. This process, giving the effect of a sliding or slipping layer of molecules adjacent to the tube wall is called 'slip flow'. Taken to the limit, as pressure is further reduced a situation eventually arises where intermolecular collisions significantly cease to occur. In this situation, gases progress by specular reflexion from tube walls, a process known as Knudsen flow. These two modes of molecular flow are diffusion processes being controlled by the concentration gradient of the molecular species concerned.

Slip flow along a circular section capillary is defined by the following equation (see Carman 1956):-

$$Q = \frac{2\pi r^3 \delta_1 \overline{V}}{3\ell} \qquad \text{Equation 1.6}$$

where r = capillary radius
ℓ = capillary length
δ_1 = factor depending on the faction of molecules undergoing diffuse reflection upon collision with capillary wall
$\overline{V}$ = molecular mean thermal velocity

so that the equation describing viscous flow with slip is obtained by adding equations 1.2 and 1.6:-

$$\frac{QP_o}{\Delta P} = \frac{\pi r^4 \overline{P}}{8\eta\ell} + \frac{2\pi r^3 \delta_1 \overline{V}}{3\ell} \qquad \text{Equation 1.7}$$

In the Knudsen region, viscous forces are virtually absent, since intermolecular collisions occur rarely. Flow in this régime is defined by the equation devised as a result of work by Knudsen (1909) and Smoluchowski (1911):-

$$\frac{QP_o}{\Delta P} = \frac{2\pi r^3 \delta_o \overline{V}}{3\ell} \qquad \text{Equation 1.8}$$

δ_o = factor depending upon fraction of molecules undergoing diffuse reflection at tube wall.

1.3.4 FLOW IN SHORT TUBES

The Hagen/Poiseuille equation (equations 1.1 and 1.2) and the equation for viscous/slip flow (equation 1.7) developed from it, strictly apply only to long tubes (where $\ell >> r$). In flow through short tubes a significant proportion of the total viscous dissipation of energy occurs beyond the tube end. This effect, which is discussed by Barr (1931), results in pressure drops across short tubes, during flow, in excess of those predicted by the Hagen/Poiseuille equation. To correct for this effect, the length term in viscous flow equations is increased by an amount dependent upon the ratio ℓ:r. Perhaps the best known of these so called 'end corrections' is that due to Couette (1891). The 'Couette' correction is used extensively in the calculation of viscosity from measurement of flow rate through capillary tubes.

A semi-empirical, mathematical treatment to describe flow through short tubes, taking slip flow into account, has been developed by Hanks and Weissberg (1964). The equation developed by them closely describes flow of gases in the viscous/slip régime, through tubes of length-to-radius ratio extending over the range 0.3 to 1100. For compactness and ease of manipulation, Hanks and Weissberg express their equation in terms of dimensionless parameters:-

$$W = W_s + \frac{Br}{\lambda} \qquad \text{Equation 1.9}$$

The dimensionless terms may be expressed in terms of physical parameters:-

$$W = \frac{4Q\overline{P}}{\pi r^2 \Delta P \overline{V}}$$

$$\beta = \frac{\pi}{8} / \left(\frac{\ell}{r}\right) + \left(\frac{3\pi}{8}\right)$$

$$W_s = \left(\frac{\beta^2}{3\pi}\right) \left(\frac{128\ell}{r}\right) + \left(\frac{27\pi^2}{4}\right)$$

where Q = volume rate of flow
$\overline{P}$ = mean gas pressure within capillary
r = capillary radius
ΔP = pressure drop across capillary
$\overline{V}$ = molecular mean thermal velocity
ℓ = capillary length

1.4 FLOW THROUGH POROUS MEDIA

Based on those derived to describe fluid transport through simple capillaries, equations have been developed to describe flow through porous media. In general these treatments are dependent upon approximating various pore shapes as equivalent simple capillaries. The subject is thoroughly discussed in various texts (see, for example, Carman, 1956 and Scheidegger, 1957, revised 1960). The pore sizes in many porous substrates are distributed fairly randomly within a broadly defined band. For example, in sedimentary rocks and consolidated sand beds the distribution of pore sizes depends, to a large extent, upon the geometry of the particles forming them and on the way in which these particles pack together. To deal with the forces resisting flow through each of the pores in such a system, individually, is clearly outside the bounds of practical possibility. Hence much more empirical treatments are generally applied to porous media than those used in simple capillary flow.

The basic law governing laminar flow of liquids through porous media is that of Darcy (1856). This law, with a development due to Carman (1938) to take account of fluid viscosity is expressed by the following equation:-

$$Q = \frac{BA\Delta P}{\eta \ell} \qquad \text{Equation 1.10}$$

where Q = volume rate of flow
A = specimen area normal to flow
ΔP = pressure drop across specimen
η = liquid viscosity
ℓ = specimen length
B = permeability constant

It will be noted that equation 1.10 (Darcy's law) is generically similar to equation 1.1 (Hagen-Poiseuille law). If 'B', the Darcy permeability constant, is set equal to $r^2/8$, the equations become identical for flow through a pipe of circular cross-section (ie 'A' = πr^2). To separate the pore radius from the permeability constant and hence to give more physical meaning to the constant, Kozeny (1927) derived an equation for laminar flow, including an average value, the mean hydraulic radius (Schiller, 1923), to describe pore size. This equation, known as the Kozeny equation, for porous media where tortuosity is small may be written:-

$$u = \frac{m^2 \Delta P}{k_o \eta \ell e} \qquad \text{Equation 1.11}$$

where u = liquid linear velocity
m = mean hydraulic radius (see below)
k_o = shape factor for flow in non-circular capillaries
ℓe = effective length of porous specimen (ie distance travelled by fluid from inlet to outlet face of specimen)

Whence volume rate of flow 'Q', is given by:-

$$Q = \frac{A\varepsilon m^2 \Delta P}{k_o \eta \ell e} \qquad \text{Equation 1.12}$$

where A = specimen area normal to flow
ε = specimen porosity (ie fraction of total volume occupied by pore space)

NB Mean hydraulic radius 'm' is defined:-

$$m = \frac{\text{pore volume}}{\text{pore surface area}} \qquad \text{Equation 1.13}$$

If hydraulic radius 'm' were a perfect parameter to represent pore size, 'k_o' would be a true constant. In practice it is found that 'k_o' varies between about 1 and 3 depending upon pore cross-sectional shape (see Carman 1956).

Modelling pore space simply as parallel uniform capillaries, Adzumi (1937) produced an equation to describe gas flow through porous media, based on the law of viscous/slip flow through capillaries of circular section (see equation 1.7 above):-

$$\frac{QP_o}{\Delta P} = \frac{\pi \bar{P} n r^4}{8\eta \ell} + \frac{2\pi\delta_1 \bar{V} n r^3}{3\ell} \qquad \text{Equation 1.14}$$

where Q = volume rate of flow
P_o = pressure of gas at flow rate measuring point
ΔP = pressure drop across specimen
$\bar{P}$ = mean gas pressure within specimen
r = capillary radius
ℓ = capillary length
δ_1 = fraction of molecules undergoing diffuse reflection at the capillary wall
η = fluid viscosity
$\bar{V}$ = molecular thermal velocity
n = number of capillaries in parallel array constituting the specimens

The pore geometry of most real porous media deviates markedly from that of capillaries of circular and uniform cross-section. Hence a more empirical treatment based on the Kozeny equation for viscous flow of liquids is more useful in most systems. This treatment involving the introduction of shape and tortuosity factors into an equation for viscous/slip flow based on the hydraulic radius and porosity concepts and containing empirical permeability coefficients was originated

by Rigden (1947). The treatment was further developed by several workers, eg Lea and Nurse (1947), Carman and Arnell (1948). This work resulted in the following equation for viscous/slip flow through porous media:-

$$\frac{uP_o}{\Delta P} = \frac{m^2\overline{P}}{k_o \quad e} + \frac{4A\varepsilon\delta_1 m\overline{V}}{3k_1 \ell e} \qquad \text{Equation 1.15}$$

Whence (see Carman, 1956):

$$\frac{QP_o}{\Delta P} = \frac{A\varepsilon m^2\overline{P}}{k_o \eta \ell e} + \frac{4A\varepsilon\delta_1 m\overline{V}}{3k_1 \ell e} \qquad \text{Equation 1.16}$$

where u = gas linear velocity

Q = gas volume flow rate

P_o = gas pressure, at flow rate measuring point

$\overline{P}$ = gas mean pressure within specimen

ε = porosity of specimen

m = mean hydraulic radius of pores

A = specimen area normal to flow

ℓe = effective pore length (average distance travelled by gas from inlet to outlet face of specimen)

δ_1 = factor dependent on fraction of ~~pores~~ molecules undergoing diffuse reflection at pore wall

$\overline{V}$ = molecular thermal velocity

η = gas viscosity

k_o = shape factor for laminar flow

k_1 = shape factor for 'slip' flow

It is recognised that the geometric parameters, 'm' and 'ℓe' introduced in the Kozeny equation and its development are not precise physical dimensional constants for pores differing markedly from the simple geometry of long uniform capillaries. They are the hydraulic radii and lengths of hypothetical pores which would give rise to the same flow characteristics as those measured experimentally for a porous medium.

1.5 FLOW IN WOOD

1.5.1 LIQUID FLOW THROUGH SOFTWOOD

Because of its obvious importance in several technological processes (section 1.1) and also because of its relevance to the physiology of the living tree, interest has been shown in the permeability of wood to liquids for a long time. Investigating the rate of flow of water through woody stems, Ewart (1905) found flow rate to decrease with time of flow. He attributed this effect simply to blockage of fine pores by solid particles.

Observations by Sutherland, Johnston and Maass (1934) suggested that water flow rate through air-dried softwood decreases rapidly with time of flow but that flow through freshly felled sapwood stems remains almost constant or decreases only slowly with duration of flow. Rate of flow of a series of liquids through a number of softwood species was measured by Buckman, Schmitz and Gortner (1935). They found a consistent reduction in flow rate with time of flow, and they observed the effect to be more pronounced with polar than with non-polar liquids. These workers suggested surface electrical effects causing resistance to flow, and sorption of polar molecules leading to reduction of pore cross-section, as possible explanations of the effect. Similar findings to those of Buckman *et al* (1935) are reported by Erickson, Schmitz and Gortner (1937) who obtained decreasing flow rates of water, zinc chloride solution and benzene through several air-dried softwoods. With water, a 90 per cent reduction in rate of flow was observed, whilst for zinc chloride solution and for benzene the decrease was usually not more than about 50 per cent. Whilst drawing no firm conclusions, Erickson *et al* believed that their data pointed to an electro-kinetic rather than a physical occlusion mechanism as the reason for decreasing permeability. The phenomenon was the subject of a thorough investigation by Anderson, Gortner and Schmitz (1941), who convincingly demonstrated that decreasing flow rate with time of flow could not be satisfactorily explained in terms of surface electro-kinetic effects (electro-osmosis and streaming potential). As an alternative, they proposed a mechanism

involving pivoting of pit membrane fibrils under the influence of flow, into a position of maximum hydrodynamic resistance. By the use of a physical model, these workers showed experimentally that their proposed mechanism was tenable. However, the hypothesis so far as wood is concerned remains purely speculative, because no evidence has been produced to suggest that the fibrils are free to pivot in the manner suggested. Using a system involving water flow through freshly felled conifer sapwood, Huber and Mertz (1958) investigated the effect of pressure gradient on flow rate. They found that the decrease in flow rate with time reduced as pressure gradient was decreased and, for applied pressure, gradients of less than 0.5 bar/m, flow rate remained constant for prolonged periods. Microscopic evidence produced by Huber and Mertz suggests that the decrease in flow rate (or permeability) is due to a shift in the position of the bordered pit membrane from a central position within the pit chamber towards the downstream pit orifice (Figure 1.4).

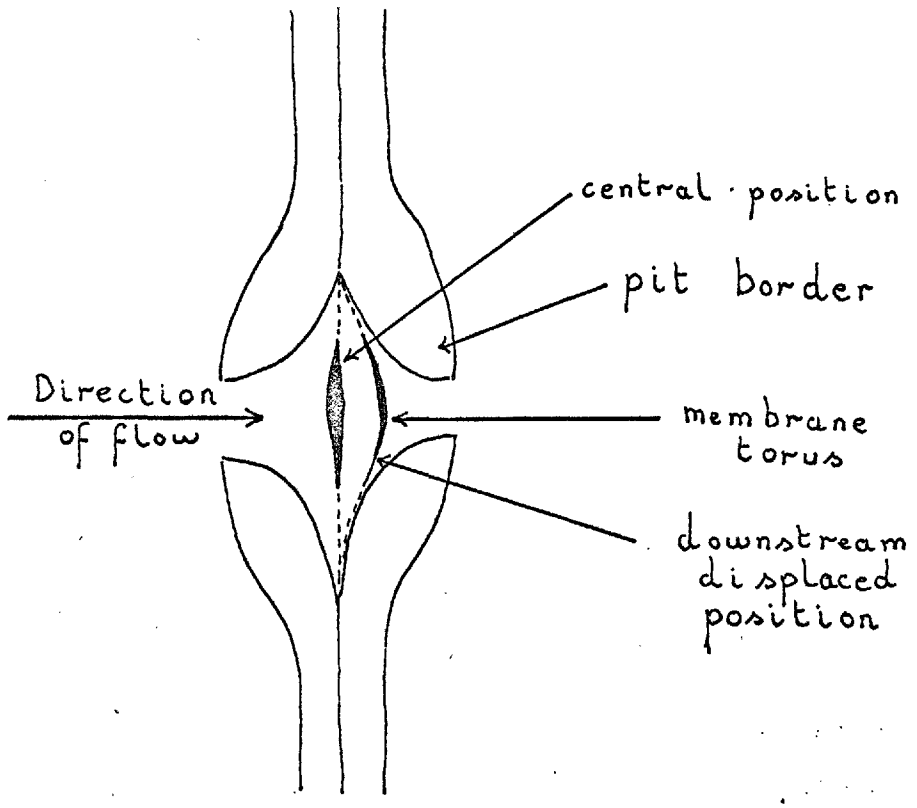


Fig 1.4 Downstream displacement of pit membrane

This displacement reduces the size of the gap between torus and pit border thus increasing its resistance to flow (for flow though a slit, rate of flow is proportional to the cube of slit width).

Working with air dry Douglas fir wood, Bailey and Preston (1970), whilst not attaining steady flow rates, observed large and irreversible decrease in permeability as applied pressure gradient was increased beyond about 100 bar/m. These workers showed the shape of their curves, relating flow rate to applied pressure differential, to be consistent with a mechanism involving membrane displacement towards the down-stream pit orifice. The findings of Bailey and Preston are thus similar in principle to those of Huber and Mertz but, whereas the former observed permeability to decrease markedly only when pressure gradients reached about 100 bar/m, the latter workers observed the decrease at gradients as small as 0.5 bar/m. The reason for this difference may be found in the type of material used in the experiments. Huber and Mertz used freshly-felled sapwood where most flow is through thin walled early wood (see section 2), whose pit membranes are relatively fragile and where only small dis-placement is needed to seal the pit. Bailey and Preston, on the other hand, worked with air-dried wood. In this material, flow is largely through late wood (Petty, 1969) where membranes appear much more robust and need to be displaced further to bring about pit closure (see section 2).

The first steady flow liquid system involving flow through air-dry wood is reported by Krier (1951). He achieved steady flow rate under constant pressure gradient for prolonged periods by removing as much air as possible from specimens and by the use of water carefully filtered through fine porosity sintered glass filters, as the permeating fluid. Using the technique of Krier, constant flow rates of water and organic liquids through both 'green' and air dry conifer wood were obtained by Erickson and Crawford (1959).

In an elegant investigation it was convincingly demonstrated by Kelso, Gertjejansen and Hossfeld (1963) that a major reason for decreasing flow rate with duration of flow is due to pore blocking by dissolved gases released from the flowing liquid. Such gas release may occur as a result of a combination of:-

i local pressure reduction due to increased flow velocity through narrow pores (Bernoulli effect)

ii the presence of particulate nuclei in the flowing liquid or in the wood.

It can easily be shown that to overcome opposing surface forces and hence force a gas bubble through a pore of submicron diameter, such as may occur in bordered pit membranes, requires an applied pressure differential of several bar. The above workers established constant rate of flow through the heartwood of air dried Sitka spruce (*Picea sitchensis*) by pre-filtration of the permeating water through a membrane filter of 0.45 micron pore size, and by reduction of dissolved gas concentration so that the water remained generally unsaturated with gas, throughout the specimen.

Since publication of the results of Kelso *et al* (1963), several workers using their techniques have attained steady flow rates of various liquids through a range of species (Sucoff, Chen and Hossfeld, 1965; Comstock, 1965, 1967; Banks, 1968; Smith and Banks, 1971). From the various data discussed it seems that steady flow through softwoods may be attained if care is taken to avoid gas or particulate embolism, and if applied force is regulated, to avoid disruption of structural elements.

The effect of magnitude of pressure differential at levels below that which causes tissue disruption, has been investigated by a number of workers. It was found by Sutherland, Johnston and Maas (1934) that rate of water flow through the dried heartwood of a number of species increases more rapidly than linearly with applied pressure differential. For

rigid porous media, Darcy's law predicts a linear relationship (section 1.4). To explain this departure from the Darcy relationship, the above workers suggested that pit membranes were stretched, under the influence of higher pressure differentials, so that membrane perforations were enlarged. For flow through two of the species investigated (white spruce and black spruce), Sutherland *et al* found the linear relationship to be obeyed. In these species they suggest, the pit membranes are sufficiently rigid to resist stretching. A greater than linear increase in rate of flow, with applied pressure differential, is also reported by Buckman, Schmitz and Gortner (1936) for flow through softwood species where longitudinal resin canals are absent. For species with resin canals, these workers observed a linear relationship over a fairly wide range of pressure differentials (1 to 8 bar). They believed that, where present, resin canals form the major fluid conduction channels and, having a simple capillary structure, closely obey Darcy's law. In species without canals, longitudinal flow routes must include pit membranes and, for these species, Buckman *et al* support the hypothesis proposed by Sutherland, Johnston and Maas (1934) that the greater than linear rate of flow increase with applied pressure differential is due to stretching of the pit membrane. It has been shown mathematically, however (Anderson, Gortner and Schmitz, 1941), that the magnitude of the permeability increase caused by increase in pressure differential is too great to be accounted for, by the membrane stretching theory. As an alternative mechanism, they propose that local reduction in pressure in small membrane pores due to the Bernoulli effect causes fibrils bounding such pores to be drawn closer together. Consequently, large pores become larger whilst small pores decrease in size. Volume rate of flow is proportional to the fourth power of pore diameter, hence the above process would account for the observed increase in permeability. The above investigations of the effect of pressure differential on rate of flow were carried out before the work of Kelso, Gertjejansen and Hossfeld (1963).

Hence the decreasing flow effect caused by gas embolism confuses them. Only after attainment of constant flow rate conditions can the effect of applied pressure differential be meaningfully investigated.

For water flow through Douglas fir heartwood, Erickson and Estep (1962) established almost constant rate of flow. They found that flow rate increased linearly over a range of applied pressure differentials from 1.5 to 5.5 bar. In the lower pressure differential range, from 0 to 1.5 bar, flow rate was observed to increase more rapidly than linearly. Erickson and Estep suggest that this greater than linear increase is due to an increasing number of small pores becoming available for flow, as gas bubbles are forced through them under the influence of increasing pressure differentials. Using the gas-removal and micro-filtration technique described earlier, Kelso, Gertjejansen and Hossfeld (1963), showed a close linear relationship between pressure differential and rate of flow of water through Sitka spruce heartwood over a range of applied pressures from 0 to 3 bar.

Thus, whilst early workers found the effect of increase in pressure differential to deviate markedly from the Darcy relationship, more recent work, where care is taken to avoid embolism, suggests quite close obedience to the law.

A further requirement of Darcy's law is for rate of flow to vary inversely with fluid viscosity. Investigating this relationship, Sutherland, Johnston and Maass (1934) found that the rate of flow through white spruce of sucrose solutions varying in concentration, decreased significantly more rapidly than predicted by the viscosity increase. These authors offer no explanation for the effect. Using a series of liquids of widely differing properties, Buckman, Schmitz and Gortner (1935) found no simple relationship between flow rate and viscosity. This is not surprising since they used both non-swelling (eg benzene) and swelling (eg water)

liquids in their series. Hence as well as viscosity effects, changes in pore geometry caused by swelling seems likely to influence flow through their specimens. In further experiments with both swelling and non-swelling liquids, Erickson, Schmitz and Gortner (1941) were unable to find a simple relationship between flow rate and viscosity. In explanation of this departure from Darcy behaviour, these workers suggest that the degree of sorption by the cell wall and the disrupting effect of the flowing liquid on the pit membrane (peptisation), may cause significant alteration to the geometry of flow determining pores.

In the conduction of these various experiments, steady flow rate conditions were not established and this factor added considerably to the difficulty of establishing the nature of any relationship.

Under steady flow rate conditions, Chen and Hossfeld (1964) were able to demonstrate an inverse relationship between viscosity and rate of flow of a series of aqueous glycerine solutions. Working with air dried eastern hemlock (*Tsuga canadensis*), Comstock (1967) showed flow rate of two non-swelling liquids (iso-octane and n-amyl-alcohol) to vary inversely with viscosity. These data suggest that individual wood specimens behave in accord with Darcy's law with respect to changes in viscosity, provided that care is taken to:-

i establish steady flow rate conditions, and

ii eliminate specimen dimensional change within an experimental series.

The scope of the work reported is limited however. Very few wood species have been investigated and the range of variation of physical parameters, eg viscosity and density of liquid, has been quite small.

1.5.2 GAS FLOW THROUGH SOFTWOOD.

As stated in section 1.1, the permeability of wood to liquids is of importance in several branches of wood science and

technology. Some importance is also attached to the process of gas transport through wood. Recent work is reported, suggesting the use of vapour phase impregnation with formaldehyde as a dimensional stabilisation treatment (Burmester, 1971), whilst impregnation with ammonia has been shown to lead to plasticisation of wood (Schuerch, 1963). Nevertheless, at present it is liquid flow processes that are of most concern to the wood technologist.

Considerable difficulties were experienced by earlier workers in measuring the permeability of wood to liquids (see section 1.5.1), and considerable technique refinement has been necessary to overcome these difficulties. In view of this, several workers have been attracted to the use of gas flow techniques to measure the basic permeability of wood to fluids. The advantages of gas flow techniques are as follows:-

i After drying, gas/liquid interfacial effects, which can lead to pores being unavailable for flow, are avoided.

ii The viscosity of gases is several orders of magnitude less than that of liquids. Hence, more rapid and easily monitored rates of flow through specimens of low permeability may be attained.

iii The lower viscous forces together with the low inertial forces associated with gas flow, are likely to have a less disruptive effect on delicate parts of the structure.

A considerable amount of work has been conducted to measure wood permeability using gas flow techniques and to establish a common mechanism of gas and liquid flow through wood.

In contrast to experience with liquid flow systems, steady flow rates under constant pressure gradients have been readily attained in gas flow systems. From the data of Stamm (1935), although not categorically stated, it can be inferred that steady flow rates of air through white pine and

western hemlock were attained for indefinite periods. Similar inference can be made from the data of Pfalzner (1950) who measured the rate of flow of oxygen and air through spruce wood. Smith and Lee (1958) made repeated permeability measurements on a number of specimens over a period of time. They found that the permeability of each of their specimens did not vary with time by more than about two per cent.

Obedience of gas flow to Darcy's law has been investigated by a number of workers. A linear relationship between air flow rate and applied pressure for a number of timbers is reported by Smith and Lee (1958). As the pressure gradient is increased further, it has been shown (Smith *circa* 1960) that a point is reached where flow rate increases at a rate less than directly proportional to pressure gradient. The apparent linear flow velocity at which this departure occurs varies with species in the range 0.4 to 4 cm/sec. It is suggested by Smith that the departure is due to a change from laminar to turbulent flow. A linear relationship between air flow rate and pressure differential for flow through Scots pine specimens is reported by Buro and Buro (1959). Almost linear behaviour between flow rate through three conifer species and applied pressure differential over the range 0-400 mm water head was obtained by Osnach (1961).

In experiments carried out with white spruce (*Picea glauca*), Sebastian, Côté and Skaar (1965), found flow rate under constant pressure differential to decrease with specimen length, faster than the inverse linear relationship predicted by Darcy's law, over the specimen length range 3-20 mm. They suggested that this is due to decrease in the number of conducting paths as specimen length is increased over this range. Similar observations have been made by Banks (1970) and Bramhall (1971). Beyond about 30 mm, these workers show flow rate to decrease with length in the manner predicted by Darcy's law. Both Banks and Bramhall, independently of one another, suggest that the effect may be explained by the following mechanism:-

Longitudinal flow through softwoods is by way of cell spaces (lumina) and cell wall interconnections (pits). It is known that in air-dried wood a high proportion of the pits are blocked (Phillips, 1933). Thus as specimen length is increased, the probability of encountering a cell in any individual flow path, in which all large pit openings are blocked, is also increased. Therefore, permeability will decrease with length. Eventually a length is reached where all potentially easy pit flow paths are blocked, and flow is controlled by 'residual' flow paths whose probability of blockage tends to zero. It has been suggested by several workers (Phillips, 1933; Osnach, 1961; Banks, 1968; Petty and Puritch, 1970; Bramhall and Wilson, 1971) that the 'residual' flow paths are the bordered pits of late wood. However, it should be recognised that in certain species, notably Scots pine, routes involving flow through ray cells and pits may make a significant contribution.

At specimen lengths where flow is controlled by these so-called 'residual' flow paths, permeability is constant with respect to length. That is, rate of flow varies inversely with specimen length.

It is clear from the above data that significant departure from Darcy's law, with respect to length variation, is observed with short softwood specimens. It has also been established in a number of investigations (Buro and Buro, 1959; Krahmer and Côté, 1963; Comstock, 1965) that permeability of both sapwood and heartwood varies unpredictably around the cross-section of a single stem. Hence, rate of flow is not necessarily related to length and cross-sectional area, in the manner predicted by Darcy's law.

In work to establish the mechanism of water vapour transport through wood, Pfalzner (1950) demonstrated the occurrence of 'slip' flow (see section 1.3.3) and showed the flow of air and nitrogen through spruce wood to be in accord with the Adzumi equation (equation 1.14). It was found by Smith and Lee (1958) that the gas flow permeability of softwoods is

significantly greater than that measured with liquids. They suggest that the discrepancy arises as a result of the occurrence in wood of fluid-conducting pores of very small diameter (< 1μm). In such pores, gas molecular mean free path is of similar magnitude to pore diameter, even at relatively high pressure (∿ 1 bar), and hence significant slip flow may be expected at such pressures (Adzumi, 1937). Further support for the viscous/slip mechanism of gas flow through softwood is provided by the evidence of Resch and Ecklund (1964) and of Sebastian, Côté and Skaar (1965). The most general equation describing viscous/slip flow through porous media is the modified Kozeny equation (equation 1.15). From this equation it is seen that total flow is made up of two components:-

i a component dependent upon mean gas pressure, which varies inversely with viscosity, and

ii a pressure independent term directly proportional to gas thermal velocity $\overline{V}$ (which is inversely related to the square root of molecular weight).

The permeability of eastern hemlock (*Tsuga canadensis*) was investigated by Comstock (1967). He showed the pressure independent or 'slip' component of flow to be inversely related to molecular weight, in accord with the modified Kozeny equation. In his work the viscosity range covered extended from about 170 only to about 190 micropoise. This range is insufficient to unequivocally demonstrate a strong relationship between the pressure dependent or 'laminar' component of flow and gas viscosity. The data of Comstock were certainly not inconsistent with the inverse relationship between laminar flow and viscosity predicted by the modified Kozeny treatment, however.

Thus, it has been shown that the Darcy relationship is only partially applicable to flow through softwood. Rate of flow in the laminar régime is proportional to applied pressure differential, but is not always inversely related to specimen length. Furthermore, it is established that flow is,

in the viscous/slip régime, at pressures around atmospheric. Thus the true relationship between rate of flow and viscosity can only be established by the use of more sophisticated equations (eg the modified Kozeny equation) where the laminar and diffusive components of flow are separated.

1.5.3 SOFTWOOD STRUCTURAL FEATURES AFFECTING GAS FLOW

Based on estimates of size and abundance, Stamm (1946) calculated the relative contribution to the total flow resistance of pits and tracheid lumina. He found that for longitudinal flow through sapwood, the pit system was responsible for about 90 per cent of the total flow resistance, whilst for heartwood this percentage may be greater than 99 per cent.

Total flow resistance of white spruce wood (*Picea glauca*) was measured experimentally by Sebastian, Côté and Skaar (1965). They compared their data with estimates of the flow resistance of cell spaces (tracheid luminae) calculated from microscopically determined geometric parameters. The results of Sebastian *et al*, showing pits in sapwood to contribute between 76 and 98 per cent of the total flow resistance and in heartwood more than 99 per cent, are in agreement with those of Stamm (1946).

Referring to equation 1.15 it is seen that a linear relationship exists between specific mass flow rate $(\frac{QP_o}{\Delta P})$ and gas mean pressure $\overline{P}$, for simple porous media. Significant departure from this linear relationship for gas flow through softwood was first observed by Smith and noted in the report of the Director, Forest Products Research (1964). The departure is in the sense that the relationship curves negatively at low mean gas pressures (Figure 1.5).

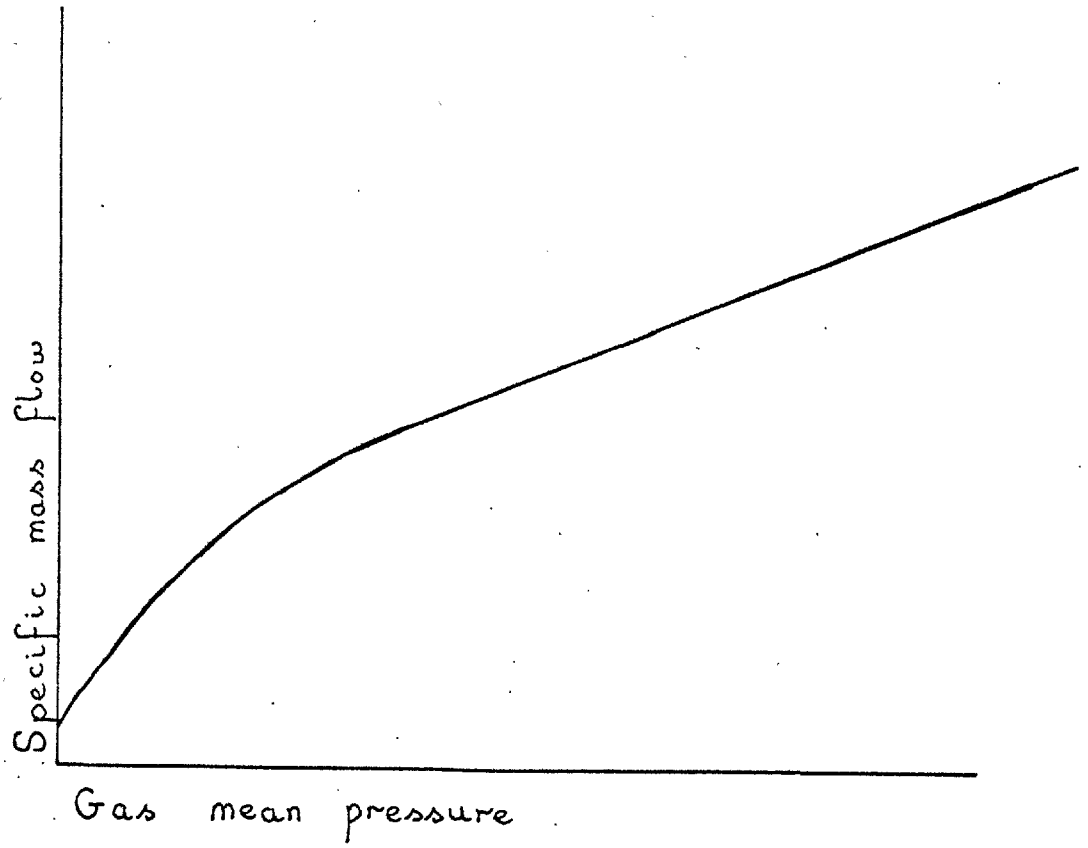


Fig 1.5 Typical curve of specific mass flow against mean pressure for flow through softwood

In a more complete report of the work (Smith and Banks, 1971) the observed deviation is attributed to the behaviour of softwood flow paths, as serially interconnected pairs of capillaries of differing diameter (d_1 and d_2) and length (l_1 and l_2) (Figure 1.6).

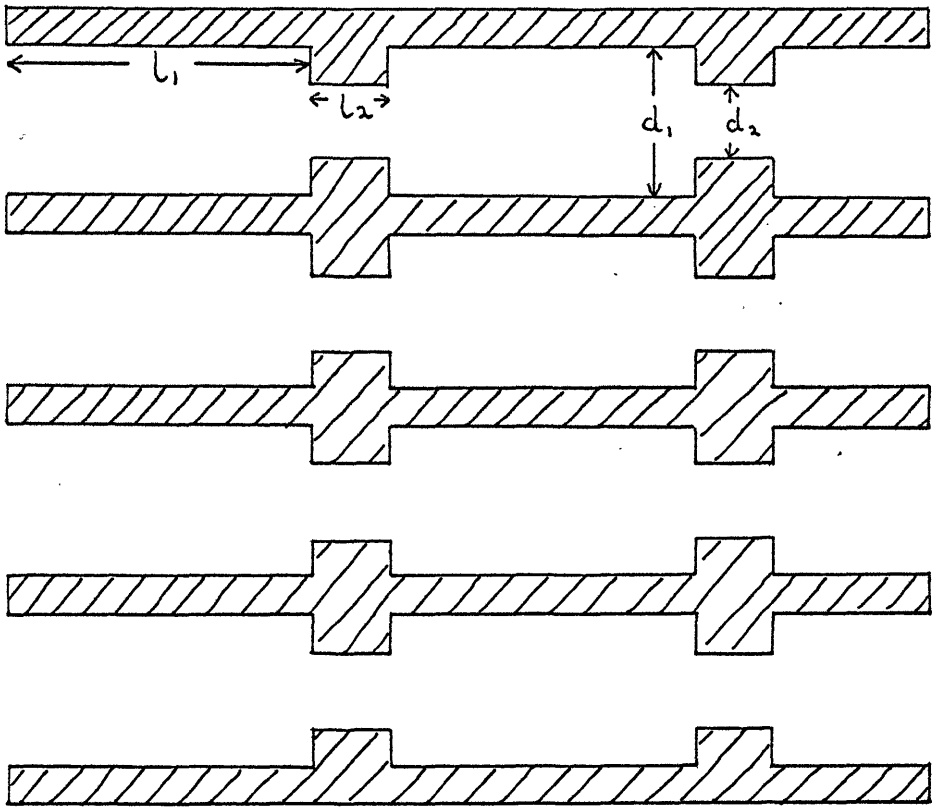


Fig 1.6 Softwood flow path model

Flow through this type of structure can be shown algebraically, to lead to curves of the type shown in Figure 1.5. Similar results were obtained by Petty (1970), who also ascribed the effect to flow through alternately wide and narrow capillaries. Both Petty (1970) and Smith and Banks (1971) related the flow path model illustrated in Figure 1.6 to softwood anatomic features. These workers agree that the long, wide capillary (Figure 1.6, capillary 'a') represents the tracheid lumen. However, whilst Smith and Banks regard capillary 'b' as some hypothetical capillary representative of

the bordered pit generally, Petty suggests that it represents the interfibrillar spaces of the bordered pit margo (Figure 1.3, page 4).

Using numerical approximation procedures the linear mass flow/mean pressure relationships were evaluated by Petty (1970) and by Smith and Banks (1971) for each of the two capillaries 'a' and 'b' forming the flow path 'repeating' pairs. It was then shown by these workers that the requirements of the modified Kozeny equation (equation 1.15) with respect to wide variation in gas viscosity and molecular weight, were met by the obtained relationships.

Thus, together with the work regarding pressure variation discussed in the previous section (section 1.5.2), the above evidence shows that gas flow through softwoods is well described by viscous/slip flow equations.

1.6 EFFECT OF SWELLING ON PERMEABILITY

It is mentioned in section 1.5.1 that no simple relationship could be established between liquid viscosity and rate of flow of various liquids differing in their ability to swell wood (Buckman, Schmitz and Gortner, 1935; Erickson, Schmitz and Gortner, 1941). The most practically important swelling molecule is water and a lot of work has been carried out in the study of the wood/water relationship. This topic is outside the scope of the present work but it may be of interest to note that it is dealt with thoroughly in standard texts by Stamm (1964) and by Kollmann and Côté (1968). During sorption of water over the range 0 to about 30 per cent, softwood swells in volume by about 10-15 per cent. This gross swelling is accompanied by some change in pore geometry (Kelsey, 1963). As early as 1935, Stamm noted a decrease in gas flow permeability associated with increase in moisture content, which he attributed to reduction in size of pit membrane pores. Similar observations are reported by Comstock (1968). It is known that molecules other than water are able to swell wood, the principal criterion governing ability to swell seeming to be an ability to form hydrogen bonds with the methanol group (Gordy, 1939). Several workers have measured experimentally the magnitude of swelling caused by various liquids (see Stamm, 1964; Browning, 1963; Morgan and Orsler, 1969). The effect of swelling induced by various liquids on permeability was investigated by Hossfeld (1972). In contrast to Stamm (1935) and Comstock (1968) who found swelling to decrease permeability, Hossfeld observed an increase in permeability with increased swelling. This conflict, which is difficult to resolve, is discussed more fully in later sections (Part 5).

1.7 SCOPE OF THE PRESENT WORK

The simplicity of the gas flow technique makes it attractive as a method to measure the permeability of wood. However, permeability to liquids is practically of much more importance

(see sections 1.5.1 and 1.5.2). Thus it is desirable to be able to relate gas flow data to liquid flow properties. Gas flow permeability is measured for specimens covering a range of species showing considerable variation in bordered pit anatomic structure (see Part 2). These gas flow data are then related to liquid flow data measured with the same specimens.

Gas flow permeability techniques are commonly used to estimate flow controlling pore sizes. The validity of these techniques for application to softwood are investigated.

The mechanism of inert liquid flow through softwood under the influence of small pressure differentials is investigated and deviations from laminar flow laws are discussed in relation to anatomic features.

It has been shown (see section 1.6) that liquids and vapours which react with wood to cause swelling of the cell wall, markedly influence softwood permeability. The evidence cited in the literature is in conflict, to some extent. Several workers, using gas flow techniques, have found that swelling leads to decreased permeability, whereas recent liquid flow work shows increased permeability associated with swelling (see section 1.6).

For one species (*Abies grandis*) a systematic and thorough investigation is conducted in this work, of the effect of swelling induced by cell wall sorption of water vapour and of organic liquids upon permeability to liquids.

Part 2 BORDERED PIT STRUCTURE

2.1 STRUCTURAL VARIATION IN BORDERED PIT MEMBRANES - SELECTION OF TEST SPECIES

It is now generally accepted that longitudinal flow through softwood is mainly by way of the tracheid/bordered pit system, with some facility for blockages in the system to be overcome by the use of radial flow paths (section 1.2). In all species, tracheid lumina are of relatively similar and simple geometry, approximating reasonably to long capillaries, allowing flow to occur in accord with the Hägen-Poiseuille law (section 1.3). It seems likely, therefore, that any major 'between species' differences in flow mechanism will be associated with variation in the structure of bordered pits, and especially of their membranes.

From examinations carried out by light microscopy, Bailey (1913) drew a remarkably accurate general description of the bordered pit membrane of the Pinaceae. With the introduction of electron microscopy, however, major advances have been made in the elucidation of membrane fine structure. Early workers carrying out electron microscopic investigations (Liese, 1951; Eicke, 1954; and Frey-Wyssling, Mühlethaler and Bosshard, 1955) observed the pit membrane to consist of an impervious central disc (the torus) surrounded by a porous fibrillar annulus (the margo) - Figure 2.1. This structure is very close to that predicted by Bailey from his light microscopy examination.

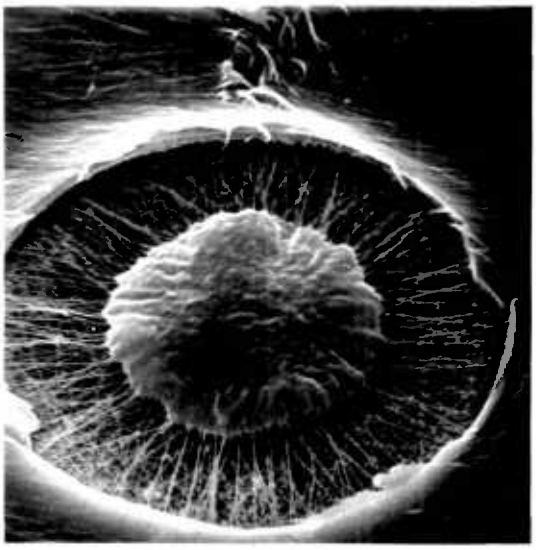


Fig 2.1 *Pinus* spp bordered pit membrane mag x3500

The above investigations were carried out with air-dried wood. In a comparative examination, however, Jayme and Fengel (1959) observed marked differences between the structure of pit membranes from 'green' and 'air-dried' specimens. In dry specimens of spruce wood they found membranes as described by Liese (1951), Eicke (1954) and Frey-Wyssling et al (1956). The membranes of 'green' (never dried) wood, however, were seen to have a uniform fibrillar appearance, without distinct torus and margo. They suggested, therefore, that the structure seen in air-dried specimens arose as a result of drying and pit aspiration (see 2.2 below). More recent work (Thomas, 1968) shows quite clearly that margo and torus are formed during cell development, and it seems that the structure observed by Jayme and Fengel was an artefact of their preparative technique.

Three species (*Picea abies*, *Araucaria angustifolia* and *Agathis labilliardierii*) were examined by Jutte and Spit (1963), who noted several between-species differences in the structure and geometry of the pits. Specimens from several genera were examined by Krahmer and Côté (1963). They observed typical *'Pinus'* type pit membranes in Douglas fir (*Pseudotsuga menziesii*), with thickened central torus and radially orientated supporting strands. In eastern and western hemlock (*Tsuga canadensis* and *T. heterophylla*), however, these workers observed irregular extensions of the torus extending into the margo zone. Fengel (1968) reports structural differences in pit membranes specifically related to genus and species. Considerable difference between early wood and late wood pit membrane structure of a single species is also reported by him. Late wood pits are observed to be generally more heavily incrusted than those of early wood, some pits in the last formed late wood having membranes totally covered by incrustant. In a detailed examination of the southern pines, Thomas (1969) found no major and consistent between-species differences in this closely-related group but, in agreement with Fengel (1968), observed considerable structural difference between early wood and late wood pits.

From the results of his own work and those of other workers, Liese (1965) classified early wood pit membranes into five types. The first of these classes, the *'Pinus'* type contains most of the timber producing temperate zone softwoods, eg pines, spruces, firs, hemlocks. The second of Liese's classes, the *'Araucaria'* type contains the commercially important South American softwood Parana pine (*Araucaria angustifolia*). Descriptions of the pit membrane structure observed in these classes are given below:-

1 *Pinus* type: fibrils in moderately dense radial pattern, with larger spaces; distinct torus by apposition.

2 *Araucaria* type: microfibrils in a radial pattern, more densely packed with narrower spaces; torus not due to

apposition, but only as matrix substance at the central region.

The remaining three classes, *'Thujopsis'* type, *'Gnetum'* type and *'Cycas'* type are made up of species with little importance as timber-producing trees. Hence for the permeability study described in this work, species are selected from the *'Pinus'* and *'Araucaria'* types described above. Within the basic *Pinus* type, Liese reports the following variations in membrane fine structure:-

Tsuga spp - erratic apparently impervious extensions of the torus extending into the margo.

Cedrus spp - more regular torus extensions giving the torus a scalloped appearance.

Several species for test are selected from the *'Pinus'* type class, to include examples with the basic type of structure described by Liese (1965) and with the structural variations described above. A list of test species with a brief description of their pit membranes is given in Table 2.1 below.

Table 2.1 TEST SPECIES

Species	Type of Membrane
Abies grandis	*Pinus* type
Picea abies	*Pinus* type
Tsuga heterophylla	*Pinus* type with extended torus
Cedrus deodara	*Pinus* type with scalloped torus
Araucaria angustifolia	*Araucaria* type

2.2 PIT ASPIRATION

In the sapwood of living trees, pit membranes are suspended centrally in the pit cavity. During air drying, however, in a high proportion of pits, the membrane is displaced and

pressed against one of the pit openings, forming a more or less efficient seal, a process known as pit aspiration.

It was demonstrated by Phillips (1933) that drying from green to below 30 per cent moisture content brought about the aspiration of some 98 per cent of pits in early wood. In late wood, however, drying led to the aspiration of only about 35 per cent of pits. Phillips suggested that the membrane displacement is caused by surface forces. By the use of physical model techniques, Hart and Thomas (1967) were able to demonstrate that membrane displacement by surface tension forces was a feasible and likely process. Subsequently a number of workers have shown experimentally that the membrane is displaced by surface tension, and fixed against the pit border by hydrogen bonds (Liese and Bauch, 1967; Comstock and Côté, 1968; Thomas and Kringstad, 1971). Several workers have demonstrated that 'green' never dried sapwood is much more permeable than air-dried wood (Banks, 1968; Comstock, 1968; Bramhall and Wilson, 1971), suggesting that fluid flow is very markedly affected by pit closure. Using a dye impregnation technique Petty and Puritch (1970) showed that whilst virtually all tracheids of 'green' grand fir (*Abies grandis*) specimens conducted fluid, conduction was restricted mainly to late wood, after air drying. This observation also strongly suggests a relationship between permeability and pit aspiration.

Hence, apart from differences in membrane structure, the condition of pits (aspirated or non-aspirated) clearly has a marked effect on permeability. Most of this work is concerned with fluid conduction through dry wood (where most pits are aspirated), because of its relevance to various wood processes. However, a limited study is included of the permeability of green wood (where virtually all pits in sapwood are non-aspirated) to liquids.

Part 3 SCANNING REFLECTION ELECTRON MICROSCOPIC STUDY OF TEST SPECIES

3.1 OBJECTIVES OF THE STUDY

The investigation of pit membrane structure described below is not intended to provide an exhaustive study of pit membrane structure. It is included to provide a record of typical membrane structures observed in the test species listed in Table 2.1. From the quite large number of membranes observed with the microscope, a smaller number were photographed and examined in greater detail to gain an idea of the range of pore sizes occurring in the various species. Many workers have shown that the technique of scanning electron microscopy is well suited to the study of wood and other plant tissue (see, for example, Wellwood, Ifju and Wilson, 1965; Echlin, 1968; Findlay and Levy, 1969 and 1970). Preparative procedures are simple and quick - allowing examination of a relatively large sample of material. The magnification range (x 30 to x 20 000) and the resolution (better than 1 000 Å) make the technique ideal for the study of pit structure.

3.2 SPECIMEN PREPARATION AND EXAMINATION TECHNIQUE

Most bordered pits lie on the radial walls of longitudinal tracheids, membranes forming part of the middle lamella/primary wall of the composite cell wall. It is convenient that softwoods cleave naturally along radial planes, these cleavage planes being along the middle lamella zone. To expose membranes, therefore, it is necessary only to split along these natural planes.

Surfaces for examination were prepared from cubes of about 5 mm side sawn from the same wood blocks used in the preparation of permeability specimens. From each test species,

specimens were prepared in air-dry condition to correspond to the condition of specimens used in permeability experiments. As mentioned in section 2.2, however, a limited study was made of the permeability of green grand fir (*Abies grandis*) wood. It has been shown by Thomas (1968) that drying in the absence of interfacial forces retains pit structure in the 'green' state. Hence to observe green pit membrane structure in grand fir, specimens were also prepared from this species, dried from green by a solvent exchange/vacuum freeze drying technique using the following system:-

1 Sap replaced by acetone.
2 Acetone replaced by benzene.
3 Benzene vacuum evaporated from the solid phase at $-5^{\circ}C$.

After drying, radial slivers, about half to one millimetre thick, were split from the 5 mm cubes, with a sharp razor blade, and mounted on metal stubs with a solvent-based glue (see Findlay and Levy, 1969). To prevent the build-up of static charge during electron bombardment in the microscope (Oatley, Nixon and Pease, 1965) the specimen surfaces were coated with a conducting film of gold/palladium about 400 Å thick, in a vacuum evaporation unit.

Specimens prepared in this way were examined with the Cambridge Instrument Company 'Stereoscan' scanning electron microscope. The instrument was operated in the emissive mode with an accelerating potential between 10 and 20 kV.

3.3 PIT MEMBRANE STRUCTURE OF TEST SPECIES

Examples of the membrane structure of the various species studied in this work are illustrated in Figures 3.1 to 3.16. The structural features observed are similar to those described in the classification of Liese (1965) - see section 2.1. In air-dried specimens early wood pits were mainly observed to be aspirated, although occasional

membranes were found in the unaspirated condition. Most late wood membranes appeared unaspirated.

3.3.1 *Abies grandis* SAPWOOD

Examples of aspirated and non-aspirated early wood pit membranes of air-dried wood are shown in Figures 3.1 and 3.2, respectively. In the aspirated membrane (Figure 3.1), a distinct impression of the pit aperture can be seen through the torus, suggesting that membrane and pit border are quite firmly pressed together. The fibrillar strands in Figure 3.1 are seen to be orientated principally radially, although some more randomly orientated fibrils can be observed between the radial strands. Structure is revealed more clearly in the non-aspirated membrane (Figure 3.2). Here the random 'between radial strand' fibrils can be very clearly distinguished. The outer anulus of the membrane appears imperforate in some areas, having a primary cell wall appearance. Both aspirated and non-aspirated membranes appear free from incrustant. In the late wood of sapwood, membranes appear to be incrusted with some amorphous substance so that fibrillar detail is obscured over large areas (Figure 3.3). In the membrane illustrated relatively few perforations remain between the incrusted fibrils. Amongst other late wood pit membranes observed, some were perforated to a greater extent whilst a few appeared virtually imperforate.

Pits of specimens prepared by the solvent exchange/freeze drying technique described above were virtually all observed to be non-aspirated. In early wood the membranes appeared free from incrusting material and the margo fibrils were seen to be aligned principally radially (Figure 3.4). In a number of pits, torus extensions similar to the *Tsuga* spp type (Liese 1965) were observed (Figure 3.5).

As in air-dried material, late wood pit membranes were seen to be heavily coated with incrustant. Where incrusting substances were absent, a fine fibrillar structure was revealed (Figures 3.6 and 3.7).

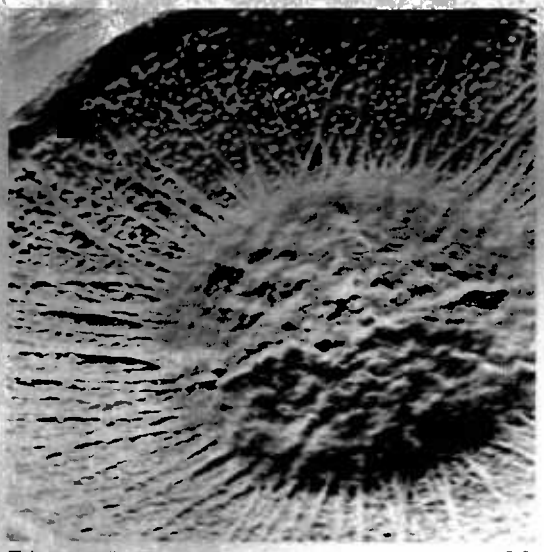


Fig 3.1 mag x 5500

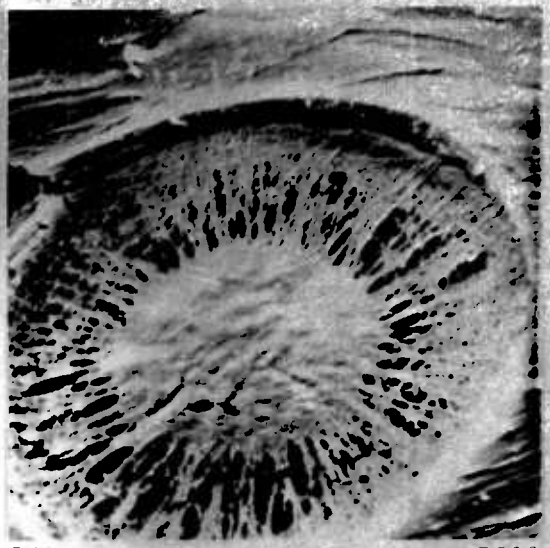


Fig 3.2 mag x 5500



Fig 3.3 mag x 5300



Fig 3.4 mag x 3800

Fig 3.1 *Abies grandis* sapwood early wood, air dried - aspirated pit membrane

Fig 3.2 *A. grandis* sapwood early wood, air dried - unaspirated pit membrane

Fig 3.3 *A. grandis* sapwood late wood, air dried - unaspirated pit membrane

Fig 3.4 *A. grandis* sapwood early wood, solvent exchange/freeze dried - unaspirated pit membrane



Fig 3.5 mag x 3600

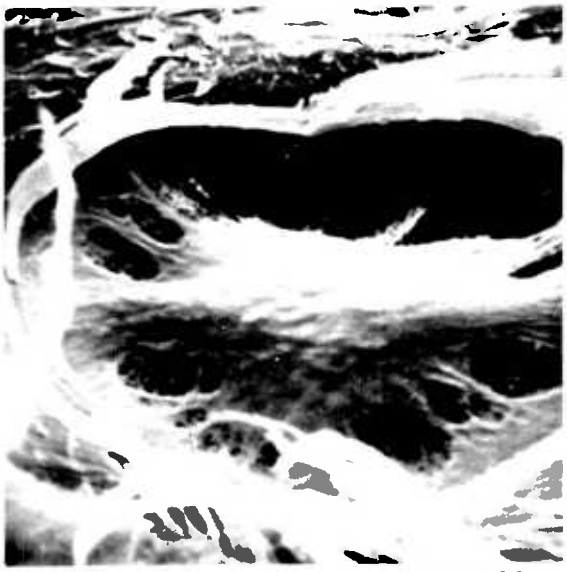


Fig 3.6 mag x 7000

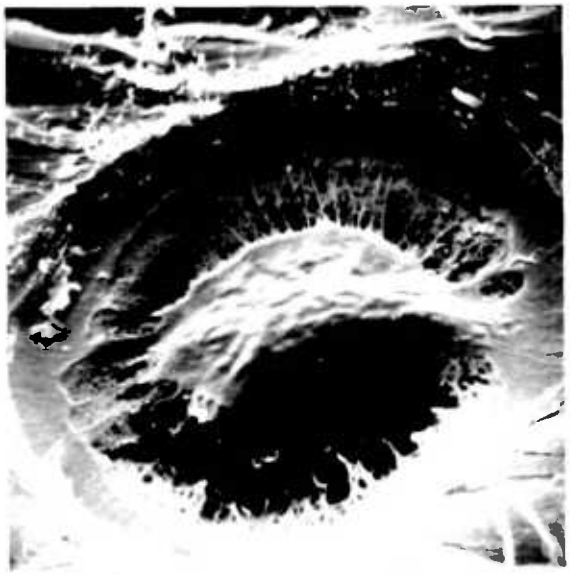


Fig 3.7 mag x 7000



Fig 3.8 mag x 4900

Fig 3.5 *Abies grandis* sapwood early wood, solvent exchange/freeze dried - pit membrane with torus extensions

Fig 3.6 *A. grandis* sapwood late wood, solvent exchange/freeze dried - pit membrane

Fig 3.7 *A. grandis* sapwood late wood, solvent exchange/freeze dried - pit membrane

Fig 3.8 *Picea abies* sapwood early wood, air dried - aspirated pit membrane

3.3.2 *Picea abies* SAPWOOD

Membrane structure in this species was observed to be similar in many respects to that seen in *Abies grandis* above. A typical early wood membrane is shown in Figure 3.8. It can be seen that the margo fibrils are orientated principally radially with some random interconnection. Incrustants are absent or sparse.

Late wood pit membranes appear heavily incrusted (Figure 3.9), often with only few apparently porous zones.

3.3.3 *Tsuga heterophylla* SAPWOOD

In the early wood of *Tsuga heterophylla* extensions of the torus running into the margo are seen in most early wood pit membranes (Figure 3.10). Apart from these torus extensions, the membranes appear essentially free from incrustant.

Late wood pits exhibit membrane structure similar to that seen in the late wood of *Abies* and *Picea* spp, a high proportion of the membrane surface appearing to be incrustant coated (Figure 3.11).

3.3.4 *Cedrus deodara* SAPWOOD

The radially orientated margo fibrils in early wood appeared more widely separated in this species (Figure 3.12) than in the other Pinaceae examined. Torus extensions giving the scalloped appearance described by Liese (1965) were not seen to be developed to any marked extent. Small, regular, torus extensions were seen to extend over about one-tenth the length of the radial margo fibrils. These together with the widely separated radial fibrils running from them may give a more scalloped appearance under lower resolution.

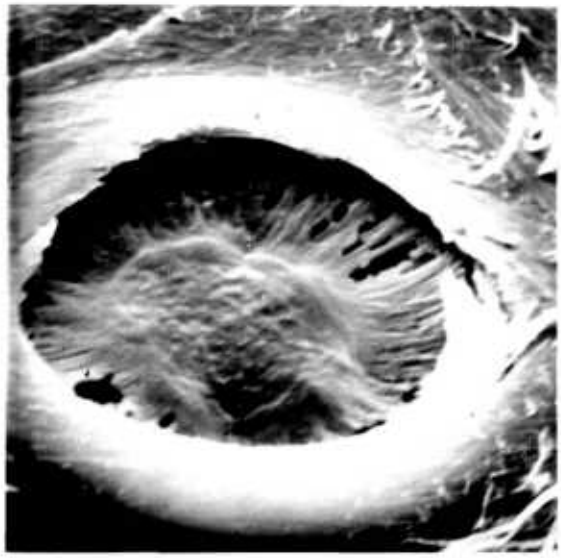


Fig 3.9 mag x 4900

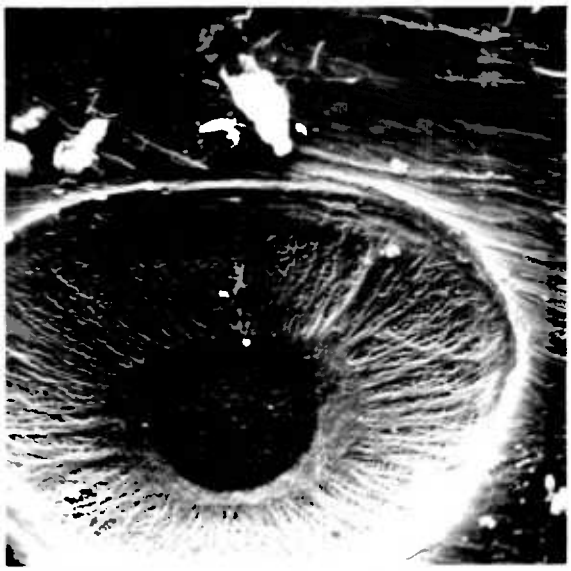


Fig 3.10 mag x 3700

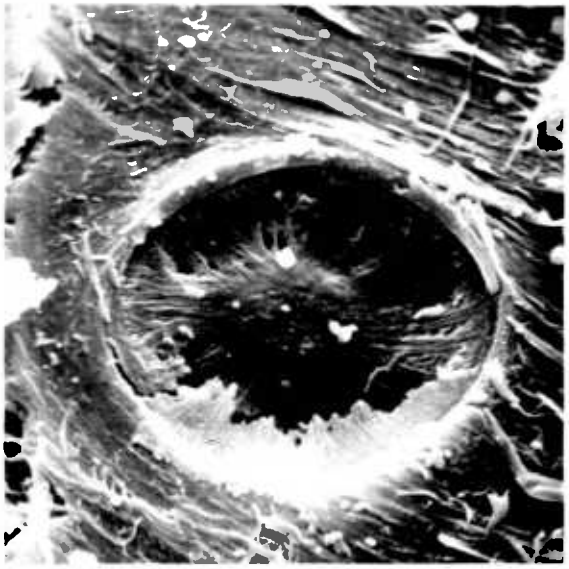


Fig 3.11 mag x 3600

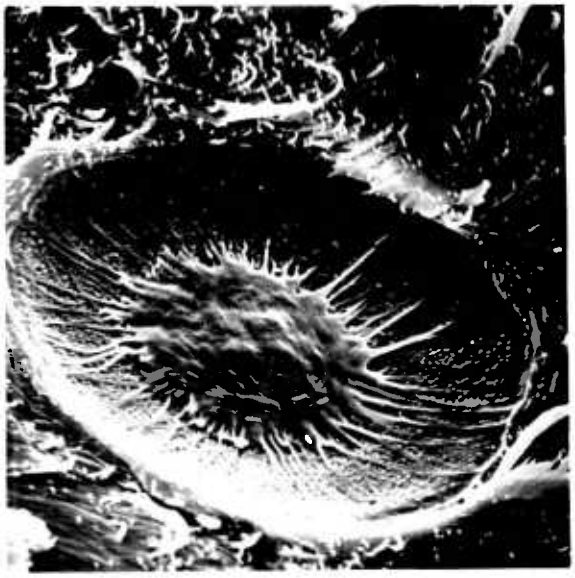


Fig 3.12 mag x 3500

Fig 3.9 *Picea abies* sapwood late wood, air dried - unaspirated pit membrane

Fig 3.10 *Tsuga heterophylla* sapwood early wood, air dried - aspirated

Fig 3.11 *T. heterophylla* sapwood late wood, air dried - unaspirated pit membrane

Fig 3.12 *Cedrus deodara* sapwood air dried - aspirated pit membrane

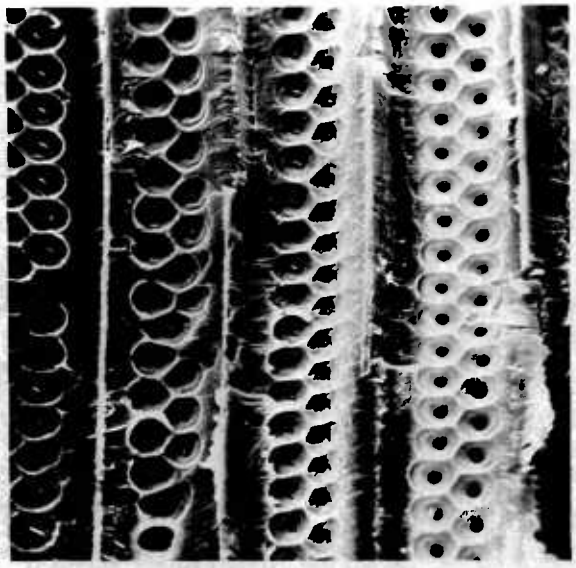


Fig 3.13 mag x 350

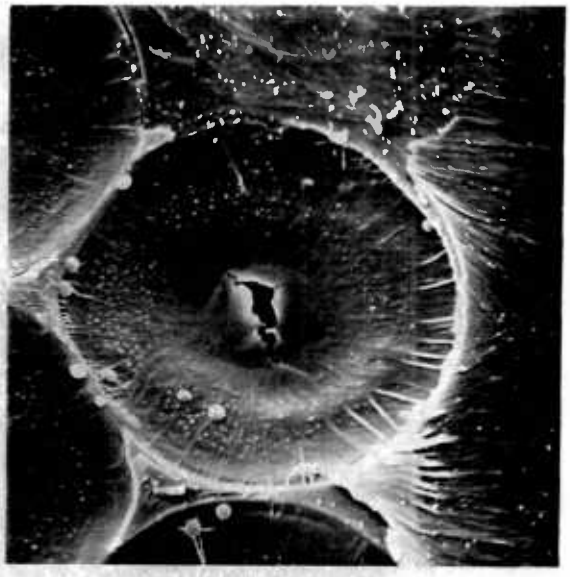


Fig 3.14 mag x 3900

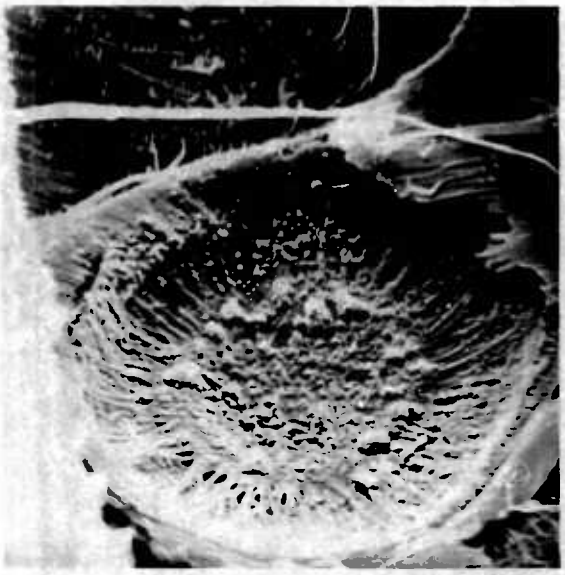


Fig 3.15 mag x 4500

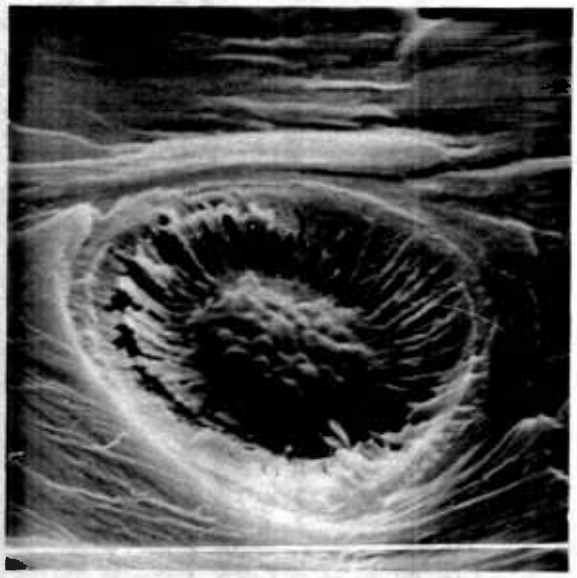


Fig 3.16 mag x 3700

Fig 3.13 *Araucaria angustifolia* air dried - group of bordered pit membranes

Fig 3.14 *A. angustifolia* air dried - pit membrane

Fig 3.15 *Abies grandis* heartwood early wood - incrusted pit membrane

Fig 3.16 *Tsuga heterophylla* heartwood early wood - incrusted pit membrane

3.3.5 *Araucaria angustifolia* SAPWOOD

The most striking features about pits in this species are their abundance and their distinct hexagonal shape, giving a honeycomb appearance to their arrangement on cell walls (Figure 3.13). As noted in the Liese classification, the tori of membranes appear unthickened. Margo fibrils are seen to be radially orientated and very widely separated (Figure 3.14). It was noticeable in the specimens examined that, in almost all pits, tori were split (Figures 3.13 and 3.14). It is possible that these splits are the result of electron beam damage in the microscope. However, the frequency of their occurrence even under low magnification (Figure 1.13) - where local heating is less severe - suggests other reasons for this damage. It seems possible that the splits may arise as a result of drying stresses, and the possibility of their occurrence throughout dried, permeability specimens is considered in the general discussion (section 7.1).

3.3.6 HEARTWOOD OF TEST SPECIES

In all the species examined, the membranes of heartwood appeared structurally similar to those of corresponding sapwood. However, it was seen that whilst in sapwood, incrustation was restricted to late wood pit membranes, in heartwood, early wood pits were frequently incrusted also (see, for example, Figures 3.15 and 3.16).

3.3.7 PIT MEMBRANE PORE SIZES

The scanning electron micrographs resulting from the above study were used to gain an idea of the range of membrane pore sizes in the test species. An immense degree of detailed geometric variation in membrane structure within each species, even between neighbouring pits in the same tracheid, was observed. Thus the limited study of pore sizes carried out (based on about ten pits per species) must not be regarded as a precise guide to pore sizes occurring throughout each

species. The measurements are intended as an 'order of magnitude' guide to membrane pore sizes in the permeability specimens used in this work. Membrane pores are approximately triangular to rectangular slit shaped (Figures 3.1 to 3.16). In Table 3.1 below, the approximate range of slit dimensions observed are cited for each species examined. Additionally, the dimensions are converted to mean hydraulic radii using equation 1.13 (section 1.4). In *Araucaria angustifolia*, all membranes appeared to be very firmly sealed against pit borders. It seems likely, therefore, in this species that flow is controlled by the observed torus splits.

In addition to membrane interfibrillar dimensions, therefore, the sizes of these splits were estimated. These lay in the range 0.25 x 1.0 micron to about 0.4 x 0.6 micron, giving an equivalent hydraulic radius about 0.1 micron.

Table 3.1

MARGO PORE DIMENSIONS FROM SCANNING ELECTRON MICROSCOPY

Species	Margo pore dimensions (micron)	
	Slit size (micron)	Equivalent hydraulic radius (micron)
Abies grandis sapwood early wood	0.08 x 0.08 to 0.6 x 1.5	0.02 to 0.2
Abies grandis sapwood late wood	0.08 x 0.08 to 0.24 x 1.6	0.02 to 0.1
Abies grandis heartwood early wood	0.08 x 0.08 to 0.9 x 1.3	0.02 to 0.25
Abies grandis heartwood late wood	0.08 x 0.3 to 0.4 x 1.7	0.03 to 0.15
Cedrus deodara sapwood	0.1 x 0.2 to 0.6 x 3.0	0.03 to 0.25
Picea abies sapwood early wood	0.1 x 3.0 to 0.3 x 3.0	0.05 to 0.15
Picea abies sapwood late wood	0.04 x 0.04 to 0.25 x 0.8	0.01 to 0.1
Tsuga heterophylla sapwood early wood	0.2 x 0.2 to 0.8 x 2.4	0.05 to 0.3
Tsuga heterophylla sapwood late wood	0.2 x 0.2 to 0.8 x 2.0	0.05 to 0.3
Tsuga heterophylla heartwood early wood	0.2 x 0.2 to 0.4 x 1.0	0.1 to 0.15
Tsuga heterophylla heartwood late wood	0.2 x 0.2 to 0.2 x 1.0	0.05 to 0.1
Tsuga canadensis sapwood	<0.1 x <0.1 to 0.6 x 2.0	<0.025 to 0.25
Tsuga canadensis heartwood	∿0.15 x 0.15	∿0.08
Araucaria angustifolia (sapwood and heartwood)	0.2 x 0.9 to 1.1 x 3.0	0.08 to 0.4

Part 4 GAS FLOW PERMEABILITY

4.1 OBJECTIVES

The flow of gases through certain softwoods is described by viscous/slip flow equations (see section 1.5.2). In this section the measurement of gas flow permeability is described. Permeability data are analysed by a numerical technique based on a simple physical flow path model. The analysis allows viscous and slip permeability constants to be separately estimated.

Viscous permeability constants estimated in this way are compared in a later section with liquid flow constants measured for the same specimens.

From the viscous and slip permeability constants, flow controlling pore sizes are estimated.

The validity of the simple flowpath model is critically examined, and the effect that oversimplification may have on the estimated values of viscous permeability constant and pore size is investigated theoretically.

4.2 APPARATUS AND EXPERIMENTAL TECHNIQUE

The apparatus used to measure gas flow rate consists of:-

i Compressed gas supply controlled by 'inlet' valve.
ii Capillary flowmeter.
iii Specimen cell with differential manometer connected across it.
iv Gas outlet manometer.
v Outlet control valve.
vi Rotary vacuum pump.

It is shown diagrammatically in Figure 4.1.

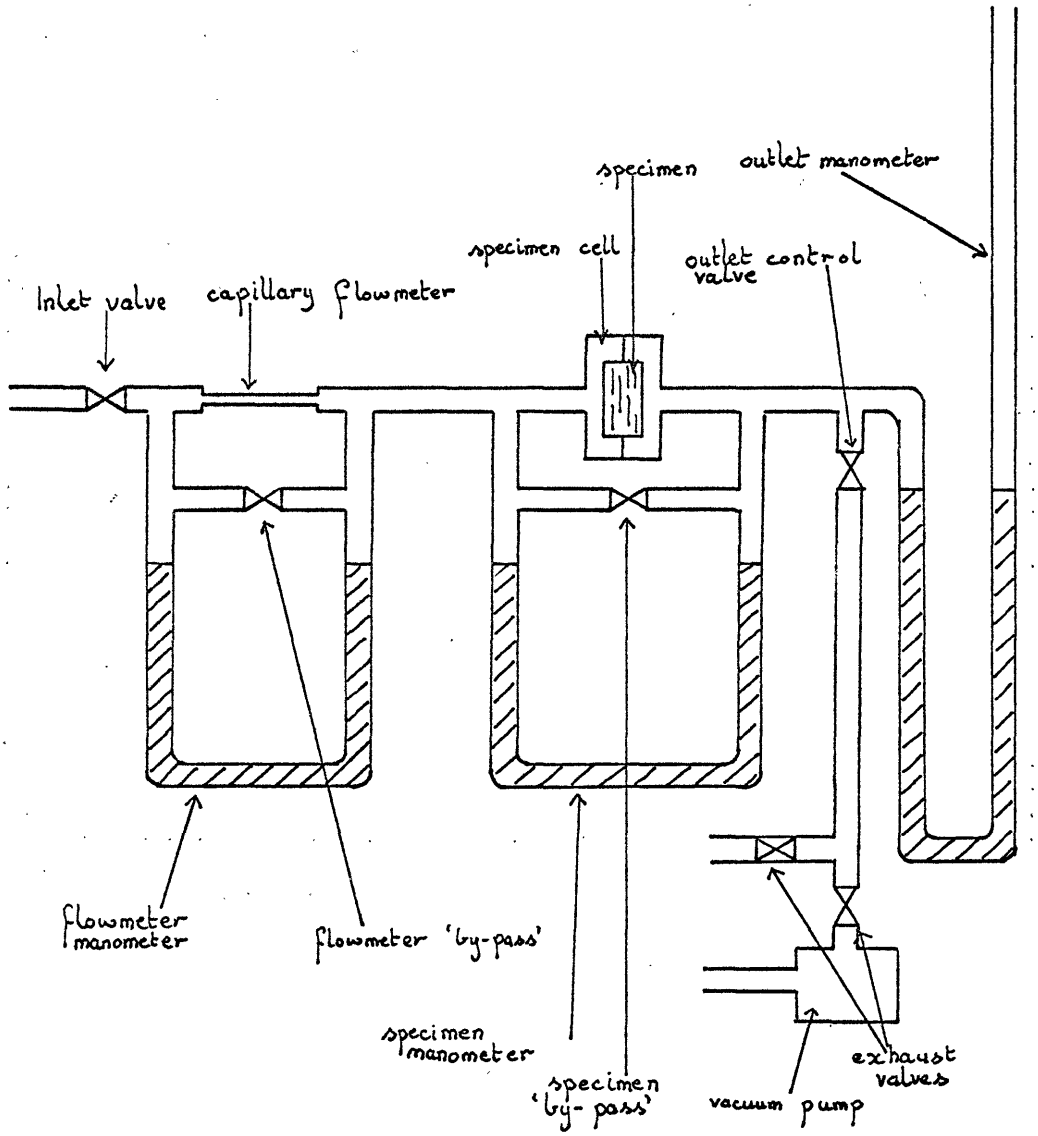


Fig 4.1 GAS FLOW PERMEABILITY APPARATUS

Gas enters the apparatus from the supply cylinder, through the inlet control valve. It flows serially through the flowmeter capillary, the wood specimen and the outlet control valve, either to exhaust at atmospheric pressure (for operating pressures greater than 1 bar absolute) or to the vacuum pump (when operating at pressures of 1 bar or less).

The capillary flowmeter consists of about 5 m of precision bore glass capillary of internal diameter 1 mm. This fairly wide bore tube was used to ensure that flow within the meter capillary is significantly free from 'slip' throughout the range of gas pressures used. This ensures that within the laminar régime of flow, the flowmeter 'constant' is independent of gas mean pressure. As a rough guide, slip flow effects assume significance when gas mean free path is of similar magnitude to capillary diameter. At the lowest pressure used in the experiments ($\sim$0.1 torr) the mean free path for the hydrogen molecule at 25^{o}C is about 0.1 mm, ie an order of magnitude less than the diameter of the flowmeter capillary.

Calibration of the flowmeter was accomplished by comparison of pressure drop across the capillary with volume rate of flow of hydrogen measured with a soap film meter connected in series with it. Over the range tested, rate of flow was found to obey the following linear relationship:-

$$Q = 0.007918\Delta P \qquad \text{Equation 4.1}$$

where Q = volume rate of flow (ml sec^{-1})

ΔP = pressure drop across flowmeter capillary (mm butyl phthalate)

The specimen cell (with a specimen in place) is illustrated diagrammatically in Figure 4.2. It is made up of two half cells constructed from brass. The half cells are threaded so that they may be tightened on to the specimen flange, sealing being effected with neoprene gaskets.

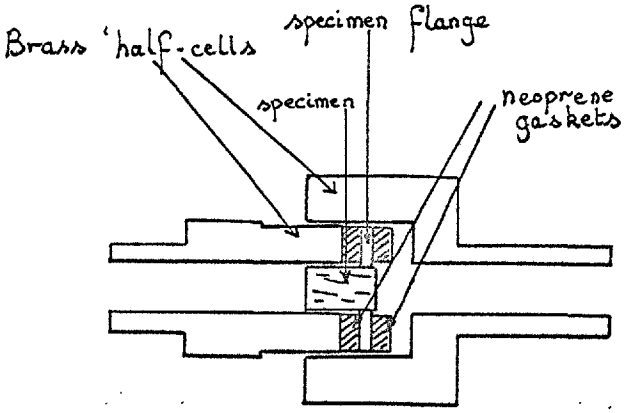


Fig 4.2 GAS FLOW PERMEABILITY, SPECIMEN CELL

Specimens were prepared by sawing cubes of about 15-20 mm side from blocks of the various species, using a small hack-saw. From selected zones of these cubes (eg early wood or late wood), test pieces, of transverse cross-section about 5 mm square, were split with a sharp razor blade. For late wood specimens it was usually necessary to cut the radial dimension rather smaller than this, to avoid the inclusion of early wood cells. Finally the transverse faces were trimmed with a razor blade to expose cleanly, transversely-cut tracheids, allowing uninterrupted fluid entry and exit. Specimens prepared in this way were then dried by evacuation over phosphorus pentoxide.

To enable easy transfer from the gas flow to the liquid flow apparatus the specimens were mounted in washers which were used as flanges enabling compressive fitting into the flow cells (see Figure 4.2). Before mounting into the washers, specimen lateral surfaces were sealed with epoxy resin, to restrict flow to the longitudinal direction. Mounting into

washers was accomplished as follows:-

1 The hole in the washer was covered on one side with adhesive tape - thus forming a shallow 'dish'.
2 A specimen transverse face was pressed on to the exposed tape in the washer centre.
3 Epoxy resin was poured into the annulus between the specimen and the washer.

This system is illustrated in Figure 4.3.

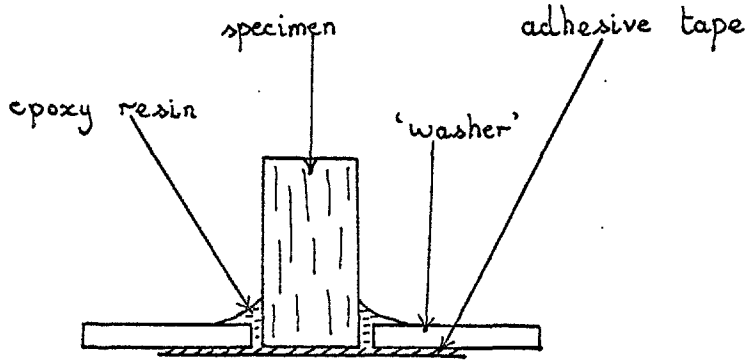


Fig 4.3 SYSTEM OF MOUNTING WOOD SPECIMENS INTO FLANGES

After allowing the resin to cure at room temperature, the adhesive tape was stripped from the specimens. Transverse surfaces were checked by low power microscopy and found to be significantly free from resin, tape adhesive and other debris. At this stage they were dried in vacuum desiccators over phosphorus pentoxide for a minimum of two days prior to gas flow experiments.

The outlet manometer contained mercury as the manometric fluid, allowing pressure to be sensed to 1 torr ($\sim 10^3$ dyn cm^{-2}) over the range 0 to 2 bar (2×10^6 dyn cm^{-2}) absolute. To measure differential pressure across the flowmeter capillary and specimen, dibutyl phthalate was used as the manometric liquid. With a vapour pressure at 25°C of 0.00016 torr and density of only about 1.05 gm ml^{-1}, this liquid is ideal for sensitive manometry at working pressures down to 1 torr. Scalar measurement to about 1 mm of fluid head enables differential pressure to be detected with a sensitivity of about 100 dyn cm^{-2} (<0.1 torr).

Specimen cell and flowmeter were fitted with by-pass valves, allowing rapid changes in gas pressure within the apparatus to be made. Connections between valves, specimen cell and flowmeter were made with glass tubing of about 10 mm bore, butt jointed and sealed with rubber pressure hose. Hence significant pressure drop occurs only across valves, flowmeter and specimen.

Before permeability experiments the apparatus was checked for leaks. This check was carried out with a specimen mounted in the cell and the equipment assembled into its operational state, as shown in Figure 4.1. With specimen and flowmeter by-pass valves open and the inlet valve closed, the apparatus was evacuated to an absolute pressure of 1 torr. The outlet valve was closed, vacuum pump removed and the apparatus allowed to stand at constant temperature (25 ± 0.5°C) for ~18 hours. Any pressure increase due to air leak was noted.

If the observed increase in pressure exceeded 10 torr, the joints were re-made and the leak test repeated. This procedure was continued until satisfactory tightness was achieved. A similar procedure was followed to ensure freedom from outward gas leak with the equipment pressurised. In this case, the apparatus was pumped to 1 bar gauge pressure with hydrogen gas, and sealed. Decrease in pressure of not more than 5 torr over a two-hour period was considered a satisfactory limit for outward leak. These limits are equivalent to inward and

outward leak rates of about 0.003 ml sec^{-1} ~~and~~ at absolute gas pressures of 5 torr and 2 bar (absolute pressure) respectively.

Once a satisfactory seal was established, the apparatus was purged of air with the permeating gas (hydrogen). This was accomplished by alternately reducing the gas pressure in the apparatus to 1 torr or less, and raising it to 2 bar absolute with hydrogen. This procedure was repeated for at least five cycles to ensure virtually complete removal of air.

Flow measurements were made with the apparatus maintained at 25 ± 0.5°C as follows:-

1 By-pass valves were opened, and hydrogen pressure within the apparatus was raised to about 2 bar absolute.
2 Inlet and outlet valves closed.
3 Specimen by-pass valve closed.
4 Inlet and outlet valves slowly opened together to give a steady pressure across the specimen (ideally this pressure should be equivalent to a head of about half to two-thirds the height of the manometer tube).
5 Flowmeter by-pass valve closed (ensuring pressure across flowmeter within manometer range).

In this condition the apparatus was allowed to stabilise until two successive sets of readings of each manometer, taken at time intervals of 15 minutes, differed by not more than 1 mm. Under these conditions, the outlet pressure (taking account of barometric pressure) and the pressure differentials across specimen and flowmeter were recorded. This procedure was repeated at about fifteen hydrogen pressures over the range 1 to 1500 torr (10^3 to 2×10^6 dyn cm^{-2}) absolute. For hydrogen pressures less than 10^6 dyn cm^{-2} absolute ('0' gauge pressure), the outlet valve exhaust was connected to a rotary vacuum pump, allowing gas flow to be measured over the range 1 to 760 torr ($\sim 10^3$ to 10^6 dyn cm^{-2}) absolute pressure.

4.3 GAS FLOW RESULTS

An example of a complete set of experimental data for a specimen is given below (Table 4.1).

Table4.1 EXPERIMENTAL DATA FOR HYDROGEN FLOW THROUGH *Tsuga heterophylla* SAPWOOD EARLY WOOD

Atmos-pheric pressure (mm Hg)	Outlet pressure (mm Hg gauge)	Pressure drop across specimen		Pressure drop across flowmeter	
		mm dibutyl phthalate	mm Hg	mm dibutyl phthalate	mm Hg
746	679	242	19.3	21	1.67
746	549	235	18.7	21.5	1.71
746	441	235	18.7	22	1.75
744	321	234	18.6	22.5	1.79
744	216	255	20.3	25.5	2.03
744	78	200	15.9	21.5	1.71
755	-74	240	19.1	27	2.15
754	-235	218	17.3	28	2.23
753	-348	174	13.8	26	2.07
753	-378	214	17.0	33	2.63
753	-514	158	12.6	31	2.47
753	-614	185	14.7	49	3.90
749	-682	178	14.2	72	5.73
753	-694	202	16.1	86	6.84
749	-732	172	13.7	126	10.03
750	-748	71	5.6	124	9.87

From the data of Table 4.1, values for the average permeating gas pressure within the specimen and the flowmeter capillary can be estimated. Referring to Figure 4.1 it is clear that approximate mean gas pressure within the specimen is given by:-

$$\overline{P} = Px + \frac{\Delta Ps}{2} \qquad \text{Equation 4.2}$$

where $\overline{P}$ = mean absolute gas pressure within specimen

Px = outlet gas pressure (absolute)

ΔPs = pressure drop across specimen.

Similarly, the mean pressure within the flowmeter capillary is given by:-

$$Po = Px + \Delta Ps + \frac{\Delta P_F}{2} \qquad \text{Equation 4.3}$$

where Po = mean absolute gas pressure within flowmeter capillary

ΔP_F = pressure drop across flowmeter capillary.

Volume rate of flow (Q), through the flowmeter, is calculated according to the relationship obtained during calibration:-

$$Q = 0.007918\Delta P \qquad \text{Equation 4.1}$$

Hence, specimen mean gas pressure ($\overline{P}$) and specific mass flow ($\frac{QPo}{\Delta P}$) may be calculated for each set of experimental conditions. These variables, obtained from the data of Table 4.1 are summarised in Table 4.2.

Table 4.2 SPECIFIC FLOW AND MEAN GAS PRESSURE DATA FOR *Tsuga heterophylla* SAPWOOD EARLY WOOD

Specific mass flow $\frac{QPo}{\Delta Ps}$(cm^3 sec^{-1})	Specimen mean gas pressure	
	mm Hg	(dyn cm^{-2}) x 10^{-6}
12.4	1434.7	1.91
12.0	1304.4	1.73
11.2	1196.4	1.59
10.4	1074.3	1.43
9.66	970.2	1.29
8.86	830.0	1.10
7.85	690.6	0.92
6.89	527.7	0.70
6.27	411.9	0.55
6.03	383.5	0.51
4.92	245.3	0.33
4.12	146.4	0.19
3.37	74.1	0.10
3.34	67.1	0.09
2.62	23.9	0.03
2.17	4.8	0.006

Mathematical analysis of the experimental data was carried out by numerical techniques using a computer programme (see section 4.4 below). For convenience, therefore the calculation

of specific mass flow ($\frac{QP_o}{\Delta P_s}$) and mean gas pressure $\overline{P}$ from the experimental manometric data was included in this programme. A listing of the program instructions is contained in the end flap, and tables of specific mass flow and mean gas pressure for each specimen, are given in Appendix 1.

4.4 MATHEMATICAL ANALYSIS OF DATA

Gas flow through simple capillaries of porous media in the viscous/slip régime is described by the modified Kozeny equation:-

$$\frac{QP_o}{\Delta P} = \frac{A\varepsilon m^2 \overline{P}}{k_o \eta \ell e} + \frac{4A\varepsilon\delta_1 m\overline{V}}{3k_1 \ell e} \quad \text{(see section 1.4)} \qquad \text{Equation 1.16}$$

That is, the relationship between specific mass flow($\frac{QP_o}{\Delta P}$) and mean gas pressure ($\overline{P}$) is linear, so that

1 Slope = $\frac{A\varepsilon m^2}{k_o \eta \ell e}$

2 Intercept with the 'y' axis = $\frac{4A\varepsilon\delta_1 m\overline{V}}{3k_1 \ell e}$

All the terms of these mathematical constants with the exception of η and $\overline{V}$ (gas viscosity and molecular thermal velocity respectively) are geometric constants of the capillaries. Therefore, equation 1.16 may be rewritten:-

$$\frac{QP_o}{\Delta P} = \frac{K_v \overline{P}}{\eta} + K_s \overline{V} \qquad \text{Equation 4.4}$$

where K_v = viscous permeability constant
K_s = slip permeability constant

(K_v and K_s are true physical constants, depending only upon the geometry of the specimen.)

It is noted in section 1.5.3 that several workers have observed gas flow through softwood to deviate from the linear relationship described by equation 4.4

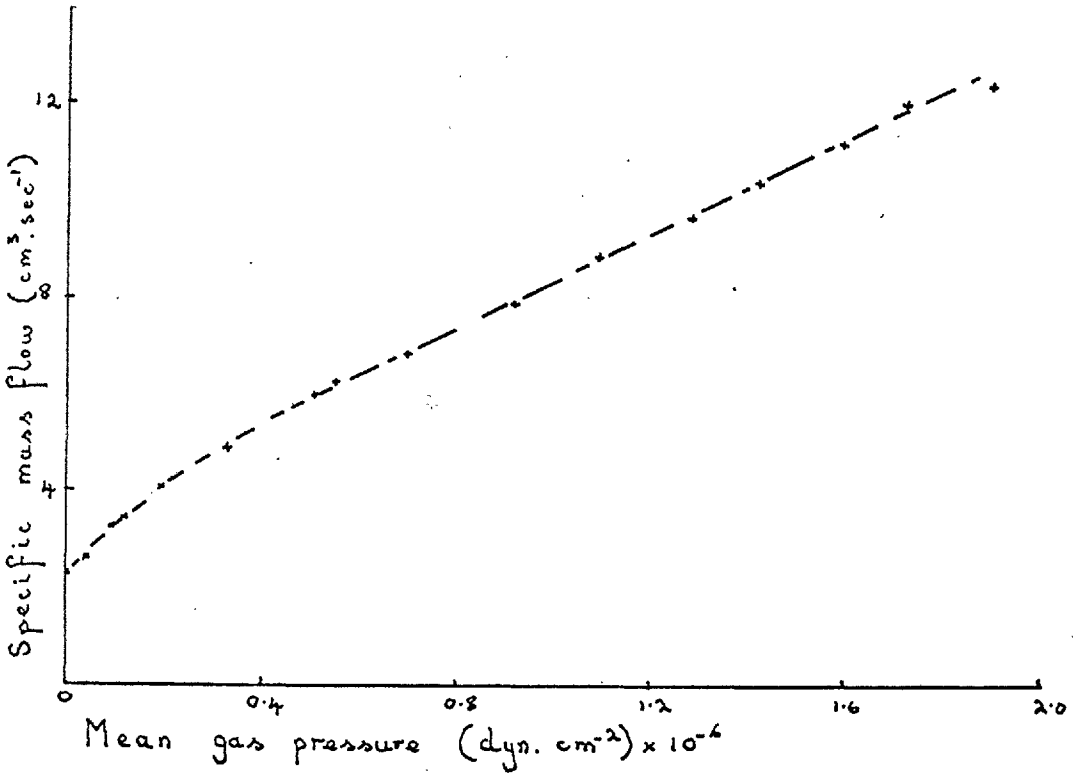


Fig 4.4 SPECIMEN THS.e. RELATIONSHIP BETWEEN SPECIFIC MASS FLOW AND MEAN GAS PRESSURE

Similar departure from linearity was observed in all the gas flow experiments carried out in this work (see, for example, Figure 4.4 which is a graph of the data of Table 4.2). It was shown by Barrer and Nicholson (1965) that this type of curve occurs as a result of flow taking place through serially interconnected capillaries or pores of alternately large and small diameter (Figure 4.5). In softwood it is believed that these pores correspond to tracheid lumina and bordered pits, respectively.

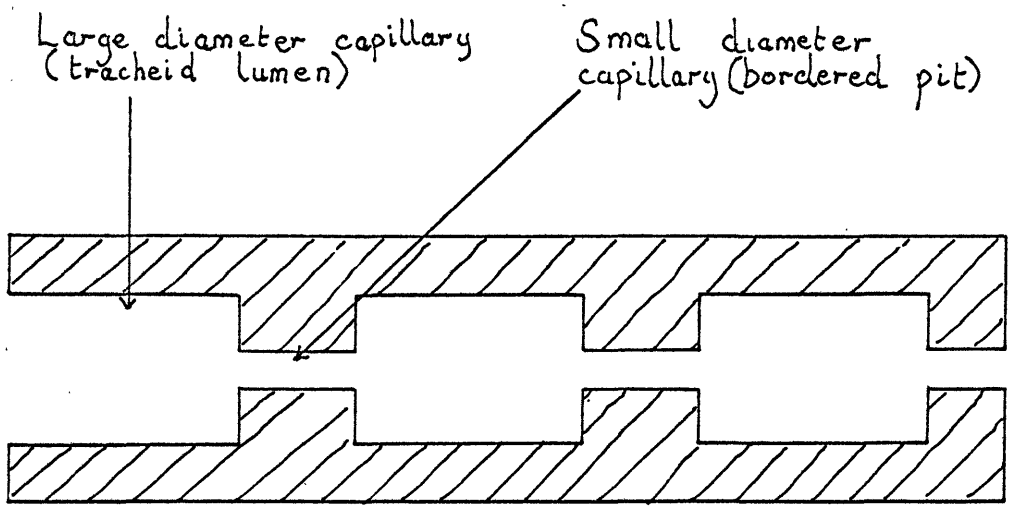


Fig 4.5 CAPILLARY SYSTEM LEADING TO NEGATIVELY DEVIATING, FLOW/PRESSURE RELATIONSHIP

By combining the equations describing flow through each type of pore or capillary, the relationship between mass flow and mean pressure, for the system, can be derived.

Let specific mass flow for capillary 1 be given by:-

$$\left(\frac{QP_o}{\Delta P}\right)_1 = \overline{Q}_1 = \frac{K_{v1}\overline{P}}{\eta} + K_{s1}\overline{V} \qquad \text{Equation 4.5}$$

and for capillary 2:-

$$\left(\frac{QP_o}{\Delta P}\right)_2 = \overline{Q}_2 = \frac{K_{v2}\overline{P}}{\eta} + K_{s_2}\overline{V} \qquad \text{Equation 4.6}$$

where $\overline{Q}_1$ and $\overline{Q}_2$ = specific mass flow for capillaries (1) and (2) respectively

Kv_1 and Kv_2 = viscous permeability constants for capillaries (1) and (2) respectively

Ks_1 and Ks_2 = slip permeability constants for capillaries (1) and (2) respectively

$\overline{P}$ = mean gas pressure

η = gas viscosity

$\overline{V}$ = gas molecular thermal velocity

Specific mass flow is a measure of gas conductance and it is a universal concept that for a serial array of conductors, the reciprocal of conductance is additive. That is:-

$$\frac{1}{\overline{Q}_R} = \frac{1}{\overline{Q}_1} + \frac{1}{\overline{Q}_2}$$

where $\overline{Q}_R$ = specific mass flow of the capillary pair.

For manipulative convenience let:-

$$\frac{K_{V1}}{\eta} = a_1$$

$$\frac{K_{V2}}{\eta} = a_2$$

$$K_{S1}\overline{V} = b_1$$

$$K_{S2}\overline{V} = b_2$$

Then:-
$$\frac{1}{\overline{Q}_R} = \frac{1}{a_1\overline{P} + b_1} + \frac{1}{a_2\overline{P} + b_2}$$

$$\text{or } \overline{Q}_R = \frac{(a_1\overline{P} + b_1)(a_2\overline{P} + b_2)}{(a_1\overline{P} + b_1) + (a_2\overline{P} + b_2)} \qquad \text{Equation 4.7}$$

Equation 4.7 may be expressed as three functions of a_1 a_2 b_1 b_2 and $\overline{P}$.

$$\overline{Q}_R = f_1(a_1,a_2,b_1,b_2)\overline{P} + f_2(a_1,a_2,b_1,b_2) - f\left[\frac{(a_1,a_2,b_1,b_2)}{\overline{P}}\right]$$

Equation 4.8

The first two terms on the right-hand side of equation 4.8 are linear in $\overline{P}$, the third term causes a non-linear effect which is markedly negative at low values of $\overline{P}$. It is assumed that longitudinal flow through softwood is mainly through alternately wide (tracheid lumina) and narrow (bordered pit) capillaries or pores (see section 1.5.3). The experimental flow data given in Appendix 1 (Tables 1 to 13), therefore, may be fitted to equation 4.8 by the use of a numerical approximation method (Newton-Raphson). From equation 4.8 estimates of a_1, b_1, a_2 and b_2 may be obtained. The values of 'a_1' and 'b_1' represent viscous and slip permeability constant respectively of the tracheid lumina; 'a_2' and 'b_2' being the corresponding constants for the bordered pit.

Equation 4.8 is solved using a computer program for each set of experimental data. The Newton-Raphson method used is given in Appendix 2, and a 'listing' of the instructions forming the computer program as well as a worked set of data is contained in the end flap. The constants a_1, a_2, b_1 and b_2 and the corresponding more general viscous and slip permeability constants (corrected for viscosity and molecular thermal velocity - see page above) K_{V1}, K_{V2}, K_{S1} and K_{S2}, are given below in Tables 4.3 and 4.4.

Table 4.3 GAS FLOW VISCOUS PERMEABILITY CONSTANTS

Specimen*	a_1 (cm^4 sec gm^{-1})10^5	a_2 (cm^4 sec gm^{-1})10^5	K_{V1} $cm^3 \times 10^8$	K_{V2} $cm^3 \times 10^8$
AGS.e	9.5	2.0	0.84	0.17
AGS.ℓ	13.0	4.5	1.11	0.39
AGH.e	5.1	1.1	0.45	0.10
AGH.ℓ	2.7	0.53	0.24	0.047
CDS	32.8	3.3	2.92	0.29
CDH	N O D E T E C T A B L E F L O W			
PAS.1	5.4	2.3	0.48	0.20
PAS.2	6.9	3.3	0.61	0.29
THS.e	6.4	0.49	0.57	0.044
THS.ℓ	4.0	1.2	0.36	0.11
THH.e	29.8	4.3	2.65	0.38
THH.ℓ	7.3	1.4	0.65	0.12
AAS	61.0	27.0	5.43	2.40
AAH	57.7	15.6	5.14	1.39

*Specimen labelling code is given below:-

First two letters define species:-

AG - *Abies grandis*

CD - *Cedrus deodara*

PA - *Picea abies*

TH - *Tsuga heterophylla*

AA - *Araucaria angustifolia*

Third letter identifies sapwood or heartwood specimen:-

S - sapwood

H - heartwood

Fourth letter (where present) identifies early wood or late wood specimen:-

e - early wood

ℓ - late wood

Where the fourth letter is omitted, the specimen is comprised of both sapwood and heartwood.

The numbers '1' and '2' appended to the *Picea abies*, 'PAS' specimens, simply identify each of two duplicate specimens of this species.

Table 4.4 SLIP FLOW PERMEABILITY CONSTANTS

Specimen	b_1 ($cm^3\ sec^{-1}$)	b_2 ($cm^3\ sec^{-1}$)	K_{S1} $(cm^2)10^8$	K_{S2} $(cm^2)10^8$
AGS.e	6.86	20.94	3.86	11.80
AGS.ℓ	8.20	37.32	4.62	21.02
AGH.e	4.56	9.96	2.57	5.61
AGH.ℓ	3.03	6.52	1.71	3.67
CDS	16.65	44.76	9.38	25.22
CDH	N O	D E T E C T A B L E	F L O W	
PAS.1	2.05	27.34	1.15	15.40
PAS.2	3.53	8.61	1.99	4.85
THS.e	3.71	4.64	2.09	2.61
THS.ℓ	3.35	12.00	1.89	6.76
THH.e	15.25	24.57	8.59	13.67
THH.ℓ	4.59	10.81	2.59	6.09
AAS	27.32	358.0	15.39	201.7
AAH	34.47	292.5	19.57	164.8

4.5 CALCULATION OF SPECIMEN VISCOUS PERMEABILITY CONSTANT FROM GAS FLOW DATA

As noted in section 4.4, the reciprocals of conductances in serial array, are additive. Viscous permeability constants measured by the gas flow technique in this work are equal to rate of flow of a gas of unit viscosity under the influence of unit pressure differential. They are, therefore, conductance values. Hence:-

$$\frac{1}{K_W} = \frac{1}{K_{V1}} + \frac{1}{K_{V2}}$$

$$\text{or } K_W = \frac{K_{V1} \cdot K_{V2}}{K_{V1} + K_{V2}} \qquad \text{Equation 4.9}$$

where K_W = viscous permeability constant for wood specimen

K_{V1} = viscous permeability constant of tracheid lumena

K_{V2} = viscous permeability constant of bordered pits

Values of viscous permeability constant (K_W) for each specimen tested, calculated from the data of Table 4.3 according to equation 4.9, are listed in Table 4.5.

Table 4.5 VISCOUS PERMEABILITY CONSTANTS ESTIMATED FROM GAS FLOW DATA

Specimen	Viscous Permeability Constant $K_W(cm^3) \times 10^8$
AGS.e	0.14
AGS.ℓ	0.29
AGH.e	0.08
AGH.ℓ	0.04
CDS	0.26
CDH	NIL
PAS.1	0.14
PAS.2	0.20
THS.e	0.04
THS.ℓ	0.08
THH.e	0.33
THH.ℓ	0.10
AAS	1.66
AAH	1.09

As stated in section 1.7, it is the objective in this work to relate gas and liquid flow data, and to investigate the effect of various imposed forces upon the permeability of specimens.

Specimens were of longitudinal length about 10 mm (within the range where permeability decreases as length is increased - see section 1.5.2). Specimens varied from one another considerably in cross-sectional area (from about 5 to 50 mm^2). Because of these two factors, the permeability constants cited in Table 4.5 are no guide to the relative permeabilities representative of the species tested. They are listed for comparison with liquid flow data measured for the same specimens, as described in a later section (section 5.2).

4.6 PORE SIZE ESTIMATION FROM GAS PERMEABILITY DATA

In Tables 4.3 and 4.4, 'viscous' (K_V) and 'slip' (K_S) permeability constants are listed for each specimen tested. It is shown (section 4.4) that 'K_V' and 'K_S' depend only upon the pore geometry of the specimens, and are defined as follows:-

$$K_V = \frac{A\varepsilon m^2}{k_o \ell e} \qquad \text{Equation 4.10}$$

$$K_S = \frac{4A\varepsilon\delta_1 m}{3k_1 \ell e} \qquad \text{Equation 4.11}$$

where A = specimen cross-sectional area normal to flow
ε = specimen porosity
m = mean hydraulic radius of flow controlling pore
ℓe = effective pore length
k_o = shape factor for viscous flow
δ_1 = factor dependent upon fraction of molecules undergoing diffuse reflection at pore wall
k_1 = shape factor for slip flow.

Dividing equation 4.10 by equation 4.11 gives an expression for 'm' the mean hydraulic radius of the flow controlling pore:-

$$m = \frac{K_V}{K_S} \cdot \frac{4k_o\delta_1}{3k_1} \qquad \text{Equation 4.12}$$

Values of the shape factor 'k_o', for pores of various shape, are given by Carman (1956). The factor δ_1, dependent upon the proportion of molecules undergoing diffuse reflection at the pore wall varies with gas and with wall roughness, from about 0.59 to 1 (Carman, 1956). For the flow of all gases through pores with high surface roughness (eg machined brass; silver oxide) 'δ_1' has a value of 0.59. Electron microscopy has shown the cell wall of wood to be extremely rough at a 'micro' level, and throughout this work a value of 0.59 is assumed for 'δ_1'.

Tracheid lumen cross-section is approximately rectangular, the ratio of side lengths varying from about 1:1 to about 3:1. Tracheid length is about 100 - 200 x lumen diameter. Values of 'k_o' appropriate to this tracheid lumen geometry (from Carman, 1956), are listed in Table 4.6.

Table 4.6 SHAPE FACTORS FOR VISCOUS/SLIP FLOW EQUATIONS (Pore cross-section = rectangular of sides 'a' and 'b')

Ratio $\frac{a}{b}$	k_o
1	1.78
2	1.94
10	2.65

From Table 4.6 it seems that the best value for k_o lies between 1.78 and about 2. A single average value (k_o = 1.89) is assumed in pore size estimation, leading to maximum error from this source of ± 6 per cent. In the 'slip' flow region k_1 = 1 for all shapes (Millikan, 1923).

Fitting these values to equation 4.12:-

$$m = 1.49\frac{K_{V1}}{K_{S1}} \qquad \text{Equation 4.13}$$

where K_{V1} = viscous permeability constant for tracheid lumen
K_{S1} = slip permeability constant for tracheid lumen

Geometric parameters for the flow controlling pore associated with the bordered pit are less easy to define.

A diagrammatic representation of a bordered pit is shown in Figure 1.3 (section 1.2). Reference to the Figure suggests that flow control may be due to one of three structural features (or to combinations of them):-

1 the margo pores
2 the complex annulus formed by the pit cavity and the torus

3 the 'slit' between torus and border in a partially aspirated pit.

Values of 'k_o' (from Carman, 1956) appropriate to these geometries are listed below in Table 4.7.

Table 4.7 SHAPE FACTOR 'k_o' FOR GAS FLOW THROUGH BORDERED PITS

	k_o
Margo pore	∿2.5
Pit chamber	2.0-3.0
Torus-border 'slit'	∿3.0

From the Table it is seen that a value of 2.5 for k_o is a reasonable approximation for the range of shapes encountered in pit structure. As for 'tracheid lumen' flow (above), $k_1 = 1$ for all shapes.

Fitting these values to equation 4.12 an expression for hydraulic radius 'm' is obtained:-

$$m = 1.97\frac{K_{V2}}{K_{S2}} \qquad \text{Equation 4.14}$$

K_{V2} = viscous permeability constant of bordered pit
K_{S2} = slip permeability constant of bordered pit

Estimated values of mean hydraulic radius for tracheid lumina are calculated from the data of Tables 4.3 and 4.4, using equation 4.13. Corresponding estimates of bordered pit pore, mean hydraulic radius are calculated using equation 4.14. These values, together with length of side of equivalent 'square cross-section' pores (calculated according to equation 1.13:-

$$m = \frac{\text{pore volume}}{\text{pore surface area}})$$

are listed in Table 4.8.

Table 4.8 PORE DIMENSIONS ESTIMATED FROM GAS FLOW DATA

Specimen	Tracheid lumen		Bordered pit	
	m(micron)	x(micron)*	m(micron)	x(micron)*
AGS.1	3.2	12.8	0.28	1.12
AGS.2	3.6	14.4	0.36	1.44
AGH.1	2.6	10.4	0.35	1.40
AGH.2	2.1	8.4	0.25	1.00
CDS.1	4.6	20.4	0.23	0.92
CDH.1	-			
PAS.1	6.2	24.3	0.25	1.00
PAS.2	4.6	18.4	1.18	4.72
THS.1	4.1	16.4	0.33	1.32
THS.2	2.8	11.2	0.32	1.28
THH.1	4.6	18.4	0.55	2.20
THH.2	3.7	14.8	0.39	1.56
AAS.1	5.3	21.2	0.23	0.92
AAH.1	3.9	15.6	0.17	0.68

* * 'x' = side length of square cross-section 'equivalent pore'

The Poiseuille equation and equations derived from it (eg the modified Kozeny equation) apply strictly only to long capillaries or pores (see section 1.3.3), ie where pore length >> pore radius. Flow through short tubes is described more precisely by the Hanks and Weissberg equation (section 1.3.3 equation 1.9):-

$$W = W_s + \frac{\beta r}{\lambda} \qquad \text{Equation 1.9}$$

If the major flow resistance of the bordered pit is centred in the pit membrane pores, pore length is small relative to pore radius (electron microscopic evidence suggests that membrane pore radius is of the order of 0.01 to about 0.2 micron - section 3.3.6, Table 3.1), whilst margo strand thickness is about 0.1 micron (see Figures 3.1 to 3.16 - section 3.3). Thus length-to-radius ratio may be less than unity.

The Hanks and Weissberg equation is semi-empirical, and was derived from work carried out with capillaries of circular cross-section. The equation cannot be applied in an absolute sense to complex-shaped pores. It seems reasonable, however, to use the equation to measure the relative effect of length-to-radius ratio. This effect is investigated by fitting a number of sets of experimental flow data to equation 1.9 and assuming a few values for pore length/pore radius in the range 0.3 (the smallest value investigated by Hanks and Weissberg) to 100. The relationship between hydraulic radius (m) and the values 'K_{V2}' and 'K_{S2}' (Tables 4.3 and 4.4) derived from equation 1.9, for various length-to-radius ratios are listed below (Table 4.9).

Table 4.9 EFFECT OF PORE LENGTH/RADIUS RATIO ON ESTIMATED HYDRAULIC RADIUS 'm'

Length/radius	Estimated hydraulic radius (m)
100	$2.11\ K_{V2}/K_{S2}$
10	$1.98\ K_{V2}/K_{S2}$
1	$1.43\ K_{V2}/K_{S2}$
0.3	$1.22\ K_{V2}/K_{S2}$

As pointed out above, the data of Table 4.9 apply strictly to pores of circular cross-section. However, they provide a guide to the magnitude of the effect of length/radius ratio upon the size estimate of more complex shaped pores. Thus data of the Table suggest that the values of bordered pit pore hydraulic radii cited in Table 4.8 (based upon a 'long capillary' model) may be significantly overestimated (by about 70 per cent) if the main resistance to flow is centred in pores of length/radius is equal to 0.3.

4.7 LIMITATIONS OF THE GAS FLOW TECHNIQUE

4.7.1 UNCERTAINTY ASSOCIATED WITH THE NUMERICAL ANALYSIS

The precision of the estimates of softwood viscous and slip permeability constants and of pore size, depends upon how accurately the constants K_{V1}, K_{V2}, K_{S1} and K_{S2} (see section 4.4) can be determined. It has been shown by Smith and Banks (1971) that slight (undetectable) experimental error in the specific mass flow/mean pressure relationship can lead to very significant error in two of the four constants, determined by numerical analysis. These workers showed that the experimental curve is dependent mainly upon the viscous permeability constant of the smaller pore (K_{V2}) and the slip constant of the large pore (K_{S1}). In the example cited by them, it is shown that up to about 30 per cent reduction in the viscous permeability constant of the large pore (K_{V1}) and increase of similar magnitude in the slip constant (K_{S2}) of the small pore, leads to no detectable change in the shape of the specific mass flow/mean pressure relationship, over the pressure range investigated (0 to 2 bar absolute). Specimen viscous permeability constant is calculated according to equation 4.9 (see section 4.5):-

$$K_W = \frac{K_{V1} \cdot K_{V2}}{K_{V1} + K_{V2}} \qquad \text{Equation 4.9}$$

From Table 4.3 it can be seen that K_{V1} is usually at least three times greater than K_{V2}. Assuming that K_{V2} is known precisely, it can easily be shown by example (using equation 4.9) that error of about 30 per cent in K_{V1} will usually lead to not more than about 6 per cent error in K_W. Even when K_{V1} is about twice K_{V2}, 30 per cent error in K_{V1} leads to only about 10 per cent error in K_W. It seems likely, therefore, that quite a large error in the estimate of K_{V1} leads to relatively small error (not more than about ± 5 per cent) in the estimate of specimen viscous permeability constant K_W.

Pore size estimation from gas flow data (section 4.6) is dependent upon the ratio of viscous to slip permeability constants (see equations 4.13 and 4.14).

Tracheid lumen:-

$$m = 1.49\frac{K_{V1}}{K_{S1}} \qquad \text{Equation 4.13}$$

Bordered pit pore:-

$$m = 1.97\frac{K_{V2}}{K_{S2}} \qquad \text{Equation 4.14}$$

Possible error of 30 per cent (± 15 per cent) in both K_{V1} and K_{S2} may, therefore, lead to error in the estimate of tracheid lumen hydraulic radius of ± 15 per cent, and in the estimate of bordered pit pore size of -13 to +18 per cent.

It must be stressed that errors of the magnitude discussed may arise as a result of undetectable experimental error, in the absence of any systematic error in parameter control and instrument calibration.

4.7.2 OVERSIMPLIFICATION OF THE FLOW PATH MODEL

Early workers measuring gas flow permeability of softwood, assumed that the material behaved as a simple capillary porous material (ie specific mass flow rate linearly related to mean pressure - see section 1.5.2). However, it was shown first by Smith (1964) that this relationship is not linear for all values of $\overline{P}$, but is visibly curved at pressures below about 1 bar. As a result of this work, the simple capillary model, assumed by the early workers, was improved by Petty (1970) and Smith and Banks (1971). These workers assumed that the curved relationship arose as the result of flow through alternately wide and narrow capillaries. (The algebra showing the logic leading to this assumption is given in section 4.4.) Consideration of softwood anatomy,

however, suggests that the above refinement is inadequate. A possible single flow path through a short length (∿ 5 mm) of softwood is shown diagrammatically in Figure 4.6 below.

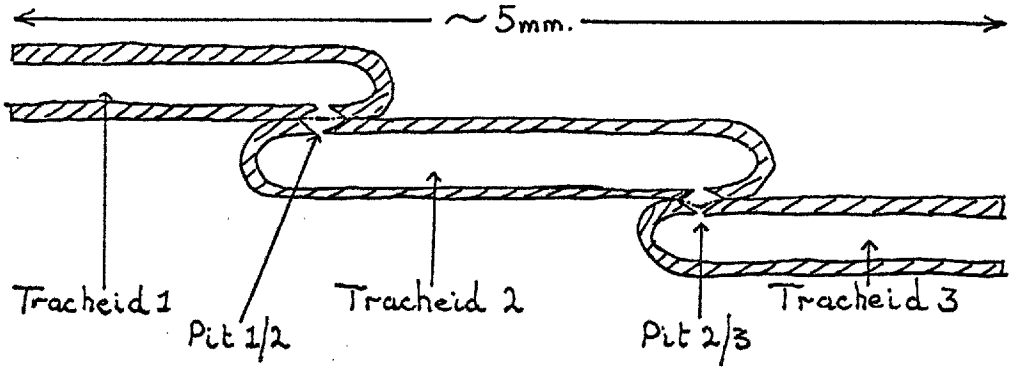


Fig 4.6 POSSIBLE FLOW PATH THROUGH A SERIES OF TRACHEIDS

In the flow path shown, let the following assumptions be made:-

1 The cross-sections of tracheids 1, 2 and 3 are identical
2 Pit 1/2 is unaspirated
3 Pit 2/3 is partially aspirated
4 All other pits (not shown) are totally sealed.

A bordered pit is shown in cross-section in Figure 4.7

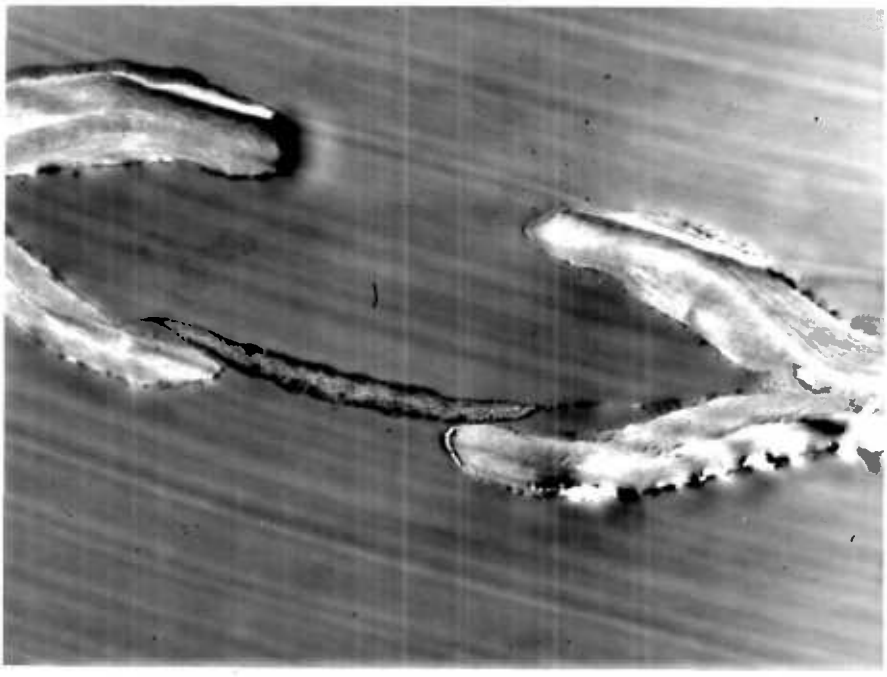


Fig 4.7 CROSS-SECTION OF BORDERED PIT. ELECTRON MICROGRAPH, MAG x9000

It is reasonable to suppose that the unaspirated pit is comprised of two pore types:-

1 the complex annulus (seen as a slit in cross-section; Figure 4.7) between torus and border
2 the parallel array of margo interfibrillar spaces.

The pore 'diameter' of the first pore type may be taken as the width of the torus-border gap (1-5μ). That of the second type of pore (margo interfibrillar space) is of the order of 0.01 to 0.1μ (see Table 3.1; section 3.3.7). During aspiration, small gaps between torus and border may remain open in a proportion of pits (see, for example, Comstock 1968a). The width of these gaps may be continuously variable between very small values (<0.1 micron) and values approaching the gap size in unaspirated pits (say about 1 micron).

Thus, the flow path illustrated in Figure 4.6 may be made up of four distinct serially interconnected pore types:-

1 tracheid lumina
2 the torus-border annulus in the unaspirated pit (1/2)
3 margo pores in the unaspirated pit (1/2)
4 'residual' torus-border pores in the partially aspirated pit (2/3).

It is impossible to predict the number of pore types in any real softwood flow path. This will depend upon the variation in pit geometry; variability in efficiency of pit aspiration, and with flow path length (and hence, number of cell wall crossings).

Tracheid length is about 2-5 mm (section 1.2) and adjacent tracheids overlap over about one-third of their length. Hence, flow paths in the specimens used in this work (length $\sim$ 10 mm) are made up of about 3 to 6 serially interconnected tracheids. Longitudinal flow, therefore, involves passage through 2 to 5 bordered pits.

As shown above, a single flow path in such a system is likely to be made up of at least 3 or 4, and possibly more, pore types.

Consider the general case, where a single flow path contains 'n' types of pore:-

Let the specific mass flow/mean pressure relationship for pore type 1 be given by:-

$$Q_1 = \alpha_1 \overline{P} + \beta_1,$$

for pore type 2, by:-

$$Q_2 = \alpha_2 \overline{P} + \beta_2,$$

and for pore type 'n', by:-

$$Q_n = \alpha_n \overline{P} + \beta_n$$

where $Q_1, Q_2 \ldots Q_n$ = specific mass flow values for pores '1', '2' .... 'n'

$\alpha_1, \alpha_2 \ldots \alpha_n$ = corresponding viscous permeability constants

$\beta_1, \beta_2 \ldots \beta_n$ = corresponding slip permeability constants.

Then, since the reciprocal of conductance in series is additive:-

$$\frac{1}{Q_R} = \frac{1}{Q_1} + \frac{1}{Q_2} \ldots + \frac{1}{Q_n} \qquad \text{Equation 4.15}$$

where Q_R = specific mass flow of the system of 'n' serially interconnected pores.

$$\text{or:-} \quad \frac{1}{Q_R} = \frac{1}{\alpha_1\overline{P} + \beta_1} + \frac{1}{\alpha_2\overline{P} + \beta_2} \ldots \frac{1}{\alpha_n\overline{P} + \beta_n}$$

which upon expansion gives an expression of the type:-

$$Q_R = f_1(\overline{P}) + Z f_2\left[\frac{(\overline{P}^{n-2} + \overline{P}^{n-3} \ldots + \overline{P})}{(\overline{P}^{n-1} + \overline{P}^{n-2} \ldots + \overline{P})}\right] \qquad \text{Equation 4.16}$$

Where Z is a numerical constant.

It will be noted that equation 4.16 is similar in form to equation 4.8, relating specific mass flow to mean pressure for gas flow through serially connected capillary pairs. Both equations tend to become linear in $\overline{P}$ at high pressures, with significant negative deviation from linearity at lower pressures. Thus, it is clear that the curvi-linear relationships between specific mass flow and mean gas pressure, obtained experimentally (Tables 1 to 13 Appendix 1) may arise as a result of gas transport along flow paths comprised of 'n' pore types, rather than of the assumed two pore system.

4.7.3 EFFECT OF FLOW PATH MODEL OVERSIMPLIFICATION ON ESTIMATION OF VISCOUS PERMEABILITY CONSTANT

Calculation of viscous permeability constants for each of the specimens tested (sections 4.4 and 4.5) is based upon the assumption that individual flow paths are comprised of two, and only two, types of pore. It is shown above,

however (section 4.7.2), that this assumption may be invalid. In this section the type and magnitude of any error resulting from the assumed simplification, is investigated.

The investigation is purely theoretical, being based on a physical model system of 3 serially connected pore types. The geometry of the pores is selected to give a reasonable approximation to pore dimensions of tracheid lumen, pit chamber and pit margo pores (Table 4.10).

Table 4.10 ASSUMED PORE GEOMETRY FOR MODEL SYSTEM

	Pore radius (micron)	Pore length (micron)
Tracheid lumen	5	3000
Pit chamber	0.5	5.0
Pit margo pore*	0.05	0.1

*It is assumed that each pit margo contains 100 pores

Let the specific mass flow $(\frac{QP_o}{\Delta P})$ for the tracheid lumen be given by:-

$$(\frac{QP_o}{\Delta P})_x = \overline{Q}_x = \alpha_x \overline{P} + \beta_x$$

For the pit chamber by:-

$$\overline{Q}_y = \alpha_y \overline{P} + \beta_y$$

and for the margo pores by:-

$$\overline{Q}_z = \alpha_z \overline{P} + \beta_z$$

where Q = volume rate of flow measured at pressure 'P_o'

ΔP = pressure difference causing flow

α_x = viscous permeability constant of tracheid lumen

β_x = slip permeability constant of tracheid lumen

$\overline{P}$ = mean pressure of gas within specimen

α_y = viscous permeability constant for bordered pit chamber

β_y = slip permeability constant for bordered pit chamber

α_z = viscous permeability constant for margo pore

β_z = slip permeability constant for margo pore

$\overline{Q}_x$, $\overline{Q}_y$ & $\overline{Q}_z$ = specific mass flow for lumen, pit chamber and margo spores respectively.

The values of α_x, β_x, α_y, β_y, α_z and β_z may be evaluated for each of the pores described by fitting the data of Table 4.10 to the Hanks and Weissberg equation (equation 1.9, section 1.3). These values are listed below:-

$$\alpha_x = 9.2 \times 10^{-10} \ (cm^2 \ sec \ gm^{-1})$$
$$\alpha_y = 0.49 \times 10^{-10} \ (cm^2 \ sec \ gm^{-1})$$
$$\alpha_z^* = 0.17 \times 10^{-10} \ (cm^2 \ sec \ gm^{-1})$$

$$\beta_x = 1.21 \times 10^{-4} \ (cm^3 \ sec^{-1})$$
$$\beta_y = 0.61 \times 10^{-4} \ (cm^3 \ sec^{-1})$$
$$\beta_z^* = 1.8 \times 10^{-4} \ (cm^3 \ sec^{-1})$$

*(NB it is assumed that the margo is comprised of '100' pores)

It is believed that the geometric constants for the tracheid lumen (Table 4.10) are a reasonable approximation to the true values for tracheids in the specimens examined experimentally. However, the geometric constants of the pit chamber and margo pores can be approximated with much less certainty. The relationship between specific mass flow and mean pressure is calculated, therefore, for several numerical examples. In each of these examples 'α_x' and 'α_y' are held constant, α_y, β_y, α_z and β_z being varied over a five- to ten-fold range. The various values of viscous and slip permeability constants used in the worked examples are listed in Table 4.11.

Table 4.11 VISCOUS AND SLIP PERMEABILITY CONSTANTS FOR MODEL FLOW PATH SYSTEM

Example	α_x $(cm^2\ sec\ gm^{-1})10^{10}$	β_x $(cm^3\ sec^{-1})10^4$	α_y $(cm^2\ sec\ gm^{-1})10^{10}$	β_y $(cm^3\ sec^{-1})10^4$	α_z $(cm^2\ sec\ gm^{-1})10^{10}$	β_z $(cm^3\ sec^{-1})10^4$
1	9.0	1.20	0.50	0.60	0.17	1.8
2	9.2	1.21	1.0	1.0	0.17	1.8
3	9.2	1.21	3.0	2.0	0.17	1.8
4	9.2	1.21	0.49	0.61	0.05	1.0
5	9.2	1.21	1.0	1.0	0.40	3.0
6	9.2	1.21	3.0	2.0	1.00	5.0

For each example the relationship between specific mass flow and mean pressure is evaluated according to equation 4.15:-

$$\frac{1}{Q_R} = \frac{1}{Q_1} + \frac{1}{Q_2} \ldots\ldots + \frac{1}{Q_n}$$ Equation 4.15 (see above)

where Q_R = specific mass flow of serially connected system of pores, Q_1, Q_2 .... Q_n

Q_1, Q_2 .... Q_n = specific mass flow values of each individual pore.

For the model 'tracheid lumen/pit chamber/margo pore' system described, equation 4.15 becomes:-

$$\frac{1}{Q_R} = \frac{1}{\overline{Q}_x} + \frac{1}{\overline{Q}_y} + \frac{1}{\overline{Q}_z}$$

$$\text{or } \frac{1}{Q_R} = \frac{1}{\alpha_x \overline{P} + \beta_x} + \frac{1}{\alpha_y \overline{P} + \beta_y} + \frac{1}{\alpha_z \overline{P} + \beta_z}$$ Equation 4.17

By fitting the data of Table 4.11 to equation 4.17 specific mass flow/mean pressure relationships are evaluated over a mean pressure range from 0 to ∿2 bar absolute, for each example listed in the Table. These relationships are given below in Table 4.12.

Table 4.12 RELATIONSHIP BETWEEN SPECIFIC MASS FLOW AND MEAN PRESSURE, FOR 3 PORE TYPE MODEL FLOW PATH SYSTEM.

$\overline{P}$ (dyn cm^2 x 10^{-6})	Specific mass flow (cm^3 sec^{-1} x 10^5)					
	Example 1	2	3	4	5	6
0.0	3.27	4.20	5.31	2.89	4.63	6.55
0.2	4.33	5.86	7.95	3.66	8.27	11.05
0.4	5.02	6.88	9.51	4.12	9.46	14.24
0.6	5.59	7.70	10.67	4.49	10.51	16.94
0.8	6.11	8.41	11.62	4.82	11.49	19.37
1.0	6.60	9.06	12.44	5.11	12.42	21.61
1.2	7.06	9.65	13.17	5.38	13.32	23.73
1.4	7.50	10.22	13.83	5.63	14.18	25.74
1.6	7.93	10.75	14.44	5.86	15.11	27.67
1.8	8.34	11.26	15.00	6.08	15.82	29.54
2.0	8.74	11.74	15.55	6.29	16.61	31.36
2.2	9.13	12.21	16.05	6.49	17.39	33.14

The curvilinear relationships described by the data of Table 4.12 are analysed into the two linear relationships which, upon serial combination, best fit the data, using the technique described in section 4.4 and Appendix 2. The apparent viscous flow constants 'a_1' and 'a_2' and slip flow constants 'b_1' and 'b_2' of the two lines extracted from the curved relationships described by the data of Table 4.12 are listed below in Table 4.13.

Table 4.13 APPARENT PERMEABILITY CONSTANTS FOR 3 PORE MODEL FLOW PATH SYSTEM

Example	Viscous permeability constant (cm^2 sec gm^{-1}) x 10^{10}		Slip permeability constant (cm^3 sec^{-1}) x 10^4	
	'a_1'	'a_2'	'b_1'	'b_2'
1	2.85	0.20	0.71	0.61
2	3.39	0.23	0.77	0.93
3	4.39	0.22	0.86	1.41
4	2.39	0.098	0.66	0.52
5	19.57	0.41	0.95	0.90
6	4.81	0.99	0.89	2.50

To check the quality of the fit between the data of Table 4.13 and the curved relationship represented by the data of Table 4.12, the following procedure is adopted.

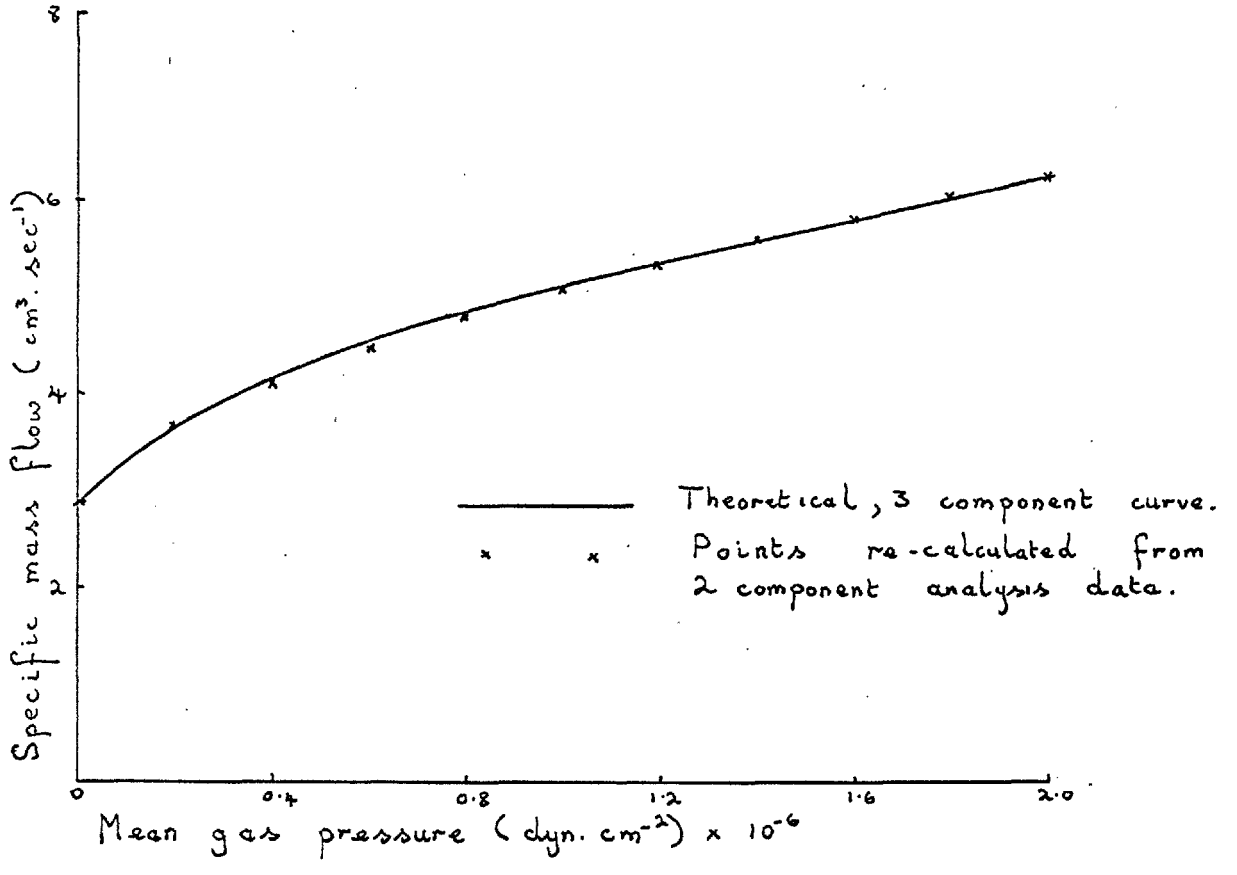


Fig 4.8 EXAMPLE 4, "GOODNESS OF FIT" BETWEEN THEORETICAL 3 COMPONENT CURVE AND 2 COMPONENT ANALYSIS

Table 4.11.

Values of viscous permeability constant estimated from the numerical analysis, based on the assumption that flow paths contain only two pore types, are calculated from the data of Table 4.13, using an equation analogous to equation 4.9.

$$\bar{A} = \frac{a_1 . a_2}{a_1 + a_2}$$

where $\bar{A}$ = estimated viscous permeability constant for the model

a_1 = viscous permeability constant of hypothetical pore 'type 1'

a_2 = viscous permeability constant of hypothetical pore 'type 2'

The true and estimated viscous permeability constants $\bar{\alpha}$ and $\bar{A}$ respectively are compared below (Table 4.14).

Table 4.14 COMPARISON OF TRUE ($\bar{\alpha}$) AND ESTIMATED ($\bar{A}$) VISCOUS PERMEABILITY CONSTANTS FOR 'THREE PORE TYPE' MODEL

Example	$\bar{\alpha}$ (cm^2 sec gm^{-1}) x 10^{10}	$\bar{A}$ (cm^2 sec gm^{-1}) x 10^{10}	Error* %
1	0.125	0.187	+ 49.6
2	0.143	0.215	+ 50.3
3	0.158	0.209	+ 32.3
4	0.045	0.094	+108.4
5	0.277	0.406	+ 46.6
6	0.693	0.820	+ 18.3

(*The '+' sign indicates that the estimated value is greater than theoretical)

For the examples worked it can be seen that use of the over-simplified flow path model always leads to a significantly high estimate of viscous permeability constant. An attempt was made to derive a general analytical proof for this,

but without success. Nevertheless, from the numerical examples worked, it seems likely that the procedure is strongly biased to give positive error. For certain geometries the magnitude of this error can be very large (over 100 per cent in worked example number 4).

From equation 4.16, it can be seen that as mean pressure $\overline{P}$ is increased, the term causing negative deviation becomes less significant, and the mass flow/mean pressure relationship becomes more truly linear. When deviation from the linear relationship becomes insignificant the slope of the line, '$f_1(\overline{P})$', is proportional to the true viscous permeability constant of the system. It seems likely, therefore, that as the mean pressure range is increased the estimated permeability constant ($\overline{A}$) will fall closer to the true value ($\overline{\alpha}$). This effect was investigated numerically for examples 3 and 4 (Table 4.11).

Using the data of Table 4.11, specific mass flow was calculated using equation 4.18, for a number of mean pressure values over the range 0 to 32 x 10^6 dyn cm^{-2} (about 0 to 32 bar). Over several increments of the full mean pressure range investigated, viscous permeability constant was estimated using the technique described above. These data, together with the true viscous permeability constants ($\overline{\alpha}$), calculated for the system, are summarised in Tables 4.15 and 4.16.

Table 4.15 COMPARISON OF TRUE ($\overline{\alpha}$) AND ESTIMATED ($\overline{A}$) VISCOUS PERMEABILITY CONSTANTS FOR EXAMPLE '3'

Mean Pressure Range (dyn cm^{-2})	Viscous permeability constant (cm^2 sec gm^{-1}) x 10^{10}		Error %
	True value $\overline{\alpha}$	Estimated value $\overline{A}$	
0-2	0.158	0.209	+32.3
0-4	0.158	0.18	+13.9
0-8	0.158	0.16	< 2
0-16	0.158	0.16	< 2
0-32	0.158	0.16	< 2

Table 4.16 COMPARISON OF TRUE ($\bar{\alpha}$) AND ESTIMATED ($\bar{A}$) VISCOUS PERMEABILITY CONSTANTS FOR EXAMPLE '4'

Mean Pressure Range ($dyn\ cm^{-2}$)	Viscous permeability constant ($cm^2\ sec\ gm^{-1}$) x 10^{10}		Error %
	True value $\bar{\alpha}$	Estimated value $\bar{A}$	
0-2	0.045	0.094	+108
0-4	0.045	0.070	+ 55.6
0-8	0.045	0.053	+ 17.8
0-16	0.045	0.047	+ 4.4
0-32	0.045	0.046	+ 2.2

From the Tables, it is clear that the magnitude of error becomes progressively less as the mean pressure range is extended. In the examples tested there is inherent error of more than 5 per cent at mean pressures up to about 5 bar for example '3', and to pressures approaching 16 bar for example '4'.

It is recognised that the pore structure of softwood is further complicated due to variability in the size of pores connected parallel, in any specimen. For example, early wood cells are significantly wider than those of late wood, whilst within early wood or late wood separately, there is smaller but still significant variation in tracheid width (Figure 4.9).

Numerical examples, taking into account variability in width of lumen and pits in parallel array have been worked. Over the range tested (about 5 to 10 fold variation in both viscous and slip permeability constants), the simplified model (ie ignoring variation in size of pores connected in parallel) was found to lead to less than 2 per cent error in estimation of permeability constant.

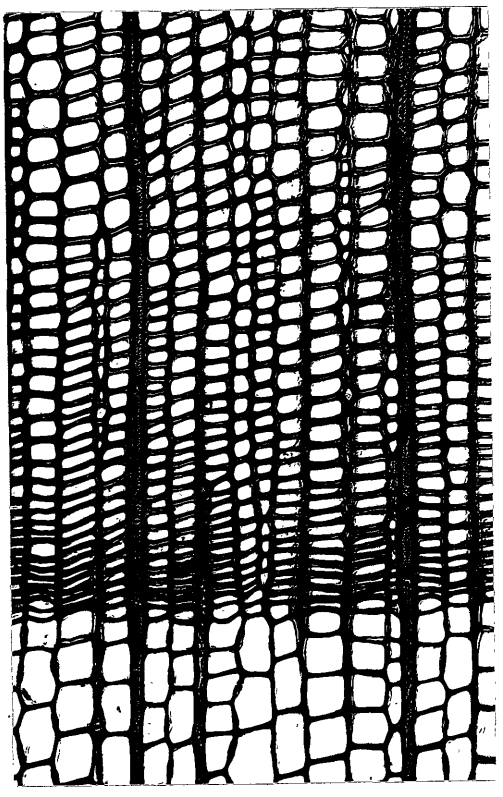


Fig 4.9 TRANSVERSE SECTION OF SOFTWOOD SHOWING VARIATION IN LINEAR CROSS-SECTION OF EARLY WOOD AND LATE WOOD CELLS

4.7.4 EFFECT OF FLOW PATH MODEL OVERSIMPLIFICATION ON PORE SIZE ESTIMATION

In section 4.6, it is shown how gas flow data are used to estimate flow controlling pore size. It is shown that the method is based on comparison of viscous and slip permeability constants. Equations are derived (equations 4.13 and 4.14) to provide an estimate of tracheid lumen and bordered pit pore sizes respectively:-

Tracheid lumen -

$$m = \frac{K_{Vl}}{K_{Sl}}.1.49 \qquad \text{Equation 4.13}$$

where m = lumen, mean hydraulic radius

K_{Vl} = lumen, viscous permeability constant

K_{Sl} = lumen, slip permeability constant

Bordered pit -

$$m = \frac{K_{V2}}{K_{S2}}.1.97 \qquad \text{Equation 4.14}$$

where m = 'bordered pit pore' mean hydraulic radius

K_{V2} = bordered pit pore, viscous permeability constant

K_{S2} = bordered pit pore, slip permeability constant.

These equations are used to estimate pore sizes for the model systems from the data of Table 4.13.

Pore sizes estimated from these data are compared with those calculated from the ~~true~~ theoretical permeability constants for each pore in the model system (Table 4.11). These data, based on a range of mean pressure extending from 0 to 2 bar, are tabulated below (Table 4.17).

Table 4.17 PORE SIZES CALCULATED FROM THEORETICAL AND ESTIMATED PERMEABILITY CONSTANTS

Example	Hydraulic radius (micron)				
	Tracheid lumen		Bordered pit		
	Theoretical	Estimated	Theoretical		Estimated
			1	2	
1	2.03	0.94	0.25	0.030	0.10
2	2.03	1.04	0.31	0.030	0.076
3	2.03	1.21	0.47	0.030	0.050
4	2.03	0.86	0.25	0.016	0.059
5	2.03	4.81	0.31	0.042	0.14
6	2.03	1.28	0.47	0.063	0.12

From the data of Table 4.17 it can be clearly seen that the pore sizes estimated do not closely match the ~~true~~ theoretical pore dimensions. In the system examined, the error in estimate of lumen radius varies from about -50 per cent to more than +200 per cent. These estimates must be regarded, therefore, as of 'order of magnitude' accuracy only. In the case of the

bordered pit pore, it appears that the single value estimated generally lies between the radii of the two serially connected pores constituting the model.

From an examination of data for a wider range of mean pressure (up to 32 bar), it is observed that the estimated ratio of viscous to slip permeability constant tends to decrease as the mean pressure range is extended. Pore size estimate entirely depends upon this ratio, and hence is strongly affected by the range of mean pressure examined. The effect for a specific example (numerical example 4) is illustrated in Table 4.18 below.

Table 4.18 EFFECT OF MEAN PRESSURE RANGE ON PORE SIZE ESTIMATE
(data from numerical example 4)

Mean Pressure Range (dyn cm^{-2}) x 10^6	Estimated hydraulic radius (micron)	
	Tracheid lumen	Bordered pit
0-2	0.86	0.059
0-4	0.54	0.036
0-8	0.38	0.022
0-16	0.34	0.018
0-32	0.29	0.017

For pores of varying size connected in parallel (in the absence of the error described above), pore radius estimated from gas flow data, is generally higher than the arithmetic mean value. It is explained in section 1.4 that the equations used to describe flow through porous media, assume a single pore radius (the mean hydraulic radius) to represent the size of fluid conducting pores. Thus, fitting of experimental flow data to these equations, allows the estimation of mean hydraulic radius 'm' (see section 4.6). The value of 'm' obtained is equal to the hydraulic radius of uniform capillaries of circular cross-section constituting a hypothetical

ideal porous specimen, which would have identical permeability characteristics to those of the experimental specimen. Since flow rate is largely controlled by the wider pores in parallel array (viscous permeability $\propto$ radius^4; slip permeability $\propto$ radius^3, for circular capillaries), it is these pores which largely determine the pore size estimate. This effect is examined for an assumed 'normal' distribution of pit pore sizes, by Petty and Preston (1969a).

4.8 GAS FLOW PERMEABILITY - SUMMARY

The relationship between specific mass flow and mean gas pressure (within the specimen) has been investigated, over a range of pressure from 0 to 2 bar (absolute), for hydrogen flow through a number of softwoods. Where practicable, flow through early wood and late wood was separately investigated. Species for examination were selected to cover a wide range of pit membrane structural features, from timbers with commercial importance. The mass flow/mean pressure relationship for all specimens was found to deviate negatively, at low pressures, from the linear relationship predicted by the modified Kozeny equation describing flow through porous media. It is believed that this deviation is due to flow taking place through serially interconnected wide (tracheid lumina) and narrow (bordered pit) pores.

By assuming a simple flow path model of alternately wide pores (of uniform and constant diameter 'd_1') and narrow pores (of uniform constant diameter 'd_2'), the gas flow data were analysed numerically to provide an estimate of 'viscous' and 'slip' permeability constants.

The limitations of the above flow path model were critically examined and it is concluded that the model is probably a gross oversimplification of softwood pore structure. A more general flow path model of 'n' pore types, serially interconnected, was constructed. It is shown that flow through this type of system can give rise to mass flow/mean pressure

relationships, indistinguishable from those for the simple '2 pore' system described above. By the use of a numerical method it is demonstrated that the assumption of a '2 pore' model to describe a more complex, 3 pore type, system, can lead to significantly high estimates of viscous permeability constant. The magnitude of likely error decreases with increase in mean pressure and is dependent upon pore geometry. For pore geometry likely to occur in softwood the error may be as much as 100 per cent, for mass flow/mean pressure relationships extending to about 2 bar.

Gas flow data are commonly used to estimate flow controlling effective pore diameter. Such estimates depend upon the relative value of viscous (K_v) and slip (K_s), permeability constants. It is observed that the estimate of the ratio $K_v:K_s$ decreases with increase in mean pressure.

Hence pore diameter estimated from gas flow data decreases markedly as mean pressure is increased. In the numerical example worked, the estimate approached constancy only when the mean pressure range extended beyond 8 bar. For these reasons, therefore, pore sizes estimated from gas flow data need to be interpreted with caution. They cannot provide a better than 'order of magnitude' guide to the size of real pores.

Furthermore, it is shown that certain possible flow controlling pores are too short to be approximated as long capillaries. This effect can lead to significant high error (up to 70 per cent in examples investigated) in pore size estimation, in addition to the errors noted above.

5 FLOW OF INERT (NON-SWELLING) LIQUIDS THROUGH DRY SOFTWOOD

5.1 OBJECTIVES

The flow of inert liquids (ie liquids which do not react with and alter the structure of softwood pores) may be described by equations of laminar or turbulent flow (see sections 1.3 and 1.4). In this section viscous permeability to liquids under creeping flow conditions, is measured. These data are compared (section 7) with corresponding gas flow data. The effect of increasing the magnitude of viscous and inertial force is investigated and discussed with respect to possible changes in flow mechanism and pore structure.

5.2 APPARATUS AND EXPERIMENTAL TECHNIQUE

The apparatus to measure liquid flow permeability consists essentially of:-

a Liquid reservoir with some means of applying pressure.
b Liquid filter.
c Specimen cell.
d Pressure gauge
e Flowmeter.

This equipment is shown diagrammatically in Figure 5.1. It is seen from the diagram that driving pressure is supplied by compressed nitrogen. This system is chosen so that completely steady pressure (free from pump oscillation) can be applied to the specimen. To avoid saturation of the permeating liquid with nitrogen (with the accompanying problems of pore blocking by gas embolism), a synthetic rubber membrane was used to separate gas and liquid in the liquid reservoir. Liquid from the reservoir was passed through a membrane filter (0.1 micron pore size) immediately prior to entry into the specimen cell. For low pressures (up to about 5×10^4 dyn cm^{-2}) a simple manometric tube was used to monitor inlet pressure, whilst for higher pressures (up to about

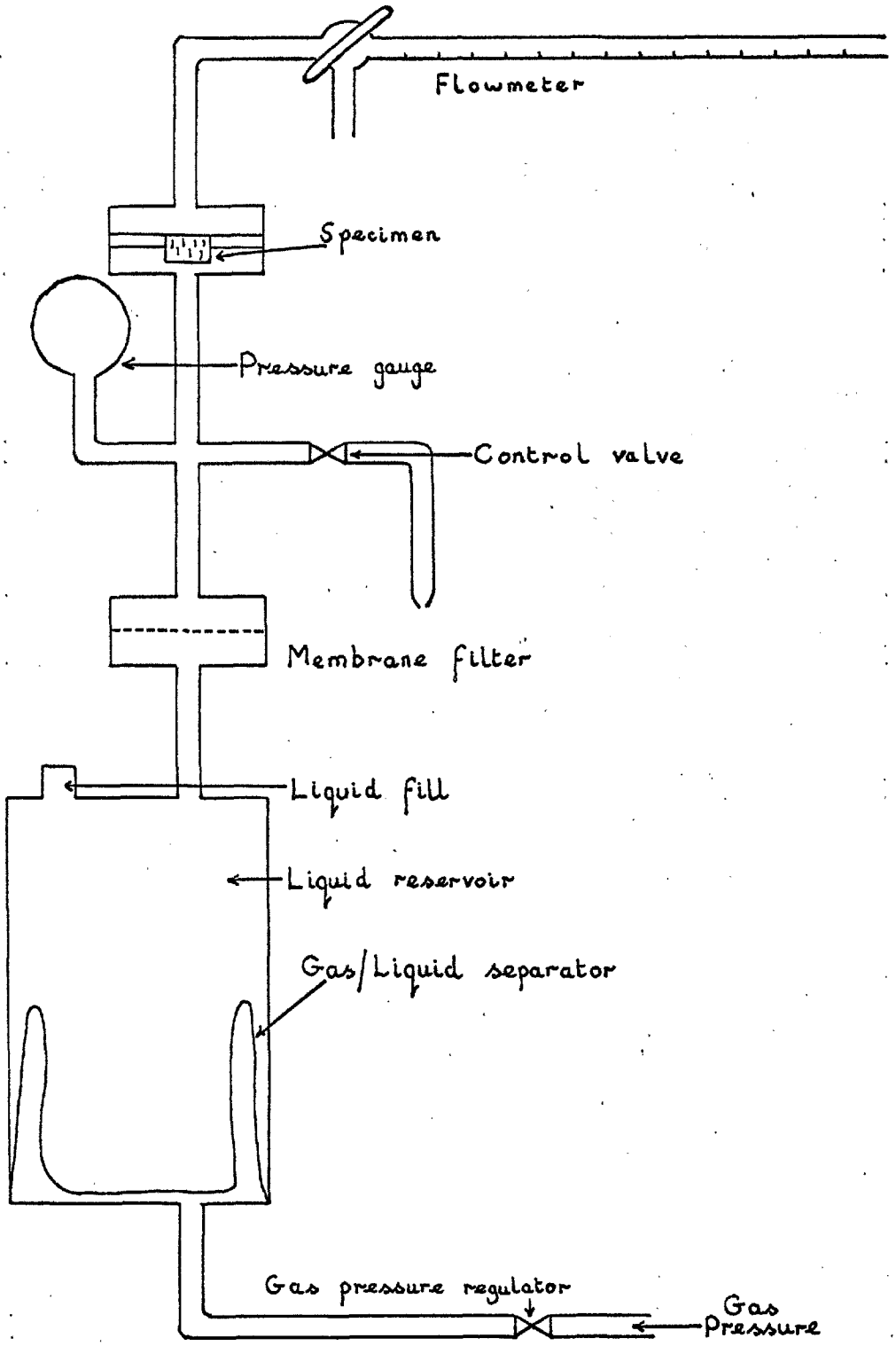


Fig 5.1 LIQUID FLOW PERMEABILITY APPARATUS

10^6 dyn cm^{-2}) a pressure transducer was employed. Throughout the work it was assumed that the permeating liquid at the flowmeter was at atmospheric pressure. The manometric tube required no calibration beyond the provision of an accurate linear scale. Calibration of the pressure transducer was carried out with a 'dead weight' tester (accurate to 0.7 x 10^3 dyn cm^{-2}) before any set of flow measurements. Pressure regulation was accomplished by a two-stage process. A gas regulator (see Figure 5.1) was used primarily, but because of the changing back pressure imposed on the system by the rubber separator and the membrane filter, it was not possible accurately to control specimen inlet pressure with this device alone. In operation, therefore, this regulator was set to give slightly higher pressure than required. Final adjustment was made by 'bleeding' excess liquid through a fine control valve in parallel with the specimen. The specimen cell consisted of a modified membrane filter holder into which specimens (as used for gas flow work, section 4.2) were sealed by compression between 'PTFE' gaskets. Small flow rates were measured with a 'burette' flowmeter (Figure 5.2) and stop watch (the burette was held near horizontal to minimise back pressure increase during flow). Higher rates of flow were

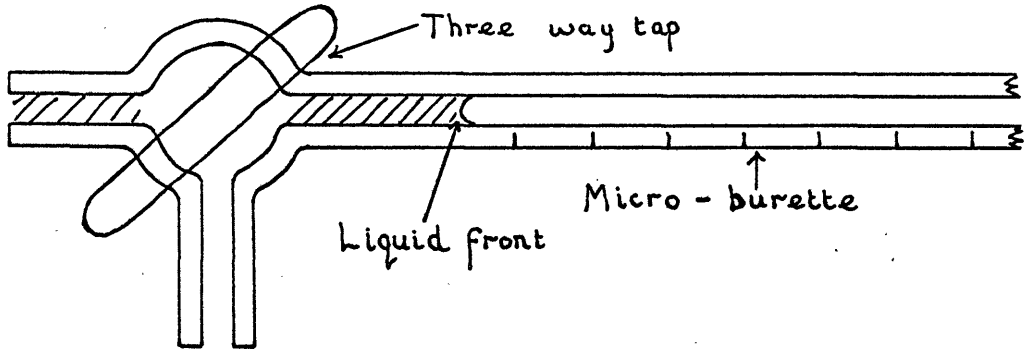


Fig 5.2 'BURETTE' FLOWMETER

monitored by collection of liquid discharge in a measuring cylinder for a measured time period.

The liquid reservoir was constructed from mild steel and the membrane filter holder and specimen holder from stainless steel. Interconnecting tubing was of glass, butt joints being sealed with appropriate synthetic rubber tubing, selected to be resistant to the particular permeating liquid in use.

Before filling the liquid reservoir, the permeating liquid was boiled for a few minutes to remove air. After filling with liquid, the reservoir was evacuated to further remove air (during this period the reservoir was hammered to induce shock waves leading to cavitation and release of residual air).

The reservoir was then returned to atmospheric pressure and sealed. To minimise re-contamination with air, pressure on the 'gas side' of the gas/liquid separator was raised slightly, to cause slow continuous flow of liquid through the membrane filter. The side-arms holding the pressure gauge and bleed valve were filled and liquid was allowed to flow slowly to waste until the reservoir attained working temperature (25°C). Temperature of the apparatus and liquid was maintained during experiments by working in a thermostatically controlled room at 25 ± 0.5°C.

Prior to mounting in the apparatus described above, specimens were dried to constant weight by evacuation over phosphorus pentoxide and impregnated with permeating liquid, by the vacuum impregnation technique described below using the apparatus shown diagrammatically in Figure 5.3.

a Specimens were placed in the impregnation jar contained in the vacuum desiccator, isolated from liquid reservoir and membrane filter, and evacuated by rotary vacuum pump to a pressure of <1 torr, for 30 minutes.

b Pressure in the jar was raised to permeating liquid vapour pressure by admitting a few drops of liquid from the reservoir, via the membrane filter (see Figure 5.3).

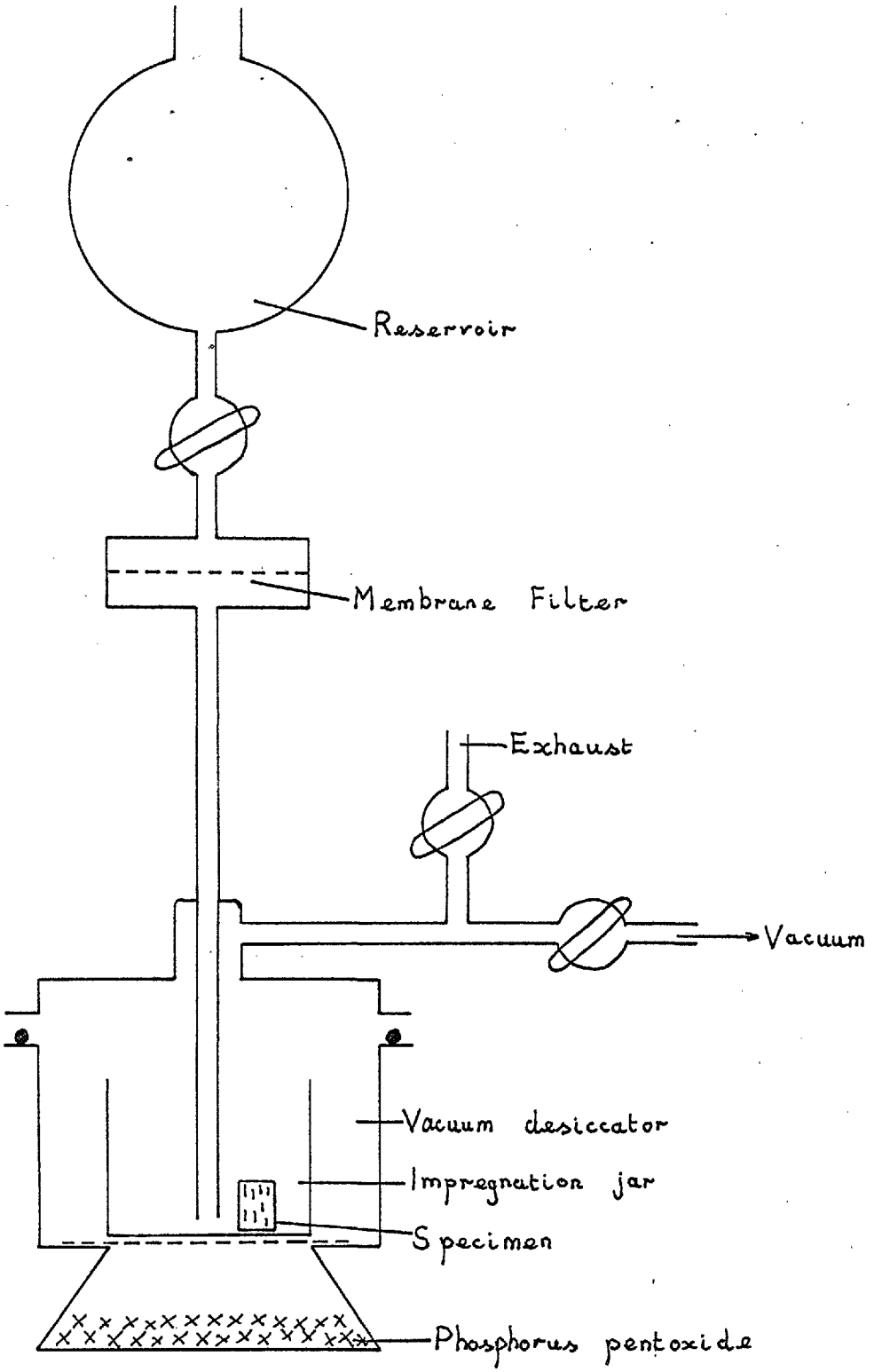


Fig 5.3 VACUUM IMPREGNATION APPARATUS

c Pumping was continued to remove vapour until pressure in the jar was re-established at less than 1 torr.

d Upon removal of vapour, residual air in the system was further diluted by admittance of a further few drops of permeating liquid.

e This dilution procedure was repeated through at least five cycles.

f Liquid was admitted to the impregnation jar to completely immerse the specimens.

g Pressure was reduced to liquid vapour pressure and the vacuum desiccator was sealed. Specimens were maintained in this condition overnight (16-24 hours).

h Pressure was raised to atmospheric by admitting air to the desiccator. Specimens were kept immersed at atmospheric pressure for at least one hour.

It is believed that this procedure led to virtual complete filling of the flowpath network of the specimens. It is possible that some pores, isolated from the main flow path system, could remain unfilled (see Petty and Preston, 1969); such pores, however, can play little or no part in gas or liquid conduction and may be disregarded.

With a slow flow to waste maintained through the inlet half of the specimen cell, specimens were quickly transferred from the impregnation jar to the permeability apparatus. Care was taken to ensure that no air became trapped at the specimen inlet face.

The apparatus was finally assembled and the pressure differential adjusted to the value required. Rate of liquid flow through the specimen was monitored for periods of at least 10 minutes, and up to 2 hours in some cases. This procedure was followed for all the test specimens, using various permeating liquids and a range of applied pressure differentials.

After completion of this series of experiments, the specimens were open stored in the laboratory to allow evaporation of

hexane. They were then re-dried to constant weight by evacuation over phosphorus pentoxide. A second series of gas flow permeability measurements were then conducted, precisely as described in Part 4. Data from these experiments are discussed in section 7. Upon completion of the second gas flow measurements, the specimens were re-impregnated with hexane as described above, for investigation of the effect of viscous force on permeability (section 5.3.3).

5.3 NON-SWELLING LIQUID FLOW RESULTS AND DISCUSSION

5.3.1 VISCOUS PERMEABILITY TO NON-SWELLING LIQUID

For each of the specimens previously used in the gas flow work (part 4), viscous permeability was measured using n.hexane as the permeating liquid. In this work, small pressure gradients were used, so that flow occurred as nearly as possible in the purely viscous régime, ie free from turbulence (see section 1.3.2).

Flow rate under measured pressure gradient was measured, using the technique described above (section 5.2).

Flow and pressure differential data are given below (Table 5.1).

Table 5.1 HEXANE FLOW DATA FOR DRY SPECIMENS

Specimen	Pressure Differential 'ΔP' (dyn cm^{-2}) x 10^{-4}	Flow Rate 'Q' (ml sec^{-1})
AGS.e	3.63	0.015
AGS.ℓ	3.56	0.030
AGH.e	3.56	0.0092
AGH.ℓ	3.56	0.0043
CDS	3.56	0.030
CDH	3.56	NO FLOW
PAS.1	3.56	0.016
PAS.2	3.56	0.022
THS.e	3.56	0.0028
THS.ℓ	3.56	0.0047
THH.e	3.56	0.035
THH.ℓ	3.56	0.011
AAS	1.20	0.053
AAH	0.65	0.022

(NB Specimen labelling code is given in section 4.4)

From the data of Table 5.1, viscous permeability constants may be measured according to equation 1.10:-

$$Q = \frac{BA\Delta P}{\eta \ell} \qquad \text{Equation 1.10}$$

where Q = volume rate of flow
A = specimen area normal to flow
ΔP = pressure differential across specimen
η = liquid viscosity
ℓ = specimen length
B = permeability constant

For any individual specimen 'A' and 'ℓ' are obviously constant - hence, as for gas flow, specimen permeability constant 'K_V' was calculated rather than the more general constant 'B' which takes account of specimen gross geometry:-

$$K_V = \frac{BA}{\ell}$$

where K_V = specimen viscous permeability constant.

Hence, from equation 1.10:

$$\frac{BA}{\ell} = \frac{Q\eta}{\Delta P} = K_V \qquad \text{Equation 5.1}$$

Values of 'K_V' calculated thus are given below in Table 5.2. (NB: The viscosity 'η' of hexane at 25°C is taken from standard tables of constants (Weart, 1973) as 0.29×10^{-2} Poise).

Table 5.2 VISCOUS PERMEABILITY CONSTANTS OF DRY SPECIMENS FROM HEXANE FLOW DATA

Specimen	Viscous permeability constant 'K_v' (cm^3) x 10^8
AGS.e	0.12
AGS.ℓ	0.24
AGH.e	0.074
AGH.ℓ	0.035
CDS	0.24
CDH	NO FLOW
PAS.1	0.13
PAS.2	0.18
THS.e	0.022
THS.ℓ	0.038
THH.e	0.29
THH.ℓ	0.089
AAS	1.28
AAH	0.98

For each of the specimens tested, hexane flow was maintained under constant pressure differential for about 40 minutes (for one specimen, 'THH.ℓ' this period was extended to about 2 hours). During the flow period, flow rate was monitored at regular intervals. These flow rate data are given in Table 5.3 below.

Table 5.3 EFFECT OF TIME OF FLOW ON FLOW RATE

Specimen	Rate of flow (ml sec^{-1}) at listed times				
	5 min	10 min	20 min	40 min	120 min
AGS.e	0.015	0.015	0.014	0.015	
AGS.ℓ	0.030	0.032	0.030	0.030	
AGH.e	0.0083	0.0092	0.0092	0.0092	
AGH.ℓ	0.0042	0.0042	0.0043	0.0043	
CDS	0.030	0.031	0.030	0.030	
CDH	NO FLOW	NO FLOW	NO FLOW	NO FLOW	
PAS.1	0.015	0.016	0.016	0.016	
PAS.2	0.020	0.021	0.022	0.022	
THS.e	0.0028	0.0028	0.0028	0.0025	
THS.ℓ	0.0047	0.0047	0.0050	0.0048	
THH.e	0.033	0.035	0.035	0.033	
THH.ℓ	0.011	0.011	0.011	0.011	0.011
AAS	0.053	0.053	0.053		
AAH	0.023	0.023	0.023		

For similar reasons given in the gas flow section (section 4.5), the permeability constants measured with n.hexane are not a true guide to the general permeability of the species tested. The data cited in Table 5.2 are used later (Part 7) for comparison with gas flow, viscous permeability data.

Earlier workers (see section 1.5.1) found difficulty in establishing steady flow through softwood under constant pressure differential. It has been shown (Kelso, Gertjejansen and Hossfeld, 1963) that the decreasing flow rate with time of flow is largely due to pore blocking by fine particles and by gas bubbles (see section 1.5.1). The techniques recommended by Kelso et al to overcome this problem were adopted in this work (section 5.2). Use of these techniques enabled steady flow under small pressure differentials (about 3.5×10^4 dyn cm^{-2}), equivalent to gradients of about 3.5 bar per metre, to be maintained for prolonged periods, up to 2 hours (see Table 5.3 above). In no case was the final flow rate lower

by more than about 10 per cent than the maximum attained flow rate. Usually, any reduction was much less than this amount.

For one of the specimens, AGH.e (*Abies grandis*, heartwood, early wood) an increase in rate of flow was observed over the initial flow period (Table 5.3). It is believed that this increase was probably due to removal of resinous extractive material from the pore structure, by the flowing liquid (this effect is discussed more fully later, in the section dealing with flow of various liquids through wood - section 6.3.4.1). The data reported are thus in agreement with those of Kelso, Gertjejansen and Hossfeld (1963), and of Comstock (1967), showing that steady flow longitudinally through softwood, can be achieved in the absence of gas or particle embolism.

5.3.2 EFFECT OF MAGNITUDE OF PRESSURE DIFFERENTIAL ON RATE OF FLOW

After measurement of permeability constant under small applied pressure differential conditions (section 5.3.1) {and the second series of gas flow experiments (see section 5.2)}, the effect of increase in pressure differential on flow rate was investigated. Generally, the same specimens used in the work described in section 5.3.1, were used for this investigation. However, two of the specimens THS.ℓ and AAS were accidentally contaminated and omitted from the series.

The range of pressure differential investigated was from about 0.04×10^6 to about 0.7×10^6 dyn cm^{-2} ($\sim$0.04 to 0.7 bar) for most specimens.

For very permeable specimens where rapid depletion of the liquid reservoir made monitoring difficult at the higher pressure differentials, the investigation was conducted over a more restricted range of pressure. To assess the magnitude of any irreversible changes in permeability, flow rates were measured for a series of increasing and decreasing pressure differentials. Flow and applied pressure data for these experiments are given in full in Appendix 1, Table 14. Specimen

permeability 'constants', calculated from these data, according to equation 5.1:-

$$K_V = \frac{Q\eta}{\Delta P} \qquad \text{Equation 5.1}$$

where K_V = specimen permeability constant
Q = volume rate of flow
η = liquid viscosity
ΔP = applied pressure differential

are given below in Table 5.4.

Table 5.4 EFFECT OF PRESSURE DIFFERENTIAL ON ESTIMATED PERMEABILITY CONSTANT

	Permeability constant ($cm^3 \times 10^8$) at listed pressure differential (Chronological order of measurement) →									
Approximate pressure differential (dyn $cm^{-2} \times 10^{-5}$) / Specimen	0.069	0.13	0.20	0.36	1.68	3.39	6.85	1.68	0.36	0.069
AGS.e				0.12	0.10	0.099	0.092	0.10	0.11	
AGS.ℓ				0.23	0.19	0.19	0.19	0.19	0.21	
AGH.e				0.080	0.057	0.055	0.052	0.051	0.059	
AGH.ℓ				0.033	0.034	0.032	0.029		0.030	
CDS				0.24	0.22	0.22			0.24	
CDH	NO FLOW									
PAS.1				0.16	0.12	0.12	0.10	0.11	0.15	
PAS.2										
THS.e				0.021	0.020	0.020	0.018	0.020	0.021	
THS.ℓ	SPECIMEN SPOILED									
THH.e				0.27	0.24	0.22	0.19	0.21	0.24	
THH.ℓ				0.089	0.078	0.074	0.060	0.063	0.079	
AAS	0.98	1.06	0.99	0.85	0.71				0.84	0.88
AAH	SPECIMEN SPOILED									

Rate of flow is observed to increase less than linearly with increase in applied pressure differential (see Table 14 Appendix 1). This effect is reflected in the decrease in viscous permeability constant with pressure differential increase (Table 5.4). For purely laminar (or viscous) flow in a rigid porous medium, rate of flow is directly proportional to applied pressure gradient (or permeability constant is independent of pressure gradient). This is a fundamental requirement of Darcy's law of flow through porous media (see section 1.4, equation 1.10).

Thus, the data of Table 5.4 suggest that either liquid flow through softwood is not entirely laminar, or the pore structure is deformed by the forces of the flowing liquid, leading to decrease in pore size or number.

It may be seen from Table 5.4 that a proportion of the permeability decrease is irreversible (ie the final measurement at low pressure differential is generally somewhat lower than the initial one at the same differential). Such irreversible change must be due to alteration of the pore structure. This alteration may result from downstream displacement of the pit membrane to make a more effective seal against the pit border as described by Huber and Mertz (1958) and by Bailey and Preston (1970), see section 1.5.1. It is also possible that the reduction may be brought about by displacement of loose extractive debris from regions where it has little effect on flow (eg the wide part of the pit chamber) to a position where it may strongly affect flow (eg the membrane margo or small gaps remaining between torus and pit border of part aspirated pits).

Much of the observed permeability reduction, however, is reversible (Table 5.4), and it is possible that this is the result of elastic distortion of the structure under the higher pressure differentials imposed. However, the departure from linearity, is consistent with the occurrence of a component of turbulent flow (see section 1.3.2).

Flow changes from a laminar to a turbulent régime, as Reynolds number increases beyond a critical value (section 1.3.2). Values of Reynolds number for various parts of the structure of one of the specimens tested are calculated below, using equation 1.5:-

$$Nr = \frac{\rho \ell e' u}{\eta} \qquad \text{Equation 1.5}$$

where Nr = Reynolds number
ρ = liquid density
$\ell e'$ = flow controlling linear dimension
u = liquid linear velocity
η = liquid viscosity

SPECIMEN - *Tsuga heterophylla* heartwood early wood (THH.e)

Cross-sectional area normal to flow $\sim$ 60 mm^2.

Tracheid cross-sectional area $\sim$ 0.002 mm^2.
Therefore number of tracheids exposed in a cross-section $\sim$ 30,000.

In early wood, a high proportion of tracheids are completely blocked and hence take no part in liquid conduction (Petty, 1970). For this relatively short specimen (about 5 tracheid lengths), let it be assumed that the conducting area amounts to about 25 per cent of the total tracheid lumen area exposed in the specimen cross-section. (ie liquid leaves the specimen through about 7500 tracheids).

Maximum rate of flow through specimen THH.e = 0.45 ml sec^{-1} (Table 14 Appendix 1). Therefore average liquid velocity (at maximum flow rate) in tracheid lumen (taking lumen cross-sectional area = 0.000012 cm^2) is given by:-

$$u = \frac{0.45}{7500 \times 0.000012} \text{ cm sec}^{-1}$$

$$= \underline{5 \text{ cm sec}^{-1}}$$

Assume $\ell e'$ = lumen diameter $\sim$ 40 micron

ρ (hexane) = 0.66 gm ml^{-1}

η (hexane) = 0.29 cP

Then, from equation 1.5 above:

$$Nr = \frac{0.66 \times 0.04 \times 5}{0.0029} = \underline{4.55}$$

Flow through straight capillaries of uniform cross-section remains laminar until Reynolds number (Nr) approaches values about 2000 (section 1.3.2). Tracheid lumen shape is a reasonable approximation to that of a uniform capillary. It seems most likely, therefore, that flow through the tracheid lumen is laminar.

From microscopic work carried out on a range of softwoods (Phillips, 1933), it seems likely that, on the average, about one pit per cell wall is unaspirated in air dried early wood. Pit membrane dimensions may be estimated from scanning electron micrographs (for *Tsuga heterophylla* see, for example, Figure 3.10). From such micrographs:-

Membrane diameter $\sim$ 16 micron

Torus diameter $\sim$ 8 micron

Therefore margo area $\sim$ 150 $micron^2$

or $\underline{1.5 \times 10^{-6}\ cm^2}$

Electron microscopic evidence suggests that about 30 per cent of the margo is pore space, therefore area of margo for liquid conduction is about $\underline{0.45 \times 10^{-6}\ cm^2}$.

Now, liquid velocity in lumen is about 5 cm sec^{-1} (see above).

Therefore liquid velocity through margo pores, is given by:

$$u = 5 \times \frac{\text{lumen cross-sectional area}}{\text{margo pore cross-sectional area}}$$

$$= 5 \times \frac{0.000012}{0.00000045} \text{ cm sec}^{-1}$$

$$= \underline{133 \text{ cm sec}^{-1}}$$

Selection of a value for $\ell e'$ in the case of margo flow, for fitting to equation 1.5, is difficult. Using pipe flow theory, the average margo pore width is the most appropriate value (section 1.3.2). If the membrane is regarded as an immersed body and treated according to Stokes law theory, then the appropriate value for $\ell e'$ is the 'diameter' of the immersed body normal to the direction of flow (see, for example, Daugherty and Franzini, 1965).

For pipe flow theory:-

$\ell e' \sim 0.3$ micron (see Table 3.1, section 3.3.7)

$u = 133 \text{ cm sec}^{-1}$

Thus, $Nr = \frac{0.66 \times 0.00003 \times 133}{0.0029} = 0.9$

As for lumen flow above, this result suggests that flow through margo pores is laminar.

For flow past an immersed body the linear dimension $\ell e'$ may be taken as:-

a average fibril width, or

b torus diameter.

a $\ell e'$ = fibril width ~ 0.2 micron

Therefore $Nr = \frac{0.66 \times 0.00002 \times 133}{0.0029} = \underline{0.6}$

b $\ell e'$ = torus diameter ~ 8 micron

Therefore $Nr = \frac{0.66 \times 0.0008 \times 133}{0.0029} = \underline{24}$

Fluid flowing past an immersed body develops a turbulent wake at very low Reynolds number (between 0.5 and 1), see section 1.3.2. It seems likely, therefore, that flow through the various pores in wood is laminar at the flow rates encountered in this work. The presence of bodies effectively immersed in a fluid stream, however (eg margo fibrils and membrane tori), may be expected to lead to some turbulent wake development. Development of wake turbulence is characterised by a less than linear increase in flow rate with increase in applied pressure differential.

The decrease in permeability encountered as pressure differential, and hence flow rate, is increased is partly reversible (upon return to lower pressure differential) and partly irreversible. The irreversible component must be due to permanent change in pore structure as a result of applied forces. It is possible that the reversible change is due to elastic structural deformation as applied force is increased. However, analysis suggests that the reversible decrease may be due to the presence of an increasing amount of wake turbulence as flow rate is increased.

The above set of calculations is based on data for one specimen only (THH.e). Approximate calculation shows, however, that similar or higher Reynolds number criteria may apply to all the specimens tested.

5.3.3 EFFECT OF VISCOUS FORCE ON PERMEABILITY

To investigate this effect the rate of flow of a series of liquids was measured, through three wood specimens. The liquids were selected to cover a wide range of viscosity, whilst being mutually miscible, of roughly similar density and causing negligible cell wall swelling. They are listed, together with relevant physical data, in Table 5.5 below.

Table 5.5 PERMEATING LIQUIDS AND THEIR PHYSICAL CONSTANTS*

Liquid	Viscosity (centipoise)	Density (gm ml^{-1})
n.hexane	0.29	0.66
carbon tetrachloride	0.90	1.60
dibenzyl ether	4.0	1.04

*Physical constants cited are values measured at 25°C obtained from published tables (Weart, 1973)

The wood specimens were selected from three different species and were chosen to include an 'all sapwood' and an 'all heartwood' specimen (see Table 5.6 below).

Table 5.6 WOOD SPECIMEN DETAILS AND DESCRIPTION

Specimen	Description
AGS.&	*Abies grandis*, sapwood, late wood
CDS	*Cedrus deodara*, sapwood (combined early wood and late wood)
THH.e	*Tsuga heterophylla*, heartwood, early wood

Using the techniques described fully in section 5.2, the permeability of each of the above specimens was measured with each of the liquids listed in Table 5.5. Transfer of specimens from one liquid to another was carried out by storage for several hours, of specimens (already saturated with a test liquid) in a large volume of the new test liquid. Each of the test liquids was carefully membrane filtered and de-aerated prior to use. To avoid re-contamination of liquid with air during the storage period, the liquid containers were held in vacuum desiccators evacuated to the vapour pressure of the liquid.

During flow rate measurement, the differential pressure was adjusted so that for each specimen, approximately similar flow rates were obtained for the three test liquids. These flow data are given below in Tables 5.7, 5.8 and 5.9.

Table 5.7 SPECIMEN AGS.ℓ - FLOW RATE DATA

Test liquid	Pressure differential (dyn cm^{-2}) x 10^{-6}	Flow rate (ml sec^{-1})
n.hexane	0.13	0.103
carbon tetrachloride	0.41	0.092
dibenzyl ether	1.33	0.065

Table 5.8 SPECIMEN CDS - FLOW RATE DATA

Test liquid	Pressure differential (dyn cm^{-2}) x 10^{-6}	Flow rate (ml sec^{-1})
n.hexane	0.13	0.092
carbon tetrachloride	0.41	0.083
dibenzyl ether	1.33	0.068

Table 5.9 SPECIMEN THH.e - FLOW RATE DATA

Test liquid	Pressure differential (dyn cm^{-2}) x 10^{-6}	Flow rate (ml sec^{-1})
n.hexane	0.069	0.057
carbon tetrachloride	0.21	0.055
dibenzyl ether	0.69	0.043

According to Darcy s law, under laminar flow conditions, rate of flow per unit pressure differential is inversely proportional to the reciprocal of viscosity:-

$$\frac{Q}{\Delta P} = \frac{BA}{\eta \ell} \qquad \text{Equation 1.10}$$

where Q = volume rate of flow

A = specimen area normal to flow direction

ΔP = pressure drop across specimen

η = liquid viscosity

ℓ specimen length

B = permeability constant

From the data of Tables 5.7 to 5.9 (above), graphs of rate of flow per unit pressure drop against reciprocal viscosity, are prepared for the three specimens investigated (Figure 5.4 below). It is seen from Figure 5.4 that the relationship between $Q/\Delta P$ and $1/\eta$ appears approximately linear for each of the specimens, suggesting that for each of these liquids flow is laminar at the rates measured.

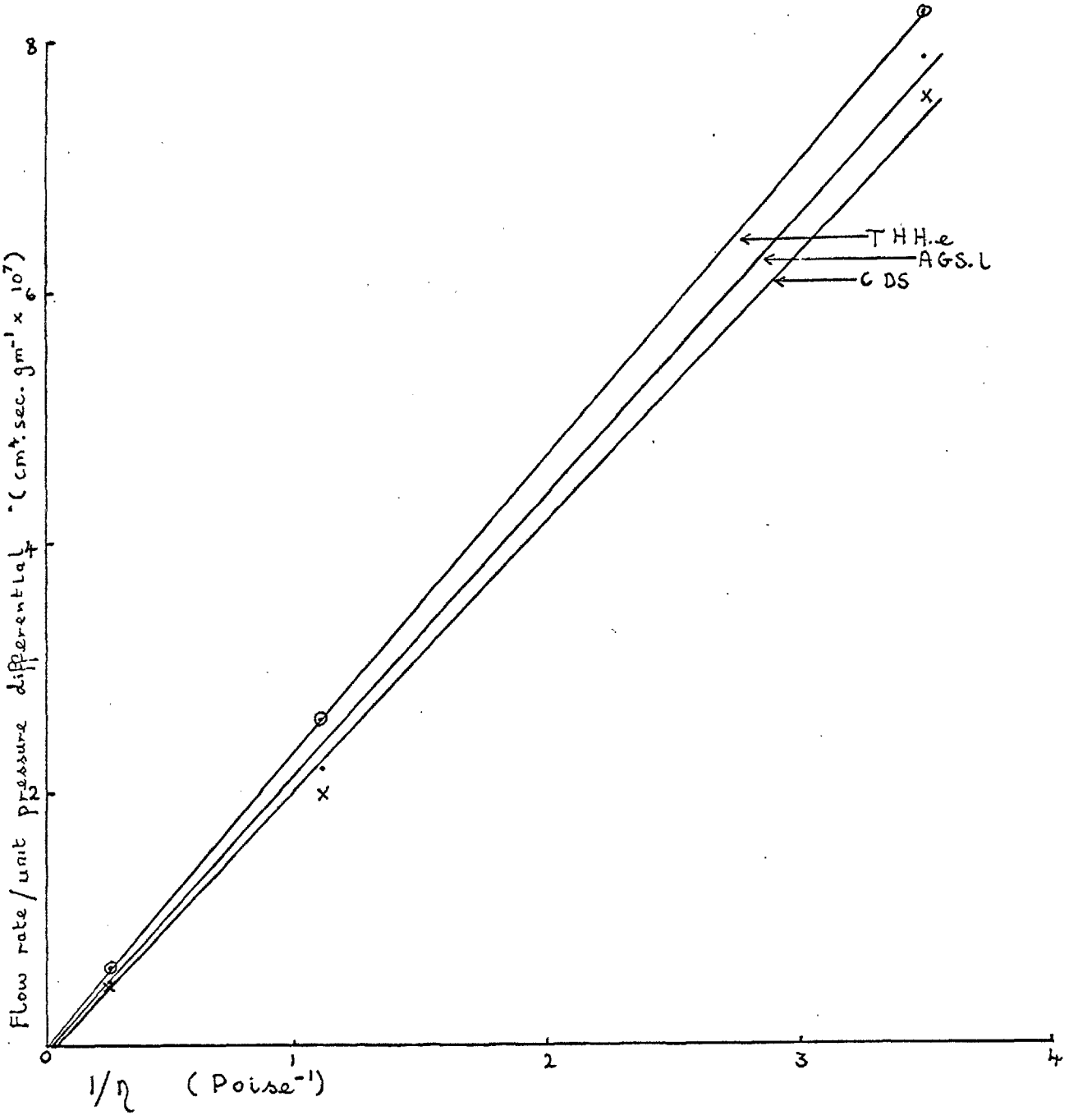


Fig 5.4 RELATIONSHIP BETWEEN LIQUID FLOW RATE AND VISCOSITY

In the laminar régime, resistance to flow is proportional to velocity and to liquid viscosity. When flow becomes turbulent, inertial forces become increasingly important and flow resistance becomes approximately proportional to the square of velocity and to liquid density (see fluid dynamic texts, eg Daugherty and Franzini (1965), and section 1.3 above). For the three specimens examined, viscous resistance parameters are calculated according to the above theory:-

$$\Omega_f = Q\eta \qquad \text{Equation 5.1}$$

where Ω_f = viscous flow resistance
Q = volume rate of flow
η = liquid viscosity

These values are tabulated below (Table 5.10).

Table 5.10 VISCOUS FORCE PARAMETERS IMPOSED BY FLOW OF TEST LIQUIDS

Specimen	Viscous force parameter Ω_f (gm cm^2 sec^{-2}) x 10^4		
	n.hexane	carbon tetrachloride	dibenzyl ether
AGS.ℓ	3.0	8.3	26.0
CDS	2.7	7.5	27.2
THH.e	1.7	5.0	17.2

From the Table it can be seen that for each specimen, viscous force increases about tenfold through the series - n.hexane - carbon tetrachloride - dibenzyl ether.

These viscous force data may be compared with the viscous force imposed by hexane at flow rates showing departure from a linear relationship with applied pressure differential (from the data of Table 5.4). These data are given below (Table 5.11).

Table 5.11 VISCOUS FORCE 'Ω_f' DUE TO HEXANE FLOW IN REGION OF DEPARTURE FROM LINEAR RELATIONSHIP WITH APPLIED PRESSURE DIFFERENTIAL

Specimen	Flow rate (ml sec^{-1})	Ω_f (gm cm^2 sec^{-2}) x 10^4
AGS.ℓ	∿ 0.10	2.9
CDS	∿ 0.13	3.8
THH.e	∿ 0.12	3.5

Comparison of the data of Tables 5.10 and 5.11 shows that higher viscous force is applied to specimens during flow of carbon tetrachloride and dibenzyl ether, than during hexane flow at the start of the departure from the linear, 'flow/applied pressure differential' relationship. It is established (Figure 5.4) that within the range investigated, flow of carbon tetrachloride and dibenzyl ether is in obedience to Darcy's law, with respect to viscosity, ie:-

$$\frac{Q}{\Delta P} \propto \frac{1}{\eta} \text{ (see equation 1.10)}$$

where Q = volume rate of flow
ΔP = applied pressure differential
η = liquid viscosity

Thus it seems unlikely that the observed permeability decrease at higher hexane flow rates, is due to structural alteration caused by increased frictional force.

Increase in hexane flow rate leads to increase in inertial force applied to the pore structure. Inertial force increases with density and with the square of liquid velocity (see above). Hence inertial force parameters may be calculated:-

$$\Omega_I = Q^2\rho$$

where Ω_I = inertial force parameter
Q = volume rate of flow
ρ = liquid density

Values of Ω_I are calculated for hexane flow rate at the start of departure from the linear relationship between flow rate and applied pressure differential (Table 5.11). These data are compared with the inertial force parameters imposed by flow of carbon tetrachloride and dibenzyl ether in Table 5.12.

Table 5.12 INERTIAL FORCES 'Ω_I' IMPOSED BY THE FLOW OF VARIOUS LIQUIDS

Specimen	Ω_I (gm cm^3 sec^{-2}) x 10^3		
	n.hexane	carbon tetrachloride	dibenzyl ether
AGS.ℓ	6.6	13.5	4.4
CDS	11.2	11.0	4.8
THH.e	9.5	4.8	1.9

It appears from the data of Table 5.12 that the inertial force imposed during flow of carbon tetrachloride is of similar magnitude to or slightly greater than that imposed by n.hexane. It is shown that flow of carbon tetrachloride under the conditions defined is in obedience to Darcy's law (see above), suggesting that inertial forces of the magnitude encountered are insufficient to cause permeability decrease due to pore structural alteration.

During flow of the test liquids, Reynolds number is varied because of the change in the density to viscosity ratio, and in flow rate. Reynolds number is given by the following equation:-

$$Nr = \frac{\rho \ell e' u}{\eta}$$ Equation 1.5

where Nr = Reynolds number

$\ell e'$ = flow controlling linear dimension

u = liquid linear velocity

η = liquid viscosity

ρ = liquid density

For any individual specimen $\ell e'$ and specimen cross-sectional area are constant. Hence:-

$$Nr \propto \frac{\rho Q}{\eta}$$

where Q = volume rate of flow.

The values of the expression '$\frac{\rho Q}{\eta}$' are calculated for hexane flow from the data of Tables 5.5 and 5.11, and for carbon tetrachloride and dibenzyl ether flow from the data of tables 5.5, 5.8 and 5.9. These values are tabulated below (Table 5.13).

Table 5.13 REYNOLDS NUMBER DATA FOR FLOW OF TEST LIQUIDS

Specimen	$\rho Q/\eta$ (cm)		
	n.hexane	carbon tetrachloride	dibenzyl ether
AGS.ℓ	∿ 23	16	2
CDS	∿ 30	15	2
THH.e	∿ 27	10	1

It can be seen from the Table that the expression '$\frac{\rho Q}{\eta}$' and hence Reynolds number, is greates for flow of n.hexane. Thus it seems that departure from the Darcy relationship is associated with increase in Reynolds number. Increase in inertial force and especially viscous force do not appear to directly lead to any departure. This lends support to the hypothesis that the reversible decrease in permeability occurring at higher hexane flow rates is due to turbulent flow (see section 5.3.2 above).

The experiments discussed were designed principally to investigate the effect of viscous force on pore structure. It must be recognised that the magnitude of the variation in inertial force (Table 5.12) and Reynolds number (Table 5.13) is insufficient to unequivocally separate effects due to these variables. It remains a possibility, therefore, that inertial force may cause structural deformation and reduction in permeability. To positively resolve this issue it is necessary to conduct an experiment where inertial force and Reynolds number are varied over a substantial range, independently of one another. Such an experiment should be possible by the use of gas and liquid flow systems, provided there is confidence that gas and liquid flow are directly related.

5.4 NON SWELLING LIQUID FLOW - SUMMARY

It is shown that constant flow rate under small pressure differential longitudinally, through the range of softwoods examined, can be maintained for long periods. To attain such steady flow conditions, it is necessary to remove fine particulate matter from the flowing liquid and to reduce the concentration of dissolved gas, to prevent particle or gas embolism of fine pores.

Increase in applied pressure differential is shown to lead to decrease in permeability. It is shown that part of this decrease is irreversible and part reversible. The irreversible component must be due to change in size or number of conducting pores, probably due to displacement of pit membranes, or to shifting of cell debris by the force of the flowing liquid.

Evidence is produced, suggesting that the reversible component of the decrease is due to an increased amount of 'wake-turbulence' as pressure differential, and hence flow rate, is increased. Increase in the magnitude of the frictional (viscous) force by an order of magnitude is shown to have no significant effect on permeability, and hence upon pore structure.

Part 6 LIQUID FLOW THROUGH SWOLLEN SOFTWOOD

6.1 SWELLING OF WOOD

A considerable degree of cell wall swelling accompanies the sorption of water and certain other liquids, by dry wood and other cellulosic materials. Thermodynamic studies suggest that the sorbed water is fixed to cellulose by hydrogen bonds (Morrison and Dziecìuch, 1959) X-ray studies show that sorption of water and other mild swelling liquids is restricted to the non-crystalline regions of cellulose (Hermans 1946; Browning 1963). Some liquids, eg pyridene, are able to penetrate the crystallites, reducing the amount of crystalline cellulose, and causing an increased amount of swelling (Browning, 1963). It is believed that sorbed molecules form first a monolayer upon and subsequently a bonded multilayer between cellulose micro fibrils (see Figure 6.1).

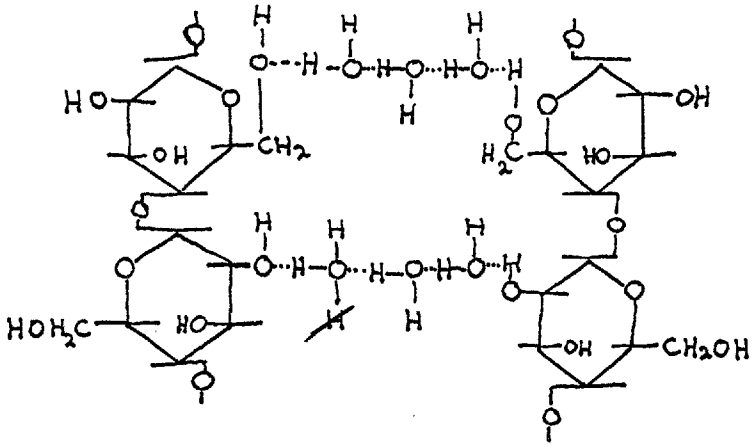


Fig 6.1 CELLULOSE/WATER, HYDROGEN BONDED MULTILAYER SYSTEM

In the water/cellulose system it is believed that the multilayer may attain a thickness of about 6 molecules.

In a totally unrestrained material, eg cellophane sheet, increase in gross dimension is accompanied by proportional increase in the size of any macro holes present. If wood

behaved in this fashion, it is clear that swelling would lead to increase in pore diameter and hence to permeability increase. The complex fibrillar nature of its cell wall prevents wood from behaving in this simple fashion, however. Wood cell walls are comprised of at least four layers of fibrils wound helically around the cell. These layers are labelled:-

a Primary wall
b Secondary wall 'S_1'
c Secondary wall 'S_2'
d Secondary wall 'S_3'

In the primary wall and the S_1 and S_3 layers of the secondary wall the helical angle (ie the angle made by the fibrils with the cell axis) is quite large (60°-90°). The helical angle in the S_2 layer, however, is relatively small (10°-30°) - Panshin and de Zeeuw, 1970 - (see Figure 6.2 below).

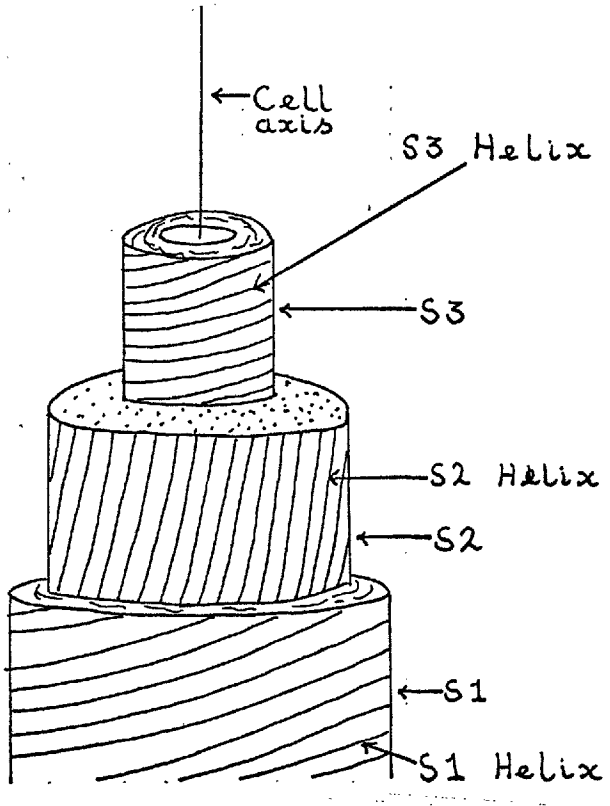


Fig 6.2 HELICAL ANGLE IN CELL WALL LAYERS

The bulk of the cell wall is contained in the S_2 layer, hence, it is this layer that mainly influences the magnitude and direction of cell wall swelling. Sorption of molecules between microfibrils in the non-crystalline zones causes this layer to swell normally to the fibril axis, and hence approximately normally to the axis of the cell. This swelling is restrained, however, by the primary wall/S_1 and by the S_3 layers which, with large helical angles, are free to swell only in the cell axial direction. The system is thus highly restrained and the relationship between macro swelling and change in pore diameter is complex (Kelsey 1963).

It is not within the scope of this work to consider in depth the mechanism of wood cell wall swelling. The foregoing is included to give a general background to the changes likely to occur during sorption. For many areas of wood technology, sorption, especially of water, is of great importance. The subject has been studied extensively by many workers over a long period of time (eg Koehler 1931, Kollmann 1935, Yintilla 1939, Frey-Wyssling 1940, Preston 1942). More recent work on this topic up to about 1960 is reviewed thoroughly by Kelsey 1963 and by Stamm 1964. Since that time interesting work on the subject has been published by Kollmann (1967); Banber (1968); Stamm and Smith (1969); Cave (1972); Boutelje (1973).

6.2 OBJECTIVES

The effect of swelling on permeability is studied in this work for one species only (*Abies grandis*). The pit membrane of this species is of the *Pinus* type (see section 2.1). Longitudinal resin canals are absent in the species (Phillips, 1948). It is believed, therefore, that results obtained with this species may be taken as representative of tracheid lumen/bordered pit flow, for the important Pinaceae family, without any complicating factor due to flow through resin canals.

Swelling is induced by exposure to moist air at various relative humidities and by impregnation with a series of pure liquids (water and aliphatic alcohols) causing various degrees of swelling.

Permeability data for specimens swollen by these two means are compared.

By comparison of the effect of swelling on the permeability of air dried and solvent exchange dried specimens, and by microscopic means, it is attempted to identify the structural elements responsible for the observed effects of swelling on permeability.

Finally, the effect of alcohols on flow through 'green' (never dried) wood is investigated.

6.3 HEXANE FLOW THROUGH WATER SWOLLEN WOOD

6.3.1 SPECIMEN PREPARATION

Specimens were prepared from two freshly felled logs of grand fir (*Abies grandis*) as described below:-

a From the central zone of each of the (1 m) logs, several discs of thickness about 30 mm were cut.

b One disc from each log was used to estimate heartwood and sapwood moisture content by the oven drying method. Of the remaining discs, three were kept in the green state by immersed storage in 50:50 ethanol/water mixture (see Erickson 1960).

6.3.1.1 CUTTING AND DRYING OF AIR DRIED SPECIMENS

a From the final three discs, four radially orientated sticks of width about 25 mm were cut from around the circumference as shown in Figure 6.3 below.

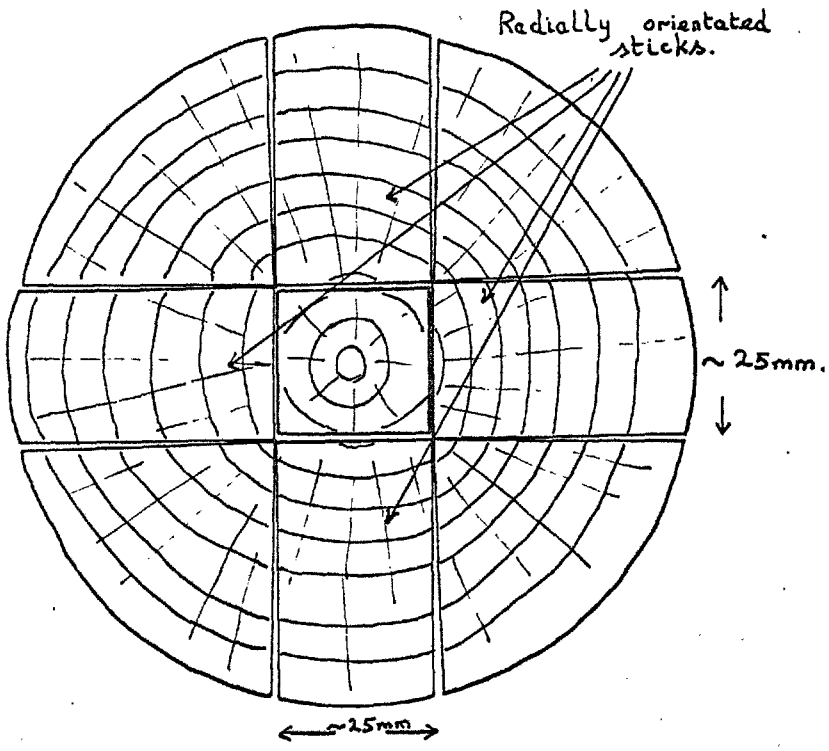


Fig 6.3 CUTTING OF RADIAL 'STICKS'

b These radial sticks were air dried gradually in controlled humidity chambers, to a final moisture content of about 6 per cent.

c At this moisture content, cylindrical air dried specimens of diameter 1 cm, were cut with a hollow drill from the sapwood and heartwood of each stick (Figure 6.4). Ends of these specimens were trimmed with a sharp razor to a length of about 1.5-2.0 cm.



Fig 6.4 PREPARATION OF CYLINDRICAL SPECIMENS

6.3.1.2 CUTTING AND DRYING OF SOLVENT DRIED SPECIMENS

a Radial sticks as shown in Figure 6.3 were quickly sawn from one of the 'green' discs from each log.

b Cylindrical specimens were cut with the hollow drill from each of these sticks (as described in section 6.3.1.1 above). During cutting of these specimens, the sticks were kept immersed in water, to prevent frictional heating and drying.

c The 'sap' from these specimens was exchanged for ethanol by storage in pure ethanol for 5 days. (Each day the resulting ethanol/sap mixture was replaced by fresh alcohol).

d After 5 days the alcohol was replaced by acetone using a similar technique.

e Finally, after 5 days' acetone storage, the acetone was replaced by hexane.

f Hexane was allowed to evaporate by open storage in the laboratory.

This technique has been shown to retain sapwood bordered pit membranes in the green (unaspirated) condition (Thomas 1969). The method retains wood, after drying, in a part swollen condition (Stamm 1964). To bring such solvent dried specimens to the shrunken condition, they were cycled a few times between 0 and $\sim$ 25 per cent moisture content, by exposure alternately to a relative humidity of 0% and 90% (measurement of tangential dimension with a micrometer showed this technique to cause normal shrinkage, about 5%, upon drying).

6.3.1.3 ADJUSTMENT OF SPECIMEN MOISTURE CONTENT

Specimens prepared as described in sections 6.3.1.1 and 6.3.1.2 were swollen by conditioning to various moisture contents within the hygroscopic range of wood. This conditioning was achieved by vacuum storage of specimens at 25^{o}C over phosphorus pentoxide (for the nominally dry condition) and over various saturated salt solutions for other moisture contents (see Table 6.1 below).

Table 6.1 MOISTURE CONTENT CONDITIONING DATA

Conditioning agent	Effective 'relative humidity' (%)	Approximate moisture content (%)
Phosphorus pentoxide (anhydrous)	0	<2
Magnesium chloride (saturated solution)	33	7
Sodium nitrite (saturated solution)	64	11
Potassium sulphate (saturated solution)	97	25

The saturated solutions used to condition the atmospheres are those recommended in a review of humidity control technique by Young (1967).

6.3.1.4 IMPREGNATION OF SPECIMENS WITH HEXANE

Specimens conditioned to various moisture contents, as described in section 6.3.1.3 above were impregnated with dry hexane. The vacuum impregnation technique used was almost identical to that described for the impregnation of dry specimens (section 5.2). To minimise the risk of moisture content change during impregnation, a quantity of the appropriate saturated salt solution (in place of phosphorus pentoxide) was contained in the vacuum desiccator (Figure 5.3) during impregnation of moist specimens.

6.3.2 FLOW MEASUREMENT

After impregnation with hexane the specimens were mounted in a modified form of the apparatus described in section 5.2. To accommodate the dimensional change associated with change in moisture content a different specimen mounting system from that shown in Figure 5.1 (section 5.2) was adopted. The cylindrical specimens described in sections 6.3.1.1 and 6.3.1.2 were held in neoprene tubing, tightened by

compression with nylon straps (see Figure 6.5).

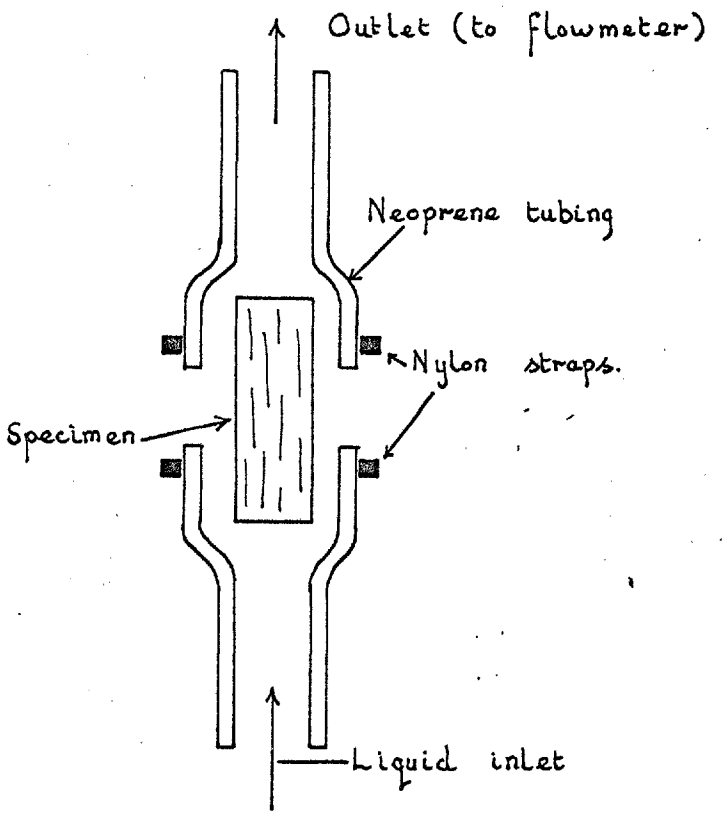


Fig 6.5 SPECIMEN MOUNTING IN NEOPRENE TUBING

Flow rate was measured under small pressure differentials ($\sim$ 3-4 x 10^4 dyn cm^{-2}), with the burette flowmeter, using the technique described previously (section 5.2).

6.3.3 SWELLING MEASUREMENT

From the radially orientated sticks described in section 6.3.1.1 obloid specimens suited to the measurement of radial and tangential swelling, were cut (Figure 6.6).

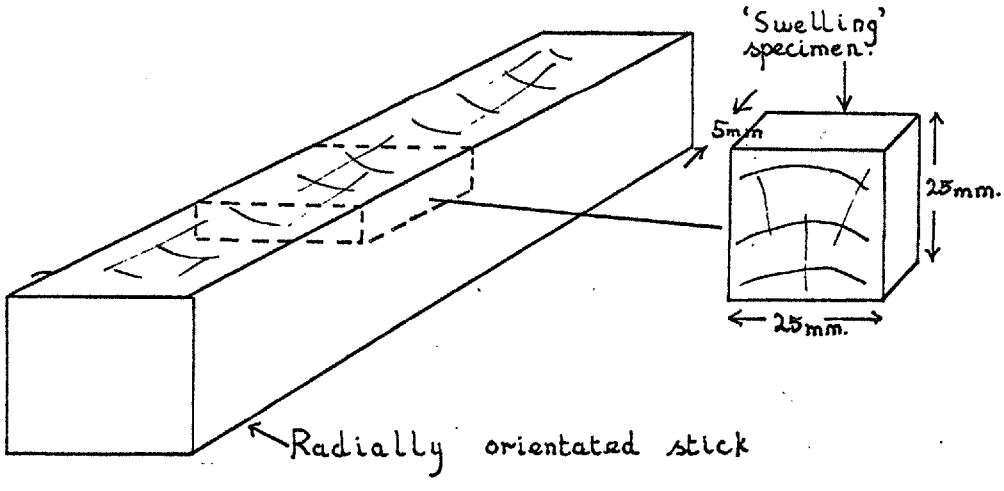


Fig 6.6 PREPARATION OF SPECIMENS FOR SWELLING MEASUREMENT

These 'obloid' specimens were air dried slowly in controlled humidity rooms, and finally vacuum dried over phosphorus pentoxide. Swelling in atmospheres over the various conditioning agents (Table 6.1) was measured with linear displacement transducers mounted in specially designed glass vacuum jars (see Figure 6.7).

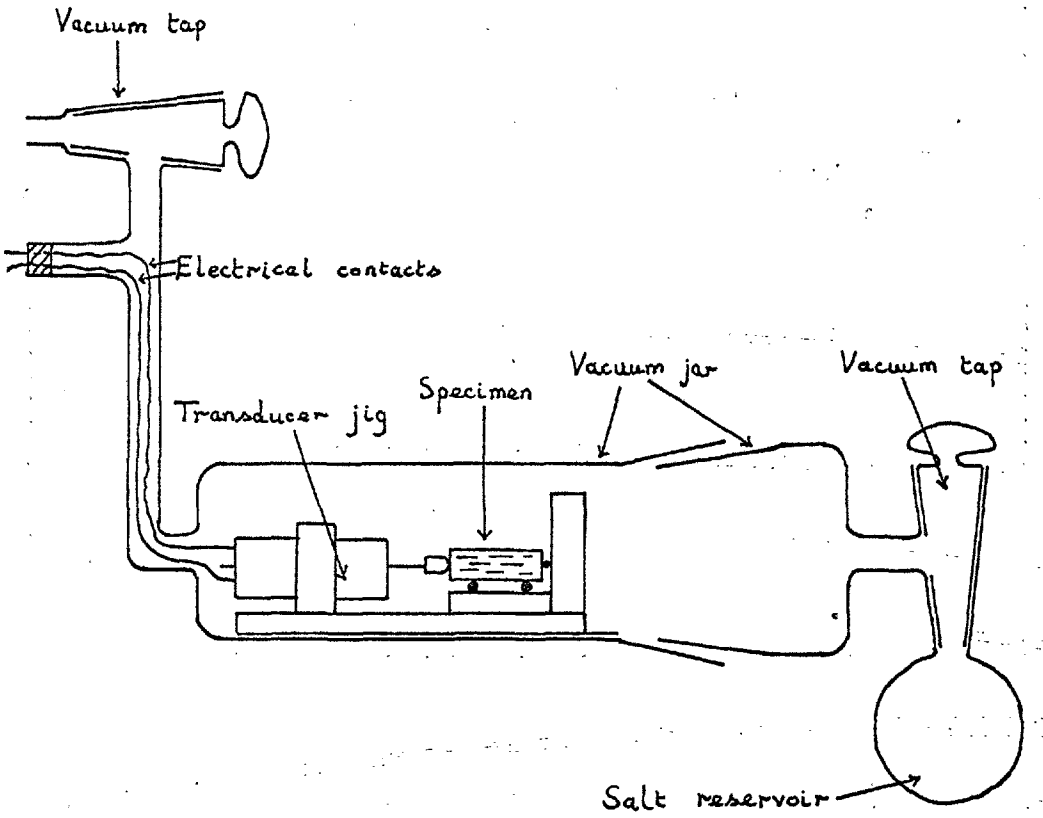


Fig 6.7 VACUUM APPARATUS TO MEASURE SWELLING IN VAPOUR

The vacuum jar is made in two parts, connected by a ground glass conical joint. At one end a salt reservoir is located which may be isolated from the specimen with a vacuum tap. A jig to hold the transducer and specimen (shown in Figure 6.8) is contained within the jar, electrical contact between the transducer and its associated energising and output recording equipment being by way of leads sealed into the glass with a rubber plug.

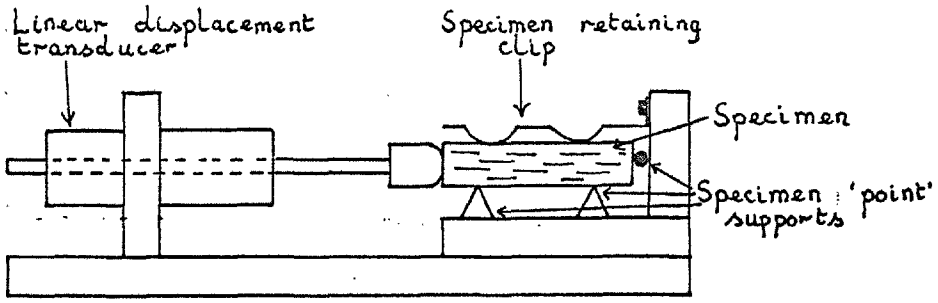


Fig 6.8 SPECIMEN AND TRANSDUCER JIG FOR MEASUREMENT OF SWELLING IN VAPOUR

Dry specimens were measured carefully with a micrometer and then mounted in the specimen jig. The conditioning salt solution was transferred to the salt reservoir and the reservoir isolated from the specimen. Whilst maintained in a thermostat at 25 ± 0.5°C the jar was evacuated and the transducer output monitored. The salt reservoir was then connected to the specimen jar and the apparatus maintained in the thermostat until attainment of equilibrium dimension. This procedure was repeated for each of the conditioning salts in turn.

The whole procedure was conducted using specimens from both the logs described in section 6.3.1.

6.3.4 RESULTS AND DISCUSSION

For clarity and convenience the specimens used throughout this part are labelled according to the code shown below:-

'a H/S b'

where 'a' = log number (1 or 2)
H = heartwood
S = sapwood
b = specimen reference number

6.3.4.1 HEXANE FLOW THROUGH MOIST 'AIR DRIED' WOOD

From the flow data obtained using the techniques described in sections 6.3.1- specimen permeability constants were calculated according to equation 5.1:-

$$K_V = \frac{Q\eta}{\Delta P} \qquad \text{Equation 5.1}$$

where Q = volume rate of flow
η = liquid viscosity
ΔP = pressure differential across specimen

These data for the various specimens examined are given below (Table 6.2).

Table 6.2 PERMEABILITY CONSTANTS FOR *Abies grandis* SAPWOOD AND HEARTWOOD AT VARIOUS MOISTURE CONTENTS

Specimen	Specimen permeability constant 'K_V' ($cm^3 \times 10^8$) at listed moisture contents			
	<2%	7%	11%	25%
1S1	0.048	0.041	0.036	0.030
1S2	0.016	0.017	0.015	0.016
2S1	0.045	0.036	0.031	0.022
1H1	0.059	0.053	0.040	0.023
1H2	0.145	0.124	0.103	0.078
2H1	0.053	0.048	0.037	0.025
2H2	0.035	0.032	0.025	0.018

It can be seen from Table 6.2 that the between-specimen variation in permeability constant, at any moisture content is quite large. To make 'between specimen' comparison of the moisture content effect easier, therefore, the data are re-expressed as dimensionless relative values (setting the value obtained at <2% moisture content for each specimen, equal to 1). These relative values are given below in Table 6.3.

Table 6.3 RELATIVE PERMEABILITY OF *Abies grandis* SAPWOOD AND HEARTWOOD SPECIMENS AT VARIOUS MOISTURE CONTENTS

Specimen	Relative permeability at listed moisture contents			
	<2%	7%	11%	25%
1S1	1.00	0.85	0.75	0.63
1S2	1.00	1.06	0.94	1.00
2S1	1.00	0.80	0.69	0.49
1H1	1.00	0.90	0.68	0.39
1H2	1.00	0.86	0.71	0.54
2H1	1.00	0.91	0.70	0.47
2H2	1.00	0.91	0.71	0.51
Mean	1.00	0.90	0.74	0.58

From Table 6.3 it is clear that on the average, permeability decreases markedly with increase in moisture content. For individual specimens, the effect is consistent except for the sapwood specimen 1S2. The permeability of this specimen remained almost constant at all moisture contents. Later evidence (see below) suggests that this may have been due to two conflicting effects: (1) permeability reduction associated with moisture content increase, and (2) permeability increase due to dissolution of cell debris during the impregnation process (see sections 6.3.1.3 and 6.3.1.4). Reversibility of the trend suggested in Table 6.3 was investigated by cycling the specimen moisture content alternately between <2 and 25 per cent moisture content. At each of these moisture contents in turn, permeability was measured using the technique described. Results, expressed as

'relative permeability' are given below in Table 6.4.

Table 6.4 RELATIVE PERMEABILITY - EFFECT OF MOISTURE CYCLING

Specimen	Relative permeability at listed moisture contents					
	1st cycle*		2nd cycle		3rd cycle	
	<2%	25%	<2%	25%	<2%	25%
1S1	1.00	0.63	1.30	0.68	1.34	0.70
1S2	1.00	1.00	2.13	1.06	2.19	1.19
2S1	1.00	0.49	1.36	0.55	1.36	0.61
1H1	1.00	0.39	1.34	0.45	1.67	0.50
1H2	1.00	0.54	1.30	0.65	1.46	0.68
2H1	1.00	0.47	1.35	0.50	1.60	0.56
2H2	1.00	0.51	1.44	0.56	1.68	0.53
Mean	1.00	0.58	1.46	0.64	1.61	0.68

*The '1st cycle' data are obtained from Table 6.3 above

The data of Table 6.4 indicate that after the first cycle, permeability decreases mainly reversibly with increase in moisture content. This is particularly true for sapwood specimens. In heartwood, it seems that a small irreversible increase occurs at each moisture content during the second and third cycles. All specimens (sap and heart) show some irreversible permeability increase between cycles '1' and '2'. This is particularly marked for specimen '1S2', where the effect 'masks' any decrease in permeability associated with moisture increase. It seems most likely that this irreversible effect is due to gradual removal of petrol soluble debris (extractives) from cells and pits, during repeated impregnation at the various moisture contents. This view is supported by the appearance of pit membranes in *Abies grandis*, before and after extraction with n.hexane (see Figure 6.9).

The scanning electron micrographs of Figure 6.9 are of heartwood early wood 'bordered pits'. In the pit of the unwashed specimen, fibrillar detail is obscured by an

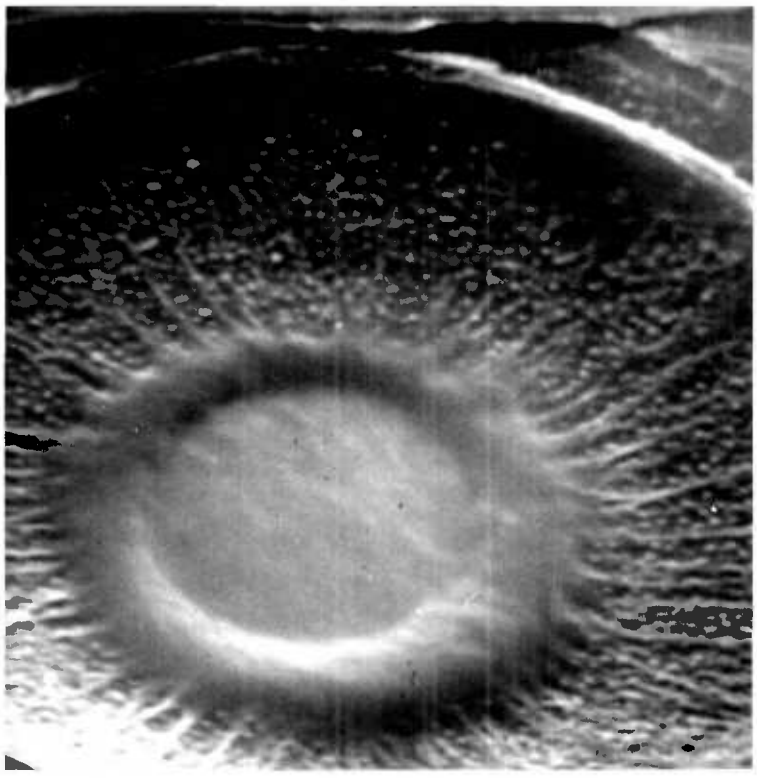


Fig 6.9a *Abies grandis* HEARTWOOD (NON WASHED) (x 7500)

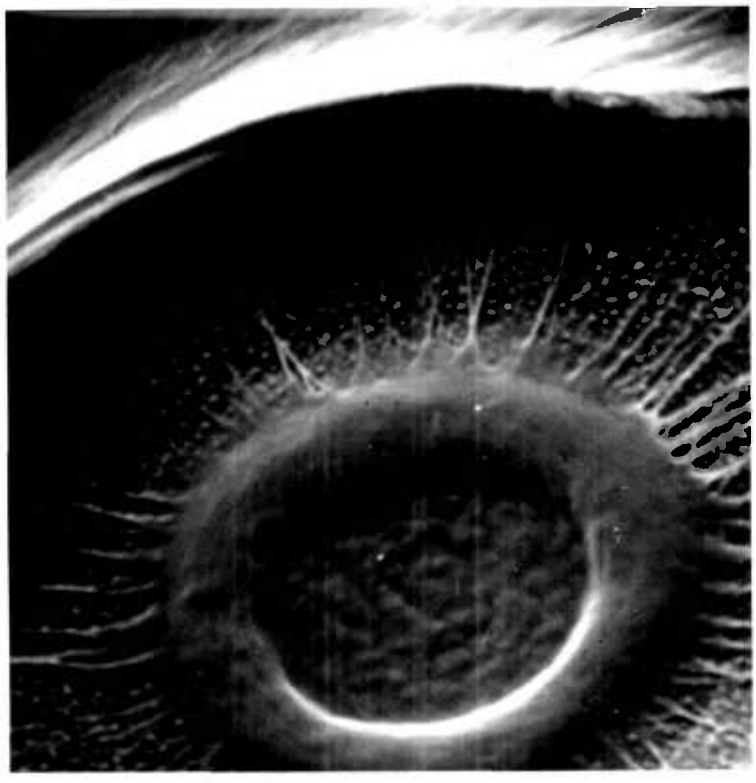


Fig 6.9b *Abies grandis* HEARTWOOD (HEXANE WASHED) (x 8000)

apparently amorphous deposit. Pit structure in the closely matched hexane washed specimen is much more clearly defined (NB solvent washing was carried out by heating prepared specimens in hexane, under reflux). This suggests that hexane is able to remove some extractive material from pit membranes. Such removal may be expected to bring about significant increase in permeability.

6.3.4.2 HEXANE FLOW THROUGH SOLVENT DRIED WOOD

As for air dried specimens (section 6.3.2.1), results are expressed as 'specimen permeability constants', calculated according to equation 5.1 (see section 6.3.2.1 above). Permeability was measured at each of the moisture contents listed in section 6.3.1.3 (Table 6.1). To check reversibility, after flow rate measurement at 25 per cent moisture content, the specimens were re-dried to <2 per cent, and permeability was re-measured. Results obtained are given below, Table 6.5.

Table 6.5 PERMEABILITY OF SOLVENT DRIED SPECIMENS AT VARIOUS MOISTURE CONTENTS

Specimen	Specimen permeability constant 'K_v' at listed moisture contents ($cm^3 \times 10^8$)				
	<2%	7%	11%	25%	<2%
1S3	2.44	1.99	1.83	1.58	1.99
1S4	2.75	2.34	1.99	1.73	2.14
2S3	2.14	1.58	1.38	1.38	1.53
2S4	1.33	1.17	1.14	0.94	1.12

For ease in comparison, the above data are re-expressed as dimensionless 'relative permeability' values (see section 6.3.2.1) and listed in Table 6.6 below.

Table 6.6 'RELATIVE PERMEABILITY' OF SOLVENT DRIED WOOD

Specimen	'Relative permeability' at listed moisture contents				
	1st cycle				2nd cycle
	<2%	7%	11%	25%	<2%
1S3	1.00	0.82	0.75	0.65	0.82
1S4	1.00	0.85	0.72	0.63	0.78
2S3	1.00	0.74	0.64	0.64	0.72
2S4	1.00	0.88	0.86	0.71	0.84
Mean	1.00	0.82	0.74	0.66	0.79

It is seen from Table 6.6 that permeability decreases with increase in moisture content. Re-drying leads to significant recovery of permeability, but to a considerably lower level than attained on the first measurement in the dry state (cf 1st and 2nd cycle measurements at <2% moisture content).

It has been shown by Huber and Merz (1958), that in the unaspirated condition, pit membranes are sensitive to very small applied pressure gradients (of the order of 0.5 bar/m). In this work pressure gradients of this magnitude were applied during flow measurements, whilst during vacuum impregnation, the initial pressure gradients applied to specimens upon vacuum release, far exceeded this value. It seems possible, therefore, that the irreversible part of the observed decrease in permeability is due to displacement, particularly of early wood pit membranes, from a central position within the pit chamber to form a more or less effective seal against one of the pit openings (see section 1.5.1, Figure 1.4).

Between <2 and 25 per cent moisture content it appears that solvent dried wood is subject to a reversible decrease in permeability of some 16 to 17 per cent (cf average relative

permeability obtained at 25 per cent moisture content and at <2 per cent moisture content '2nd cycle'). It can be seen that the results obtained from the four individual specimens are fairly consistent, the range of the reversible permeability decrease extending from 11 per cent (specimen 2S3) to 21 per cent (specimen 1S3).

6.3.4.3 SWELLING DUE TO MOISTURE SORPTION

Swelling associated with conditioning to the various test moisture contents was measured by the technique described in section 6.3.1.6. Data from these measurements expressed as percentage linear increase in dimension (based on specimen dry dimension) are tabulated below (Table 6.7).

Table 6.7 SWELLING OF DRY *Abies grandis* DUE TO MOISTURE SORPTION

Moisture content (per cent)	Swell (per cent dry dimension)					
	Tangential			Radial		
	Specimen 1	Specimen 2	Mean	Specimen 1	Specimen 2	Mean
<2	0.0	0.0	0.0	0.0	0.0	0.0
7	0.6	1.1	0.9	0.7	0.7	0.7
11	2.0	1.9	2.0	1.2	1.4	1.3
25	4.2	4.4	4.3	2.5	2.6	2.6

From the linear swell data of Table 6.5, volumetric swell was calculated (assuming that longitudinal swelling is negligible). These data are given below (Table 6.8).

Table 6.8 VOLUMETRIC SWELL DUE TO MOISTURE SORPTION

Moisture content (per cent)	Mean volumetric swell (per cent of dry volume)
<2	0.0
7	1.6
11	3.3
25	7.0

The data of Table 6.8 show a similar 'moisture content/swell' relationship to other recorded data for softwoods of similar density (see Stamm 1964).

NB The above swelling data were obtained with specimens, air and vacuum dried from green (see section 6.3.1.6). Measurement of solvent dried specimens (section 6.3.1.2) with calipers, at the test moisture contents, showed that these specimens underwent a similar degree of swelling during moisture sorption.

6.4 SWELLING LIQUID FLOW THROUGH DRY WOOD

In this section the measurement of specimen permeability using a range of liquids causing swelling of the non-crystalline zones of cellulose, is described. The liquids used in ascending order of swelling power are listed below:-

a n hexane
b n butanol
c n propanol
d ethanol
e methanol
f water

6.4.1 SPECIMEN PREPARATION

6.4.1.1 CUTTING AND CONDITIONING OF SPECIMENS

From the air dried radial sticks taken from the freshly felled logs (section 6.3.1.1), cylindrical specimens of diameter about 1 cm and length 1.5-2.0 cm were cut, precisely as described for hexane flow specimens (section 6.3.1.1). Two sets of heartwood and two of sapwood specimens were prepared, and labelled according to the code given in section 6.3.4.

One set of heartwood and one of sapwood were vacuum dried over phosphorus pentoxide. The remaining two sets were solvent extracted prior to vacuum drying.

Solvent extraction was carried out to remove hexane and methanol soluble material prior to flow measurement with these liquids. The extraction procedure adopted was as follows:-

a Specimens were vacuum impregnated with a miscible mixture of n.hexane, methanol and acetone.

b Specimens so impregnated were boiled under reflux 8 hours per day for 10 days. Each day the solvent mixture was replaced by fresh liquid to avoid concentration and possible saturation with extractive material. During the 16 hours per day not under reflux, the specimens were allowed to soak in the cold solvent mixture.

c After this period, solvent was allowed to evaporate. To ensure normal shrinkage, specimens were brought to fibre saturation moisture content by exposure to water saturated air for a day, prior to drying.

d Specimens were dried gradually in controlled humidity chambers and finally vacuum dried over phosphorus pentoxide to a moisture content less than 2 per cent.

6.4.2 IMPREGNATION AND FLOW MEASUREMENT

After cutting and drying as described in 6.4.1.1 above, dry specimens were impregnated with n.hexane as described in section 5.2. Rate of flow under small pressure differential was measured using the technique prescribed in section 6.3.2. Upon completion of flow measurement with hexane, specimens were transferred to n.butanol and maintained at n.butanol vapour pressure in a vacuum desiccator for about 24 hours. This allowed some diffusive replacement of n.hexane by n.butanol. Butanol flow rate was then measured using the method described for hexane flow. To ensure virtual complete removal of hexane, care was taken to ensure the flow of about ten times the specimen pore volume, of n.butanol, prior to flow rate measurement.

This procedure was followed for each of the test liquids in turn.

Water was found to cause little further swelling beyond that attained in methanol (see section 6.4.4.2 below). Therefore, because of the experimental difficulty encountered in measuring water flow rate (because of its high viscosity and surface tension), it was omitted from the series of experiments with solvent extracted specimens.

After permeability measurement of solvent extracted specimens with methanol, reversibility of the effect of swelling liquid was checked, by flow measurement alternately with hexane and methanol. During this procedure, care was taken to ensure that specimens were dry and shrunken prior to any measurement with hexane.

6.4.3 MEASUREMENT OF SWELLING CAUSED BY SORPTION OF TEST LIQUIDS

Obloid specimens identical to those described for measurement of swelling by water sorption (section 6.3.3, Figure 6.6) were prepared. These were cut from the same radially orientated sticks used in preparation of permeability specimens (section 6.4.1.1 above). The specimens were dried to about 6 per cent, by exposure at 30% relative humidity and then by evacuation over phosphorus pentoxide. After drying, the specimens were measured accurately with a micrometer and mounted in jigs as shown in Figure 6.10 below.

Specimens in the swelling jigs were immersed in n hexane and swelling observed until the dimension remained constant for a period of 4 hours. Any dimensional change was noted, and then the n hexane was replaced by n butanol. Again dimension change was noted until no further change occurred for 4 hours. This procedure was repeated in turn for the liquid series listed in section 6.4 - radial and tangential swelling being measured with each of the liquids.

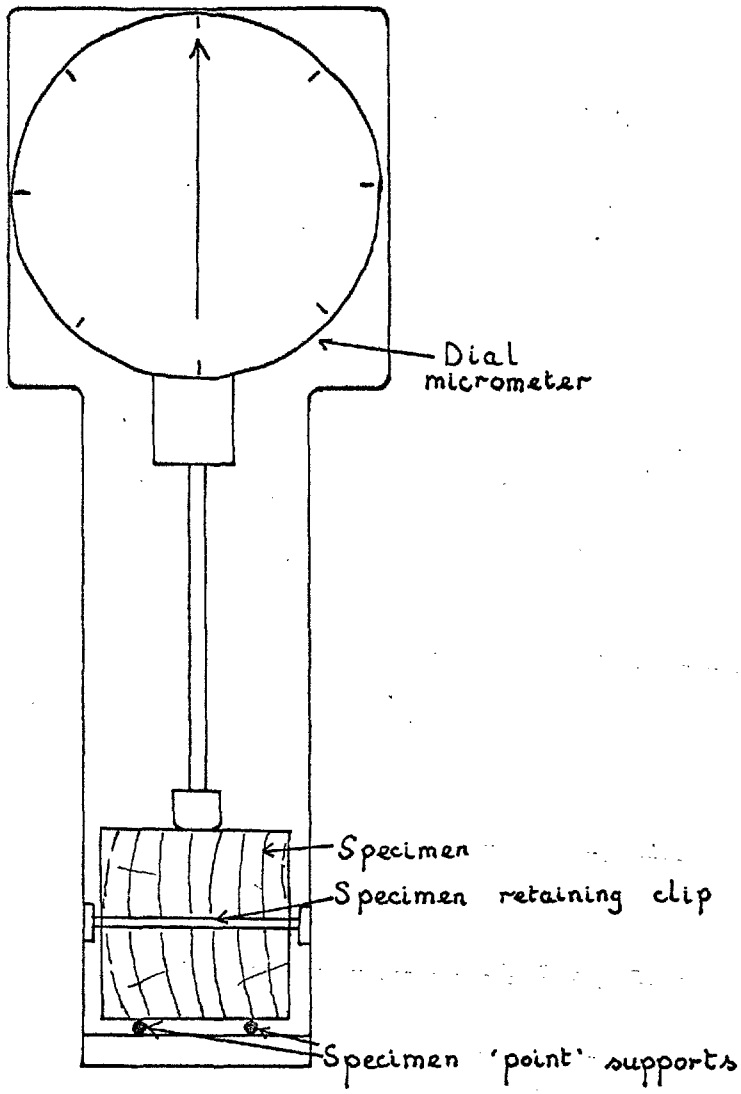


Fig 6.10 DIAL MICROMETER JIG TO MEASURE SWELLING BY IMMERSION IN LIQUIDS

6.4.4 RESULTS AND DISCUSSION

6.4.4.1 PERMEABILITY MEASUREMENT

Throughout this series, rates of flow were measured under pressure differentials of about 5×10^4 dyn cm^{-2} ($\sim$ 0.05 bar). Liquid temperature was maintained at about 25°C, and the viscosities of the various liquids were taken from published tables (Weart, 1973).

The first series of measurements was made using non-solvent washed specimens, specimen permeability constants being calculated according to equation 5.1:-

$$K_V = \frac{Q\eta}{\Delta P} \qquad \text{Equation 5.1}$$

where K_V = specimen permeability constant
Q = volume rate of flow
η = liquid viscosity
ΔP = applied pressure differential

These data are given below (Table 6.9).

Table 6.9 PERMEABILITY TO SWELLING LIQUIDS BEFORE SOLVENT EXTRACTION

Specimen	Specimen permeability constant 'K_V' ($cm^3 \times 10^8$) to listed liquids					
	n hexane	n butanol	n propanol	ethanol	methanol	water
1S5	0.072	0.068	0.053	0.043	0.039	0.043
2S5	0.197	0.179	0.169	0.130	0.112	0.119
2S6	0.221	0.204	0.196	0.150	0.162	0.133
1H3	0.074	0.069	0.054	0.052	0.077	0.089
1H4	0.052	0.047	0.041	0.037	0.063	0.081
2H3	0.069	0.062	0.054	0.053	0.100	0.150
2H4	0.055	0.053	0.046	0.039	0.057	0.081

From the above Table it can be seen that permeability decreases through the liquid series n.hexane to ethanol. However, measurement with the final two liquids in the series (methanol

and water) leads to some increase in permeability. This effect is particularly marked with the heartwood specimens (1H3, 1H4, 2H3, 2H4). In any porous medium, viscous flow permeability can be increased only by increase in number or effective diameter of flow controlling pores. Swelling due to water sorption causes permeability decrease (see section 6.3.4). In the present series, swelling caused by sorption of n.butanol, n.propanel and ethanol, also seems to be accompanied by permeability decrease. It seems inconsistent, therefore, that the further swelling due to sorption of methanol and of water (see section 6.4.4.2 below) should cause some increase in permeability. The observed increase seems likely, therefore, to be due to changes in pore geometry other than those due to cell wall swelling. Such changes are most likely due to removal of incrustant material or to de-aspiration of pit membranes (ie breaking of the seal between torus and border - see section 2.2). Consequently, permeability to n hexane and the series of alcohols was measured for a further set of specimens, pre-treated by solvent extraction with a mixture of hexane, methanol and acetone (section 6.4.4.1).

Results obtained for these specimens are given below (Table 6.10).

Table 6.10 PERMEABILITY OF SOLVENT EXTRACTED SPECIMENS TO SWELLING LIQUIDS

Specimen	Specimen permeability constant 'K_V' ($cm^3 \times 10^8$)				
	n hexane	n butanol	n propanol	ethanol	methanol
1S6	0.069	0.050	0.036	0.023	0.016
2S7	0.037	0.022	0.014	0.009	0.008
1H5	0.062	0.059	0.035	0.020	0.017
1H6	0.149	0.127	0.088	0.059	0.053
2H5	0.065	0.053	0.031	0.018	0.014
2H6	0.117	0.090	0.060	0.044	0.040

The data of Table 6.10 show a much more consistent decrease in permeability through the liquid series, after solvent extraction. Reversibility of this observed effect was checked

by measurement of permeability alternately with n hexane and methanol, as described in section 6.4.2. Data from this experiment expressed as 'relative permeability', taking the first 'n. hexane' value for each specimen equal to '1' (see section 6.3.4.1 above) are given below (Table 6.11).

Table 6.11 RELATIVE PERMEABILITY TO n HEXANE AND METHANOL

Specimen	Relative permeability to stated liquid				
	1st cycle		2nd cycle		3rd cycle
	Hexane	Methanol	Hexane	Methanol	Hexane
1S6	1.00	0.24	0.94	0.26	0.93
1S7	1.00	0.21	1.03	0.20	1.03
1H5	1.00	0.27	1.32	0.29	1.56
1H6	1.00	0.36	1.14	0.32	1.27
2H5	1.00	0.22	1.13	0.20	1.39
2H6	1.00	0.34	1.07	0.29	1.23
Mean	1.00	0.27	1.11	0.26	1.24

From the data of Table 6.11 it can be seen that the decrease in permeability measured with methanol compared with the value obtained for hexane flow, is largely reversible. For sapwood specimens (1S6 and 1S7) the reversibility is almost complete. In the case of heartwood (1H5, 1H6, 2H5, 2H6) a small irreversible increase in permeability is observed as flow proceeds. Heartwood is known to contain more extractive material than sapwood (see section 3.3.6). It is likely that the solvent extraction procedure carried out prior to flow experiments, may not have completely removed this material. During the flow experiments, such extractive substances are likely to be removed by the action of the flowing liquids.

It is believed, therefore, that the more consistent behaviour to swelling liquid flow after solvent washing (compare Tables 6.9 and 6.10) is due to removal of extractive material. After such treatment permeability is affected mainly by decrease in size and/or number of pores associated with sorption of test liquid by the cell wall. In specimens not pre-extracted with solvent two conflicting processes seem likely to occur:-

a Pore size and/or number is decreased by sorption of swelling liquids.

b Pore size and/or number is increased by removal of extractives.

This is supported by scanning electron microscopic evidence. In specimens taken from heartwood prior to solvent extraction, pit membrane detail was ill defined due to the presence of apparently amorphous substance, coating the margo. Solvent extraction with hexane appeared to remove some of this substance, making margo structure somewhat more clearly defined (see Figure 6.9, section 6.3.4). Further washing with methanol brought about great clarity of membrane structural detail (Figure 6.11), suggesting the further removal of extractive substances. Additionally the membranes of many pits after methanol extraction seem to have been partly de-aspirated and degraded (Figures 6.11 and 6.12). In the pit shown in Figure 6.11, there is a distinct impression of the border impressed on to the torus, suggesting that it has been tightly aspirated. However, the margo appears to be partially detached from the border, suggesting that it is only partially and lightly aspirated. The membranes of the two pits shown in Figure 6.12 seem to have been weakened by methanol treatment and to have fractured. These two effects were observed in a high proportion of pits in methanol extracted wood and are in contrast to the generally intact and tightly aspirated appearance of pits in non-washed and hexane washed wood (Figure 6.9).

It has been shown by Bauch, Liese and Schulz (1968) that phenolic, lignin or lignin-like compounds are present in the heartwood pit membranes of *Abies alba* (a closely related species to *Abies grandis*). In a later study (Bauch and Berndt, 1973) spectral and histochemical techniques were used to show the presence of phenolic substances in both sapwood and heartwood pit membranes of four *Abies* species including those of *A. grandis*. These workers showed that a proportion of this material is removed by extraction with ethanol/benzene mixture. Thus, it seems likely that the observed pit

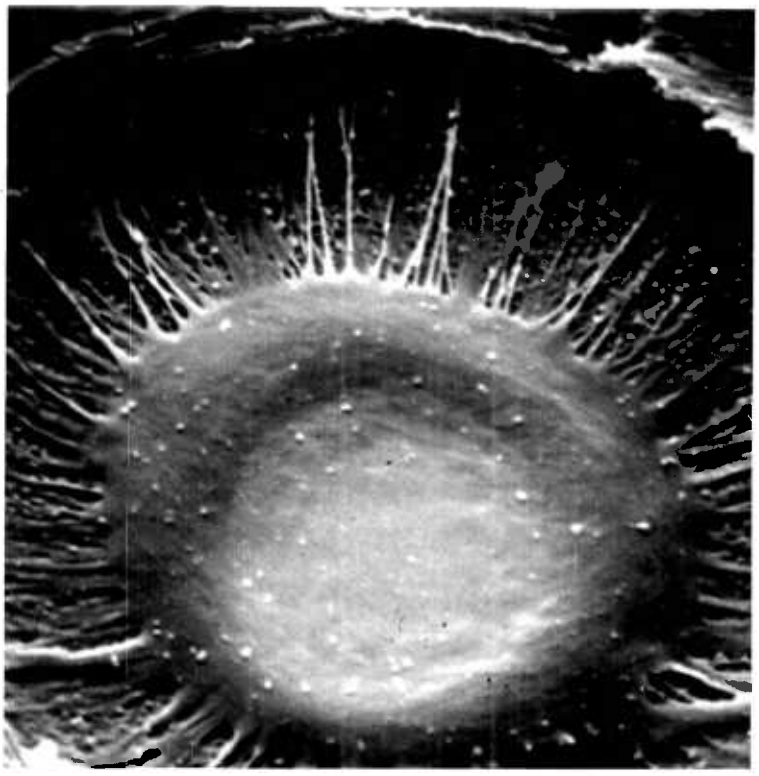


Fig 6.11 *Abies grandis* HEARTWOOD (METHANOL WASHED) (x 8000)



Fig 6.12 *Abies grandis* HEARTWOOD (METHANOL WASHED) (x 3000)

membrane structural changes described above (Figures 6.9, 6.11 and 6.12) caused by extraction with methanol, may be due to removal of such polyphenolic substances.

6.4.4.2 SWELLING MEASUREMENT

Linear swelling radially and tangentially due to sorption of the test liquids, was measured by the technique described in section 6.4.3. These data, expressed as percentage linear swell, based on dry dimension are recorded below (Table 6.12).

Table 6.12 SWELLING OF DRY *Abies grandis* DUE TO SORPTION OF VARIOUS LIQUIDS

Replacement liquid	Linear swell (per cent of dry dimension)					
	Tangential			Radial		
	Specimen 1	Specimen 2	Mean	Specimen 1	Specimen 2	Mean
n.hexane	0.0	0.0	0.0	0.0	0.0	0.0
n.butanol	3.0	3.2	3.1	0.8	0.6	0.7
n.propanol	3.6	4.0	3.8	1.8	1.5	1.7
ethanol	4.4	4.8	4.6	2.0	1.7	1.9
methanol	4.9	5.4	5.2	2.3	1.9	2.1
water	5.4	5.8	5.6	2.5	2.0	2.3

As in the case of swelling due to water vapour sorption (section 6.3.4.3), volumetric swell was calculated from the above data, assuming that longitudinal swelling is insignificant (see Table 6.13 below).

Table 6.13 VOLUMETRIC SWELL OF DRY *Abies grandis* DUE TO SORPTION OF VARIOUS LIQUIDS

Liquid	Volumetric swell (per cent of dry volume)
n.hexane	0.0
n.butanol	3.8
n.propanol	5.6
ethanol	6.6
methanol	7.4
water	8.0

The data of Tables 6.12 and 6.13 are in general agreement with published results for swelling of softwoods by aliphatic alcohols and water (see, for example, Browning, 1963; Stamm, 1964). Immersion in a non-polar liquid (n·hexane) caused no swelling, the degree of swelling in alcohols, increasing with decrease in chain length (and hence polarity).

6.5 LIQUID FLOW THROUGH GREEN WOOD

It is known that the pore structure of softwood, particularly of sapwood is significantly altered by initial drying from the green state. In freshly felled, 'green' wood almost all bordered pits are in the conducting 'non-aspirated' condition. During drying, however, most pits, especially in early wood, are aspirated (see section 2.2). In this section the measurement of permeability of 'green' *Abies grandis* to a range of swelling liquids, is described.

6.5.1 SPECIMEN PREPARATION

Cylindrical specimens of sapwood and heartwood were cut from discs taken from each of the two freshly felled logs and stored in ethanol/water mixture (see section 6.3.1). These specimens were cut with the hollow drill as described for air dry specimens (section 6.3.1.1), and labelled in accord with the code described in section 6.3.4. During cutting of green specimens, the discs were kept immersed in water to prevent drying due to frictional heating (as in the preparation of specimens for solvent exchange drying (section 6.3.1.2). Prior to flow measurement, specimens were end trimmed with a sharp razor blade to a length of 1.5 to 2.0 cm. Trapped air in these specimens was replaced by immersion in de-ionised water, cleaned by filtration through a membrane filter of 0.2 micron, pore size. Whilst maintaining the specimens immersed in water, the specimens were subjected alternately to reduced pressure (water vapour pressure) and atmospheric pressure. This procedure was carried on until few air

bubbles could be observed leaving the specimens during the reduced pressure periods. Thus as much air as possible was replaced by water.

6.5.2 FLOW MEASUREMENT

Flow rate of water through specimens impregnated with water, as described in section 6.5.1 above was measured by the technique described for hexane flow (section 6.3.2). After completion of water flow measurement, the water saturated specimens were transferred to membrane filtered methanol and stored in vacua overnight to allow solvent exchange by diffusion. Flow rate of methanol was monitored using the same technique as for water flow, and the process was repeated in turn for each of the liquids:-

Water
Methanol
Ethanol
n.propanol
n.butanol

6.5.3 MEASUREMENT OF DIMENSIONAL CHANGE DUE TO LIQUID EXCHANGE

Shrinkage during exchange of water for the various alcohols listed in section 6.5.2 was measured using wafer specimens cut from the same discs as the cylindrical permeability specimens (see section 6.5.1). These specimens were prepared precisely as those used in the determination of swelling of dry wood (section 6.3.3). Linear tangential and radial dimensions were measured by micrometer and the specimens were placed in the jigs described in section 6.4.3 (Figure 6.10). These wet specimens in the jigs were immersed in methanol for 24 hours. During this period the methanol in the jar was replaced twice with fresh pure liquid, to maintain low water content conditions. Shrinkage tangentially and radially (using separate specimens) during soaking in methanol was measured and the

procedure was repeated in turn for each of the liquids listed in section 6.5.2.

6.5.4 RESULTS AND DISCUSSION

6.5.4.1 PERMEABILITY MEASUREMENT

As for swelling liquid flow through dry wood (section 6.4.4.1), flow rates were measured under small pressure differential ($\sim 5 \times 10^{-4}$ dyn cm^{-2}) conditions. Liquid temperature was maintained at about 25°C, and the liquid viscosities at the precise temperature during flow, were obtained from tables (see section 6.4.4.1). Results are expressed as specimen permeability constants (K_V):-

$$K_V = \frac{Q\eta}{\Delta P} \qquad \text{Equation 5.1}$$

where Q = volume rate of flow
η = liquid viscosity
ΔP = pressure differential causing flow.

These data, calculated from the flow measurements described in section 6.5.2, are given below (Tables 6.14 and 6.15).

Table 6.14 PERMEABILITY OF 'GREEN' SAPWOOD TO VARIOUS LIQUIDS

Specimen	Specimen permeability 'K_V' ($cm^3 \times 10^8$) measured with stated liquids				
	Water	Methanol	Ethanol	n.propanol	n.butanol
1S8	0.021	0.075	0.070	0.070	0.060
1S9	0.278	0.321	0.327	0.339	0.350
2S8	0.433	0.487	0.481	0.499	0.519
2S9	0.627	0.641	0.669	0.683	0.676

Table 6.15 PERMEABILITY OF 'GREEN' HEARTWOOD TO VARIOUS LIQUIDS

Specimen	Specimen permeability 'K_v' ($cm^3 \times 10^8$) measured with stated liquids				
	Water	Methanol	Ethanol	n.propanol	n.butanol
1H8	0.087	0.223	0.243	0.257	0.266
1H9	0.023	0.088	0.089	0.099	0.099
2H8	0.142	0.284	0.287	0.309	0.319
2H9	0.004	0.015	0.022	0.024	0.027

Inspection of the Tables suggests some increase in permeability associated with decrease in the polar character of the test liquids. The effect is confused to some extent by the large 'between specimen' variability in permeability. To help overcome this confusion, as in the case of dried specimens (section 6.4.4.1), the data of Tables 6.14 and 6.15 are re-expressed as relative permeability values - setting the water flow value for each specimen equal to 1. These relative data are given in Tables 6.16 and 6.17 below.

Table 6.16 RELATIVE PERMEABILITY OF 'GREEN' SAPWOOD TO VARIOUS LIQUIDS

Specimen	Relative permeability to stated liquid				
	Water	Methanol	Ethanol	n.propanol	n.butanol
1S8	1.00	3.57	3.33	3.33	2.86
1S9	1.00	1.15	1.18	1.22	1.26
2S8	1.00	1.12	1.11	1.15	1.20
2S9	1.00	1.02	1.07	1.09	1.08
Mean	1.00	1.72	1.67	1.70	1.60

Table 6.17 RELATIVE PERMEABILITY OF 'GREEN' HEARTWOOD TO VARIOUS LIQUIDS

Specimen	Relative permeability to stated liquid				
	Water	Methanol	Ethanol	n.propanol	n.butanol
1H8	1.00	2.56	2.79	2.95	3.06
1H9	1.00	3.83	3.87	4.30	4.30
2H8	1.00	2.00	2.02	2.18	2.25
2H9	1.00	3.75	5.50	6.00	6.75
Mean	1.00	3.04	3.55	3.86	4.09

From these re-expressed data it becomes clear that the largest permeability increase occurs with the first solvent exchange (ie from water to methanol). It can also be seen that the increase is much more marked for heartwood than for sapwood specimens. Although not checked microscopically, it seems most likely that this effect is similar to that observed during flow of the same liquid series through air dried wood (section 6.4.4.1). There it was observed that methanol was most effective in the removal of extractive material from pit membranes especially from heartwood, and also appeared to cause some de-aspiration of pits (see Figures 6.11 and 6.12 - section 6.4.4.1).

After this initial increase in permeability associated with change from water to methanol flow, permeability of sapwood remains almost constant, irrespective of the liquid used for flow measurement. In heartwood (Table 6.17), permeability continues to increase through the series, ethanol-n.propanol-n.butanol, although to a much smaller extent than in the initial water-methanol step.

Reversibility of these observed effects of the various liquids on permeability was checked, by re-measurement of flow rate with each liquid in reverse order. These data, expressed as relative permeability values (with the n.butanol values from Tables 6.16 and 6.17, for comparison) are given below (Tables 6.18 and 6.19).

Table 6.18 RELATIVE PERMEABILITY OF 'GREEN' SAPWOOD TO VARIOUS LIQUIDS

Specimen	Relative permeability to stated liquid				
	n.butanol	n.propanol	ethanol	methanol	water
1S8	2.86	3.00	2.76	3.57	3.19
1S9	1.26	1.14	1.07	1.19	1.05
2S8	1.20	1.11	1.09	1.10	1.03
2S9	1.08	1.09	1.02	1.08	0.99
Mean	1.60	1.59	1.49	1.74	1.57

Table 6.19 RELATIVE PERMEABILITY OF 'GREEN' HEARTWOOD TO VARIOUS LIQUIDS

Specimen	Relative permeability to stated liquid				
	n.butanol	n.propanol	ethanol	methanol	water
1H8	3.06	2.85	2.81	2.92	2.56
1H9	4.30	3.96	3.87	3.74	2.30
2H8	2.25	2.06	2.00	1.99	1.42
2H9	6.75	6.00	6.00	6.25	4.00
Mean	4.09	3.72	3.67	3.73	2.57

Comparison of the data of Tables 6.16 and 6.17 with those of Tables 6.18 and 6.19 indicates that the longer carbon chain length (and less polar) alcohols (butanol, propanol and ethanol) have a reversible effect on permeability - permeability increasing slightly, with increased chain length. Re-introduction of methanol, however, causes an increase in permeability beyond that obtained during the first methanol flow experiment, especially in heartwood specimens. Subsequent water flow leads to significant permeability reduction, but to a level considerably higher than the first water flow value, however (see Tables 6.16 to 6.19). It appears, therefore, that the first exposure to methanol causes a large, irreversible permeability increase, particularly in heartwood. As discussed above, this effect is probably due to dissolution of extractive material, and possibly to some de-aspiration of pits. Additionly a reversible increase in permeability is observed during flow with the series of alcohols and water associated with increase in carbon chain length (or decrease in polarity).

The largest part of this reversible effect is associated with the change from water to methanol. This effect has been further investigated for heartwood. Flow rate through the heartwood specimens was measured alternately with water and methanol, using the technique described in section 6.5.2. Relative permeability data from these experiments are given below (Table 6.20).

Table 6.20 RELATIVE PERMEABILITY TO WATER AND METHANOL

Specimen	Relative permeability to stated liquid			
	1st cycle		2nd cycle	
	Methanol	Water	Methanol	Water
1H8	2.92	2.56	2.98	2.79
1H9	3.74	2.30	2.92	2.63
2H8	1.99	1.42	1.91	1.60
2H9	6.25	4.00	6.25	4.00
Mean	3.73	2.57	3.52	2.76

The data of the Table suggest a significant reversible decrease in permeability to water, compared with that for methanol flow. The difference between the methanol and water flow values is less for the second cycle than for the first. The possible reason for this effect is discussed in the section dealing with the relationship between permeability and swelling of green wood - section 6.6.3.

6.5.4.2 DIMENSIONAL CHANGE

Tangential and radial shrinkage due to replacement of water by alcohols was measured as described in section 6.5.3. Results, expressed as linear shrinkage, based on original, water-swollen dimensions, are tabulated below (Table 6.21).

Table 6.21 LINEAR SHRINKAGE DUE TO REPLACEMENT OF WATER BY ALCOHOLS

Replacement liquid	Linear shrinkage (per cent of water-swollen dimension)					
	Tangential			Radial		
	Specimen 1	Specimen 2	Mean	Specimen 1	Specimen 2	Mean
Water	0.00	0.00	0.00	0.00	0.00	0.00
Methanol	0.18	0.15	0.17	0.04	0.04	0.04
Ethanol	0.21	0.18	0.20	0.08	0.08	0.08
n.propanol	0.21	0.18	0.20	0.08	0.08	0.08
n.butanol	0.34	0.28	0.31	0.08	0.08	0.08

As for swelling of dried specimens (section 6.4.4.2), mean volumetric dimensional change was calculated from the above data, making the assumption that longitudinal shrinkage is insignificant. These calculated data are given below (Table 6.22).

Table 6.22 VOLUMETRIC SHRINKAGE DUE TO REPLACEMENT OF WATER BY ALCOHOLS

Replacement liquid	Mean volumetric shrinkage (per cent of water-swollen volume)
Water	0.00
Methanol	0.21
Ethanol	0.28
n.propanol	0.28
n.butanol	0.39

The data of Tables 6.21 and 6.22 show that measureable and significant shrinkage occurs during replacement of water by the series of aliphatic alcohols. This dimensional change, however, is less than 10 per cent of the change due to swelling of dry wood in a similar alcohol series. This observation is consistent with data reported by Stamm and Hansen (1935). These workers replaced water by alcohol, and alcohol by benzene, and observed an accompanying shrinkage equivalent to about 18-20 per cent of the total shrinkage occurring during drying from water.

It is seen from the data of Table 6.22, that more than half the shrinkage occurring during the solvent exchange process takes place in the replacement of water by methanol. The possible significance of this is discussed in section 6.6.2, dealing with the relationship between permeability and swelling.

6.6 THE RELATIONSHIP BETWEEN PERMEABILITY AND SWELLING

In sections 6.3, 6.4 and 6.5, permeability measurements made with wood specimens swollen by various methods, are described

and discussed. The method of swelling and degree of swelling attained is also commented upon.

In this section, the effect of swelling on permeability is collated and discussed and a mechanism is proposed to explain the observed permeability reduction associated with swelling.

6.6.1 THE EFFECT OF SWELLING ON THE PERMEABILITY OF AIR DRIED WOOD

Air dried wood specimens were swollen by two methods:-

a Exposure to water vapour.

b Exposure to a series of swelling liquids (aliphatic alcohols).

Flow rate through water swollen specimens was measured with n.hexane, and through alcohol swollen wood, with the appropriate alcohol (see sections 6.3.4 and 6.4.4). Swelling induced by exposure to water vapour and to the series of alcohols is recorded in sections 6.3.4.3 and 6.4.4.2.

From the data of Tables 6.3, 6.4 and 6.8 a relationship between 'relative' permeability and degree of swelling may be obtained. This relationship is shown in graphical form in Figure 6.13 below.

In section 6.3.4, it is described how permeability is measured for 3 cycles of moisture content change from <2 to ∿25 per cent. Results for the 3 cycles are given in Figure 6.13. It is shown (section 6.3.4.1) that during the first cycle, hexane flow may bring about a significant removal of extractive material tending to increase permeability and to reduce the magnitude of permeability decrease, associated with moisture sorption. Thus, the true permeability reduction, resulting from moisture content increase from <2 to 25 per cent, is better indicated by the data of the second and third cycles. From Figure 6.13 it can be seen that this reduction,

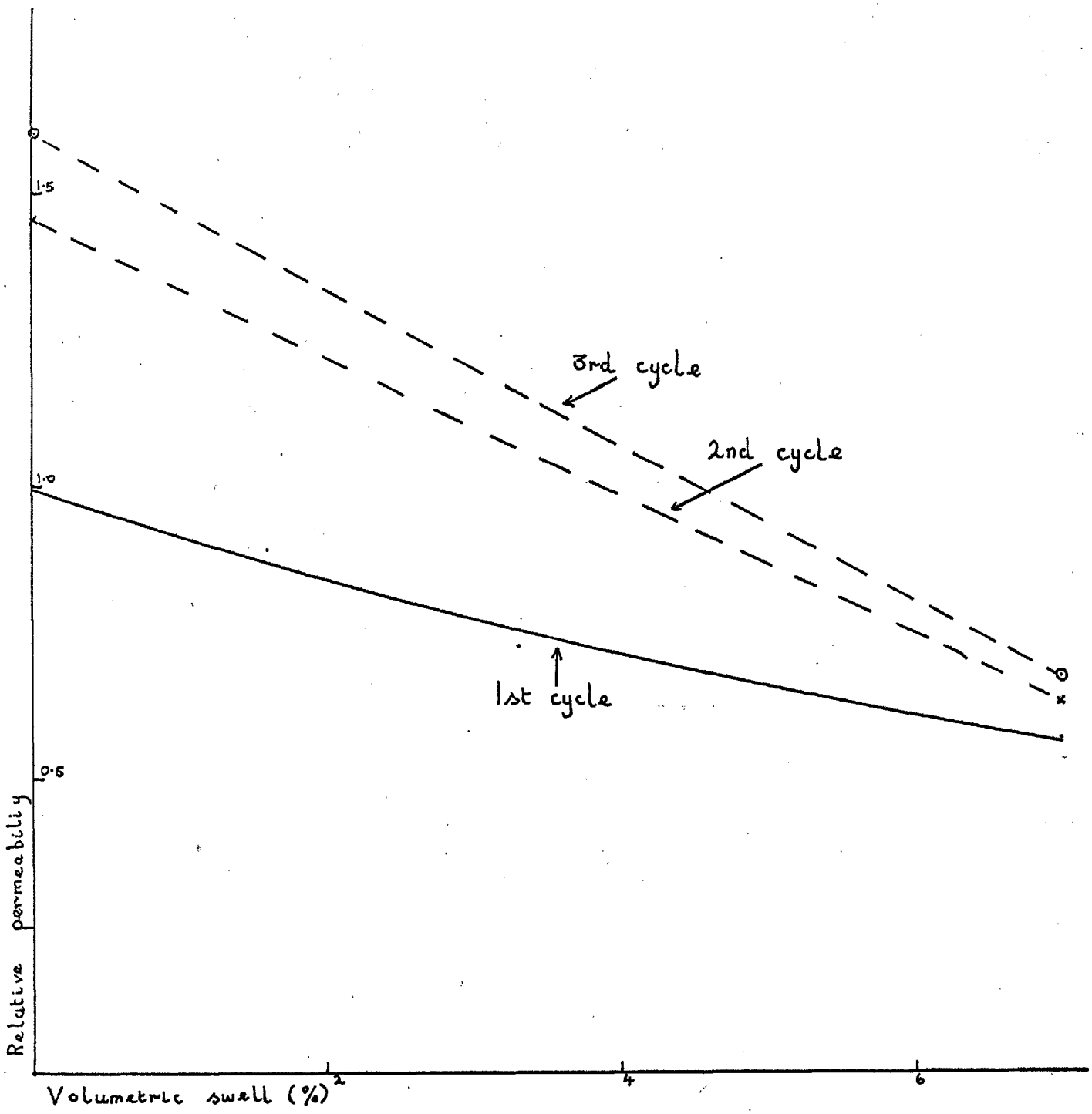


Fig 6.13 RELATIONSHIP BETWEEN PERMEABILITY OF AIR DRIED WOOD AND SWELLING DUE TO MOISTURE SORPTION

associated with about 7 per cent volumetric swell, amounts to some 60 per cent of the non-swollen value.

Similarly, a relationship between permeability and swelling in alcohols may be drawn from the data of Tables 6.10, 6.11 and 6.13 (sections 6.4.4.1 and 6.4.4.2). As for hexane flow through moisture swollen wood (Figure 6.13), data are shown for cycling between the shrunken and swollen state. The relationship is illustrated graphically (Figure 6.14).

Comparison of Figures 6.13 and 6.14 shows a marked similarity in the relationship between permeability and swelling, for specimens swollen by the two methods described. Specimens swollen by sorption of alcohols show a smaller tendency to increase in permeability irreversibly during cycling. This is probably because most of the alcohol and hexane soluble extractives are removed by the solvent extraction process carried out before flow measurement on these specimens (see section 6.4.4.1).

Although similar, reversible, decrease in permeability is observed for both methods of swelling, the magnitude of the decrease is somewhat greater for alcohol swollen material. For moisture swollen wood, gross volumetric swelling from 0 to 7 per cent leads to about 60 per cent permeability reduction (see above). From Figure 6.14 it can be calculated that a similar level of swelling due to alcohol sorption causes about 70 per cent reduction in permeability. This difference, which appears to be consistent for almost all specimens tested, may be explained on the basis of the known reactivity to methanol of phenolic extractive and cell wall structural (lignin) material. Specimens used in the alcohol flow series of experiments were subjected to solvent extractions with hot hexane/methanol/acetone mixture (sections 6.4.1.1 and 6.4.4.1). Additionally, these specimens were, of course, in contact with alcohols during flow experiments.

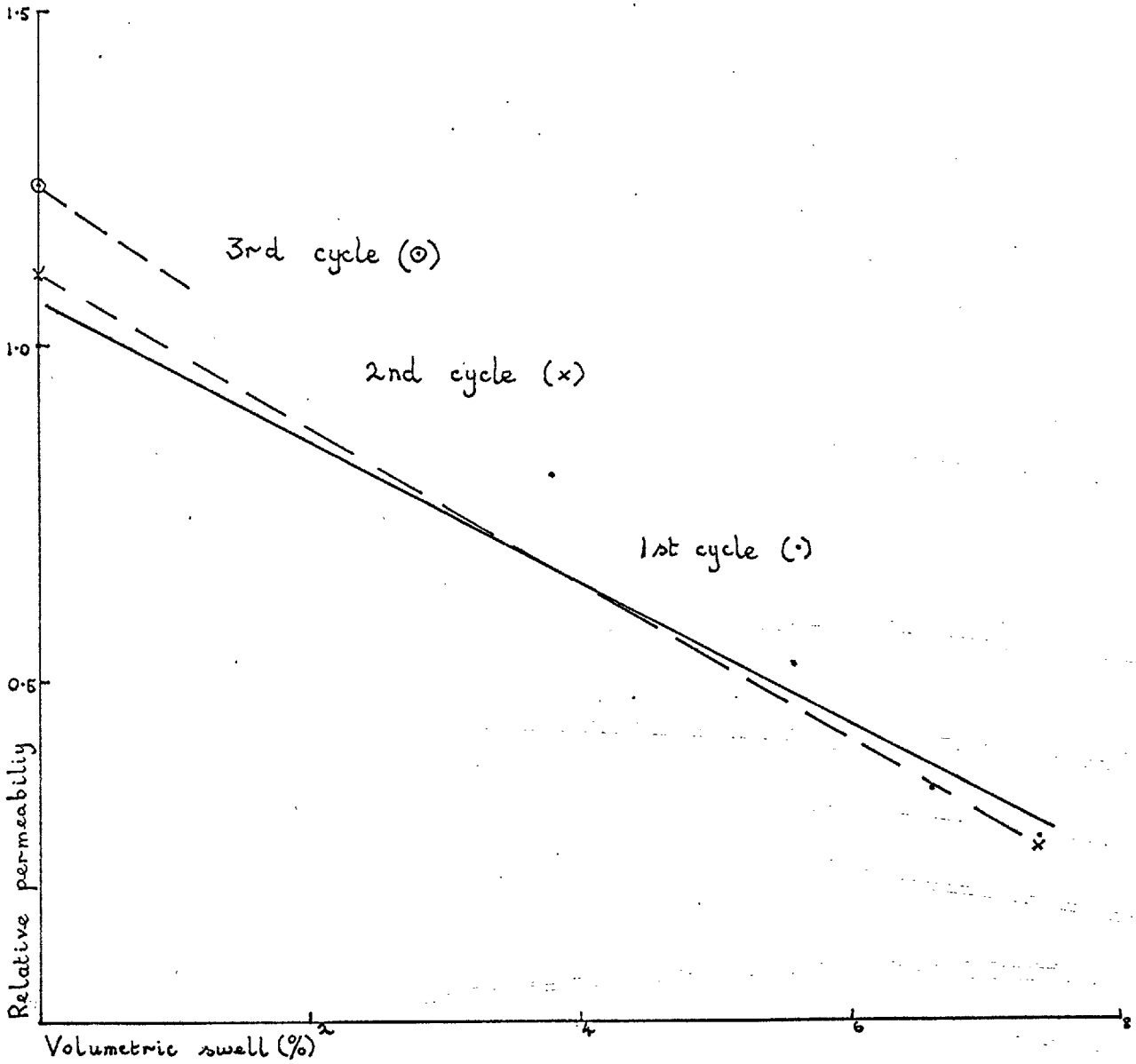


Fig 6.14 RELATIONSHIP BETWEEN PERMEABILITY OF AIR DRIED WOOD AND SWELLING DUE TO ALCOHOL SORPTION

Bordered pit membranes, which exert a strong influence on fluid flow rate, are known to be rich in polyphenolic materials. Removal of these materials (see section 6.4.4.1) may reduce the restraint of membranes to dimensional change caused by sorption. Hence, for the same degree of gross swelling, certain critical structures may show a greater dimensional change due to sorption, after exposure to alcohols - especially methanol.

Permeability is an extremely sensitive guide to change in pore dimension (volume rate of flow 'Q' $\propto$ pore radius 'r' to the fourth power - section 1.3.1, equation 1.1). Additionally, account should be taken of the probable weakening of restraint due to removal of phenolic substances by methanol. With these two effects in mind it seems likely that the relationships between permeability and gross swelling obtained for the two methods of swelling, are due to a common mechanism. This suggests that cell wall swelling is directly responsible for the observed, reversible, permeability decrease.

6.6.2 THE EFFECT OF SWELLING ON THE PERMEABILITY OF 'SOLVENT EXCHANGE' DRIED WOOD

From the data of Tables 6.6 and 6.8, the relationship between 'relative' permeability of solvent exchange dried wood and gross swelling is obtained. This relationship is shown graphically in Figure 6.15, below.

From the Figure it is clear that permeability is decreased by swelling. The decrease is considerably less, however, than for dry wood (Figures 6.13 and 6.14). Permeability of specimens of solvent exchange dried wood is reduced by 16 to 34 per cent for a gross volumetric swell of 7 per cent. In air-dried wood, swollen by the same amount, permeability is reduced by 60 to 70 per cent (section 6.6.1 above). This reduced sensitivity to sorption and dimensional change is believed to be associated with the lower degree of pit

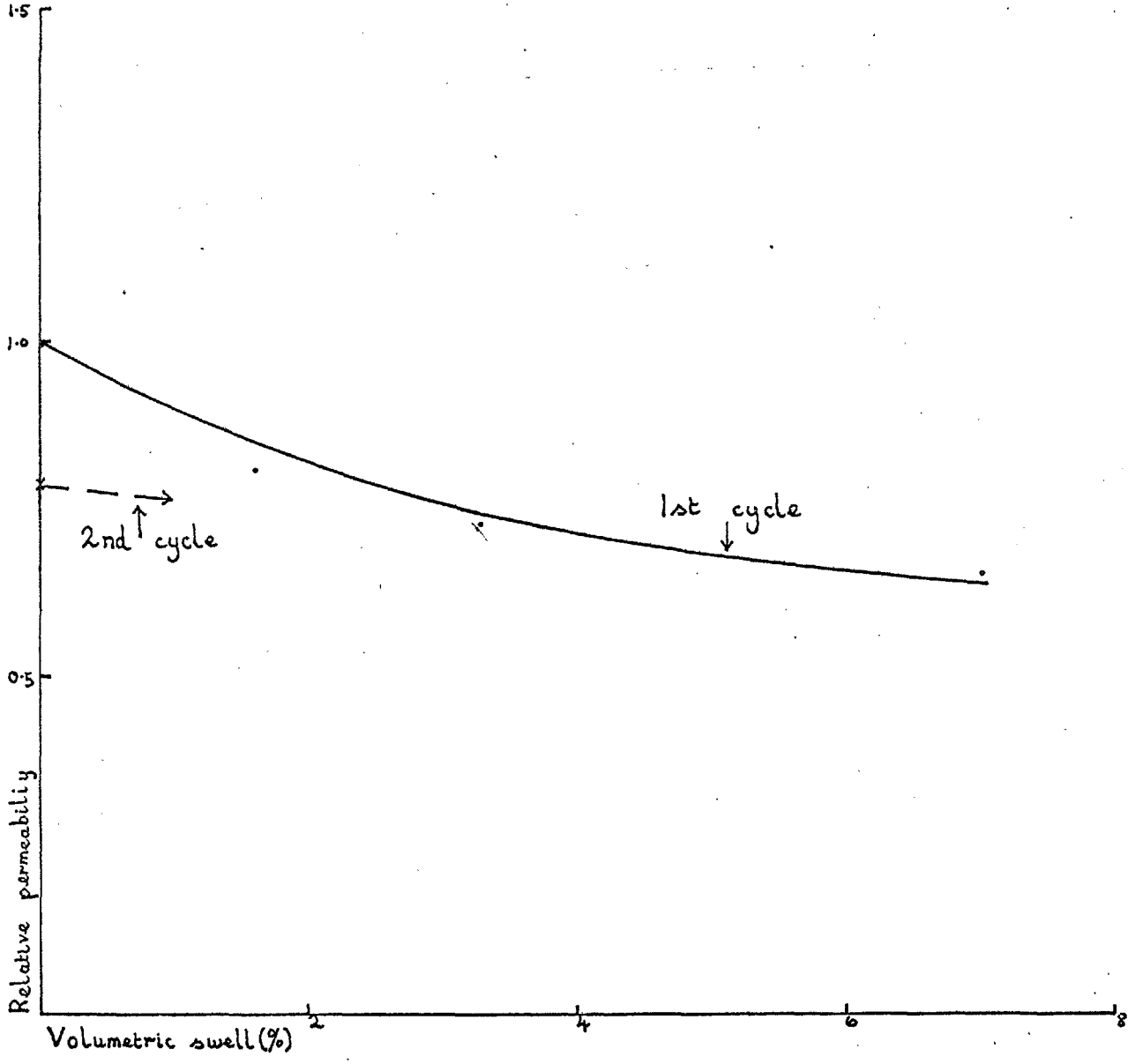


Fig 6.15 RELATIONSHIP BETWEEN PERMEABILITY OF SOLVENT DRIED WOOD AND SWELLING DUE TO MOISTURE SORPTION

aspiration in solvent exchange dried wood (section 6.3.1.2), and is discussed more fully in section 6.6.4 below.

6.6.3 THE EFFECT OF DIMENSION CHANGE ON THE PERMEABILITY OF GREEN WOOD

The shrinkage of green wood, associated with the replacement of water by aliphatic alcohols is recorded in section 6.5.4.2 (Tables 6.21 and 6.22). Compared with the total dimensional change occurring during air drying and re-soaking with alcohols, this amount is very small (section 6.3.4.2). Nevertheless, significant dimensional change is observed (Table 6.22) and the relationship between this change and permeability (from section 6.5.4.1, Tables 6.18, 6.19 and 6.20) is illustrated in Figure 6.16, below. The irreversible change associated mainly with the first exposure to methanol, discussed in section 6.5.4.1, is clearly illustrated in Figure 6.16 (first cycle data, shrinkage step 0 to 0.21 per cent). Thereafter, sapwood permeability remains almost constant. This is consistent with the data obtained for 'solvent exchange' dried specimens (Figure 6.15). In wood dried by this technique, as in 'green' sapwood, most bordered pits are unaspirated. Such material shows a scarcely detectable permeability reduction associated with shrinkage by <1 per cent from the fully swollen state.

Heartwood behaves similarly to sapwood, after the first cycle, except for the shrinkage step from 0 to 0.21 per cent (the water-methanol step). Over this range significant permeability reduction (~30 per cent) accompanies swelling. Further experimental data suggest that the magnitude of this reduction becomes less, as cycling proceeds (see section 6.5.4, Table 6.19). This gradually 'reducing' effect seems likely to be due to the gradual removal of material slowly dissolved by methanol (eg polyphenolic extractive and cell wall structural substances) from pit membranes and the walls of pit chambers, as described in section 6.4.4.1.

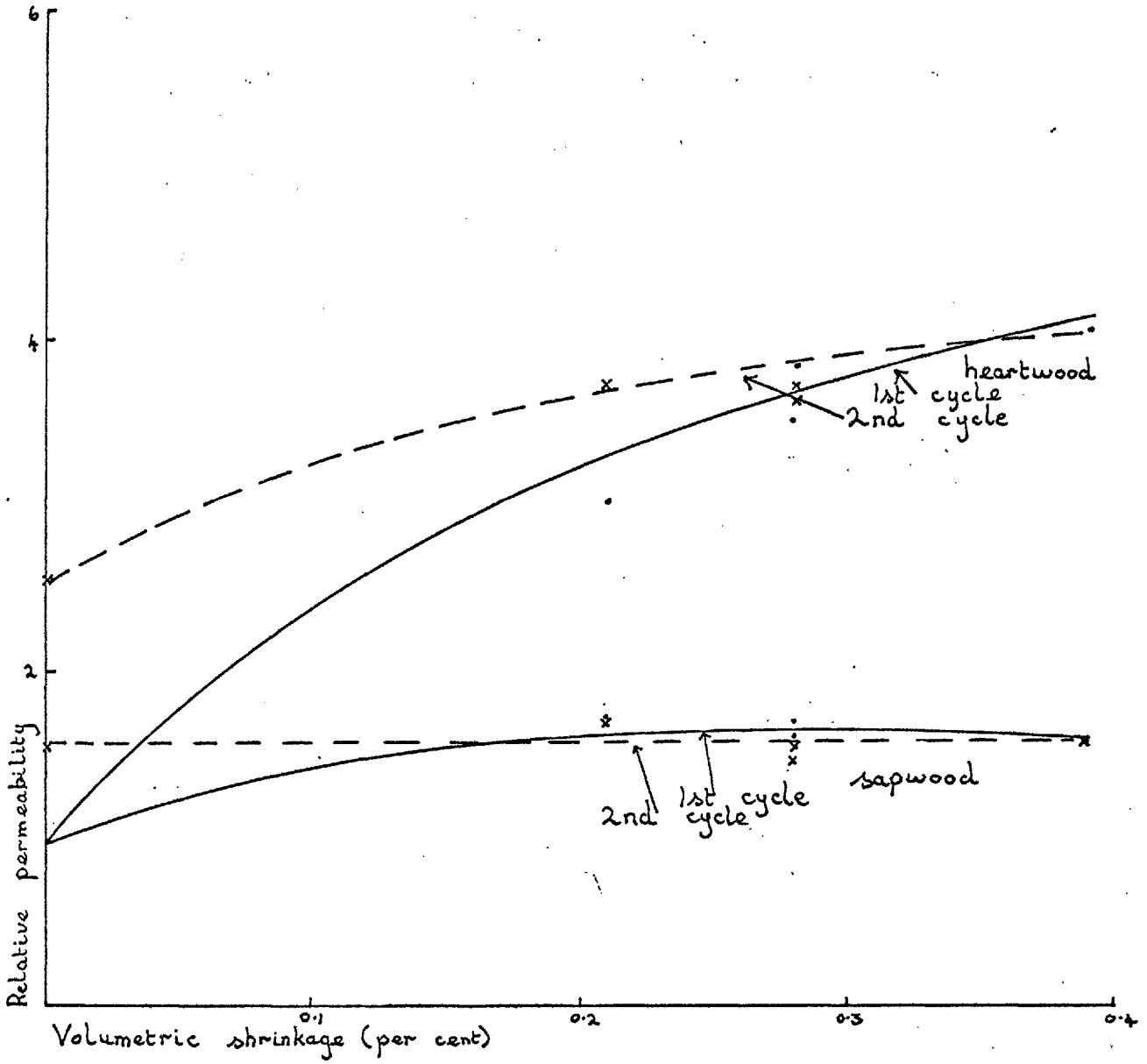


Fig 6.16 RELATIONSHIP BETWEEN PERMEABILITY OF 'GREEN' WOOD AND SHRINKAGE DUE TO SOLVENT EXCHANGE

It must be recognised, however, that in dealing with 'green' wood it was impossible to be certain that all air was removed from specimens. Hence, gas embolism effects (section 1.5.1) may lead to considerable experimental error. The differences observed may be due to the more effective blocking of pores by gas, during the flow of a high surface tension liquid (water), than during low surface tension liquid (alcohol) flow.

6.6.4 MECHANISM OF PERMEABILITY DECREASE CAUSED BY SWELLING

Many workers have shown that the principal longitudinal fluid pathways in softwood are comprised of the tracheid-bordered pit system (see section 1.2). Therefore, the reduction in permeability observed as wood swells must be due to either:-

a reduction in 'diameter' or number of tracheid lumina, or

b reduction in diameter or number of border pit pores,

or to a combination of both these effects.

The effect of swelling on the cross-sectional dimensions of tracheids has been studied by several workers (Clarke 1930; Beiser 1933; Nakato 1958). This work is reviewed and summarised by Kelsey (1963). The data of these workers show no consistency of behaviour for all species tested. In some species, tracheid lumina expand and, in others, contract during gross shrinkage. Boutelje (1962) measured the cross-section of tracheid lumina on wet and dried thin sections of Swedish pine (*Pinus sylvestris*). He found the lumina of early wood tracheids to shrink by about 4 per cent during drying, whilst in late wood, drying caused some 4 per cent expansion of lumen cross-section. Some workers have disputed that measurements made with thin sections provide a true guide to the behaviour of 'bulk' wood (Lindsay and Chalk, 1954; Barclay, 1955). For softwoods, however, it is shown by

Boutelje (1973) that such measurements do provide a reasonable guide to the behaviour of larger specimens of wood.

In this work, an optical microscopic technique was used to estimate change in lumen cross-section during drying from the water saturated to the vacuum dry condition. Transverse sections, about 15 micron thick, were cut from blocks taken from the test logs (section 6.3.1). These were 'wet' mounted between glass slides. Selected fields were photographed through the microscope, and prints of known magnification (x640) were prepared. The sections were then dried in air and finally in vacua over phosphorus pentoxide, whilst 'lightly' supported between nylon gauzes. They were then dry mounted, and the same fields were re-photographed and examined at precisely the same magnification as used for the sections when wet. An example of one of the 'fields' examined is shown in Figure 6.17 below.

Cell cross-sections were estimated from the photographs by measurement of the tangential and radial dimensions with a caliper micrometer. From these data shrinkage caused by drying was calculated. The complete data for about 70 cells measured are recorded in Appendix 1, Tables 15 and 16 and are summarised below (Tables 6.23 and 6.24).

Table 6.23 EARLY WOOD - DIMENSIONAL CHANGE OF TRACHEID LUMENA CAUSED BY DRYING

Number of cells measured	Average lumen width (micron)					
	Radial			Tangential		
	Wet	Dry	Shrinkage(%)*	Wet	Dry	Shrinkage(%)*
42	32.65	32.80	-0.5	26.09	24.53	+6.0

*'+' sign indicates dimensional decrease (shrinkage);
'-' sign indicates dimensional increase (expansion).



Fig 6.17a (x 450)

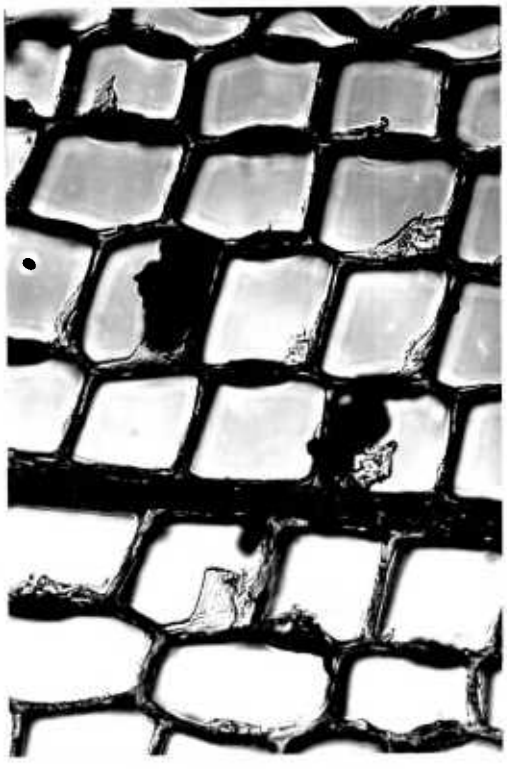


Fig 6.17b (x 450)

Abies grandis EARLY WOOD, TRANSVERSE SECTION, 'a' WET (SWOLLEN)
'b' DRY (SHRUNKEN)

Table 6.24 LATE WOOD - DIMENSIONAL CHANGE OF TRACHEID LUMENA CAUSED BY DRYING

Number of cells measured	Average lumen width (micron)					
	Radial			Tangential		
	Wet	Dry	Shrinkage(%)*	Wet	Dry	Shrinkage(%)*
27	8.28	8.75	-5.7	16.56	16.56	±0.0

*'+' sign indicates dimensional decrease (shrinkage);
'-' sign indicates dimensional increase (expansion).

It is seen from Tables 6.23 and 6.24 that the cross-sectional area of tracheid lumina of early wood is reduced during drying (and gross shrinkage) by some $5\frac{1}{2}$ per cent. In late wood, on the other hand, gross shrinkage leads to some 6 per cent increase in lumen cross-sectional area. These data are in reasonable agreement with those reported for Swedish pine by Boutelje (1962).

It has been found by a number of workers that the main resistance to laminar flow (~75 to 90 per cent), through air dried softwood, is centred in the bordered pits (see section 1.5.3). Gas flow measurement reported in this work (section 4.4) is in reasonable agreement with these findings. The data of Table 4.3 (section 4.4) suggest that in *Abies grandis* sapwood specimens, about 60 per cent of resistance to flow is due to the pit system whilst, in heartwood, the pits account for about 85 per cent of flow resistance. It is shown in section 4.7.3 that viscous permeability is subject to some overestimation by the technique used. Better viscous flow data are obtained if a permeability is measured at higher mean gas pressure. It is shown in section 4.7.4 that at the gas pressure used in this work, pit pore size relative to lumen diameter is overestimated. Hence, the contribution to total flow resistance of the pit system is ~~over~~under estimated. It is likely, therefore, that the resistance to flow due to pits, in the specimens used in this work, accounts for 70 per cent or more of the total flow resistance.

Let the hexagonal, cross-sectional shape of the early wood tracheids (Figure 6.17) be approximated as circular. Then, from the Hagen-Poiseuille law (equation 1.1, section 1.3):-

$$Q \propto r^4$$

where Q = volume rate of flow
r = tube radius

It is shown above that early wood lumina expand in cross-sectional area by some $5\frac{1}{2}$ per cent, during wetting from vacuum dry to fibre saturation. Therefore, effective radius 'r' is increased by about 2.7 per cent.

Thus, from the relationship given above ($Q \propto r^4$) it may be calculated that the permeability of early wood lumina is increased by wetting, by about 11 per cent. Late wood tracheid lumen cross-section is approximately rectangular slit shaped. For capillaries of this shape, it has been shown (Bird, Stewart and Lightfoot, 1960), that rate of flow, and hence permeability, is proportional to the cube of slit width. Increase in moisture content of late wood from vacuum dry, to fibre saturation, causes about 5.7 per cent reduction in width (Table 6.24). This shrinkage, therefore, must lead to about 16 per cent decrease in the permeability of latewood tracheid lumina.

It is shown above that the tracheid lumina are probably responsible for not more than 30 per cent of the total resistance to longitudinal fluid flow, through softwood. Thus, some 70 per cent (at least) of the total resistance to flow is centred in the pit system. This resistance may be caused by two or more types of capillary (see section 4.7.2), rather than a single one. Nevertheless, to a reasonable approximation, about 70 per cent of flow resistance may be associated with the bordered pit system, represented as a single 'effective' capillary. For capillaries connected in series, the reciprocal of conductance is additive (section 4.4), ie resistance is additive. The permeability of late

wood tracheid lumina is decreased, during gross swelling from the shrunken to the fully water swollen state, by about 16 per cent (see above).

Let the resistance of dry late wood be equal to 1 unit. Then (from the above argument), in dry wood:-

$$\text{Lumen resistance} = \underline{0.3 \text{ units}}$$
$$\text{Pit system resistance} = \underline{0.7 \text{ units}}$$

In water swollen wood:-

Permeability (the reciprocal of resistance) is reduced by 16 per cent. Therefore, resistance is increased by about 19 per cent. Thus, in fully water swollen wood:-

$$\text{Lumen resistance} = \frac{0.3 \times 119}{100} = \underline{0.357 \text{ units}}$$

Therefore, in the absence of any effect on 'pit' permeability, gross swelling, to the fully water swollen state, increases resistance to flow from

$$\underline{1.000 \text{ units}} \text{ to } \underline{1.057 \text{ units}}$$

Hence, in late wood permeability being the reciprocal of resistance is decreased by about 5 per cent, due to the observed decrease in late wood lumen cross-section.

In early wood, it is shown above that gross swelling leads to an increase in the permeability of tracheid lumina. Thus, the observed large permeability decrease observed during volumetric swelling of vacuum dried wood, to the water or methanol swollen condition (sections 6.3.4 and 6.4.4) cannot occur as a result of the observed dimensional change of tracheid lumina. It is reasonable to suppose, therefore, that these large decreases (about 60-80 per cent) of permeability values measured in the shrunken condition (Tables 6.4 and 6.11), occur as a result of changes in pit geometry.

6.6.4.1 EFFECT OF CELL WALL SWELLING ON PIT STRUCTURE

From the electron microscopic evidence cited in sections 1.2 and 3.3 a physical model of the bordered pit structure of *Abies grandis* may be constructed. This model is illustrated below (Figure 6.18).

To a reasonable first approximation it can be taken that volume rate of flow through pores is proportional to the fourth power of pore radius (section 1.4). Hence, flow rate may be strongly influenced by margo pores and by 'torus-border' slits (Figure 6.18) which are of relatively small 'diameter', and probably to only a small degree by the pit aperture, which is relatively large in diameter.

In an investigation of the chemical nature of pit membranes in *Pinus taeda*, it has been shown by Nicholas (1966) that the margo is comprised of mainly cellulose. *Abies* belongs to the same family of gymnosperms (the Pinaceae) as *Pinus*, and it is assumed that the pit margo in *Abies grandis* is also mainly cellulosic. It is reported by Stamm (1964) that cotton cellulose fibrils swell volumetrically by about 35 per cent for a moisture content change from dry to fibre saturation. It is explained in section 6.1, that swelling of cellulose fibrils caused by sorption, occurs normally to the fibril axis (ie longitudinal swelling is virtually zero).

For most softwoods, moisture content at fibre saturation is about 28 per cent (on a dry weight basis). Within this range, external (gross) swelling is approximately proportional to moisture content (Stamm 1964). From Table 6.13 (section 6.4.4.1), it is seen that saturation of dry wood with water causes about 8 per cent volumetric swelling. Hence, assuming that fibrils are of circular cross-section, 8 per cent gross external swell is equivalent to some 16 per cent increase in margo fibril thickness.

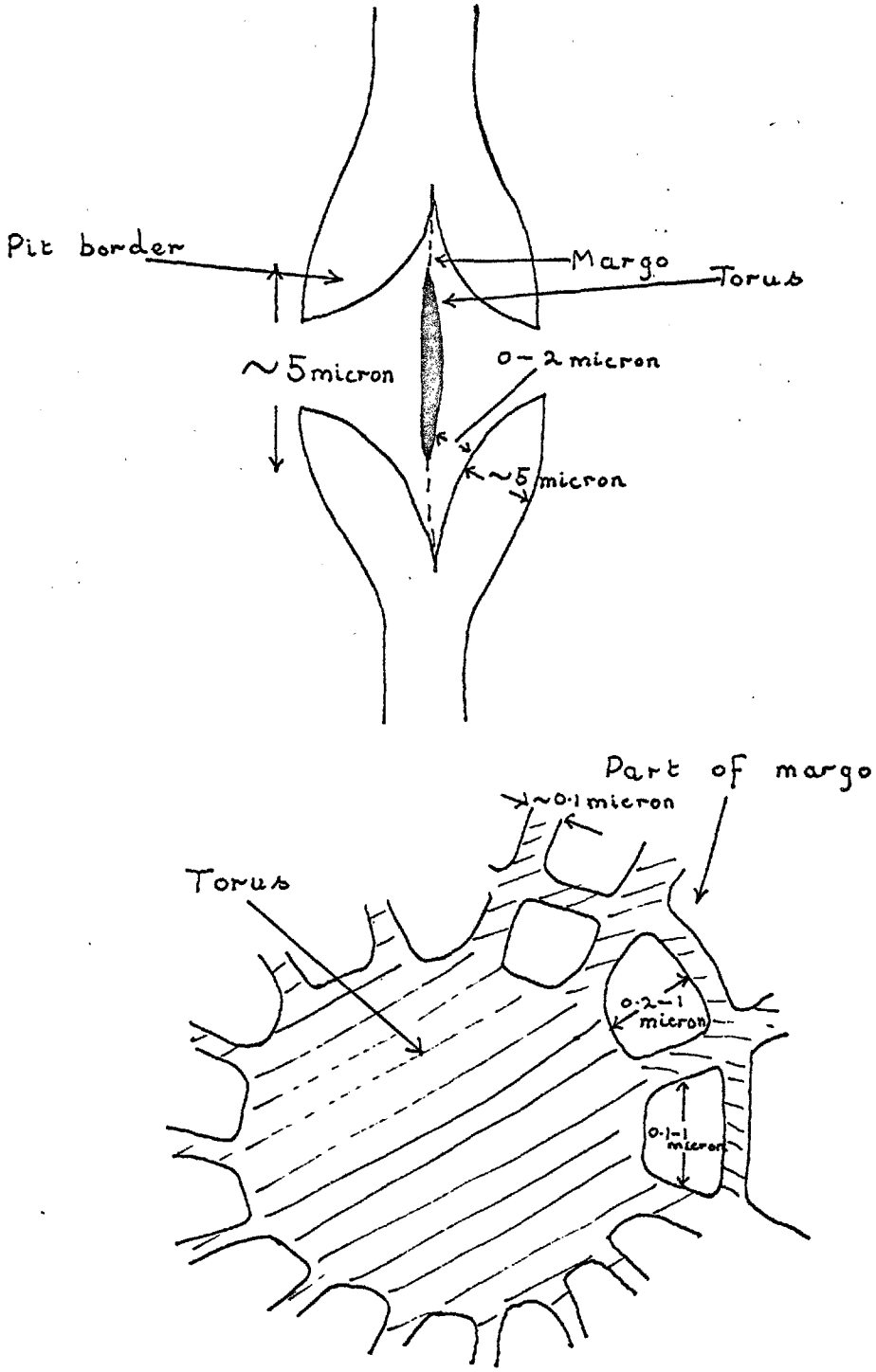


Fig 6.18 'MODEL' BORDERED PIT STRUCTURE

Consider a single pore formed by the intersection of two parallel pairs of fibrils (Figure 6.19).

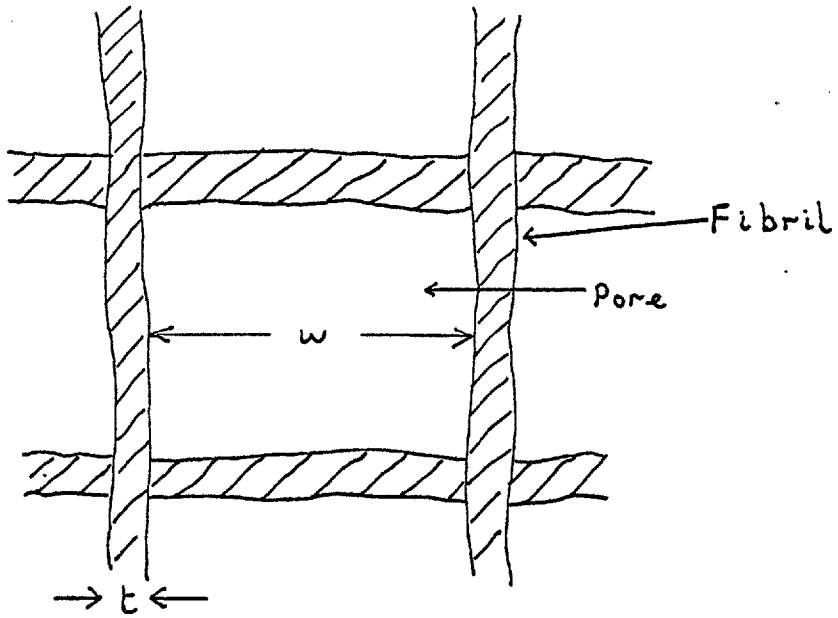


Fig 6.19 SINGLE MARGO PORE

In the dry (unswollen) state let the ratio of fibril thickness to pore width $(\frac{t}{w})$ be equal to 'α'.

Since margo fibrils are probably mainly cellulosic, it is reasonable to assume that they swell in direct proportion to the external swelling of wood specimens. This being so, pore width is related to external swelling by the following relationship:-

$$W_x = W_o(1 - \frac{0.16 \times \alpha}{8}) \qquad \text{Equation 6.1}$$

where W_x = margo pore width in wood swollen externally by 'x' per cent

W_o = margo pore width in dry (unswollen) wood

x = external swelling (per cent)

α = ratio of fibril thickness to pore width, in the unswollen state

For a pore of square cross-section, hydraulic radius 'm' (section 1.4, equation 1.13) is given by:-

$$m = \frac{W^2}{4W} = \frac{W}{4}$$

where W = pore width

From equation 1.16 (section 1.4) it can be seen that rate of flow 'Q' is controlled by:-

$$Q \propto A\varepsilon m^2$$

where A = specimen cross-sectional area
ε = specimen porosity
m = pore hydraulic radius

For a single pore of square cross-section:-

$$A = W^2$$
$$\varepsilon = 1.0$$

Therefore:-

$$Q \propto W^4$$

But, pore width 'W' varies with change in external dimension (see equation 6.1 above). Therefore, rate of flow (which is directly proportional to permeability) varies with gross external swelling:-

$$Qx \propto K_{Vx} \propto \{W_o(1 - \frac{0.16 \times \alpha}{8})\}^4 \qquad \text{Equation 6.2}$$

where Qx = volume rate of flow through a specimen swollen externally by x per cent.
K_{Vx} = specimen viscous permeability at 'x' per cent external swelling
W_o = pore width in dry wood
x = external swelling (per cent
α = dry fibril thickness to pore width ratio

Let $K_{Vx} = 1$ when 'x' = 0

then $W_o = 1$

Thus the variation in 'relative' permeability (see section 6.3.4.1) with external swelling, may be calculated for any value of 'α'. Such relationships for a number of 'α' values are shown graphically in Figure 6.20. Data from sections 6.3.4 and 6.4.4, relating permeability to water swollen and alcohol swollen, air/vacuum dried wood respectively, are plotted on Figure 6.20. These data show that the relationship between permeability and swelling caused by moisture sorption, is of the type predicted. Where swelling is induced by sorption of alcohols, however, the experimental relationship seems to depart somewhat from the shape of the theoretical curves. For small amounts of swelling (sorption of n butanol and n propanol) the experimentally obtained permeability seems to be somewhat higher than predicted. The experimental evidence supporting this observation is sparse, and more data are needed to confirm the shape of the curve. However, it does suggest that the less polar liquids affect pit pore structure somewhat less than is predicted by the magnitude of their effect on gross dimension. This effect may be related to a difference in distribution of cell wall constituents in the pit compared with that in the cell wall as a whole (see, for example, Nicholas 1966; Bauch and Berndt 1973).

In general the experimental data shown on Figure 6.20, suggest that for the wood examined 'α' lies between 1 and 2. That is, on the average, dry wall thickness is equal to or up to twice, dry pore width.

In late wood, margo pores are bounded by relatively wide fibrillar bundles (Figures 3.6 and 3.7), and a value of 'α' between 1 and 2 seems reasonable for this material.

Pit membranes in early wood have many pores where pore width is greater than the thickness of the bounding fibrils by a factor of 5 to 10 times. For such pore geometry (α = 0.1 to 0.2), gross swelling of 8 per cent leads to some 5 to 15 per cent permeability reduction (see Figure 6.20). The experimental relationships between permeability and swelling suggest, therefore, that in specimens comprised of both early wood and late wood, flow occurs mainly through late wood cells and pits. Similar data relating permeability to swelling caused by moisture sorption, were obtained in gas flow experiments conducted by Comstock (1968). From these data, he concluded that the major flow controlling pores in air dried wood, were formed by gaps left between torus and pit border in partially aspirated pits (Figure 6.20). As far as

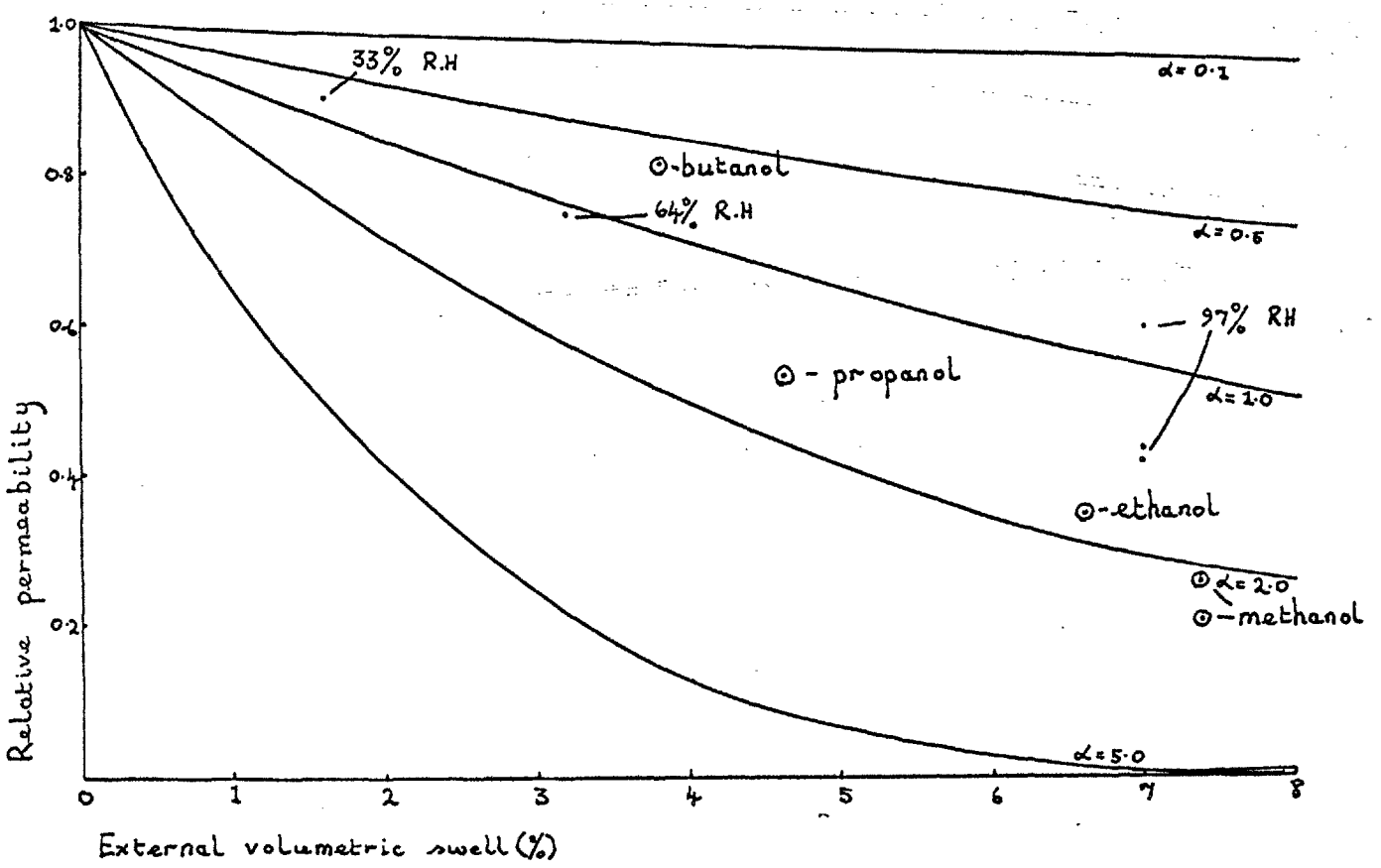


Fig 6.20 RELATIONSHIP BETWEEN RELATIVE PERMEABILITY AND EXTERNAL SWELL.

NB LINES ARE THEORETICAL CURVES FOR VARIOUS VALUES OF 'α'; EXPERIMENTAL DATA ARE REPRESENTED BY '.' FOR MOISTURE SORPTION AND '⊙' FOR ALCOHOL SORPTION

can be judged from microscopic evidence the value of 'α' for such pores is likely to be equal to or greater than unity. Hence, Comstock's interpretation is reasonable and could be applied to the data obtained in this work. However, it has long been established that almost all pits in air dried early wood are aspirated, whereas a high proportion of late wood pits remain unaspirated, and able to conduct fluid freely (Phillips, 1933; Liese and Bauch, 1967). Several workers have produced experimental evidence showing most primary longitudinal conduction in air dried softwood, to be through late wood cells and pits (Osnach, 1961; Petty and Puritch, 1970; Bramhall and Wilson, 1971). The work of Petty and Puritch is particularly interesting. These workers, using *Abies grandis* wood, showed by a dye technique, that liquid flow through water swollen specimens of length about 12 mm, was restricted to the early wood/late wood boundary. This evidence supports the hypothesis proposed above that the observed permeability/swell relationship is due to flow control by late wood pit membranes. With the present data, it is impossible to unequivocally decide which of the two explanations of the effect is the correct one. The question could be resolved by the separate determination of the relationship between permeability and swelling for specimens comprised of exclusively early wood and exclusively late wood cells.

In solvent exchange dried wood almost all pits in both early wood and late wood remain unaspirated (see section 6.3.1.2). Early wood cells were more abundant than late wood cells in the specimens examined in this work. Tracheid lumina in early wood are of greater diameter (Figure 6.17) and bordered pits occur more abundantly in early wood than in late wood (Stamm, 1964). Where pits are unaspirated (as in solvent exchange dried specimens), therefore, most conduction is through early wood. External swelling of about 7 per cent caused by water sorption in solvent exchange dried specimens in this work, led to some 17 per cent, reversible permeability decrease (section 6.3.4.2). These data suggest that for this material, 'α' lies between 0.1 and 0.5. Such a value is in

the range to be expected where flow is controlled substantially by the membrane of unaspirated early wood pits (see above).

The results discussed above are in agreement with those of a number of earlier workers (see section 1.6). In particular the data agree closely with the gas flow data of Comstock (1968) - see this section, above. A completely different relationship between liquid flow permeability and swelling has been reported by Hossfeld (1972). He measured the rate of flow of a series of binary liquid mixtures (dioxane/water; tertiary butanol/water and iso propanol/water), through northern white cedar wood (*Thuja occidentalis*). Hossfeld found a permeability maximum corresponding to the maximum observed tangential swell. At the 'high swell' end of his relationships, however, permeability appears to decrease markedly with increased water fraction. This latter effect suggests that sorption of water by pit elements may cause swelling with accompanying pore size decrease, as observed in this work.

The differences between the behaviour of *Abies grandis* wood and *Thuja occidentalis* specimens may be due to differences in pit structure between the two species. Pit membranes in *Thuja* have no thickened torus (Bauch, Liese and Schultze, 1972), and it may be that they are able to conduct swelling liquids by a diffusion mechanism. The evidence produced in the present work, suggests that most liquid flow through *Abies* is in the laminar régime. It should be recognised, however, that the use of binary liquids leads to the establishment of a complex, 'three component' system (component 'a'/ component 'b'/cell wall). In such a system some structural elements may preferentially sorb one or other of the liquid components. Hence, it is difficult to relate with confidence, gross dimensional changes in such systems, to effects on discrete cell elements (eg pit membranes). It is difficult, therefore, to draw firm conclusions from the experimental flow data of Hossfeld (1972).

6.6.5 LIQUID FLOW THROUGH SWOLLEN SOFTWOOD - SUMMARY

For the species investigated (*Abies grandis*), it is shown that cell wall swelling of air dried wood, induced by sorption of moisture, causes a marked, reversible decrease in longitudinal permeability. The magnitude of this decrease amounts to about 60 per cent, for some 7 per cent volumetric swelling (equivalent to a moisture content change from vacuum dryness to about 25 per cent).

In the system where swelling of air dried wood was induced by the low molecular weight aliphatic alcohols (methanol to n.butanol), opposing effects were observed. Initially, permeability was seen to decrease with increased swelling, caused by sorption of butanol and propanol. Upon the introduction of ethanol and especially of methanol, however, the further swelling caused by these liquids was accompanied by an increase in permeability. Evidence is cited, suggesting that this increase was due to increase in size and/or number of pores, due to extractive removal and to some de-aspiration of bordered pits. Specimens pre-extracted with methanol/hexane/acetone, and then caused to swell by sorption of the alcohol series, were found to show a consistent, reversible decrease in permeability with increased swelling, throughout the swelling range. The magnitude of the permeability decrease appeared to be somewhat greater for these solvent extracted, alcohol swollen specimens, than for those swollen by moisture sorption (about 70 per cent reduction for 7 per cent volumetric swell). It is believed that this enhanced effect may be due to the removal of some matrix material from pit membranes leading to reduction of restraint against swelling forces.

Specimens dried by a solvent exchange process, to retain all bordered pits in the unaspirated state, were found to be considerably less affected by cell wall swelling. In this material, as for air dried wood, swelling caused a reversible

permeability decrease. However, the magnitude of this decrease, corresponding to 7 per cent volumetric swelling, was only about 17 per cent, compared with 60 to 70 per cent for air dried wood.

A model pore system is constructed and, from this, the theoretical relationship between the ratio of pore wall thickness to pore diameter 'α', and change in permeability with swelling, is derived. It is shown that the magnitude of this change in air dried wood is consistent with control of flow by late wood pit membranes. The much smaller permeability decrease associated with swelling of solvent exchange dried specimens, suggests that most conduction by this material is through early wood.

In 'green' (never dried) wood, replacement of water by successively less polar alcohols caused only a small degree of shrinkage (about 0.4 per cent total volumetric shrinkage during the exchange of water through the series, methanol → ethanol → n propanol → n.butanol). This small degree of dimensional change had no measureable effect on the permeability of sapwood. In heartwood, however, a marked 'part reversible' increase (about 30 per cent) in permeability was observed during exchange from water to methanol. About half the total shrinkage (about 0.2 per cent) occurred over this step. It is unlikely that the small observed dimensional change can, alone, account for this increase. Two possible reasons are suggested to explain the effect:-

a Gradual removal of extractive and/or matrix substance from pit membranes.

b Less interference with flow, by any small air bubbles remaining in the pore structure, during the flow of low surface tension liquids (the alcohols) than during the flow of water, a liquid of much higher surface tension.

Part 7 GENERAL DISCUSSION

This thesis is divided into several major parts, each of which is discussed in some detail. Nevertheless, conclusions reached in one part have relevance to other parts. The purpose of this 'General Discussion', therefore is to bring these separate conclusions together and briefly to consider their interrelationships and significance.

7.1 THE RELATIONSHIP BETWEEN PERMEABILITY TO GASES AND INERT LIQUIDS

It has been shown in section 1.4 that for rigid porous media, laminar flow of gases and liquids are directly relatable (equations 1.12 and 1.14). In section 4.5 (Table 4.5), viscous permeability constants calculated from gas flow data, are listed. For the same series of specimens, inert liquid flow, viscous permeability constants are given in Table 5.2 (section 5.3.1). It is noted also in section 5.3.1 that hydrogen flow permeability was re-measured after measurement of hexane flow rate under low pressure differential conditions. Permeability constants from this series of experiments were calculated precisely as described for the first series of gas flow measurements (section 4.5). The whole of these permeability data are summarised below (Table 7.1).

Table 7.1

VISCOUS PERMEABILITY CONSTANTS MEASURED WITH GAS AND NON-SWELLING LIQUID

Specimen	Viscous permeability constant (cm^3) x 10^8		
	Gas flow before hexane flow	Liquid flow	Gas flow after hexane flow
AGS.e	0.14	0.12	0.13
AGS.ℓ	0.29	0.24	0.27
AGH.e	0.08	0.074	0.09
AGH.ℓ	0.04	0.035	0.036
CDS	0.26	0.24	0.26
PAS.1	0.14	0.13	0.15
PAS.2	0.20	0.18	0.20
THS.e	0.04	0.022	0.040
THS.ℓ	0.08	0.038	0.055
THH.e	0.33	0.29	0.31
THH.ℓ	0.10	0.089	0.10
AAS	1.66	1.28	1.75
AAH	1.09	0.98	1.18

From the above Table it is seen that gas flow permeability after liquid flow is sometimes higher and sometimes lower than that measured before liquid flow. It has been shown in an earlier section (4.7.1) that gas flow measurement is unlikely to be subject to experimental error greater than about 5 per cent. The differences in permeability measured before and after liquid flow, although small in absolute terms, often fall outside this limit. Hence, it is believed that they are real, and not artefacts of experimental error. They must, therefore, be due to pore structural changes, probably induced by the flowing liquid, or by surface forces generated during evaporation of hexane prior to the second series of gas flow experiments. Steady liquid flow rate was achieved for each of the specimens, so that any structural change caused by liquid flow experiments, must have occurred before monitoring commenced, eg during impregnation. Such changes may result from particulate filtration by fine pores, leading to pore blocking and hence permeability decrease, and to removal of extraneous deposits by solvent extraction, leading to increased permeability. It is likely that these two processes occur simultaneously, sometimes one dominating and sometimes

the other. Particulate matter to cause blocking, may be introduced adventitiously in spite of the precautions taken (section 5.2). Since steady flow conditions were achieved for all specimens, however (section 5.3.1), it seems more likely that blocking is due to the shifting of fine cell debris from large pores (where its presence has little effect), into fine pores (eg pit membrane openings), where it may cause significant pore size reduction.

During evaporation of hexane, prior to the second series of gas flow measurements, the specimen pores are subject to surface tension forces. These, although unable to cause total aspiration of pits (see section 6.3.1.2) may be sufficient to displace unaspirated membranes, sufficiently to cause a small permeability change.

The differences between the first and second gas flow measurements do not exceed 10 per cent (with one exception), generally the difference is much less than this. Assuming a circular pore cross-section, flow rate and hence permeability is proportional to the fourth power of pore diameter (section 1.3.1, equations 1.1 and 1.2). The observed differences may be caused, therefore, by changes in pore diameter of less than 3 per cent.

The various mechanisms suggested are not offered as definitive reasons for the measured differences in permeability. They are cited to illustrate the high potential for alteration, that exists in a micro-porous medium such as softwood, subjected to the forces necessary to conduct liquid flow experiments.

With the information available, it is impossible to say with certainty, which of the two sets of gas flow data are the more directly related to liquid flow results. If the changes leading to the observed reduction in gas flow were caused during liquid impregnation and flow, then the second gas flow series are the best to use. If, on the other hand, the

changes occurred after liquid flow rate measurement (eg during hexane evaporation), then the more relevant gas flow data for comparison, are those carried out before liquid flow. Because of this uncertainty the relationship is investigated between liquid flow and both sets of gas flow permeability data. Regression lines fitted by the least squares method, relating liquid and gas flow results are illustrated in Figure 7.1, below.

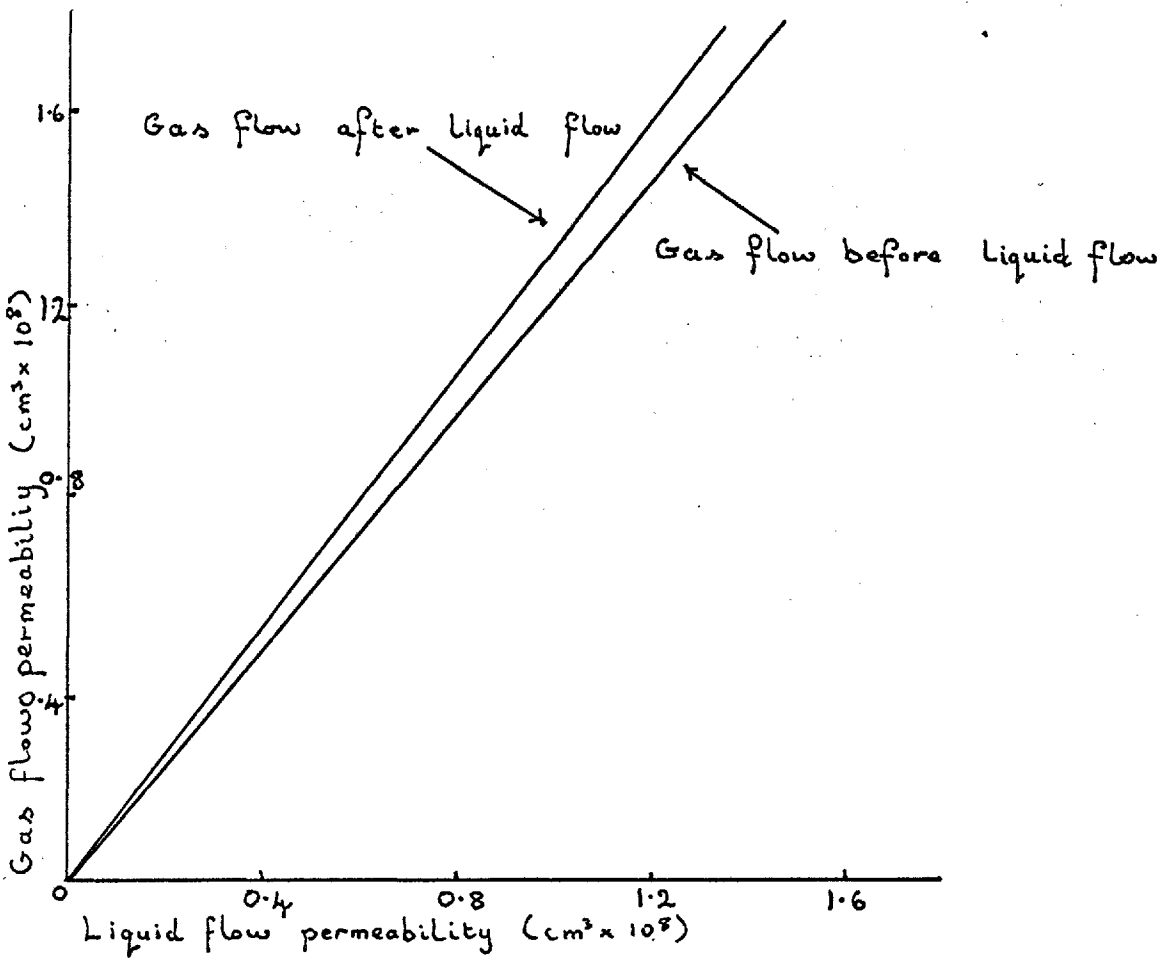


Fig 7.1 RELATIONSHIP BETWEEN PERMEABILITY MEASURED BY GAS AND LIQUID FLOW TECHNIQUES

For exact equivalence between gas and liquid flow data, the slope of the regression lines should be unity. Slopes calculated from the lines of Figure 7.1 turn out to be the following:-

First gas flow compared with liquid flow, slope = 1.23
Second gas flow compared with liquid flow, slope = 1.32

That is, on the average, gas flow permeability is estimated between 23 and 32 per cent higher than corresponding liquid flow data. Correlation coefficient for each pair of data sets is found to be 0.99, suggesting a functional relationship between gas and liquid flow viscous permeability.

It is indicated in this section (above), that the pore structure of softwood may be sensitive to the forces applied during liquid flow. Such forces may be responsible for part of the observed difference between gas and liquid flow permeability. However, it is believed that there is a more likely, systematic reason for the difference. It is argued (section 4.7.2) that the flow path model used in the analysis of gas flow data is oversimplified. Such oversimplification is shown (section 4.7.3) to cause significant overestimation of gas flow permeability. In the numerical examples investigated (0-2 bar), the magnitude of this overestimation was found to be in the range 18-108 per cent. Hence, the average difference between gas and liquid flow data observed experimentally (23-32 per cent) may be easily accounted for by this effect. It is shown in section 4.7.3 that the magnitude of the error associated with the oversimplification of the flow path model, decreases as working gas pressure is increased. Hence by working at higher pressure (probably up to about 5 bar), closer agreement between gas and liquid flow permeability should be attained. Experimental apparatus to test this hypothesis was not developed. However, in work carried out by Comstock (1967) closer agreement was obtained between gas (nitrogen and helium) and liquid (amyl alcohol and iso octane) permeability data for flow through a single species (*Tsuga canadensis*). The gas flow measurements conducted by Comstock, were carried out over a higher pressure range (1 to 3 bar, absolute) than those described in this work (0 to 2 bar, absolute). It is likely that the closer agreement between gas and liquid data reported by Comstock, resulted from this small technique variation.

Gas flow techniques are much simpler to apply to dry softwoods than are liquid flow methods. Hence it is attractive to use gas flow methods to measure wood permeability. The work reported in this thesis, however, shows that considerable error may be introduced by the use of these methods. Where very large differences in permeability are sought, gas flow procedures may be confidently used. If only small differences are under investigation, on the other hand, these methods may give misleading results. It is shown (section 4.7.3) that the error potential is markedly reduced as working pressure is increased. Above some critical pressure, the differences between gas and liquid permeability data become insignificant. Provided gas flow measurements are conducted at pressures in excess of this critical value, which may need experimental determination for each species of interest, gas flow methods may be confidently employed to predict liquid flow properties.

7.2 PORE SIZE MEASUREMENT

Several workers in the past have used gas flow permeability data to estimate flow controlling pore sizes (eg Sebastian, Côté and Skaar, 1965; Comstock, 1967; Petty, 1970; Smith and Banks, 1971). It has been shown that, in softwoods, longitudinal flow rate may be significantly influenced both by the tracheid lumen and by the interconnecting pits between adjacent tracheids (see section 1.5.3). Tracheid lumen diameter is well documented and typical values for similar species to those tested have been abstracted from the literature (Panshin and De Zeeuw, 1970). Pit membrane pore sizes estimated by scanning electron microscopy are tabulated in section 3.3.7, Table 3.1. These data are compared with flow controlling pore sizes, obtained from gas flow data (section 4.6) in Tables 7.2 and 7.3 below.

Table 7.2

TRACHEID LUMEN PORE SIZE

Species	Pore hydraulic radius (Micron)	
	Microscopy (literature)	Gas flow
Abies grandis sapwood early wood	∿10	3.2
Abies grandis sapwood late wood	∿ 5	3.6
Abies grandis heartwood early wood	∿10	2.6
Abies grandis heartwood late wood	∿ 5	2.1
Cedrus deodara sapwood	5-10	4.6
Cedrus deodara heartwood	5-10	No flow
Picea abies sapwood 1	5-10	6.2
Picea abies sapwood 2	5-10	4.6
Tsuga heterophylla sapwood early wood	∿10	4.1
Tsuga heterophylla sapwood late wood	∿ 5	2.8
Tsuga heterophylla heartwood early wood	∿10	4.6
Tsuga heterophylla heartwood late wood	∿ 5	3.7
Araucaria angustifolia sapwood	5-10	3.9
Araucaria angustifolia heartwood	5-10	3.9

Table 7.3

BORDERED PIT PORE SIZE

Species	Pore hydraulic radius (micron)	
	Microscopy (margo pores)	Gas flow
Abies grandis sapwood early wood	0.02-0.2	0.28
Abies grandis sapwood late wood	0.02-0.1	0.36
Abies grandis heartwood early wood	0.02-0.25	0.35
Abies grandis heartwood late wood	0.03-0.15	0.25
Cedrus deodara sapwood	0.03-0.25	0.23
Cedrus deodara heartwood		
Picea abies sapwood 1	0.05-0.15	0.25
Picea abies sapwood 2	0.01-0.1	1.18
Tsuga heterophylla sapwood early wood	0.05-0.3	0.33
Tsuga heterophylla sapwood late wood	0.05-0.3	0.32
Tsuga heterophylla heartwood early wood	0.1-0.15	0.55
Tsuga heterophylla heartwood late wood	0.05-0.1	0.39
Araucaria angustifolia sapwood *Araucaria angustifolia* heartwood	0.08-0.4	0.17-0.23

Comparison of the microscopic and gas flow data of Table 7.2 suggests that there is only approximate agreement between the two methods. It is clear that direct microscopic observation must give a reasonable estimate of tracheid lumen diameter. It follows, therefore, that the gas flow method is subject to marked error. This is in accord with the conclusions drawn from the theoretical examination of the effect of flow path model oversimplification on pore size estimation (section 4.74). In that section it is shown by numerical example that estimation of lumen diameter by gas flow technique may be subject to error in excess of 100 per cent.

It is shown in section 4.7.2 that the softwood bordered pit may be better represented as a serially connected pair of capillaries, than as a single capillary. Furthermore, in the same section, it is argued that the flow controlling pores of pits in serially interconnected tracheids may differ from one another, depending on their state of aspiration. It is quite unrealistic, therefore, to represent bordered pit pore size by a single value which has any physical reality. A more sophisticated (3-capillary type) model is investigated by numerical example in section 4.7.2. It is shown that for this model, pit pore sizes estimated using the gas flow method lie between the true sizes of the two capillary types forming the pit system (section 4.6). In the numerical examples worked, the estimate lay consistently closer to the size of the smaller of these capillaries. This is reasonable, since rate of laminar flow is dependent upon the fourth power of pore radius (for a pore of circular cross-section). Hence, flow rate is most strongly influenced by the smallest pores in a serially interconnected system.

From the foregoing, it is seen that it is unlikely that pit pore size estimated by the gas flow method, can be associated with specific softwood pores, having physical reality. It is likely that these estimated pore sizes have an order of magnitude similarity to those 'real' pores

constituting the centres of greatest flow resistance. Which pores constitute these centres is difficult to define with confidence. It is shown for example, in section 6.6.4.1, that in air dried late wood, margo interfibrillar spaces may largely control flow. In early wood, on the other hand, the main resistance to flow may be located in small gaps remaining between torus and border in partially aspirated pits.

The great attraction of pore size estimates based on flow measurement, is that the sizes estimated must relate to those pores directly involved in fluid conduction. Hence, any differences in the size of flow controlling pores caused by applied processes may be qualitatively assessed, without *a priori* knowledge of the pores involved.

Pore sizes estimated by gas flow methods depend on a reliable estimate of viscous and 'slip' permeability constants. It is shown in section 4.7.4 that below some critical working pressure, these constants and hence pore sizes calculated from them, are unreliable. Hence it is essential to work at gas pressures greater than this critical value to obtain meaningful pore size data. Provided that care is taken to meet this requirement, estimation of pore sizes from gas flow data may be a useful technique, for the limited application described above.

7.3 PERMEABILITY OF NON-SWOLLEN AND SWOLLEN WOOD

The relationship between the permeabilities of swollen and non-swollen wood is comprehensively discussed in Part 6. However, because of the potential technical importance of the effect of swelling, some aspects of more practical interest are further discussed below.

7.3.1 EFFECT OF ATMOSPHERIC CONDITIONS

Wood responds quite quickly to changes in the relative humidity of the atmosphere surrounding it (see for example, Banks 1973). It is seen from the data of section 6.3.4, that quite small changes in moisture content, induced by changes in atmospheric relative humidity, produce significant permeability changes. Hence, in conducting permeability experiments, it is essential to control experimental conditions so that any changes in specimen moisture content during flow measurement, are avoided.

On a more practical level, it must be remembered that rate of impregnation with non-swelling fluids may be decreased significantly by increase in wood moisture content within the hygroscopic range (ie up to about 30 per cent).

7.3.2 IMPREGNATION WITH VARIOUS LIQUIDS

Commercial impregnation of wood (eg wood preservation, dimensional stabilisation, etc) involves the use of various liquids. These include non-swelling systems, based on hydrocarbon solvents, and rapidly swelling ones such as those utilising water as the solvent. As indicated above (section 7.3.1), where non-swelling systems are involved, wood moisture content prior to impregnation is likely to markedly influence rate of penetration. Hence, where rate of penetration is the prime consideration it may be profitable to specify drying to the lowest practicable moisture content, prior to impregnation with this type of liquid.

During impregnation with swelling liquids (eg water-based ones), however, the wood immediately ahead of the moving liquid front will absorb water as a result of diffusional movement. Hence, in such systems, water transport is always through wood which is significantly fully swollen - irrespective of its state prior to impregnation. In this type of system, therefore, provided free water is absent from cell

spaces (ie moisture content at or below fibre saturation), further drying is likely to have little effect on penetration rate.

7.4 RELATIONSHIP BETWEEN PERMEABILITY AND RATE OF PENETRATION

In this work, the permeability of wood is studied under steady state conditions, ie constant rate of flow through specimens is maintained under the influence of constant pressure gradient. This mode of flow is described by the simple Darcy Law relationship (see section 1.4):-

$$Q = \frac{BA\Delta P}{\eta \ell} \qquad \text{Equation 1.10}$$

where Q = volume rate of flow
A = specimen area normal to flow direction
ΔP = pressure drop across specimen
η = liquid viscosity
ℓ = specimen length
B = specimen permeability constant.

Most practical liquid flow situations, however, involve the penetration of wood by a moving liquid front. This type of penetration for uniform porous media is described by a differential form of Darcy's law:-

$$\frac{dQ}{dt} = \frac{BA\Delta P}{\eta \ell} \qquad \text{Equation 7.1}$$

where t = time of flow;
all other symbols are as defined for equation 1.10 above.

Hence, for simple, uniform porous substrates, rate of penetration is predictable from a knowledge only of the steady state permeability constant.

7.4.1 EFFECT OF PORE BLOCKAGE

Evidence is cited in section 1.5.2 that wood may not behave as a simple, uniform porous medium. For example, in dry softwood, it has been shown (see section 1.5.2) that longitudinal permeability decreases markedly with increase in specimen length over the range 0 to about 30 mm. This decrease is due to a proportion of softwood pores being totally blocked, after air drying. Hence relationships derived to predict rate of penetration must take into account the change of permeability with flow path length. Rate of penetration, therefore, will depart significantly from that predicted by the Darcy relationship (equation 7.1).

7.4.2 EFFECT OF SURFACE FORCES

A liquid front advancing into a capillary is subject to surface forces. The magnitude and direction of these forces is related to:-

a liquid surface tension
b solid/liquid/vapour, contact angle
c capillary radius,

by the following equation:-

$$P = \frac{2\gamma \cos \theta}{r} \qquad \text{Equation 7.2}$$

(see basic texts on surface physics)

where P = surface force, expressed as effective pressure aiding or resisting pore penetration
γ = liquid surface tension
θ = contact angle
r = pore radius

For values of 'θ' less than 90°, cos θ and hence 'P' is positive and liquid is attracted into the capillary. For values of 'θ' greater than 90°, 'P' is negative, resisting

liquid entry into the capillary. The magnitude of 'P' increases rapidly with decrease in capillary radius 'r' (Figure 7.2).

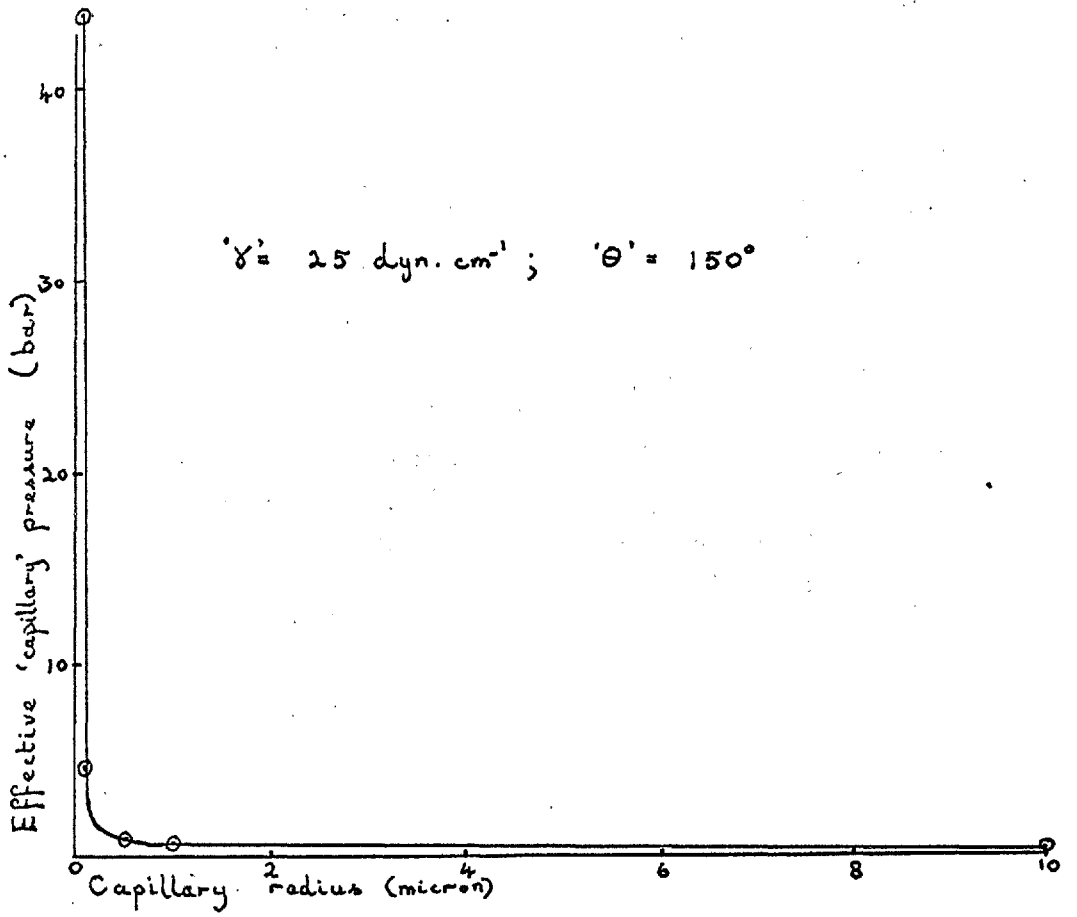


Fig 7.2 RELATIONSHIP BETWEEN EFFECTIVE CAPILLARY PRESSURE, AND CAPILLARY RADIUS

In an idealised porous medium (Figure 7.3) as for capillaries (above) it is clear from equation 7.2 that penetration is assisted by surface forces for 'θ' less than 90° and hindered where 'θ' is greater than 90°. Softwood departs significantly from such an idealised system. The larger pores (tracheid lumina) are not uniform, but cover a range of pore radii from about 3 to 30 micron (see section 1.2). Furthermore, these larger pores are interconnected by smaller ones (cell wall pits) - see Figure 7.4 below.

In such a system, the rate of penetration of the larger tracheids is greater than the smaller ones (since linear flow rate is proportional to r^2 - see section 1.4). Hence,

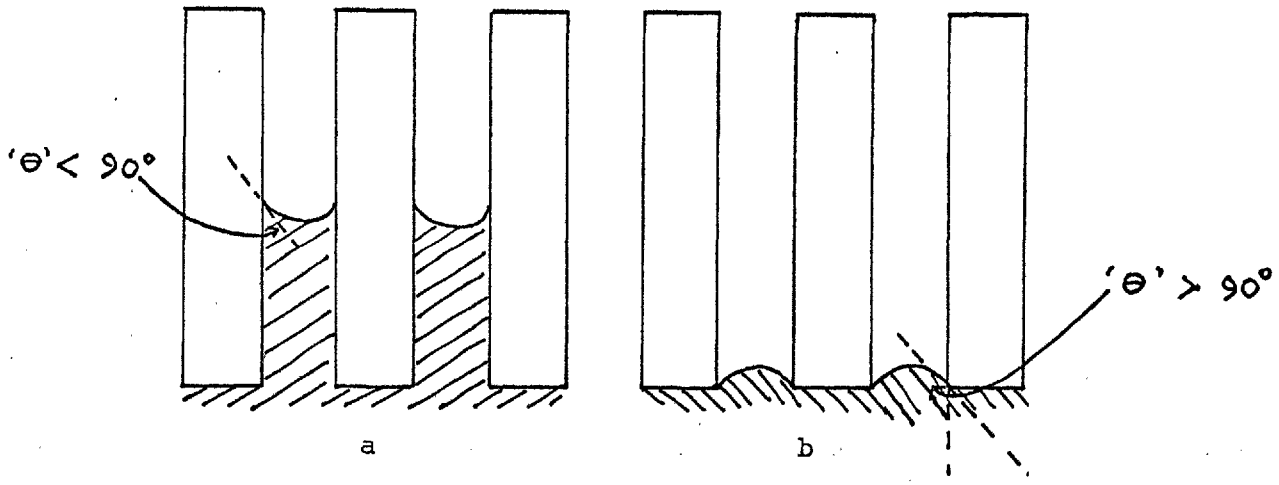


Fig 7.3 CAPILLARY PENETRATION IN POROUS MEDIA,
'a' CONTACT ANGLE 'θ' < 90°
'b' CONTACT ANGLE 'θ' > 90°

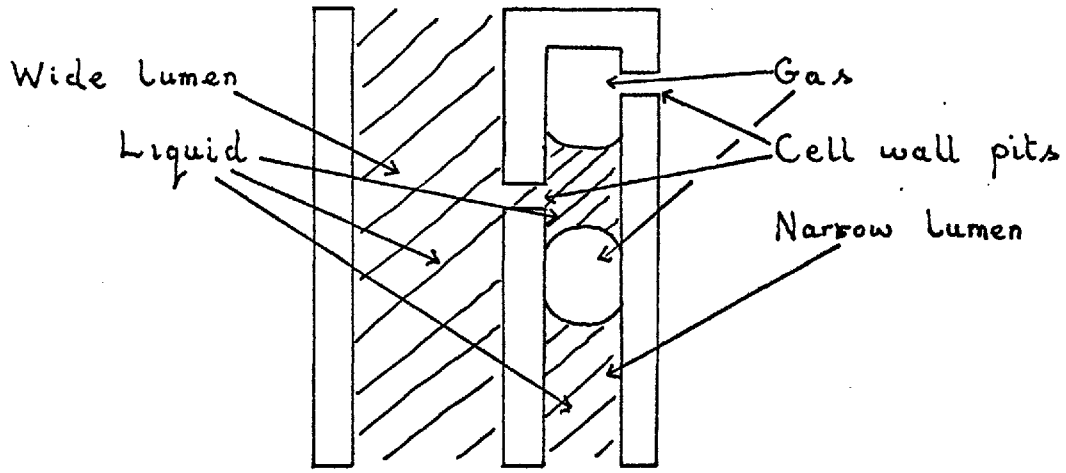


Fig 7.4 LIQUID PENETRATION INTO SOFTWOOD STRUCTURE

periodically the situation illustrated in Figure 7.4 is likely to arise, where a gas or vapour bubble is entrapped in the liquid stream. In such a system as for simple capillaries, if the contact angle 'θ' is less than 90°, initially, the advancing liquid front will spontaneously penetrate small pores encountered, whilst in systems where 'θ' is greater than 90° such penetration may be prevented by capillary pressure (see this section, above). Where gas bubbles are present, low contact angle or 'wetting' liquids may present a high resistance to penetration in some situations (Figure 7.5).

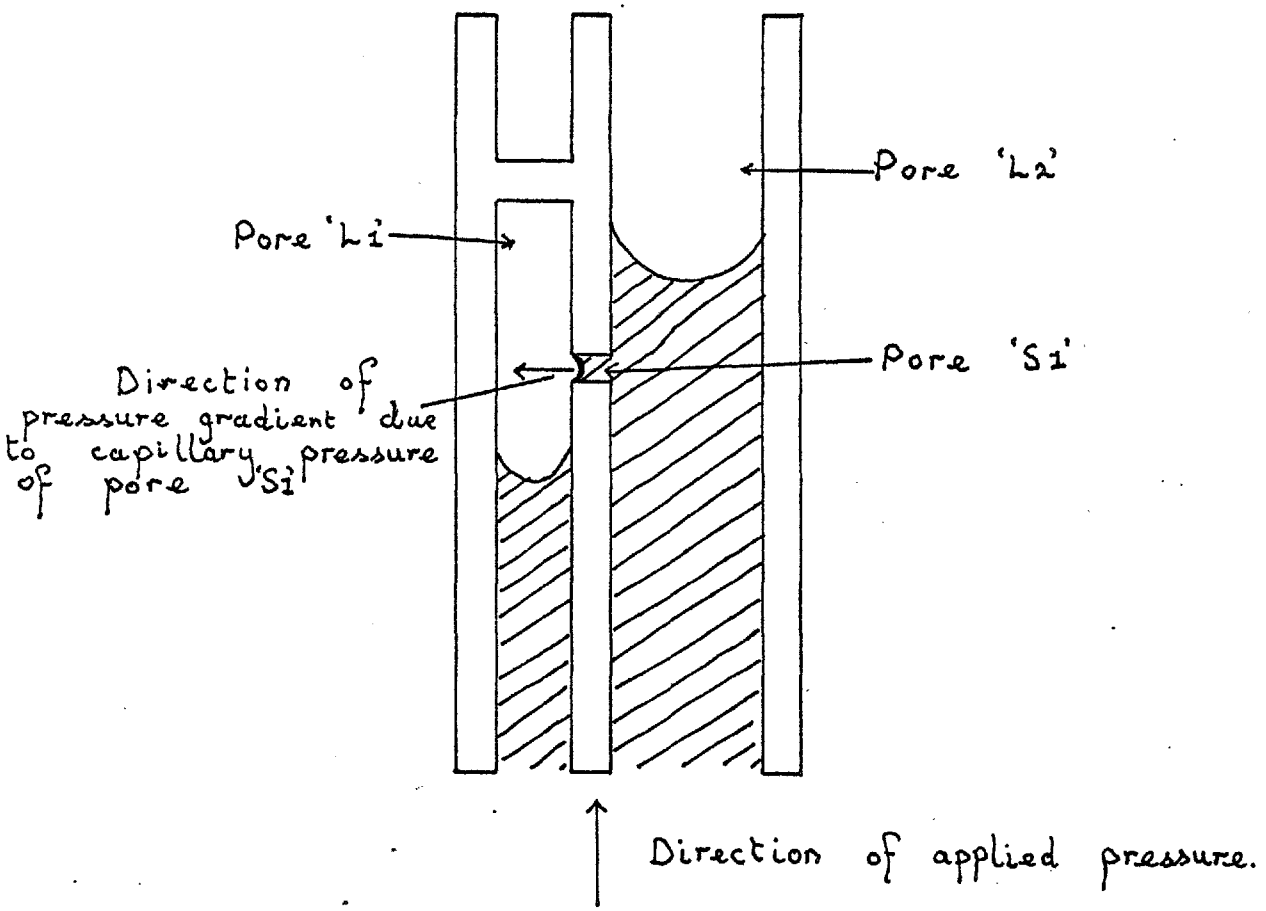


Fig 7.5 LIQUID PENETRATION, SHOWING HIGH RESISTANCE TO FLOW IN LOW CONTACT ANGLE SYSTEM

In the system shown in Figure 7.5, a high capillary pressure is generated in the small pore S_1. This high pressure operates in the direction shown by the arrow. Hence, further flow utilising the potential flow path $L_1 \rightarrow S_1 \rightarrow L_2$,

cannot occur unless the applied pressure differential across S_1 exceeds the capillary pressure of the pore. Thus it may be seen that for both 'wetting' (contact angle $<90^{\circ}$) and non-wetting (contact angle $>90^{\circ}$) systems, surface forces can occur in wood pores, resisting penetration by impregnant liquids.

From the foregoing it will be appreciated that whilst wood permeability is a major property effecting penetration of wood, it is not the only one. Flow routes into and through softwood, involves very small pores interconnected in a complex manner. Because of this, surface forces are likely to arise, grossly influencing rate and possibly depth of penetration.

From equation 7.2 above it is seen that the magnitude of the surface force (capillary pressure) resisting pore penetration, is proportional to liquid surface tension 'γ'. Therefore to minimise the risk of adversely effecting impregnation by surface effects, impregnant liquids should be selected with as low surface tension as possible.

Part 8 CONCLUSIONS AND SUGGESTIONS FOR FURTHER WORK

8.1 GAS FLOW PERMEABILITY MEASUREMENT

Gas flow measurement techniques are relatively simple and steady flow conditions can be easily achieved. Flowpaths in softwood are comprised of serially interconnected pores of widely varying diameter. Because of this feature it has been shown that estimation of viscous flow permeability, of all species tested, is subject to considerable error. This error is systematic and is always positive (ie estimates tend to be higher than true values). The magnitude of the error decreases with increase in working gas pressure. Numerical worked examples suggest that at gas pressures above about 5 bar the systematic error becomes insignificant. Facilities were not available to check the above finding experimentally. It would be useful to conduct such a check by the conduction of gas flow permeability measurements over a range of working pressures.

8.2 PORE SIZE ESTIMATION

Gas flow methods have often been used to estimate flow controlling pore size. As for estimation of permeability constant (section 8.1, above) it is shown that the method is extremely sensitive to the pressure of the flowing gas. Numerical examples demonstrated a marked decrease in estimated pore size as pressure increased in the range 0 to about 8 bar. Only above this pressure range did it approach a constant value. Thus it is essential to work at a sufficiently high pressure to eliminate this systematic error in order to obtain meaningful pore size data. The true magnitude of this 'critical' pressure, needs to be determined experimentally for wood species of interest.

It is further shown that even in the absence of the above systematic error, the pore sizes estimated relate to 'effective' pores. Because of softwood structural complexity they cannot be readily related to physically real wood capillaries.

The method is likely to be useful to make a comparative assessment of the effect of various experimental processes on pore structure.

8.3 NON SWELLING LIQUID FLOW

By careful filtration and de-aeration techniques, steady flow of liquid under small pressure differential, for prolonged time periods, was attained through non-swollen wood of all the species tested. Within the flow range investigated, increase in frictional drag was found to have no effect on permeability. Increase in pressure differential and hence of flow rate of a single liquid (n hexane) caused up to 30 per cent decrease in permeability. Some of this decrease was irreversible and has been ascribed to pore blocking by debris. The larger part of the permeability decrease, however, was reversible. Calculation of approximate Reynolds Number suggests that this reversible decrease was due to an increase in 'wake turbulence' (see section 5.3.2) at increased flow rate. Nevertheless, it remains possible that it resulted from elastic deformation of pore structure due to increased inertial force. To resolve this uncertainty it is necessary to measure permeability in systems where Reynolds Number and inertial force are independently varied.

8.4 EFFECT OF SWELLING ON PERMEABILITY

For the species examined (*Abies grandis*), swelling caused a marked permeability decrease. In air dried specimens this decrease amounted to some 60 to 70 per cent for cell wall swelling from the shrunken to the fully water swollen state.

In solvent dried wood the magnitude of the effect of swelling on permeability was found to be much less (only about 17 per cent for swelling from the shrunken to water swollen state).

It is believed that this difference in behaviour of air dried and solvent dried wood results from differences in major flow paths through these two types of material. In air dried wood, most early wood pits are aspirated, and it is likely that flow is mainly through late wood pits, where the ratio of membrane pore 'diameter' to pore wall thickness is small. Most pits in solvent dried wood, on the other hand, are un-aspirated. In this material, therefore, flow is largely by way of early wood pits where the pore diameter to pore wall thickness ratio is large.

Measurements of the effect of swelling on early wood and late wood of solvent dried wood separately, would be useful to test this hypothesis. It is pointed out above (section 7.2) that the gas flow method is useful to measure the effect of applied processes on effective pore size. This method could usefully be applied in further investigations of the effect of swelling. Effective pore sizes could be estimated for specimens swollen to various degrees by carrying out flow measurement with gases conditioned to various levels of relative humidity.

8.4.1 DE-ASPIRATION OF PIT MEMBRANES

Certain swelling liquids, notably methanol, appeared to cause some de-aspiration of bordered pits. This effect could have considerable commercial significance. A statistically designed experiment to investigate, microscopically, the possibility of systematically causing de-aspiration would be worth while.

Membranes in aspirated pits are believed to be fixed against pit borders initially by hydrogen bonding. It is likely that deposition of extractive material also contributes (sections 3.3 and 6.4.4). Hence to bring about de-aspiration

a combination of hydrogen bond donor/acceptor and extractive solvent properties may be required. It is indicated in section 6.4.4.1 that methanol is likely to combine these properties effectively.

8.5 THE RELATIONSHIP BETWEEN GAS AND LIQUID FLOW

For all species tested, it seems likely that longitudinal viscous permeability to gases and non-swelling liquids is identical. However, it was found that estimation of viscous permeability with gases at about atmospheric pressure led to significant positive error (ie estimated values were higher than true ones - see section 8.1). Results from numerical examples suggest that better estimates of viscous permeability from gas flow data may be achieved by working at increased pressure (about 5 bar).

As noted in section 8.1, facilities were not available to investigate experimentally the relationship between liquid flow and gas flow at the suggested increased pressure. An experimental study of this relationship would be worth while.

8.6 PENETRATION OF WOOD BY LIQUIDS

In addition to permeability, penetration, ie liquid front advance, into wood may be strongly effected by surface forces. Theoretical considerations suggest that such forces of sufficient magnitude to retard or resist liquid penetration may be generated.

To attain most rapid and deepest penetration with impregnant, it is desirable to treat wood in the non-swollen state with a low viscosity liquid. Additionally, to minimise the effect of the surface forces mentioned above, impregnants of low surface tension should be selected. Where impregnation is with a swelling liquid (eg an aqueous solution), the penetrated region and a zone a little way ahead of it is likely to be

fully swollen, irrespective of starting moisture content, due to the proximity of liquid water and water vapour. Hence, in this situation, further drying below fibre saturation point is unlikely significantly to increase penetration rate.

ACKNOWLEDGEMENTS

The work for this thesis was carried out at the Building Research Establishment, Princes Risborough Laboratory and Imperial College, Department of Botany, under the University of London 'Public Research Institutions' scheme.

I should like to thank the head of the Princes Risborough Laboratory, Dr E J Gibson for allowing and encouraging me to pursue the study.

My sincere thanks are recorded to Dr J F Levy, my Director of Studies and to my supervisor, Dr J W W Morgan, for helpful discussion and criticism during the period of study.

Many of the staff of the Princes Risborough Laboratory and of Imperial College offered help and advice on numerous occasions. I express my thanks to them; especially to Mr Peter Throsby who developed the computer program and gave invaluable advice on the mathematical analysis of data, and to Dr J M Dinwoodie and Mr E Adams who instructed me in the arts of electron microscopy of biological material.

I cannot overstress the debt which I owe to Mr D N R Smith who pioneered the early studies on wood permeability. He gave me the opportunity to follow up his studies and without his guidance this investigation would not have been undertaken.

I express my appreciation for the co-operation of Mrs Hilda Barnard, who typed the thesis, and to Mr John Russell who produced the photographic prints.

Finally I record my thanks to my wife, who not only tolerated an undecorated house for three years, but still found enthusiasm at the end to help with editing and compilation.

Appendix 1

DATA TABLES

Tables 1 to 13: MASS FLOW/MEAN PRESSURE DATA FOR HYDROGEN FLOW THROUGH TEST SPECIMENS

Table 1

Specimen AGSe	
$\frac{Qp_o}{\Delta p}$ ($cm^3\ sec^{-1}$)	$\bar{p}$ ($dyn\ cm^{-2}$)
46.4	2.06×10^6
44.0	1.87
40.8	1.68
39.2	1.57
35.9	1.39
33.6	1.27
30.4	1.08
25.9	0.85
23.4	0.71
21.1	0.56
17.8	0.42
14.5	0.27
13.3	0.22
10.5	0.13
6.8	0.03
5.4	0.007

Table 2

Specimen AGS.ℓ	
$\frac{Qp_o}{\Delta p}$ (cm^3 sec^{-1})	$\bar{p}$ (dyn cm^{-2})
84.1	1.93×10^6
78.2	1.75
71.3	1.66
66.6	1.48
63.1	1.36
58.0	1.20
52.2	1.03
47.0	0.88
42.5	0.77
36.7	0.61
32.7	0.51
26.0	0.35
17.6	0.16
16.0	0.14
9.5	0.04
7.8	0.009
7.2	0.006

Table 3

Specimen AGH.e	
$\frac{Qp_o}{\Delta p}$ (cm^3 sec^{-1})	$\bar{p}$ (dyn cm^{-2})
22.9	1.82×10^6
21.3	1.64
20.0	1.48
18.9	1.35
16.8	1.17
15.3	1.02
14.8	0.96
13.1	0.83
11.5	0.66
10.3	0.53
8.5	0.36
6.5	0.19
4.2	0.04
3.2	0.005

Table 4

Specimen AGH.ℓ	
$\frac{Qp_o}{\Delta p}$ ($cm^3\ sec^{-1}$)	$\bar{p}$ ($dyn\ cm^{-2}$)
13.3	2.06×10^6
12.7	1.86
11.2	1.68
11.0	1.51
10.1	1.37
9.7	1.18
8.6	1.02
7.9	0.88
7.2	0.74
6.1	0.58
5.3	0.40
3.9	0.18
3.4	0.12
2.4	0.03
2.2	0.009

Table 5

Specimen CDS	
$\frac{Qp_o}{\Delta p}$ ($cm^3\ sec^{-1}$)	$\bar{p}$ ($dyn\ cm^{-2}$)
89.55	1.82×10^6
84.35	1.66
80.89	1.55
76.24	1.40
71.92	1.25
66.11	1.08
63.41	0.99
56.86	0.83
54.69	0.73
49.20	0.58
45.56	0.49
42.69	0.43
38.12	0.33
32.04	0.21
27.43	0.14
22.43	0.079
19.68	0.048
12.33	0.003

Table 6

Specimen PAS.1	
$\frac{Qp_o}{\Delta p}$ ($cm^3\ sec^{-1}$)	$\bar{p}$ (dyn cm^{-2})
33.8	1.91×10^6
30.9	1.74
28.1	1.58
25.7	1.39
22.4	1.19
20.8	1.10
15.3	0.78
12.4	0.60
11.2	0.53
8.7	0.38
7.2	0.29
5.3	0.18
3.2	0.07
2.0	0.008
2.8	0.04

Table 7

Specimen PAS.2	
$\frac{Qp_o}{\Delta p}$ ($cm^3\ sec^{-1}$)	$\bar{p}$ (dyn cm^{-2})
45.2	1.86×10^6
40.6	1.64
37.2	1.49
34.6	1.38
30.6	1.20
27.3	1.05
24.2	0.91
21.7	0.80
16.9	0.59
14.3	0.47
12.8	0.40
10.8	0.32
7.9	0.19
6.1	0.12
4.4	0.061
2.7	0.006

Table 8

Specimen THS.e	
$\frac{Qp_o}{\Delta p}$ ($cm^3\ sec^{-1}$)	$\bar{p}$ ($dyn\ cm^{-2}$)
12.4	1.91×10^6
12.0	1.73
11.3	1.59
10.4	1.43
9.65	1.28
8.85	1.09
7.85	0.92
6.89	0.70
6.27	0.55
6.03	0.51
4.92	0.33
4.12	0.19
3.34	0.09
3.37	0.10
2.62	0.03
2.17	0.007

Table 9

Specimen THS.ℓ	
$\frac{Qp_o}{\Delta p}$ ($cm^3\ sec^{-1}$)	$\bar{p}$ ($dyn\ cm^{-2}$)
22.9	1.83×10^6
21.4	1.65
20.1	1.55
18.5	1.32
16.9	1.17
16.2	1.06
14.4	0.93
13.8	0.84
12.3	0.73
10.1	0.50
8.7	0.39
7.0	0.25
5.6	0.15
3.7	0.04
2.7	0.007

Table 10

Specimen THH.e	
$\frac{Qp_o}{\Delta p}$ (cm^3 sec^{-1})	$\bar{p}$ (dyn cm^{-2})
87.1	1.83×10^6
85.1	1.78
80.3	1.65
73.2	1.48
68.6	1.36
62.4	1.19
57.3	1.05
45.6	0.74
41.5	0.63
33.9	0.47
27.8	0.31
24.9	0.24
17.3	0.09
10.8	0.01
14.7	0.06

Table 11

Specimen THH.ℓ	
$\frac{Qp_o}{\Delta p}$ (cm^3 sec^{-1})	$\bar{p}$ (dyn cm^{-2})
29.5	1.89×10^6
27.9	1.76
25.7	1.60
23.5	1.42
20.9	1.23
19.7	1.05
17.3	0.90
14.7	0.74
14.0	0.61
13.2	0.58
10.9	0.41
9.7	0.31
7.8	0.19
4.6	0.04
3.3	0.003

Table 12

Specimen AAS	
$\frac{Qp_o}{\Delta p}$ (cm^3 sec^{-1})	$\overline{p}$ (dyn cm^{-2})
546.1	1.85×10^6
507.9	1.65
479.2	1.51
441.9	1.34
398.2	1.17
383.6	1.07
344.0	0.92
318.5	0.82
299.9	0.73
258.5	0.58
228.4	0.47
206.2	0.40
162.0	0.27
118.1	0.16
80.8	0.09
59.5	0.05
29.4	0.002

Table 13

Specimen AAH	
$\frac{Qp_o}{\Delta p}$ (cm^3 sec^{-1})	$\overline{p}$ (dyn cm^{-2})
383.0	1.88×10^6
366.2	1.74
344.4	1.58
308.2	1.36
287.0	1.18
264.3	1.03
246.1	0.92
220.5	0.75
191.9	0.62
168.5	0.48
145.0	0.37
124.0	0.28
104.9	0.21
76.6	0.12
43.4	0.03
33.0	0.003

Table 14

RATE OF FLOW OF n.HEXANE UNDER VARIOUS PRESSURE DIFFERENTIALS

Specimen \ Pressure differential (dyn cm^{-2} x 10^{-5})	Flow rate (ml sec^{-1}) at listed pressure differential (Chronological order of measurement →)									
	0.069	0.13	0.20	0.36	1.68	3.39	6.85	1.68	0.36	0.069
AGS.e				0.015	0.06	0.12	0.22	0.058	0.014	
AGS.ℓ				0.028	0.11	0.23	0.45	0.11	0.027	
AGH.e				0.010	0.033	0.065	0.12	0.03	0.007	
AGH.ℓ				0.004	0.020	0.038	0.070		0.004	
CDS				0.030	0.128	0.26			0.030	
CDH				N O F L O W						
PAS.1				0.020	0.070	0.14	0.24	0.062	0.018	
THS.e				0.003	0.012	0.023	0.043	0.012	0.003	
THS.ℓ				S P E C I M E N C O N T A M I N A T E D						
THH.e				0.033	0.053	0.26	0.45	0.12	0.03	
THH.ℓ				0.011	0.045	0.087	0.14	0.037	0.010	
AAH	0.023	0.047	0.067	0.11	0.41				0.11	0.022

Table 15 TRACHEID DIMENSIONS, *Abies grandis* EARLY WOOD

Specimen	Cell	Radial width (micron)		Tangential width (micron)	
		swollen	shrunken	swollen	shrunken
1	a	33	32	21	20
	b	34	33	18	15
	c	31	31	12	11
	d	40	40	24	25
	e	47	48	34	29
	f	28	28	16	15
	g	32	33	25	25
	h	40	40	28	26
	i	40	41	38	35
2	a	29	31	22	21
	b	28	28	29	27
	c	18	18	23	21
	d	27	24	25	25
	e	40	41	24	23
3	a	38	38	31	30
	b	35	35	30	26
	c	32	32	26	25
	d	29	29	19	15
	e	32	31	21	19
	f	33	33	12	12
	g	30	31	20	20
	h	33	33	20	20
	i	34	36	30	28
	j	30	31	18	16
	k	29	29	24	23
	l	34	33	23	21
	m	44	45	28	26
	n	33	33	24	22
	o	31	31	23	22
	p	27	27	30	30
	q	29	29	30	28
4	a	30	30	28	27
	b	34	34	31	30
	c	31	30	31	29
	d	38	39	36	34
	e	35	35	27	25
	f	31	31	35	33
	g	29	29	35	33
	h	29	30	31	30
	i	34	34	32	30
	j	29	30	34	33
	k	33	33	31	29
	Mean*	32.7	32.8	26.2	24.6

*NB Small differences in averages are apparent, between values cited in these tables and those given in table 6.23. This is because, to avoid 'rounding' errors, the averages used for permeability calculation (section 6.6.4) are calculated from the direct measurements made on the calibrated micrographs

Table 16 TRACHEID DIMENSIONS, *Abies grandis* LATE WOOD

Specimen	Cell	Radial width (micron)		Tangential width (micron)	
		swollen	shrunken	swollen	shrunken
1	a	6.5	7.0	14.5	14.8
	b	5.3	5.8	11.9	12.5
	c	4.7	5.6	12.8	11.9
	d	10.0	11.1	24.5	25.3
	e	7.8	8.6	22.3	22.2
	f	5.8	4.8	23.0	22.0
	g	6.6	7.2	19.5	18.4
	h	6.4	7.5	23.0	23.3
	i	3.6	3.6	20.2	19.7
	j	8.0	8.4	16.4	17.5
	k	7.5	8.6	19.7	19.1
	l	4.2	4.4	15.8	15.8
2	a	8.8	9.1	15.6	15.5
	b	7.5	7.8	17.0	18.4
	c	9.5	9.8	15.8	16.7
	d	12.5	11.9	15.3	14.8
	e	17.2	17.2	13.1	12.5
	f	5.5	6.3	12.0	12.2
	g	5.2	6.4	14.5	13.8
	h	5.8	8.8	14.1	13.3
	i	6.6	6.6	14.4	13.3
	j	8.9	9.4	21.6	19.5
	k	9.1	8.9	20.5	20.3
	l	12.3	13.9	15.6	18.4
	m	11.9	11.9	10.8	9.4
	n	13.3	13.1	11.4	11.3
	o	12.8	12.8	13.9	13.9
	Mean*	8.3	8.8	16.6	16.4

*NB Small differences in averages are apparent, between values cited in these tables and those given in table
This is because, to avoid 'rounding' errors, the averages used for permeability calculation (section
are calculated from the direct measurements made on the calibrated micrographs

Appendix 2

ANALYSIS OF SPECIFIC MASS FLOW/MEAN GAS PRESSURE RELATIONSHIP

The relationship between specific flow and mean pressure is significantly non-linear for low values of mean gas pressure (section 4.4). It is shown that this non-linearity is probably due to flow in the viscous/slip régime, through serial networks of capillaries of different diameters. In section 4.4 softwood structure is treated, to a first approximation, as parallel 'bundles' of flow paths, each flow path consisting of alternately large diameter (tracheid lumina) and small diameter (bordered pit) capillaries. Flow through such a system of capillary 'pairs' is described by the following equation:-

$$\overline{Q}_R = \frac{(a_1\overline{P} + b_1)(a_2\overline{P} + b_2)}{(a_1\overline{P} + b_1) + (a_2\overline{P} + b_2)} \qquad \text{Equation 4.7}$$

where $\overline{Q}_R$ = specific mass flow of the capillary pair
a_1 = a viscous permeability constant for capillary 1
a_2 = a vsicous permeability constant for capillary 2
b_1 = a slip permeability constant for capillary 1
b_2 = a slip permeability constant for capillary 2
$\overline{P}$ = mean gas pressure
(see section 4.4)

The experimental data of section 4.3 and Appendix 1 defines the relationship between $\overline{Q}_R$ and $\overline{P}$ for each specimen. The problem is then, to evaluate the constants a_1, a_2, b_1 and b_2.

NEWTON-RAPHSON METHOD

The problem cannot be solved by a direct method because there is only one relationship involved, namely that between $\frac{Qp_o}{\Delta p}$ and $\overline{P}$, and there are four unknowns, the constants a_1, b_1, a_2 and b_2 to be evaluated. The problem can be treated

iteratively by using an approximation technique usually known as the Newton-Raphson method (Stack, 1970)*.

This problem can be formulated as:-

$$\underset{\sim}{y} = \underset{\sim}{\underset{\sim}{f}}(\underset{\sim}{x} , \theta)$$

Where θ can be any number of constants, in this case 4, ie a_1, b_1, a_2 and b_2. So the problem reduces to choosing θ to minimise $\|\underset{\sim}{y} - \underset{\sim}{\underset{\sim}{f}}(\underset{\sim}{x} , \theta)\|^2$, called the norm and in fact the square of the error between $\underset{\sim}{y}$ and the approximation to $\underset{\sim}{\underset{\sim}{f}}(\underset{\sim}{x} , \theta)$, least squares).

Let the norm be denoted by 2V and $\underset{\sim}{\underset{\sim}{f}}(\underset{\sim}{x} , \theta)$ by $\underset{\sim}{f}$.

Then:- $$V = \tfrac{1}{2}\|\underset{\sim}{y} - \underset{\sim}{\underset{\sim}{f}}(\underset{\sim}{x} , \theta)\|^2 = \tfrac{1}{2}\langle \underset{\sim}{y} - \underset{\sim}{f} , \underset{\sim}{y} - \underset{\sim}{f} \rangle$$
$$= \tfrac{1}{2}\langle \underset{\sim}{y} , \underset{\sim}{y} \rangle - \langle \underset{\sim}{y} , \underset{\sim}{f} \rangle + \tfrac{1}{2}\langle \underset{\sim}{f} , \underset{\sim}{f} \rangle$$

The scalar product of a matrix (also called the inner product) can be written,

$$\langle \underset{\sim}{y} , \underset{\sim}{f} \rangle \equiv \underset{\sim}{y}^T \underset{\sim}{f} \equiv \sum_{i=1}^{n} y_i \cdot f_i$$

Where y^T is the transpose of the 'n' dimensional vector $\underset{\sim}{y}$, and y_i is the ith term in the vector $\underset{\sim}{y}$.

Hence:- $$V = \tfrac{1}{2}\underset{\sim}{y}^T \underset{\sim}{y} + \tfrac{1}{2}\underset{\sim}{\underset{\sim}{f}}^T \underset{\sim}{\underset{\sim}{f}} - \underset{\sim}{y}^T \underset{\sim}{\underset{\sim}{f}}$$

From the definition of differentiation the differential coefficient of V with respect to θ may be written as,

$$V(\theta + \delta\theta) = \tfrac{1}{2}\langle \underset{\sim}{y} - \underset{\sim}{f} - \underset{\sim}{f}_\theta \delta\theta , \underset{\sim}{y} - \underset{\sim}{f} - \underset{\sim}{f}_\theta \delta\theta \rangle$$
$$= \tfrac{1}{2}\langle \underset{\sim}{y} - \underset{\sim}{f} , \underset{\sim}{y} - \underset{\sim}{f} \rangle + \tfrac{1}{2}\langle \underset{\sim}{f}_\theta \delta\theta , \underset{\sim}{f}_\theta \delta\theta \rangle - \langle \underset{\sim}{f}_\theta \delta\theta , \underset{\sim}{y} - \underset{\sim}{f} \rangle .$$

---

*Stack P A, 1970, Introduction to Numerical Methods. London, MacMillan.

Hence to first order,

$$V(\theta + \delta\theta) = \tfrac{1}{2}\langle \underset{\sim}{y} - \underset{\sim}{f} , \underset{\sim}{y} - \underset{\sim}{f} \rangle - \langle \underset{\sim}{f}_\theta \delta\theta , \underset{\sim}{y} - \underset{\sim}{f} \rangle$$

$$V_\theta = \frac{\delta V}{\delta\theta} = \underset{\delta\theta \to 0}{\text{Lim}} \left(\frac{V(\theta + \delta\theta) - V(\theta)}{\delta\theta} \right)$$

$$\delta\theta V_\theta = \tfrac{1}{2}\langle \underset{\sim}{y} - \underset{\sim}{f} , \underset{\sim}{y} - \underset{\sim}{f} \rangle - \langle \underset{\sim}{f}_\theta \delta\theta , \underset{\sim}{y} - \underset{\sim}{f} \rangle - \tfrac{1}{2}\langle \underset{\sim}{y} - \underset{\sim}{f} , \underset{\sim}{y} - \underset{\sim}{f} \rangle$$

Therefore

$$V = \frac{-\langle \underset{\sim}{f}_\theta \delta\theta , \underset{\sim}{y} - \underset{\sim}{f} \rangle}{\delta\theta}$$

$$= -\langle \underset{\sim}{f}_\theta , \underset{\sim}{y} - \underset{\sim}{f} \rangle$$

$$= -\underset{\sim}{f}^T_\theta (\underset{\sim}{y} - \underset{\sim}{f})$$

$$V_{\theta\theta} \equiv \frac{\delta^2 V}{\delta\theta^2} = \underset{\sim}{f}_\theta{}^T \underset{\sim}{f}_\theta + \text{terms which} \to 0 \text{ near the true value.}$$

$$\delta\theta = -V_{\theta\theta}^{-1} V_\theta = (\underset{\sim}{f}_\theta{}^T \underset{\sim}{f}_\theta)^{-1} \underset{\sim}{f}_\theta{}^T (\underset{\sim}{y} - \underset{\sim}{f})$$

The iteration can thus be formulated as,

$$\theta_i + 1 = \theta_i + \delta\theta_i$$

Where $\theta_i + 1$ is the $(i + 1)^{th}$ iteration.

The iteration can be speeded up by factoring $\delta\theta_i$ by α, such that

$$\theta_i + 1 = \theta_i + \alpha . \delta\theta_i$$

Where $0 < \alpha \leq 1$.

α can in fact be greater than unity, and in the computer program is allowed to vary between zero and two. However as the iteration converges, α approaches unity. α is chosen such that $V(\theta_i + \alpha\delta\theta_i) < V(\theta_i)$ in fact ultimately so that $V(\theta_i + \alpha\delta\theta_i)$ is a minimum

In this case, $V = \langle \underset{\sim}{y} - \underset{\sim}{f} , \underset{\sim}{y} - \underset{\sim}{f} \rangle$

Where $(\underset{\sim}{y} - \underset{\sim}{f})$ is the error.

A program listing written in FORTRAN IV language, based on the algebraic process described is presented in the end flap. This incorporates examples of experimental data input and output from the program, in the evaluation of the constants a_1, b_1, a_2 and b_2.

REPERENCES

ADZUMI H (1937)

The flow of gaseous mixtures through capillaries. I. The viscosity of binary gaseous mixtures. *Bull Chem Soc Japan*, 12 199-226.

ANDERSON B E, GORTNER R H & SCHMITZ H (1941)

Factors affecting the decreasing rate of flow of liquids through wood. *Univ of Minnesota Agr Exp Stn Tech Bull* 146

BAILEY I W (1913)

The preservative treatment of wood. *For Quart*, 11, 5-21.

BAILEY P J & PRESTON R D (1969)

Some aspects of softwood permeability. I. Structural studies with Douglas fir sapwood and heartwood. *Holzforschung*, 23, 113-120.

BAILEY P J & PRESTON R D (1970)

Some aspects of softwood permeability. II. Flow of polar and non-polar liquids through sapwood and heartwood of Douglas fir. *Holzforschung*, 24, 37-45.

BANBER N F (1968)

A theoretical model of shrinking wood. *Holzforschung*, 22, 97-103.

BANKS W B (1968)

A technique for measuring the lateral permeability of wood. *J Inst Wood Sci* No 20, 35-41.

BANKS W B (1970)

Some factors affecting the permeability of Scots pine and Norway spruce. *J Inst Wood Sci*, 5, 10-17.

BANKS W B (1971)

Structure of the bordered pit membrane in certain softwoods as seen by scanning electron microscopy. *J Inst Wood Sci*, 5 (4) 12-15.

BANKS W B (1973)

Water uptake by Scots pine sapwood, and its restriction by the use of water repellents. *Wood Sci & Tech*, 7, 271-284.

BARCLAY R M (1955)

The effect of the middle lamella and anatomical structure on the tangential shrinkage of hardwoods. *J Oxf For Soc* 4 (3) 5-8.

BARR G (1931)

A monograph of viscometry.
Oxford Univ Press, London.

BAUCH J & BERNDT H (1973)

Variability of the chemical composition of pit membranes of gymnosperms. *Wood Sci & Tech*, 7, 6-19.

BAUCH J, LIESE W & SCHULZ F (1968)

Uber die Entwicklung und staffliche Zusammensetzung der Hoftüpfelmembranen von Längstracheiden in Coniferen. *Holzforschung*, 22, 145-53.

BAUCH J, LIESE W & SCHULTZE R (1972)

The morphological variability of the bordered pit membranes in gymnosperms. *Wood Sci & Tech*, 6, 165-184.

BEHR A E, SACHS I B, KUKACHKA B F & BLEW J O (1969)
Microscopic examination of pressure-treated wood.
For Prod J, 19, 31-40.

BEISER von W (1933)
Mikrophotographische Quellungsuntersuchungen von Fichten und Buchenholz on Mikrotomschnitten im durchfallenden Licht und on Holzklotzchen im auffallenden Licht. *Kolloidzeitschrift*, 65 (2) 203-211.

BIKERMAN J J (1958)
Surface chemistry.
Academic Press, NY.

BIRD R B, STEWARD W E & LIGHTFOOT E N (1960)
Transport phenomena.
John Wiley & Sons Inc, NY, London.

BOND W N (1922)
Viscosity determinations by means of orifices and short tubes. *Proc Phys Soc*, 34, 139.

BOUTELJE J B (1962)
On shrinkage and change in microscopic void volume during drying as calculated from microtome cross sections of Swedish pine. *Svensk Papperstidn*, 65 (6) 209-

BOUTELJE J (1973)
On the relationship between structure and the shrinkage and swelling of the wood in Swedish pine and spruce. *Svensk Papperstidn*, 76, 78-83.

BRAMHALL G (1971)
The validity of Darcy's Law in the axial penetration of wood. *Wood Sci & Tech*, 5, 121-134.

BRAMHALL G & WILSON J W (1971)
Axial gas permeability of Douglas fir micro-sections dried by various techniques. *Wood Science*, 3, 223-230.

BROWN F L & BAKER H M (1970)
Scanning electron microscopy of mature Douglas fir earlywood intertracheid pitting. *Wood & Fiber*, 2, 52-64.

BROWNING B L (1963)
The wood-water relationship
in - "The Chemistry of Wood", ed B L Browning, Interscience, London.

BUCHANAN M A (1963)
Extraneous components of wood
in - "The Chemistry of Wood", ed B L Browning, Interscience, London.

BUCKMAN S J, SCHMITZ H & GORTNER R A (1935)
A study of certain factors influencing the movement of liquids in wood. *J Phys Chem*, 39, 103-120.

BURMESTER A (1971)
On the improvement of wood with formaldehyde. *Holz als Roh- und Werkstoff*, 28, 184-188.

BURO A & BURO E A (1959a)
Contribution to the knowledge of how liquids penetrate into pine wood. *Holzforschung*, 13, 71-77. *Trans US Dept Ag For Serv*, FPL-624, 1965.

BURO A & BURO E A (1959b)
Studies on the permeability of wood. *Holz als Roh; und Werkstoff*, 17, 461-474.

CARMAN P C (1938)
Determination of the specific surface of powders I.
J Soc chem Ind, London (Trans), 57, 225-234.

CARMAN P C (1956)
Flow of gases through porous media.
Butterworths Scientific Publications, London.

CARMAN P C & ARNELL J C (1948)
Surface area measurements of fine powders using modified permeability equations. *Can J Res*, A26, 128.

CAVE I D (1972)
A theory of the shrinkage of wood.
Wood Sci & Tech, 6, 284-292.

CHEN P Y S & HOSSFELD R S (1964)
The effect of viscosity on the permeability of Sitka spruce to aqueous glycerine. *TAPPI*, 47, 750-752.

CLARKE S H (1930)
The differential shrinkage of wood.
Forestry, 4, 93-104.

COMOLET R (1949)
Sur l'écoulement laminaire dans un tube courbe.
CR Acad, Paris, 229, 342-343.

COMSTOCK G L (1965)
Longitudinal permeability of green eastern hemlock.
For Prod J, 15, 441-449.

COMSTOCK G L (1967)
Longitudinal permeability of wood to gases and non-swelling liquids. *For Prod J*, 17, 41-46.

COMSTOCK G L (1968)
Relationship between permeability of green and dry eastern hemlock. *For Prod J*, 18, 20-23.

COMSTOCK G L (1968a)

Physical and structural aspects of the longitudinal permeability of wood. Syracuse University, State University College of Forestry, *PhD thesis*.

COMSTOCK G L & CÔTÉ W A (1968)

Factors affecting permeability and pit aspiration in coniferous sapwood. *Wood Sci & Tech*, 2, 279-291.

CÔTÉ W A & KRAHMER R L (1962)

The permeability of coniferous pits demonstrated by electron microscopy. *TAPPI*, 45, 119-122.

COUETTE (1890)

Ann Chim Phys, 21
(Cited, Barr G, 1921 - A monograph of viscometry. London, Oxf Univ Press).

DARCY H P G (1856)

Les fontaines publiques de la ville de Dijon. Victor Dalmont, Paris.

DAUGHERTY R L & FRANZINI J B (1965)

Fluid mechanics with engineering applications (6th edition). McGraw-Hill, New York and London.

DODGE R A & THOMPSON M J (1937)

Fluid mechanics.
London, McGraw-Hill.

ECHLIN P (1968)

The use of the scanning reflection electron microscope in the study of plant and microbial material. *J Roy Microscopical Soc*, 88, 407-418.

EICKE R (1954)
Beitrag zur Frage des Hoftüpfelbaues der Koniferen. *Berichte der Deutschen Botanischen Gesellschaft*, 67, 123-127.

EISNER F (1931)
Das Wederstandsproblem.
Proc Third Int Cong App Mech, Stockholm.

ERICKSON H D (1960)
The effects of storage conditions and time upon permeability of green sapwood. *AWPA Proc*, 56, 156-165.

ERICKSON H D & BALATINECZ J J (1964)
Liquid flow paths into wood using polymerisation techniques - Douglas fir and styrene. *For Prod J*, 14, 293-299.

ERICKSON H D & CRAWFORD R (1959)
The effects of several seasoning methods on the permeability of wood to liquids. *AWPA Proc*, 55, 210-220.

ERICKSON H D & ESTEP E M (1962)
Permeability of Douglas fir heartwood from Western Washington. *For Prod J*, 12, 313-324.

ERICKSON H D, SCHMITZ H & GORTNER R A (1937)
The permeability of woods to liquids and factors affecting the rate of flow. *Univ of Minnesota, Agr Exp Stn Tech Bull* 122.

EWART R D (1905)
The ascent of water in trees.
Roy Soc Lond Philos Trans 198B:41-85.

FENGEL von D (1968)
Zur Variation der Hoftüpfelgestalt bei verschiedenen Nadelholzern. *Holz als Roh- und Werkstoff*, 26, 296-304.

FINDLAY G W D & LEVY J F (1969)
Scanning electron microscopy as an aid to the study of wood anatomy and decay. *J Inst Wood Sci* No 23, 57-63.

FINDLAY G W D & LEVY J F (1970)
Wood anatomy in three dimensions.
J Linn Soc, 63, 71-74.

FREY-WYSSLING A (1940)
Die Ursache der anisotropen Schwindung des Holzes.
Holz als Roh- und Werkstoff, 3, 349.

FREY-WYSSLING A, MÜHLETHALER K & BORSHARD H H (1965)
Das Elektronenmikroskop im Dienste der Bestimmung von Pinus-Arten. *Holz als Roh- und Werkstoff*, 13, 245-

GORDY W J (1939)
Spectroscopic comparison of the proton-attracting properties of liquids. *J Chem Physics*, 7, 93-99.

GRIFFIN G J (1919)
Bordered pits in Douglas fir - a study of the positions of the torus in mountain and lowland specimens in relation to creosote penetration. *J Forestry*, 17, 813-822.

GRIFFIN G J (1924)
Further note on the position of the tori in bordered pits in relation to penetration of preservatives.
J Forestry, 22 (6) 82-83.

HANKS R W & WEISSBERG H L (1964)
Slow viscous flow of rarefied gases through short tubes. *J Appl Phys*, 35, 142-144.

HART C A & THOMAS R J (1967)
Mechanism of bordered pit aspiration as caused by capillarity. *For Prod J*, 17, 61-68.

HERGT H F A & CHRISTENSEN G N (1972)
Capillary absorption by wood related to surface properties. *Holzforschung*, 26, 26-31.

HERMANS P H (1946)
Contribution to the physics of cellulose fibres. Elsevier - Amsterdam, London.

HONEYMAN J (1959)
Recent advances in the chemistry of cellulose and starch. Heywood & Co Ltd, London.

HOSSFELD R (1972)
The effect of degree of swelling of wood on its permeability to liquids. *Holzforschung*, 26, 70-76.

HUBER B & MERZ W (1958)
On the significance of bordered pit closure for the axial water conductivity of conifers. *Plants*, 51, 645-672.

JAYME G & FENGEL D (1959)
Untersuchungen über den Feinbau der Hoftüpfelschliesshäute in Fichtenholz unter Anwendung einer Feucht-Proparationsmethode. *Holz als Roh- und Werkstoff*, 17, 226-230.

JOHNSON H W & MAAS O (1930)
Penetration studies. The path of liquid penetration in Jack pine. *Canad J Research*, 3, 140-173.

JUTTE S M & SPIT B J (1963)
The submicroscopic structure of bordered pits on the radial walls of tracheids in Parana pine, kauri and European spruce. *Holzforschung*, 17, 168-175.

KAYE G W C & LABY T H (1956)
Tables of physical and chemical constants (11th edition). Longmans, Green and Co, London, New York and Toronto.

KELSEY K E (1963)
A critical review of the relationship between the shrinkage and structure of wood. *CSIRO Australia, Divn of For Prod Tech Paper* No 28.

KELSO W C, GERTJEJANSEN R O & HOSSFELD R L (1963)
The effect of air blockage upon the permeability of wood to liquids. *Univ Minn Agr Exp Stan Tech Bull* 242.

KLINKENBERG L J (1941)
Permeability of porous media to liquids and gases. *Amer Petrol Inst, Drill Prod Pract,* 200.

KNUDSEN M (1909)
Die Gesetze der Molekularströmung und der inneren Reibungsströmung der Gase durch Röhren. *Ann Phys, Lpz,* 28, 75-130.

KOEHLER A (1931)
Longitudinal shrinkage of wood.
Trans Amer Soc Mech Engrs Wood Ind Div, 53

KOLLMANN F (1935)
Die Bedeutung der Physik fur die moderne Holzforschung.
Z Forst- und Jagdw, 67, 75.

KOLLMANN F (1967)
Sorption and diffusion in wood.
Colloques Internationaux du Centre National de la Recherche Scientifique No 160.

KOLLMANN F F P & CÖTÉ W A (1968)
Principles of wood science and technology, I Solid wood. Springer-Verlag, Berlin, Heidleberg, New York.

KOZENY J (1927)

Uber kapillare Leitung des Wassers im Boden (Aufstieg, Versickerung und Anwendung auf die Bewässerung. *Sber Akad Wiss Wien* IIa, 136, 271-306.

KRAHMER R L & CÔTÉ W A (1963)

Changes in coniferous wood cells associated with heartwood formation. *TAPPI*, 46, 42-49.

KRIER J P (1951)

Factors causing decreasing rate of longitudinal flow of liquid through freshly cut woody stems. *PhD thesis*, University of Yale.

KUNDT A & WARBURG E (1875)

Phil Mag, 50, 53 (cited Carman, P C 1956, The flow of gases through porous media. London, Butterworth).

LEA F M & NURSE R W (1947)

Symposium on particle size analysis. *Inst of Chem Eng and Soc of Chem Ind*, February, p 47.

LIESE W (1951)

Demonstration elektronenmikroskopischer Aufnahmen von Nadelholztüpfeln. *Ber Dtsch Bot Ges*, 64, 31-32.

LIESE W (1954)

Der Feinbau der Hoftüpfel im Holz der Koniferen. *Proc Int Conf Electr Micr*, London, p 550.

LIESE W (1965)

Cellular ultrastructure of woody plants (ed W A Côté) Syracuse University Press.

LIESE W & BAUCH J (1967)

On the closure of bordered pits in conifers. *Wood Sci & Tech*, 1, 1-13.

LINDSAY F W & CHALK L (1954)

The influence of rays on the shrinkage of wood. *Forestry*, 27, 16-24.

MACLEAN J D (1928)

Relation of treating variables to the penetration and absorption of preservatives into wood. Part IV. Experiments on mountain Douglas fir, eastern hemlock and cork bark fir. *Proc Amer Wood Pres Assoc*, 52-72.

MILLIKAN R A (1923)

The general law of a fall of a small spherical body through a gas, and its bearing upon the nature of molecular reflection from surfaces. *Phys Rev*, 22, 1-23.

MORGAN J W W & ORSLER R J (1969)

The interaction of wood with organic solvents. *Holzforschung*, 23, 1-5.

MORGAN J W W & ORSLER R (1969)

The interaction of wood with organic solvents. II. Its significance for extractive location. *Holzforschung*, 23, 48-51.

MORRISON J L & DZIECIUCH M A (1959)

The thermodynamic properties of the system cellulose-water vapour. *Canad J of Chem*, 37, 1379-1390.

NAKATO K (1958)

On the cause of anisotropic shrinkage and swelling of wood. X. On the relationship between the microscopic structure and the anisotropic shrinkage in transverse section. *J Jap Wood Res Soc*, 4, 183-186.

NICHOLAS D D (1966)

Structure and chemical composition of the pit membrane in relation to the permeability of loblolly pine. *PhD thesis*. North Carolina State University, Raleigh.

OATLEY C W, NIXON W C & PEASE R F W (1965)
Scanning electron microscopy (*in 'Advances in electronics and electron physics'*, Vol 21, ed Manton, L, London, Academic Press).

OSNACH N A (1961)
On the permeability of wood.
Derev Prom, 10, 11-13. (Can Dept For and Rur Devel, Translation No 99).

PANSHIN A J & de ZEEUW C (1970)
Text Book of Wood Technology (3rd edition).
McGraw-Hill, New York; London.

PETTY J A (1967)
The movement of fluids through wood cell walls with special reference to timber preservation. *PhD thesis*, University of Leeds, Dept of Biophysics.

PETTY J A (1970)
Permeability and structure of the wood of Sitka spruce.
Proc Roy Soc Lond, B 175, 149-166.

PETTY J A (1972)
The aspiration of bordered pits in conifer wood.
Proc Roy Soc Lond, B 181, 395-406.

PETTY J A & PRESTON R D (1969a)
The dimensions and number of pit membrane pores in conifer wood. *Proc Roy Soc*, B 172, 137-151.

PETTY J A & PRESTON R D (1969b)
The removal of air from wood.
Holzforschung, 23, 9-15.

PETTY J A & PURITCH G S (1970)
The effects of drying on the structure and permeability of the wood of *Abies grandis*. *Wood Sci & Tech*, 4, 140-154.

PFALZNER P M (1950)

On the flow of gases and water vapour through wood. *Can J of Research,* A, 28, 389-410.

PHILLIPS E W J (1933)

Movement of the pit membrane in coniferous woods, with special reference to preservative treatment. *Forestry,* 7, 109-120.

PHILLIPS E W J (1948)

Identification of softwoods by their microscopic structure. *For Prod Res Bull* 22, London, HMSO.

PRANDTL L (1923)

Engerbnisse der aerodynamischen Versuchsanstalt zu Göttingen. R Oldenbourg K G, Munich.

PRESTON R D (1942)

Anisotropic contraction of wood and of its constituent cells. *Forestry,* 16, 32.

REPORT - DIRECTOR, FOREST PRODUCTS RESEARCH (1964)

Permeability of timber - mechanism of gas flow. pp 20-22, London, HMSO.

RESCH H & ECKLUND B A (1964)

Permeability of wood exemplified by measurements on redwood. *For Prod J,* 14, 199-206.

REYNOLDS O (1883)

An experimental investigation of the circumstances which determine whether motion of water will be direct or sinuous and of the law of resistance in parallel channels. *Phil Trans Roy Soc,* London.

RIGDEN P J (1947)

The specific surface of powders. A modification of the theory of the air permeability method. *J Soc Chem Ind,* London. Trans, 66, 130-136.

SACHS I B (1963)
Torus of the bordered pit membrane in conifers.
Nature, 198, 906-907.

SARKANEN K V (1963)
Wood lignins (*in 'The Chemistry of Wood'*, ed Browning, B L - Wiley, New York & London.

SCARTH G W (1928)
The structure of wood and its penetrability.
Paper Trade J, 86, 53-58.

SCHEIDEGGER A E (1957)
The physics of flow through porous media.
London - Oxford University Press; University of Toronto Press. (Revised edition published 1960.)

SCHILLER L (1923)
Über den Strömungswiderstand von Rohren verschiedenen Querschnitts und Rauhigkeitsgrades. *Z angew Math Mech*, 3, 2-13.

SCHUERCH C (1963)
Plasticizing wood with liquid ammonia.
Ind Eng Chem, 55, 39-

SEBASTIAN L P, CÔTÉ W A & SKAAR C (1965)
Relationship of gas phase permeability to ulstra-structure of white spruce wood. *For Prod J*, 15, 394-404.

SMITH D N R (*circa* 1960)
Unpublished data, Building Research Establishment, Princes Risborough Laboratory.

SMITH D N R (1963)
The permeability of wood to liquids and gases.
Food & Agr Org of the UN, 5th Conference on Wood Technology, held at FPL, Madison, Wisconsin, USA.

SMITH D N R & LEE E (1958)
The longitudinal permeability of some hardwoods and softwoods. *For Prod Res Spec Rep* 13. London, HMSO.

SMITH D N R & BANKS W B (1971)
The mechanism of flow of gases through coniferous wood. *Proc Roy Soc London*, B, 177, 197-223.

SMOLUCHOWSKI von M (1911)
Zur theorie dur Warmeleitung in Verdunnten gasen und dur dabei auftretenden Drudekrafte. *Ann Phys Lpz*, 35, 983-1004.

STAMM A J (1935)
The effect of changes in the equilibrium relative vapour pressure upon the capillary structure of wood. *Physics*, 6, 334-342.

STAMM A J (1946)
Passage of liquids, vapors and dissolved materials through softwoods. *US Dept of Agr Tech Bull* No 929.

STAMM A J (1964)
Wood and Cellulose Science.
Ronalds Press Co, New York.

STAMM A J & HANSEN L A (1935)
Minimizing wood shrinkage and swelling.
Ind Eng Chem, 27, 1480-1484.

STAMM A J & SMITH W E (1969)
Laminar sorption and swelling theory for wood and cellulose. *Wood Sci & Tech*, 3, 301-323.

STAMM A J & TARKOW H (1950)
Penetration of cellulose fibres.
J Phys and Colloid Chem, 54, 745-

STEMSRUD F (1956)
Über die Fernstruktur der Hoftüpfel-Schliesshaut von Nadelhölzern. *Holzforschung*, 10, 69-75.

STRASBURGER E (1891)
Histologische Beitrage, iii, 31.

SUCOFF E I, CHEN P Y S & HOSSFELD R L (1965)
Permeability of unseasoned xylem of northern white cedar. *For Prod J*, 15, 321-324.

SUTHERLAND J H, JOHNSTON H W & MAASS O (1934)
Further investigation of the penetration of liquids into wood. *Can J Res*, 10, 36-72.

THOMAS R J (1968)
The development and ultrastructure of the bordered pit membrane in the southern yellow pines. *Holzforschung*, 22, 38-44.

THOMAS R J (1969)
The ultrastructure of southern pine bordered pit membranes as revealed by specialized drying techniques. *Wood & Fiber*, 1, 110-123.

THOMAS R J & KRINGSTAD K P (1971)
The role of hydrogen bonding in pit aspiration. *Holzforschung*, 25, 143-149.

THOMAS R J & NICHOLAS D D (1966)
Pit membrane structure in loblolly pine as influenced by solvent exchange drying. *For Prod J*, 16, 53-56.

TIEMANN H D (1910)
The physical structure of wood in relation to its penetrability by preservative fluids. *American Ry Engin and Maintenance of Way Assoc, Bull* 120, 359-375.

TOPAKOGLU C (1951)

Steady laminar flow of an incompressible fluid through a curved pipe of circular cross section. *Pamphlet Istanbul Univ*, 30 pp.

VINTILA E (1939).

Untersuchungen über Raumgewicht und Schwindmass von Frich- und Spätholz bei Nadelhölzern. *Holz als Roh- und Werkstoff*, 2, 12.

WARDROP A B & DAVIES G W (1958)

Some anatomical factors relating to the penetration of water into the xylem of gymnosperms. *Aust J Bot*, 6 (2) 96-102.

WARDROP A B & DAVIES G W (1961)

Morphological factors relating to the penetration of liquids into wood. *Holzforschung*, 15, 129-141.

WEAST R D (ed) (1973)

Handbook of Chemistry and Physics. 54th edn. CRC Press, Cleveland, Ohio.

WEISS H F (1912)

The structure of commercial woods in relation to the injection of preservative. *Proc Am Wood Pres Assoc*, 8, 159-187.

WELLWOOD R W, IFJU G & WILSON J W (1964)

Inter increment physical properties of certain western Canadian coniferous species, *in 'Cellular Ultrastructure of Woody Plant'*, ed Côté W A, Syracuse Univ Press.

YOUNG J F (1967)

Humidity control in the laboratory using salt solutions - a review. *J of Appl Chem*, 17, 241-245.

```
      PROGRAM BARTTWO(DATAIN,OUTPUT,TAPE5=DATAIN,TAPE6=OUTPUT)          DEK000      2
C                                                                       DEK000      3
C                                                                       DEK000      4
C***********************************************************************DEK000      5
C**********                                                   **********DEK000      6
C**********  FLUID MECHANICS IN TIMBER    W.B. BANKS  4/2/70  **********DEK000      7
C**********                                                   **********DEK000      8
C**********          CDC 6400 DOUBLE PRECISION VERSION        **********DEK000      9
C**********                                                   **********DEK000     10
C**********             UPDATED TO 01 JUNE 1973               **********DEK000     11
C**********                                                   **********DEK000     12
C***********************************************************************DEK000     13
C                                                                       DEK000     14
C     FLOW OF GAS THROUGH A CAPILLARY VARIES AS PRESSURE ACCORDING TO   DEK000     15
C     THE LINEAR RELATIONSHIP, Q = A*P + B, WHERE Q IS THE MASS FLOW    DEK000     16
C     A IS THE VISCOUS FLOW COEFFICIENT( P IS THE PRESSURE AND B IS THE DEK000     17
C     SLIP FLOW COEFFICIENT.  SOFTWOOD CAN BE IDEALISED AS A SYSTEM OF  DEK000     18
C     ALTERNATE LARGE AND SMALL RADIUS CAPILLARIES.                     DEK000     19
C     FLOW THROUGH THESE CAPILLARIES IN SERIES OBEYS THE FOLLOWING      DEK000     20
C     EQUATION  1/Q = 1/Q1 + 1/Q2                                       DEK000     21
C     OR          Q = (A1*P+B1)(A2*P+B2)/( (A1+A2)*X + (B1+B2) )        DEK000     22
C     CURVES OF THESE EXPRESSIONS ARE OBTAINED EXPERIMENTIALLY          DEK000     23
C     THIS PROGRAM IS USED TO OBTAIN THE LINEAR RELATIONSHIPS Q1        DEK000     24
C     AND Q2 FROM THE EXPERIMENTAL CURVES                               DEK000     25
C                                                                       DEK000     26
C     FLOW THROUGH THE LARGE TYPE OF CAPILLARY IS GIVEN BY              DEK000     27
C     Y1= A1*X + B1, WHERE A1 AND B1 ARE CONSTANTS.                     DEK000     28
C     FLOW THROUGH THE SMALL TYPE OF CAPILLARY IS GIVEN BY              DEK000     29
C     Y2= A2*X + B2, WHERE A2 AND B2 ARE CONSTANTS.                     DEK000     30
C     HENCE FLOW THROUGH BOTH CAPILLARIES IN SERIES IS GIVEN BY         DEK000     31
C     1/Y = 1/Y1 + 1/Y2, OR  Y=(A1*X+B1)*(A2*X+B2)/((A1+A2)*X+(B1+B2))  DEK000     32
C                                                                       DEK000     33
C     PROGRAM GENERATES A SUMMARY OF ITERATIONS WHICH CAN BE LISTED     DEK000     34
C     BY CALLING SUBROUTINE SUMARY(ITCAN)                               DEK000     35
C                                                                       DEK000     36
C     METHOD                                                            DEK000     37
C     NEWTON-RAPHSON ITERATION                                          DEK000     38
C                                                                       DEK000     39
C                                                                       DEK000     40
C     DICTIONARY OF SYMBOLIC ADDRESSES                                  DEK000     41
C                                                                       DEK000     42
C     IDATA      IS DATA SET NUMBER                                     DEK000     43
C     NDATA      IS NUMBER OF DATA POINTS                               DEK000     44
C     ITCNT      IS ITERATION COUNTER                                   DEK000     45
C     ITMAX      IS MAXIMUM NUMBER OF ITERATIONS TO BE COMPLETED        DEK000     46
C     CVALUE     IS VALUE OF CONVERSION TEST                            DEK000     47
C     ALPHA      IS FACTOR OF DELTA'S USED IN NEXT ITERATION            DEK000     48
C     IWRITE     IS USED TO CONTROL OUTPUT                              DEK000     49
C     RDSQ       IS RECIPROCAL OF DENOMINATOR SQUARED                   DEK000     50
C                                                                       DEK000     51
C                                                                       DEK000     52
C     X(I)       IS INTERNAL NAME FOR PBAR(I)                           DEK000     53
C     Y(I)       IS INTERNAL NAME FOR Q(I)                              DEK000     54
C     A(I,J)     IS LEAST SQUARES MATRIX                                DEK000     55
C     ATRANS(I,J) IS TRANSPOSE OF A MATRIX                              DEK000     56
C     C(I,J)     IS PRODUCT OF PREMULTIPLICATION OF ATRANS(I,J) AND A(I,J DEK000     57
C     Z(I)       IS PRODUCT OF ATRANS(I,J) AND Y(I)                     DEK000     58
C     DLTA(I)    IS DELTA VECTOR                                        DEK000     59
C     YV(I)      IS VECTOR Y                                            DEK000     60
```

```
C     A1        IS SLOPE OF CURVE FOR LARGE CAPILLARY FLOW                    DEK000     61
C     B1        IS INTERCEPT ON Y1 AXIS OF ABOVE CURVE                        DEK000     62
C     A2        IS SLOPE OF CURVE FOR SMALL CAPILLARY FLOW                    DEK000     63
C     B2        IS INTERCEPT ON Y2 AXIS OF ABOVE CURVE                        DEK000     64
C                                                                             DEK000     65
C     SUBSCRIPTED VARIABLES USED IN GENERATING ITERATION SUMMARY              DEK000     66
C     ALPMIN(IT)   USED TO STORE ALPHAS                                       DEK000     67
C     VMIN(IT)     USED TO STORE MINIMUM V FUNCTIONS                          DEK000     68
C     GRAD(IT)     USED TO STORE NORM OF GRADIENT  (FIRST DERIVATIVE)         DEK000     69
C     AONE(IT)     USED TO STORE A1'S                                         DEK000     70
C     BONE(IT)     USED TO STORE B1'S                                         DEK000     71
C     ATWO(IT)     USED TO STORE A2'S                                         DEK000     72
C     BTWO(IT)     USED TO STORE B2'S                                         DEK000     73
C                                                                             DEK000     74
C     ALLOCATION OF GLOBAL STORAGE FOR THIS PROGRAM                           DEK000     75
C                                                                             DEK000     76
C                                                                             DEK000     77
000002       COMMON                                                           DEK000     78
            A/BLOCKA/ A(200,  6)                                              DEK000     79
            C/BLOCKC/ C( 6, 6)                                                DEK000     80
            D/BLOCKD/ DLTA( 6)                                                DEK000     81
            S/BLOCKS/ DSQ(200)                                                DEK000     82
            M/BLOCKM/ ALPMIN(128), VMIN(128), GRAD(128)                       DEK000     83
            P/BLOCKP/ PARAM( 6)                                               DEK000     84
            T/BLOCKT/ TPARAM(128, 6)                                          DEK000     85
            X/BLOCKX/ X(200)                                                  DEK000     86
            Y/BLOCKY/ Y(200)                                                  DEK000     87
            V/BLOCKV/ YV(200)                                                 DEK000     88
            Z/BLOCKZ/ Z(200)                                                  DEK000     89
C                                                                             DEK000     90
000002       DOUBLE PRECISION A                                               DEK000     91
000002       DOUBLE PRECISION ALPHA                                           DEK000     92
000002       DOUBLE PRECISION ALPINC                                          DEK000     93
000002       DOUBLE PRECISION ALPMIN                                          DEK000     94
000002       DOUBLE PRECISION ALPRNG                                          DEK000     95
000002       DOUBLE PRECISION ALPTMP                                          DEK000     96
000002       DOUBLE PRECISION C                                               DEK000     97
000002       DOUBLE PRECISION CVALUE                                          DEK000     98
000002       DOUBLE PRECISION DLTA                                            DEK000     99
000002       DOUBLE PRECISION DSQ                                             DEK000    100
000002       DOUBLE PRECISION EPS                                             DEK000    101
000002       DOUBLE PRECISION GRAD                                            DEK000    102
000002       DOUBLE PRECISION PARAM                                           DEK000    103
000002       DOUBLE PRECISION TPARAM                                          DEK000    104
000002       DOUBLE PRECISION VDLTA                                           DEK000    105
000002       DOUBLE PRECISION VLAST                                           DEK000    106
000002       DOUBLE PRECISION VMIN                                            DEK000    107
000002       DOUBLE PRECISION VTEMP                                           DEK000    108
000002       DOUBLE PRECISION X                                               DEK000    109
000002       DOUBLE PRECISION Y                                               DEK000    110
000002       DOUBLE PRECISION YV                                              DEK000    111
000002       DOUBLE PRECISION Z                                               DEK000    112
C                                                                             DEK000    113
C     INPUT DATA                                                              DEK000    114
C     READ DATA SET NUMBER     (FORMAT I5)                                    DEK000    115
000002    10 READ(5,500) IDATA,NDATA                                          DEK000    116
000012   500 FORMAT(2I5)                                                      DEK000    117
C     IF IDATA = 100 STOP                                                     OCT28A      1
000012       IF( IDATA.EQ.100 ) GO TO 999                                     OCT28A      2
000014       WRITE(6,600) IDATA,NDATA                                         DEK000    118
000024   600 FORMAT(45H1FLUID MECHANICS OF TIMBERS, DATA SET NUMBER , I5 ,/   DEK000    119
           +       35H0NUMBER OF BITS OF DATA IN THIS SET, I5 ,///)          DEK000    120
```

```
      C     NPARAM       IS NUMBER OF PARAMETERS TO BE DETERMINED                  DEK000   125
000024        NPARAM = 4                                                          DEK000   126
      C                                                                           DEK000   127
      C     IF IDATA = ZERO PROGRAM IS IN TEST MODE                               DEK000   128
000025        IF( IDATA.NE. 0 ) GO TO 101                                         DEK000   129
000026        CALL DATAGN(NPARAM, NDATA, PARAM )                                  DEK000   130
000031        GO TO 102                                                           DEK000   131
000032    101 CONTINUE                                                            DEK000   132
      C     IF IDATA SIX CALL GENSIX                                            DEK000   133
000032        IF( IDATA.NE.6 ) GO TO 107                                          DEK000   134
      C                                                                           DEK000   135
000034        READ(5,510) XND                                                     DEK000   136
000042    510 FORMAT(D20.8)                                                       DEK000   137
      C                                                                           DEK000   138
000042        CALL GENSIX(NPARAM,NDATA,XND)                                       DEK000   139
000045        GO TO 102                                                           DEK000   140
000046    107 CONTINUE                                                            DEK000   141
      C                                                                           DEK000   142
      C     IF IDATA GREATER THAN 90000,                                        OCT28A     3
      C     CALL SPECIAL SUBROUTINE TO READ X AND Y DIRECTLY                    OCT28A     4
000046        IF( IDATA.LT.90001 ) GO TO 108                                      OCT28A     5
000051        CALL PQIN(NPARAM,NDATA)                                             DEK000   146
000053        GO TO 102                                                           DEK000   147
000054    108 CONTINUE                                                            DEK000   148
      C                                                                           DEK000   149
      C     NORMAL DATA INPUT SUBROUTINE                                        DEK000   150
000054        CALL DATAIN(NPARAM, NDATA)                                          DEK000   151
      C                                                                           DEK000   152
000056    102 CONTINUE                                                            DEK000   153
      C     WRITE INPUT DATA AS CHECK                                           DEK000   154
      C                                                                           DEK000   155
000056        WRITE (6,600) IDATA,NDATA                                           DEK000   156
      C                                                                           DEK000   157
      C     WRITE INITIAL VALUES OF CONSTANTS A1,B1,A2,B2,A3,B3                 DEK000   158
      C                                                                           DEK000   159
000066        IF(NPARAM.EQ. 4) WRITE(6,601) (PARAM(I), I=1,NPARAM)                DEK000   160
000077    601 FORMAT(11H/INPUT DATA, //,                                          DEK000   161
             1  8H  A1  = , 1PD20.8, / ,                                         DEK000   162
             2  8H  B1  = , 1PD20.8, / ,                                         DEK000   163
             3  8H  A2  = , 1PD20.8, / ,                                         DEK000   164
             4  8H  B2  = , 1PD20.8, //)                                         DEK000   165
000077        IF(NPARAM.EQ. 6) WRITE(6,602) (PARAM(I), I=1,NPARAM)                DEK000   166
000110    602 FORMAT(11H0INPUT DATA, //,                                          DEK000   167
             1  8H  A1  = , 1PD20.8, / ,                                         DEK000   168
             2  8H  B1  = , 1PD20.8, / ,                                         DEK000   169
             3  8H  A2  = , 1PD20.8, / ,                                         DEK000   170
             4  8H  B2  = , 1PD20.8, / ,                                         DEK000   171
             5  8H  A3  = , 1PD20.8, / ,                                         DEK000   172
             6  8H  B3  = , 1PD20.8, // )                                        DEK000   173
      C                                                                           DEK000   174
      C     WRITE VALUES OF PBAR AND Q                                          DEK000   175
      C                                                                           DEK000   176
000110        WRITE(6,604)                                                        DEK000   177
000114    604 FORMAT( 4H0  I, 10X, 5H PBAR, 16X, 2H Q, // )                       DEK000   178
      C                                                                           DEK000   179
000114        DO 110 I=1,NDATA                                                    DEK000   180
000116        WRITE(6,606) I, X(I), Y(I)                                          DEK000   181
000131    110 CONTINUE                                                            DEK000   182
000134    606 FORMAT( 1X, I4, 1P2D20.8 )                                          DEK000   183
      C                                                                           DEK000   184
      C     ZEROISE DELTA VECTOR                                                DEK000   185
```

```
000134          DO 125 I=1,NPARAM                                                DEK000   186
000141          DLTA(I) = 0.000D+00                                              DEK000   187
000143       125 CONTINUE                                                        DEK000   188
                                                                                 DEK000   189
          C                                                                      DEK000   190
          C     SET ITERATION COUNTER TO START FROM ZERO                         DEK000   191
000144          ITCNT = -1                                                       DEK000   192
          C                                                                      DEK000   193
          C     SET INITIAL VALUES FOR EXAMINING ALPHA RANGE                     DEK000   194
          C     ALPRNG  IS RANGE OF ALPHA TO BE EXAMINED                         DEK000   195
000145          ALPRNG = 2.000D+00                                               DEK000   196
          C     ALPINC  IS INCREMENT OF ALPHA TO BE USED                         DEK000   197
000150          ALPINC = 0.010D+00                                               DEK000   198
          C                                                                      DEK000   199
000152          IND = ALPRNG/ALPINC + 0.100                                      DEK000   200
          C                                                                      DEK000   201
          C     SET CONVERGENCE VALUE FOR ITERATION                              DEK000   202
000171          CVALUE = 1.000D-10                                               DEK000   203
          C     WRITE CONVERGENCE VALUE FOR ITERATION                            DEK000   204
000173          WRITE(6,603) CVALUE                                              DEK000   205
000201       603 FORMAT(36H0CONVERGENCE VALUE FOR ITERATION IS , 1PD14.6,  //  )  DEK000   206
          C                                                                      DEK000   207
          C     SET MAXIMUM NUMBEROF ITERATIONS TO BE COMPLETED                  DEK000   208
000201          ITMAX = 127                                                      DEK000   209
          C     WRITE VALUE OF ITMAX                                             DEK000   210
000202          WRITE(6,654) ITMAX                                               DEK000   211
000210       654 FORMAT(32H0MAXIMUM NUMBER OF ITERATIONS IS, I10  )               DEK000   212
          C                                                                      DEK000   213
          C                                                                      DEK000   214
          C*********************************************************************DEK000   215
          C                                                                      DEK000   216
          C     START OF ITERATION PROCEDURE                                     DEK000   217
          C                                                                      DEK000   218
000210    1000 CONTINUE                                                        DEK000   219
          C     CURRENT VALUE OF ITERATION                                       DEK000   220
000210          ITCNT = ITCNT + 1                                                DEK000   221
          C                                                                      DEK000   222
          C     CHOOSE ALPHA TO GIVE MINIMUM V FUNCTION                          DEK000   223
000212          ALPHA = 0.000D+00                                                DEK000   224
000214          CALL OPTALP(NPARAM,NDATA,ALPHA,VLAST)                            DEK000   225
          C                                                                      DEK000   226
000217          VTEMP = VLAST                                                    DEK000   227
          C     IND SET OUTSIDE ITERATION LOOP                                   DEK000   228
000222          DO 235 I=1,IND                                                   DEK000   229
000223          ALPHA = FLOAT(I)*ALPINC                                          DEK000   230
000231          CALL OPTALP(NPARAM,NDATA,ALPHA,VDLTA)                            DEK000   231
          C     SELECT MINIMUM VDLTA AND NOTE VALUE OF ALPHA                     DEK000   232
000234          IF( VTEMP.LE.VDLTA ) GO TO 235                                   DEK000   233
000237          VTEMP = VDLTA                                                    DEK000   234
000241          ALPTMP = ALPHA                                                   DEK000   235
000244       235 CONTINUE                                                        DEK000   236
          C                                                                      DEK000   237
          C                                                                      DEK000   238
000247          ALPHA = ALPTMP                                                   DEK000   239
          C     UPDATE CONSTANTS A1 B1 A2 B2 A3 B3                               DEK000   240
000251          DO 237 I=1,NPARAM                                                DEK000   241
000261          PARAM(I) = PARAM(I) + ALPHA*DLTA(I)                              DEK000   242
000272       237 CONTINUE                                                        DEK000   243
          C                                                                      DEK000   244
          C     GATHER DATA FOR SUMMARY                                          DEK000   245
          C     IT  IS USED AS SUBSCRIPT FOR FORMING SUMMARY OF ITERATION        DEK000   246
000274          IT = ITCNT + 1                                                   DEK000   247
          C     ALPMIN(IT)  IS USED TO STORE SUMMARY OF ALPHA
```

```
000275          ALPMIN(IT) = ALPHA                                              DEK000   248
      C         VMIN(IT)  IS USED TO STORE SUMMARY OF MINIMUM VFUNCTION         DEK000   249
000301          VMIN(IT) = VTEMP                                                DEK000   250
      C                                                                         DEK000   251
000305          DO 129 I=1,NPARAM                                               DEK000   252
000316          TPARAM(IT,I) = PARAM(I)                                         DEK000   253
000320      129 CONTINUE                                                        DEK000   254
      C                                                                         DEK000   255
000322          IF( NPARAM.EQ. 4 ) CALL AFOUR( NPARAM, NDATA )                  DEK000   256
000326          IF( NPARAM.EQ. 6 ) CALL ASIX ( NPARAM, NDATA )                  DEK000   257
      C                                                                         DEK000   258
      C         PREMULTIPLY TRANSPOSE OF A BY A MATRIX                          DEK000   259
      C                                                                         DEK000   260
000332          DO 220 I=1,NPARAM                                               DEK000   261
000334          DO 240 J=1,NPARAM                                               DEK000   262
000335          C(I,J) = 0.000D+00                                              DEK000   263
000342          DO 260 K=1,NDATA                                                DEK000   264
000357          C(I,J) = C(I,J) + A(K,I) * A(K,J)                               DEK000   265
000370      260 CONTINUE                                                        DEK000   266
000372      240 CONTINUE                                                        DEK000   267
000374      220 CONTINUE                                                        DEK000   268
      C                                                                         DEK000   269
      C         PREMULTIPLY TRANSPOSE OF A MATRIX BY Y VECTOR                   DEK000   270
      C                                                                         DEK000   271
000376          DO 280 I=1,NPARAM                                               DEK000   272
000377          Z(I) = 0.000D+00                                                DEK000   273
000402          DO 300 K=1,NDATA                                                DEK000   274
000414          Z(I) = Z(I) + A(K,I) * YV(K)                                    DEK000   275
000425      300 CONTINUE                                                        DEK000   276
000427      280 CONTINUE                                                        DEK000   277
      C                                                                         DEK000   278
      C         CALCULATE NORM OF GRADIENT                                      DEK000   279
      C         GRADIENT IS FIRST DERIVATIVE OF V FUNCTION                      DEK000   280
      C                                                                         DEK000   281
000431          GRAD(IT) = 0.000D+00                                            DEK000   282
000435          DO 304 I=1,NPARAM                                               DEK000   283
000444          GRAD(IT) = GRAD(IT) + Z(I)*Z(I)                                 DEK000   284
000455      304 CONTINUE                                                        DEK000   285
      C                                                                         DEK000   286
000456          GRAD(IT) =DSQRT(GRAD(IT))                                       DEK000   287
      C         WRITE GRADIENT VECTOR AND NORM                                  DEK000   288
      C                                                                         DEK000   289
      C         CAPTION REQUIRED OUTSIDE LOOP FOR NPARAM = 4 AND 6              DEK000   290
      C                                                                         DEK000   291
      C                                                                         DEK000   292
      C         TEST IF CONVERGENCE IS ADEQUATE                                 DEK000   293
000466          IF( GRAD(IT).LT.CVALUE ) GO TO 197                              DEK000   294
      C                                                                         DEK000   295
      C         CALL INVERSION SUBROUTINE                                       DEK000   296
000472          EPS = 1.000D-100                                                DEK000   297
000474          NCOL = 1                                                        DEK000   298
      C         NOTE  INVERSION PROCEDURE WILL WORK IF DIMENSIONED STORAGE IS    DEK000   299
      C         GREATER THAN ACTUAL MATRIX SIZE                                 DEK000   300
000475          NDIM = 6                                                        DEK000   301
      C                                                                         DEK000   302
000476          CALL DGELG( NPARAM, NCOL, EPS , IER)                            DEK000   303
      C         IF MATRIX SINGULAR GO TO NEXT DATA SET                          DEK000   304
000501          IF( IER.NE. 0 ) GO TO 197                                       DEK000   305
      C         COPY SOLUTION TO DELTA VECTOR                                   DEK000   306
000502          DO 308 I=1,NPARAM                                               DEK000   307
000511          DLTA(I) = Z(I)                                                  DEK000   308
000513      308 CONTINUE                                                        DEK000   309
```

```
      C                                                                      DEK000    310
      C                                                                      DEK000    311
      C     TEST IF LIMIT OF ITERATIONS HAS BEEN REACHED                     DEK000    312
000515      IF( ITCNT.LT.ITMAX ) GO TO 1000                                  DEK000    313
      C                                                                      DEK000    314
      C                                                                      DEK000    315
000517  197 CONTINUE                                                         DEK000    316
      C                                                                      DEK000    317
000517      CALL SUMARY(IDATA, ITCNT, NPARAM)                                DEK000    318
      C                                                                      DEK000    319
      C     WRITE VALUE OF PARAMETERS                                        DEK000    320
      C                                                                      DEK000    321
000522      IF( NPARAM.EQ.4 ) WRITE(6,690) ITCNT,(PARAM(I),I = 1,NPARAM)     DEK000    322
000535  690 FORMAT(26H1VALUES OF CONSTANTS AFTER, I5,11H ITERATIONS, //,      DEK000    323
         1  7H  A1 = , 1PD20.8, / ,                                          DEK000    324
         2  7H B1 = , 1PD20.8, / ,                                           DEK000    325
         3  7H A2 = , 1PD20.8, / ,                                          DEK000    326
         4  7H B2 = , 1PD20.8, /    )                                       DEK000    327
000535      IF( NPARAM.EQ.6 ) WRITE(6,680) ITCNT, (PARAM(I),I = 1,NPARAM)    DEK000    328
000550  680 FORMAT(26H1VALUES OF CONSTANTS AFTER, I5,11H ITERATIONS, //,      DEK000    329
         1  7H  A1 = , 1PD20.8, / ,                                          DEK000    330
         2  7H  B1 = , 1PD20.8, / ,                                          DEK000    331
         3  7H  A2 = , 1PD20.8, / ,                                          DEK000    332
         4  7H  B2 = , 1PD20.8, / ,                                          DEK000    333
         5  7H  A3 = , 1PD20.8, / ,                                          DEK000    334
         6  7H  B3 = , 1PD20.8, //  )                                        DEK000    335
      C                                                                      DEK000    336
      C     S/R CHECK WRITES VALUES OF Q BASED ON CURRENT A1 B1 A2 B2        DEK000    337
000550      CALL CHECK(NPARAM, NDATA)                                        DEK000    338
      C                                                                      DEK000    339
      C     PROCESS NEXT DATA SET                                            DEK000    340
000552      GO TO 10                                                         DEK000    341
      C                                                                      DEK000    342
000553  999 STOP                                                           DEK000    343
      C                                                                      DEK000    344
000555      END                                                              DEK000    345
      C                                                                      DECK02      2

UNUSED COMPILER SPACE
015100


      SUBROUTINE DATAGN( NPARAM, NDATA, PARIN )                            DECK02      3
      C                                                                    DECK02      4
      C*********************************************************************DECK02      5
      C**********                                                 **********DECK02      6
      C**********          VERSION  25 APRIL 1970                 **********DECK02      7
      C**********                                                 **********DECK02      8
      C*********************************************************************DECK02      9
      C                                                                    DECK02     10
      C                                                                    DECK02     11
      C     DATAGN CALCULATES DATA FOR TESTING MAIN PROGRAM                DECK02     12
      C     LINEAR COMPONENTS ARE                                          DECK02     13
      C       Y1 = A1*X + B1                                               DECK02     14
      C       Y2 = A2*X + B2                                               DECK02     15
      C     THIS SUBROUTINE THEN CALCULATES Y VALUES FOR                   DECK02     16
      C       1/Y = 1/Y1 + 1/Y2                                            DECK02     17
      C                                                                    DECK02     18
      C                                                                    DECK02     19
      C     STORAGE FOR THIS S/R                                           DECK02     20
      C                                                                    DECK02     21
      C     LABELED COMMON STORAGE                                         DECK02     22
```

```
000005          COMMON                                                          DECK02     23
                X/BLOCKX/ X(200)                                                DECK02     24
                Y/BLOCKY/ Y(200)                                                DECK02     25
000005          DIMENSION PARAM( 6)                                             DECK02     26
000005          DIMENSION PARIN( 6)                                             DECK02     27
      C                                                                         DECK02     28
000005          DOUBLE PRECISION PARAM                                          DECK02     29
000005          DOUBLE PRECISION PARIN                                          DECK02     30
000005          DOUBLE PRECISION X                                              DECK02     31
000005          DOUBLE PRECISION XINC                                           DECK02     32
000005          DOUBLE PRECISION Y                                              DECK02     33
000005          DOUBLE PRECISION YA                                             DECK02     34
000005          DOUBLE PRECISION YB                                             DECK02     35
000005          DOUBLE PRECISION YC                                             DECK02     36
      C                                                                         DECK02     37
      C                                                                         DECK02     38
000005          WRITE(6,600)                                                    DECK02     39
000010    600 FORMAT(21H0PROGRAM IN TEST MODE, /// )                            DECK02     40
      C                                                                         DECK02     41
      C     SET CONSTANTS FOR LINEAR RELATIONSHIPS                            DECK02     42
000012          PARAM( 1) = 1.000D+00                                           DECK02     43
000015          PARAM( 2) = 0.500D+00                                           DECK02     44
000017          PARAM( 3) = 2.000D+00                                           DECK02     45
000022          PARAM( 4) = 1.500D+00                                           DECK02     46
000024          PARAM( 5) = 3.000D+00                                           DECK02     47
000027          PARAM( 6) = 1.000D+00                                           DECK02     48
      C                                                                         DECK02     49
      C     WRITE INPUT DATA AS CHECK                                         DECK02     50
000031          IF(NPARAM.EQ. 4) WRITE(6,605) (PARAM(I), I=1,NPARAM)            DECK02     51
000044    605 FORMAT( 11H0INPUT DATA, // ,                                      DECK02     52
                1  6H A1 = , 1PD20.7, / ,                                      DECK02     53
                2  6H B1 = , 1PD20.7, / ,                                      DECK02     54
                3  6H A2 = , 1PD20.7, / ,                                      DECK02     55
                4  6H B2 = , 1PD20.7, / )                                      DECK02     56
000044          IF(NPARAM.EQ. 6) WRITE(6,615) (PARAM(I), I=1,NPARAM)            DECK02     57
000057    615 FORMAT(11H0INPUT DATA, // ,                                       DECK02     58
                1 6H A1 = , 1PD20.7, / ,                                       DECK02     59
                2 6H B1 = , 1PD20.7, / ,                                       DECK02     60
                3 6H A2 = , 1PD20.7, / ,                                       DECK02     61
                4 6H B2 = , 1PD20.7, / ,                                       DECK02     62
                5 6H A3 = , 1PD20.7, / ,                                       DECK02     63
                6 6H B3 = , 1PD20.7, / )                                       DECK02     64
      C                                                                         DECK02     65
      C        **********          **********          **********          *** DECK02     66
      C                                                                         DECK02     67
      C     INVESTIGATE EFFECT OF INCREASING NDATA                            DECK02     68
      C                                                                         DECK02     69
      C        **********          **********          **********          *** DECK02     70
      C                                                                         DECK02     71
      C     SET RANGE FOR AUTOMATIC GENERATION OF X                           DECK02     72
000057          XST = 0.0000E+00                                                DECK02     73
000060          XND = 2.0000E+00                                                DECK02     74
000061          XRANGE = XND - XST                                              DECK02     75
000062          XINC = XRANGE/FLOAT(NDATA - 1)                                  DECK02     76
      C                                                                         DECK02     77
      C     GENERATE X VALUES                                                 DECK02     78
000066          DO 100 I =1,NDATA                                               DECK02     79
000074          X(I) = XINC * FLOAT( I - 1 )                                    DECK02     80
000103    100 CONTINUE                                                          DECK02     81
      C                                                                         DECK02     82
      C     CALCULATE Y VALUES CORRES PONDING TO X VALUES AND WRITE TO O/P     DECK02     83
000104          WRITE(6,620)                                                    DECK02     84
```

```
000112      620 FORMAT( 9H0Y VALUES,//,                                                  DECK02     85
               1 3X, 2H I, 10X, 2H X, 18X, 2H Y, //  )                                 DECK02     86
                                                                                        DECK02     87
            C                                                                           DECK02     88
000114            DO 110 I=1,NDATA                                                      DECK02     89
            C     SET PARIN(I) FOR THIS SUBROUTINE                                      DECK02     90
000120            YA = PARAM(1)*X(I) + PARAM(2)                                         DECK02     91
000132            YB = PARAM(3)*X(I) + PARAM(4)                                         DECK02     92
000143            YC = PARAM(5)*X(I) + PARAM(6)                                         DECK02     93
000155            IF(NPARAM.EQ. 4) Y(I) = (YA*YB)/(YA+YB)                               DECK02     94
000206            IF(NPARAM.EQ. 6) Y(I) = (YA*YB*YC)/(YB*YC + YA*YC + YA*YB)            DECK02     95
000260            WRITE(6,630) I, X(I), Y(I)                                            DECK02     96
000274      630 FORMAT( I5, 1P2D20.6 )                                                  DECK02     97
000276      110 CONTINUE                                                                DECK02     98
            C                                                                           DECK02     99
            C     SET INITIAL VALUES OF A1 A2 B1 AND B2 WHICH ARE CALLED                DECK02    100
000301            PARIN( 1) = 2.000D+00                                                 DECK02    101
000303            PARIN( 2) = 1.000D+00                                                 DECK02    102
000306            PARIN( 3) = 4.000D+00                                                 DECK02    103
000311            PARIN( 4) = 3.000D+00                                                 DECK02    104
000314            PARIN( 5) = 6.000D+00                                                 DECK02    105
000317            PARIN( 6) = 2.000D+00                                                 DECK02    106
            C                                                                           DECK02    107
            C                                                                           DECK02    108
000322            RETURN                                                                DECK02    109
            C                                                                           DECK02    110
000323            END                                                                   GENSIX      2
            C

UNUSED COMPILER SPACE
016500
```

```
            SUBROUTINE GENSIX(NPARAM,NDATA,XND)                                         GENSIX      3
            C                                                                           GENSIX      4
            C*************************************************************************GENSIX      5
            C**********                                                    **********  GENSIX      6
            C**********                VERSION 01 JUNE1973                 **********  GENSIX      7
            C**********                                                    **********  GENSIX      8
            C*************************************************************************GENSIX      9
            C                                                                           GENSIX     10
            C                                                                           GENSIX     11
            C     SUBROUTINE GENSIX READS IN SIXPARAMETERS                              GENSIX     12
            C     A1,B1,A2,B2,A3,B3 AND CALCULATES                                      GENSIX     13
            C     1/Y = 1/Y1 + 1/Y2 + 1/Y3                                              GENSIX     14
            C     WHERE Y1 = A1*X + B1                                                  GENSIX     15
            C           Y2 = A2*X + B2                                                  GENSIX     16
            C           Y3 = A3*X + B3                                                  GENSIX     17
            C     STORAGE FOR THIS S/R                                                  GENSIX     18
            C                                                                           GENSIX     19
            C     LABELED COMMON STORAGE                                                GENSIX     20
000005            COMMON                                                                GENSIX     21
                 X/BLOCKX/ X(200)                                                       GENSIX     22
                 Y/BLOCKY/ Y(200)                                                       GENSIX     23
                 P/BLOCKP/ PARAM( 6)                                                    GENSIX     24
000005            DIMENSION PARIN( 6)                                                   GENSIX     25
            C                                                                           GENSIX     26
000005            DOUBLE PRECISION PARAM                                                GENSIX     27
000005            DOUBLE PRECISION PARIN                                                GENSIX     28
000005            DOUBLE PRECISION X                                                    GENSIX     29
000005            DOUBLE PRECISION XINC                                                 GENSIX     30
000005            DOUBLE PRECISION Y                                                    GENSIX     31
000005            DOUBLE PRECISION YA                                                   GENSIX     32
```

```
000005          DOUBLE PRECISION YB                                              GENSIX     33
000005          DOUBLE PRECISION YC                                              GENSIX     34
          C                                                                      GENSIX     35
          C                                                                      GENSIX     36
000005          WRITE(6,600)                                                     GENSIX     37
000010      600 FORMAT(40H0PROGRAM IN BINOMIAL/POLYNOMIAL FIT MODE,///)          GENSIX     38
          C     READ DATA SET NUMBER                                             GENSIX     39
000012          READ(5,510) EX                                                   GENSIX     40
000020      510 FORMAT( I5 )                                                     GENSIX     41
          C     WRITE EXAMPLE NUMBER                                             GENSIX     42
000022          WRITE(6,640) EX                                                  GENSIX     43
000030      640 FORMAT(18H0EXAMPLE NUMBER    ,I5)                                GENSIX     44
000032          LPARAM = 6                                                       GENSIX     45
          C     READ IN SIX PARAMETERS A1,B1,A2,B2,A3,B3                         GENSIX     46
          C                                                                      GENSIX     47
000033          READ(5,500) (PARIN(I),I=1,LPARAM)                                GENSIX     48
000042      500 FORMAT( D20.8 )                                                  GENSIX     49
          C                                                                      GENSIX     50
          C     WRITE INPUT DATA AS CHECK                                        GENSIX     51
000044          WRITE(6,615) (PARIN(I), I=1,LPARAM)                              GENSIX     52
000053      615 FORMAT(46H0INPUT DATA FOR SIX PARAMETER CURVE GENERATION,//,     GENSIX     53
                1 6H A1 = , 1PD20.7, / ,                                       GENSIX     54
                2 6H B1 = , 1PD20.7, / ,                                       GENSIX     55
                3 6H A2 = , 1PD20.7, / ,                                       GENSIX     56
                4 6H B2 = , 1PD20.7, / ,                                       GENSIX     57
                5 6H A3 = , 1PD20.7, / ,                                       GENSIX     58
                6 6H B3 = , 1PD20.7, / )                                       GENSIX     59
          C                                                                      GENSIX     60
          C     SET RANGE FOR AUTOMATIC GENERATION OF X                          GENSIX     61
000055          XST = 0.0000E+00                                                 GENSIX     62
000055          XRANGE = XND - XST                                               GENSIX     63
          C                                                                      GENSIX     64
          C     SET NUMBER OF DATA SETS TO BE GENERATED                          GENSIX     65
          C                                                                      GENSIX     66
          C        **********          **********          **********       *** GENSIX     67
          C                                                                      GENSIX     68
          C     INVESTIGATE EFFECT OF INCREASING NDATA                           GENSIX     69
          C                                                                      GENSIX     70
          C        **********          **********          **********       *** GENSIX     71
          C                                                                      GENSIX     72
000057          XINC = XRANGE/FLOAT(NDATA - 1)                                   GENSIX     73
          C                                                                      GENSIX     74
          C     GENERATE X VALUES                                                GENSIX     75
000063          DO 100 I =1,NDATA                                                GENSIX     76
000070          X(I) = XINC * FLOAT( I - 1 )                                     GENSIX     77
000077      100 CONTINUE                                                         GENSIX     78
          C                                                                      GENSIX     79
          C     CALCULATE Y VALUES CORRESPONDING TO X VALUES AND WRITE TO O/P     GENSIX     80
000100          WRITE(6,620)                                                     GENSIX     81
000106      620 FORMAT( 9H0Y VALUES,// ,                                         GENSIX     82
               1 3X, 2H I, 10X, 2H X, 18X, 2H Y, //  )                         GENSIX     83
          C                                                                      GENSIX     84
000110          DO 110 I=1,NDATA                                                 GENSIX     85
          C     SET PARIN(I) FOR THIS SUBROUTINE                                 GENSIX     86
000114          YA = PARIN(1)*X(I) + PARIN(2)                                    GENSIX     87
000126          YB = PARIN(3)*X(I) + PARIN(4)                                    GENSIX     88
000137          YC = PARIN(5)*X(I) + PARIN(6)                                    GENSIX     89
000151          IF(LPARAM.EQ.6) Y(I) = (YA*YB*YC)/(YB*YC + YA*YC + YA*YB)        GENSIX     90
000223          WRITE(6,630) I, X(I), Y(I)                                       GENSIX     91
000237      630 FORMAT( I5, 1P2D20.6 )                                           GENSIX     92
000241      110 CONTINUE                                                         GENSIX     93
          C                                                                      GENSIX     94
```

```
000244          READ(5,500) (PARAM(I),I=1,NPARAM)                                GENSIX    95
                C                                                                GENSIX    96
                C                                                                GENSIX    97
000253          RETURN                                                           GENSIX    98
                C                                                                GENSIX    99
000254          END                                                              GENSIX   100
                C                                                                DECK03     2

UNUSED COMPILER SPACE
017000


                SUBROUTINE DGELG(M,N,EPS,IER)                                    DECK03     3
                C                                                                DECK03     4
                C*****************************************************************DECK03     5
                C**********                                             **********DECK03     6
                C**********      NEW VERSION INTRODUCED ON 29 MAY 1969  **********DECK03     7
                C**********                                             **********DECK03     8
                C**********            UPDATED TO 05 JUNE 1969          **********DECK03     9
                C**********                                             **********DECK03    10
                C*****************************************************************DECK03    11
                C                                                                DECK03    12
                C       SUBROUTINE DGELG        NOW MODIFIED TO SUIT HBPG        DECK03    13
                C                                                                DECK03    14
                C       PURPOSE                                                  DECK03    15
                C          TO SOLVE A GENERAL SYSTEM OF SIMULTANEOUS LINEAR EQUATIONS.DECK03  16
                C                                                                DECK03    17
                C       USAGE                                                    DECK03    18
                C          CALL DGELG(R,A,M,N,EPS,IER)        NOW CHANGED SEE BELOWDECK03    19
                C       CALL DGELG(M,N,EPS,IER).....A AND R NOW IN BLOCK COMMON  DECK03    20
                C                                                                DECK03    21
                C       DESCRIPTION OF PARAMETERS                                DECK03    22
                C          R      - DOUBLE PRECISION M BY N RIGHT HAND SIDE MATRIX DECK03    23
                C                   (DESTROYED). ON RETURN R CONTAINS THE SOLUTIONS DECK03    24
                C                   OF THE EQUATIONS.                            DECK03    25
                C          A      - DOUBLE PRECISION M BY M COEFFICIENT MATRIX     DECK03    26
                C                   (DESTROYED).                                 DECK03    27
                C          M      - THE NUMBER OF EQUATIONS IN THE SYSTEM.         DECK03    28
                C          N      - THE NUMBER OF RIGHT HAND SIDE VECTORS.         DECK03    29
                C          EPS    - DOUBLE PRECISION INPUT CONSTANT WHICH IS USED AS DECK03  30
                C                   RELATIVE TOLERANCE FOR TEST ON LOSS OF       DECK03    31
                C                   SIGNIFICANCE.                                DECK03    32
                C          IER    - RESULTING ERROR PARAMETER CODED AS FOLLOWS     DECK03    33
                C                   IER=0  - NO ERROR,                           DECK03    34
                C                   IER=-1 - NO RESULT BECAUSE OF M LESS THAN 1 OR DECK03  35
                C                            PIVOT ELEMENT AT ANY ELIMINATION STEPDECK03    36
                C                            EQUAL TO 0,                         DECK03    37
                C                   IER=K  - WARNING DUE TO POSSIBLE LOSS OF SIGNIFI-DECK03 38
                C                            CANCE INDICATED AT ELIMINATION STEP K+1,DECK03 39
                C                            WHERE PIVOT ELEMENT WAS LESS THAN OR DECK03  40
                C                            EQUAL TO THE INTERNAL TOLERANCE EPS TIMESDECK03 41
                C                            ABSOLUTELY GREATEST ELEMENT OF MATRIX A.DECK03  42
                C                                                                DECK03    43
                C       REMARKS                                                  DECK03    44
                C          INPUT MATRICES R AND A ARE ASSUMED TO BE STORED COLUMNWISE DECK03 45
                C          IN M*N RESP. M*M SUCCESSIVE STORAGE LOCATIONS. ON RETURN DECK03  46
                C          SOLUTION MATRIX R IS STORED COLUMNWISE TOO.           DECK03    47
                C          THE PROCEDURE GIVES RESULTS IF THE NUMBER OF EQUATIONS M IS DECK03 48
                C          GREATER THAN 0 AND PIVOT ELEMENTS AT ALL ELIMINATION STEPS DECK03 49
                C          ARE DIFFERENT FROM 0. HOWEVER WARNING IER=K - IF GIVEN - DECK03  50
                C          INDICATES POSSIBLE LOSS OF SIGNIFICANCE. IN CASE OF A WELL DECK03 51
                C          SCALED MATRIX A AND APPROPRIATE TOLERANCE EPS, IER=K MAY BE DECK03 52
```

```
C           INTERPRETED THAT MATRIX A HAS THE RANK K. NO WARNING IS      DECK03     53
C           GIVEN IN CASE M=1.                                           DECK03     54
C                                                                        DECK03     55
C        SUBROUTINES AND FUNCTION SUBPROGRAMS REQUIRED                   DECK03     56
C           NONE                                                         DECK03     57
C                                                                        DECK03     58
C        METHOD                                                          DECK03     59
C           SOLUTION IS DONE BY MEANS OF GAUSS-ELIMINATION WITH          DECK03     60
C           COMPLETE PIVOTING.                                           DECK03     61
C                                                                        DECK03     62
C     ..................................................................DECK03     63
C                                                                        DECK03     64
C                                                                        DECK03     65
C                                                                        DECK03     66
C     LABELLED COMMON DECLARATIONS                                       DECK03     67
000006      COMMON                                                       DECK03     68
           C/BLOCKC/ C( 6, 6)                                            DECK03     69
           Z/BLOCKZ/ R( 6)                                               DECK03     70
C                                                                        DECK03     71
C     SYMBOLIC ADDRESS A IS LOCAL TO THIS ROUTINE                        DECK03     72
000006      DIMENSION A(36)                                              DECK03     73
C                                                                        DECK03     74
000006      DOUBLE PRECISION A                                           DECK03     75
000006      DOUBLE PRECISION AZERO                                       DECK03     76
000006      DOUBLE PRECISION C                                           DECK03     77
000006      DOUBLE PRECISION EPS                                         DECK03     78
000006      DOUBLE PRECISION PIV, PIVI, TB, TOL                          DECK03     79
000006      DOUBLE PRECISION R                                           DECK03     80
C                                                                        DECK03     81
C     COPY C MATRIX AS ONE DIMENSIONAL ARRAY CLOSED UP COL BY COL        DECK03     82
000006      DO 400 I=1,M                                                 DECK03     83
000007      L = M*(I-1)                                                  DECK03     84
000012      DO 410 J=1,M                                                 DECK03     85
000021      K = L + J                                                    DECK03     86
000022      A(K) = C(J,I)                                                DECK03     87
000030  410 CONTINUE                                                     DECK03     88
000033  400 CONTINUE                                                     DECK03     89
C                                                                        DECK03     90
C                                                                        DECK03     91
000036      IF(M)23,23,1                                                 DECK03     92
C     SEARCH FOR GREATEST ELEMENT IN MATRIX A                            DECK03     93
000037    1 IER=0                                                        DECK03     94
000040      PIV = 0.000D+00                                              DECK03     95
000042      MM=M*M                                                       DECK03     96
000044      NM=N*M                                                       DECK03     97
000046      DO 3 L=1,MM                                                  DECK03     98
000047      TB=DABS(A(L))                                                DECK03     99
000052      IF(TB-PIV)3,3,2                                              DECK03    100
000063    2 PIV=TB                                                       DECK03    101
000066      I=L                                                          DECK03    102
000067    3 CONTINUE                                                     DECK03    103
000072      TOL=EPS*PIV                                                  DECK03    104
C     A(I) IS PIVOT ELEMENT. PIV CONTAINS THE ABSOLUTE VALUE OF A(I).    DECK03    105
C                                                                        DECK03    106
C                                                                        DECK03    107
C     START ELIMINATION LOOP                                             DECK03    108
000100      LST=1                                                        DECK03    109
000101      DO 17 K=1,M                                                  DECK03    110
C                                                                        DECK03    111
C     TEST ON SINGULARITY                                                DECK03    112
000102    4 IF(IER)7,5,7                                                 DECK03    113
000103    5 IF(PIV-TOL)6,6,7                                             DECK03    114
```

```
000112          6 IER=K-1                                                       DECK03   115
000114          7 PIVI = 1.000D+00/A(I)                                         DECK03   116
000130            J=(I-1)/M                                                     DECK03   117
000134            I=I-J*M-K                                                     DECK03   118
000136            J=J+1-K                                                       DECK03   119
                C     I+K IS ROW-INDEX, J+K COLUMN-INDEX OF PIVOT ELEMENT     DECK03   120
                C                                                             DECK03   121
                C     PIVOT ROW REDUCTION AND ROW INTERCHANGE IN RIGHT HAND SIDE R  DECK03   122
000140            DO 8 L=K,NM,M                                               DECK03   123
000145            LL=L+I                                                      DECK03   124
000146            TB=PIVI*R(LL)                                               DECK03   125
000157            R(LL)=R(L)                                                  DECK03   126
000166          8 R(L)=TB                                                     DECK03   127
                                                                              DECK03   128
                C     IS ELIMINATION TERMINATED                               DECK03   129
000174            IF(K-M)9,18,18                                              DECK03   130
                C                                                             DECK03   131
                C     COLUMN INTERCHANGE IN MATRIX A                          DECK03   132
000200          9 LEND=LST+M-K                                                DECK03   133
000202            IF(J)12,12,10                                               DECK03   134
000204         10 II=J*M                                                      DECK03   135
000207            DO 11 L=LST,LEND                                            DECK03   136
000216            TB=A(L)                                                     DECK03   137
000220            LL=L+II                                                     DECK03   138
000221            A(L)=A(LL)                                                  DECK03   139
000226         11 A(LL)=TB                                                    DECK03   140
                C                                                             DECK03   141
                C     ROW INTERCHANGE AND PIVOT ROW REDUCTION IN MATRIX A      DECK03   142
000236         12 CONTINUE                                                    DECK03   143
000236            DO 13 L=LST,MM,M                                            DECK03   144
000244            LL=L+I                                                      DECK03   145
000245            TB=PIVI*A(LL)                                               DECK03   146
000256            A(LL)=A(L)                                                  DECK03   147
000265         13 A(L)=TB                                                     DECK03   148
                                                                              DECK03   149
                C     SAVE COLUMN INTERCHANGE INFORMATION                     DECK03   150
000273            A(LST)=J                                                    DECK03   151
                C                                                             DECK03   152
                C     ELEMENT REDUCTION AND NEXT PIVOT SEARCH                 DECK03   153
000276            PIV = 0.000D+00                                             DECK03   154
000301            LST=LST+1                                                   DECK03   155
000302            J=0                                                         DECK03   156
000303            DO 16 II=LST,LEND                                           DECK03   157
000307            PIVI=-A(II)                                                 DECK03   158
000312            IST=II+M                                                    DECK03   159
000313            J=J+1                                                       DECK03   160
000315            DO 15 L=IST,MM,M                                            DECK03   161
000317            LL=L-J                                                      DECK03   162
000320            A(L)=A(L)+PIVI*A(LL)                                        DECK03   163
000333            TB=DABS(A(L))                                               DECK03   164
000337            IF(TB-PIV)15,15,14                                          DECK03   165
000350         14 PIV=TB                                                      DECK03   166
000353            I=L                                                         DECK03   167
000354         15 CONTINUE                                                    DECK03   168
000357            DO 16 L=K,NM,M                                              DECK03   169
000364            LL=L+J                                                      DECK03   170
000365         16 R(LL)=R(LL)+PIVI*R(L)                                       DECK03   171
000412         17 LST=LST+M                                                   DECK03   172
                C     END OF ELIMINATION LOOP                                 DECK03   173
                C                                                             DECK03   174
                C                                                             DECK03   175
                C     BACK SUBSTITUTION AND BACK INTERCHANGE                  DECK03   176
```

```
000416       18 IF(M-1)23,22,19                                                 DECK03   177
000420       19 IST=MM+M                                                        DECK03   178
000421          LST=M+1                                                         DECK03   179
000423          DO 21 I=2,M                                                     DECK03   180
000425          II=LST-I                                                        DECK03   181
000426          IST=IST-LST                                                     DECK03   182
000427          L=IST-M                                                         DECK03   183
000430          L=A(L)+.5D0                                                     DECK03   184
000437          DO 21 J=II,NM,M                                                 DECK03   185
000441          TB=R(J)                                                         DECK03   186
000444          LL=J                                                            DECK03   187
000446          DO 20 K=IST,MM,M                                                DECK03   188
000452          LL=LL+1                                                         DECK03   189
000454       20 TB=TB-A(K)*R(LL)                                                DECK03   190
000472          K=J+L                                                           DECK03   191
000473          R(J)=R(K)                                                       DECK03   192
000502       21 R(K)=TB                                                         DECK03   193
000512       22 GO TO 99                                                        DECK03   194
          C                                                                     DECK03   195
          C                                                                     DECK03   196
          C     RETURN FOR SINGULAR MATRIX                                      DECK03   197
000513       23 IER=-1                                                          DECK03   198
000514       99 CONTINUE                                                        DECK03   199
          C                                                                     DECK03   200
000514          IF( IER.EQ. 0 ) GO TO 999                                       DECK03   201
000515          WRITE(6,699) IER                                                DECK03   202
000523      699 FORMAT(24H0MATRIX SINGULAR, IER = , I5, // )                    DECK03   203
000526      999 CONTINUE                                                        DECK03   204
000526          RETURN                                                          DECK03   205
000527          END                                                             DECK03   206
          C                                                                     DECK05     2

UNUSED COMPILER SPACE
016200


          SUBROUTINE DATAIN(NPARAM, NDATA)                                      DECK05     3
          C                                                                     DECK05     4
          C                                                                     DECK05     5
          C*************************************************************************** DECK05     6
          C**********                                                 ********** DECK05     7
          C**********              UPDATED TO 12 MAY  1970            ********** DECK05     8
          C**********                                                 ********** DECK05     9
          C*************************************************************************** DECK05    10
          C                                                                     DECK05    11
          C                                                                     DECK05    12
          C     DATAIN PROCESSES INPUT DATA                                     DECK05    13
          C                                                                     DECK05    14
000004          COMMON                                                          DECK05    15
               P/BLOCKP/ PARAM( 6)                                              DECK05    16
               X/BLOCKX/ X(200)                                                 DECK05    17
               Y/BLOCKY/ Y(200)                                                 DECK05    18
000004          DIMENSION P1(200), SPECP(200), FLOWP(200)                       DECK05    19
000004          DOUBLE PRECISION C                                              DECK05    20
000004          DOUBLE PRECISION C1                                             DECK05    21
000004          DOUBLE PRECISION DTWO                                           DECK05    22
000004          DOUBLE PRECISION G                                              DECK05    23
000004          DOUBLE PRECISION F1                                             DECK05    24
000004          DOUBLE PRECISION F2                                             DECK05    25
000004          DOUBLE PRECISION FLOWP                                          DECK05    26
000004          DOUBLE PRECISION P                                              DECK05    27
000004          DOUBLE PRECISION P1                                             DECK05    28
```

```
000004          DOUBLE PRECISION P2                                          DECK05     29
000004          DOUBLE PRECISION P3                                          DECK05     30
000004          DOUBLE PRECISION PARAM                                       DECK05     31
000004          DOUBLE PRECISION SPECP                                       DECK05     32
000004          DOUBLE PRECISION U                                           DECK05     33
000004          DOUBLE PRECISION X                                           DECK05     34
000004          DOUBLE PRECISION Y                                           DECK05     35
        C                                                                    DECK05     36
000004          DO 130 I=1,NPARAM                                            DECK05     37
000011          PARAM(I) = 0.0000+00                                         DECK05     38
000013      130 CONTINUE                                                     DECK05     39
        C                                                                    DECK05     40
        C       READ VALUES OF PARAMETERS      (PARAM(I) )                   DECK05     41
000014          READ(5,550) ( PARAM(I), I=1,NPARAM)                          DECK05     42
        C       DETAIL OF FORMAT FOR READING CONSTANTS.   D20.5              DECK05     43
        C       DECIMAL POINT IN COLUMN 11                                   DECK05     44
        C       D IN COLUMN 17                                               DECK05     45
        C       SIGN OF EXPONENT IN COLUMN 18                                DECK05     46
        C       EXPONENT IN COLUMNS  19 AND 20,  RIGHT JUSTIFIED             DECK05     47
000025      550 FORMAT( D20.5 )                                              DECK05     48
        C                                                                    DECK05     49
        C       SET DATA COUNTER                                             DECK05     50
000027          I = 0                                                        DECK05     51
000027      100 I = I + 1                                                    DECK05     52
000031          READ(5,500) P1(I), SPECP(I), FLOWP(I)                        DECK05     53
000045      500 FORMAT( 3D20.5 )                                             DECK05     54
        C       IF LAST DATA HAS BEEN READ IN START PROCESSING               DECK05     55
000047          IF(P1(I).GT.10000.000) GO TO 125                             DECK05     56
000053          GO TO 100                                                    DECK05     57
000053      125 CONTINUE                                                     DECK05     58
        C                                                                    DECK05     59
        C       HENCE DETERMINE NUMBER OF DATA SETS READ IN                  DECK05     60
000053          NDATA = I-1                                                  DECK05     61
        C                                                                    DECK05     62
        C       SET MANOMETER CONSTANTS                                      DECK05     63
000055          F1 = 0.079570D+00                                            DECK05     64
000057          F2 = 0.007918D+00                                            DECK05     65
        C                                                                    DECK05     66
        C       WRITE TITLE AND MANOMETER FACTORS.                           DECK05     67
        C                                                                    DECK05     68
000062          WRITE(6,600) F1, F2                                          DECK05     69
000071      600 FORMAT( 18H0EXPERIMENTAL DATA, ///,                          DECK05     70
                   1 22H MANOMETER FACTOR F1 =, D20.8, /,                    DECK05     71
                   2 22H MANOMETER FACTOR F2 =, D20.8, / )                   DECK05     72
        C                                                                    DECK05     73
        C       SET CONVERSION FACTOR FOR MM HG TO DYNES/SQ. CM              DECK05     74
        C                                                                    DECK05     75
000073          C = 1.353410D+00                                             DECK05     76
000075          G = 980.6650D+00                                             DECK05     77
000100          C1 = G * C                                                   DECK05     78
        C       SET DOUBLE PRECISION TWO                                     DECK05     79
000106          DTWO = 2.000D+00                                             DECK05     80
        C                                                                    DECK05     81
        C       CALCULATE PBAR AND Q CALLED X AND Y IN THIS SUBROUTINE       DECK05     82
000110          DO 110 I=1,NDATA                                             DECK05     83
000121          P2 = F1 * SPECP(I)                                           DECK05     84
000127          P3 = F1 * FLOWP(I)                                           DECK05     85
000135          U = F2 * FLOWP(I)                                            DECK05     86
000143          P = P1(I) + P2 + P3/DTWO                                     DECK05     87
000167          Y(I) = U*P/P2                                                DECK05     88
000204          X( I)    = C1 * ( P1(I) + P2/DTWO )                          DECK05     89
000231      110 CONTINUE                                                     DECK05     90
```

```
      C     WRITE DATA AND CALCULATED RESULTS                                  DECK05    92
000234        WRITE(6,620)                                                     DECK05    93
000241    620 FORMAT(1H0,3X,1HI,5X,15HOUTLET PRESSURE,3X,17H SPECIMEN DELTA P,  DECK05    94
           12X,17HFLOWMETER DELTA P,8X,4HPBAR,17X,1HQ, // )                    DECK05    95
000243        DO 120 I=1,NDATA                                                 DECK05    96
000244        WRITE(6,640) I, P1(I), SPECP(I), FLOWP(I), X(I), Y(I)            DECK05    97
000272    120 CONTINUE                                                         DECK05    98
000274    640 FORMAT( I5,5D20.8 )                                              DECK05    99
000274    999 CONTINUE                                                         DECK05   100
000274        RETURN                                                           DECK05   101
000275        END                                                              DECK05   102
      C                                                                        DECK06     2

UNUSED COMPILER SPACE
017100


            SUBROUTINE CHECK( NPARAM, NDATA)                                   DECK06     3
      C                                                                        DECK06     4
      C*************************************************************************DECK06     5
      C***********                                                  ***********DECK06     6
      C***********          VERSION  26 APRIL 1970                  ***********DECK06     7
      C***********                                                  ***********DECK06     8
      C*************************************************************************DECK06     9
      C                                                                        DECK06    10
      C     CHECK CALCULATES VALUES OF Q BASED ON CURRENT VALUES OF            DECK06    11
      C     A1 B1 A2 B2 AS CHECK ON ACCURACY OF ITERATION                      DECK06    12
      C     THE DIFFERENCE BETWEEN THE ORIGINAL VALUES OF Q AND                DECK06    13
      C     THE NEW VALUES OF Q ARE WRITTEN                                    DECK06    14
      C                                                                        DECK06    15
      C                                                                        DECK06    16
      C     LABELED COMMON STORAGE                                             DECK06    17
000004        COMMON                                                           DECK06    18
           P/BLOCKP/ PARAM( 6)                                                 DECK06    19
           X/BLOCKX/ X(200)                                                    DECK06    20
           Y/BLOCKY/ Y(200)                                                    DECK06    21
000004        DOUBLE PRECISION DIFF                                            DECK06    22
000004        DOUBLE PRECISION PARAM                                           DECK06    23
000004        DOUBLE PRECISION TEMP1                                           DECK06    24
000004        DOUBLE PRECISION TEMP2                                           DECK06    25
000004        DOUBLE PRECISION TEMP3                                           DECK06    26
000004        DOUBLE PRECISION X                                               DECK06    27
000004        DOUBLE PRECISION Y                                               DECK06    28
000004        DOUBLE PRECISION YNEW                                            DECK06    29
      C                                                                        DECK06    30
      C     WRITE TITLE OF OUTPUT                                              DECK06    31
      C                                                                        DECK06    32
000004        WRITE(6,600)                                                     DECK06    33
000007    600 FORMAT(25H0SUBROUTINE CHECK ENTERED, // )                        DECK06    34
      C                                                                        DECK06    35
      C     WRITE NEW VALUES OF Q AND DIFFERENCES                              DECK06    36
      C                                                                        DECK06    37
000011        WRITE(6,610)                                                     DECK06    38
000014    610 FORMAT(4X , 1HI, 12X, 5H PBAR, 16X, 2H Q, 16X, 5HNEW Q, 12X,     DECK06    39
           1 10HDIFFERENCE, /  )                                               DECK06    40
      C                                                                        DECK06    41
000016        DO 100 I=1,NDATA                                                 DECK06    42
000022        TEMP1 = PARAM(1)*X(I) + PARAM(2)                                 DECK06    43
000033        TEMP2 = PARAM(3)*X(I) + PARAM(4)                                 DECK06    44
000045        TEMP3 = PARAM(5)*X(I) + PARAM(6)                                 DECK06    45
000056        IF(NPARAM.EQ. 4) YNEW = (TEMP1*TEMP2)/(TEMP1+TEMP2)              DECK06    46
```

```
000107          IF(NPARAM.EQ. 6) YNEW = (TEMP1*TEMP2*TEMP3)/                    DECK06     47
                1 (TEMP2*TEMP3 + TEMP1*TEMP2 + TEMP1*TEMP3)                     DECK06     48
000160          DIFF = Y(I) - YNEW                                              DECK06     49
000167          WRITE(6,620) I, X(I), Y(I), YNEW, DIFF                          DECK06     50
000206      620 FORMAT( I5, 1P4D20.6 )                                          DECK06     51
000210      100 CONTINUE                                                        DECK06     52
          C                                                                     DECK06     53
          C                                                                     DECK06     54
000212          RETURN                                                          DECK06     55
000212          END                                                             DECK06     56
          C                                                                     DECK08      2

UNUSED COMPILER SPACE
017400


          SUBROUTINE OPTALP(NPARAM,NDATA,ALPHA,V )                              DECK08      3
          C                                                                     DECK08      4
          C*********************************************************************DECK08      5
          C**********                                                 **********DECK08      6
          C**********                VERSION  10 MAY  1970            **********DECK08      7
          C**********                                                 **********DECK08      8
          C*********************************************************************DECK08      9
          C                                                                     DECK08     10
          C                                                                     DECK08     11
          C     OPTALP IS USED TO FIND THE OPTIMUM VALUE OF ALPHA TO            DECK08     12
          C     MINIMISE COST FUNCTION V                                        DECK08     13
          C                                                                     DECK08     14
000006          COMMON                                                          DECK08     15
               D/BLOCKD/ DLTA( 6)                                               DECK08     16
               P/BLOCKP/ PARAM( 6)                                              DECK08     17
               X/BLOCKX/ X(200)                                                 DECK08     18
               Y/BLOCKY/ Y(200)                                                 DECK08     19
          C                                                                     DECK08     20
000006          DIMENSION F(200)                                                DECK08     21
000006          DIMENSION TPARAM( 6)                                            DECK08     22
000006          DOUBLE PRECISION ALPHA                                          DECK08     23
000006          DOUBLE PRECISION DLTA                                           DECK08     24
000006          DOUBLE PRECISION ERROR                                          DECK08     25
000006          DOUBLE PRECISION F                                              DECK08     26
000006          DOUBLE PRECISION PARAM                                          DECK08     27
000006          DOUBLE PRECISION TEMP1                                          DECK08     28
000006          DOUBLE PRECISION TEMP2                                          DECK08     29
000006          DOUBLE PRECISION TEMP3                                          DECK08     30
000006          DOUBLE PRECISION TPARAM                                         DECK08     31
000006          DOUBLE PRECISION V                                              DECK08     32
000006          DOUBLE PRECISION X                                              DECK08     33
000006          DOUBLE PRECISION Y                                              DECK08     34
          C                                                                     DECK08     35
          C     CALCULATE CURRENT VALUES OF PARAMETERS                          DECK08     36
000006          DO 105 I=1,NPARAM                                               DECK08     37
000015          TPARAM(I) = PARAM(I) + ALPHA*DLTA(I)                            DECK08     38
000026      105 CONTINUE                                                        DECK08     39
          C                                                                     DECK08     40
000030          V = 0.000D+00                                                   DECK08     41
          C                                                                     DECK08     42
000035          DO 100 I=1,NDATA                                                DECK08     43
000051          TEMP1 = TPARAM(1)*X(I) + TPARAM(2)                              DECK08     44
000063          TEMP2 = TPARAM(3)*X(I) + TPARAM(4)                              DECK08     45
000075          TEMP3 = TPARAM(5)*X(I) + TPARAM(6)                              DECK08     46
          C                                                                     DECK08     47
000107          IF(NPARAM.EQ. 4) F(I) = (TEMP1*TEMP2)/(TEMP1+TEMP2)             DECK08     48
```

```
000140          IF(NPARAM.EQ. 6) F(I) = (TEMP1*TEMP2*TEMP3)/                    DECK08     49
                1 (TEMP2*TEMP3 + TEMP1*TEMP3 + TEMP1*TEMP2)                     DECK08     50
      C         HENCE NORM CAN BE CALCULATED                                    DECK08     51
000213          ERROR = Y(I) - F(I)                                             DECK08     52
000221          V = V + ERROR*ERROR                                             DECK08     53
000232        100 CONTINUE                                                      DECK08     54
      C                                                                         DECK08     55
000235          RETURN                                                          DECK08     56
000235          END                                                             DECK08     57
      C                                                                         DECK12      2

UNUSED COMPILER SPACE
017300


                SUBROUTINE SUMARY(IDATA, ITCNT, NPARAM)                         DECK12      3
      C                                                                         DECK12      4
      C*************************************************************************DECK12      5
      C**********                                                   **********  DECK12      6
      C**********              VERSION  10 MAY  1970                **********  DECK12      7
      C**********                                                   **********  DECK12      8
      C*************************************************************************DECK12      9
      C                                                                         DECK12     10
      C                                                                         DECK12     11
      C     SUMARY LISTS SUMMARY OF ITERATIONS                                  DECK12     12
000005          COMMON                                                          DECK12     13
               M/BLOCKM/ ALPMIN(128), VMIN(128), GRAD(128)                      DECK12     14
               T/BLOCKT/ TPARAM(128, 6)                                         DECK12     15
      C                                                                         DECK12     16
000005          DOUBLE PRECISION ALPMIN                                         DECK12     17
000005          DOUBLE PRECISION GRAD                                           DECK12     18
000005          DOUBLE PRECISION TPARAM                                         DECK12     19
000005          DOUBLE PRECISION VMIN                                           DECK12     20
      C                                                                         DECK12     21
000005          WRITE(6,600) IDATA                                              DECK12     22
000012        600 FORMAT(42H1SUMMARY OF ITERATIONS FOR DATA SET NUMBER, I10 )   DECK12     23
                                                                                DECK12     24
000014          WRITE(6,620)                                                    DECK12     25
000020        620 FORMAT( 4H0  I,7X,                                            DECK12     26
               1  6H ALPHA,                                                     DECK12     27
               2 21H          COST FUNCTION,                                   DECK12     28
               3 14H       GRADIENT,                                           DECK12     29
               4 13H       A1      ,                                           DECK12     30
               5 13H       B1      ,                                           DECK12     31
               6 13H       A2      ,                                           DECK12     32
               7 13H       B2      ,                                           DECK12     33
               8 13H       A3      ,                                           DECK12     34
               9 13H       B3      , // )                                      DECK12     35
      C                                                                         DECK12     36
      C     CYCLE SUMMARY OF ITERATION                                          DECK12     37
000022          IND = ITCNT + 1                                                 DECK12     38
000024          DO 100 I=1,IND                                                  DECK12     39
000025          IT = I - 1                                                      DECK12     40
000026          WRITE(6,630) IT, ALPMIN(I), VMIN(I),GRAD(I),                    DECK12     41
                1 (TPARAM(I,J), J=1,NPARAM)                                     DECK12     42
000072        100 CONTINUE                                                      DECK12     43
000075        630 FORMAT( 1X, I3, 1PD15.4, 1PD21.12,1PD13.4,1P6D13.5 )          DECK12     44
      C                                                                         DECK12     45
      C                                                                         DECK12     46
      C                                                                         DECK12     47
000075          RETURN                                                          DECK12     48
000075          END                                                             DECK12     49
```

```
      C                                                                 DECK14     2
UNUSED COMPILER SPACE
017600


            SUBROUTINE AFOUR( NPARAM, NDATA )                           DECK14     3
      C                                                                 DECK14     4
      C*****************************************************************DECK14     5
      C**********                                                *********DECK14     6
      C**********                VERSION  15  MAY  1970          *********DECK14     7
      C**********                                                *********DECK14     8
      C*****************************************************************DECK14     9
      C                                                                 DECK14    10
      C                                                                 DECK14    11
      C     AFOUR CALCULATES A MATRIX WHICH IS RECTANGULAR (N*4)        DECK14    12
      C     AFOUR ALSO CALCULATES Y VECTOR                              DECK14    13
      C     RDSQ   IS RECIPROCAL OF DENOMINATOR SQUARED                 DECK14    14
      C                                                                 DECK14    15
      C                                                                 DECK14    16
      C     LABELLED COMMON DECLARATIONS                                DECK14    17
000004        COMMON                                                    DECK14    18
           A/BLOCKA/ A(200,  6)                                         DECK14    19
           P/BLOCKP/ PARAM( 6)                                          DECK14    20
           X/BLOCKX/ X(200)                                             DECK14    21
           Y/BLOCKY/ Y(200)                                             DECK14    22
           V/BLOCKV/ YV(200)                                            DECK14    23
      C                                                                 DECK14    24
000004        DOUBLE PRECISION A                                        DECK14    25
000004        DOUBLE PRECISION PARAM                                    DECK14    26
000004        DOUBLE PRECISION DONE                                     DECK14    27
000004        DOUBLE PRECISION RDSQ                                     DECK14    28
000004        DOUBLE PRECISION TEMP1                                    DECK14    29
000004        DOUBLE PRECISION TEMP2                                    DECK14    30
000004        DOUBLE PRECISION TEMP3                                    DECK14    31
000004        DOUBLE PRECISION TEMP4                                    DECK14    32
000004        DOUBLE PRECISION TEMP5                                    DECK14    33
000004        DOUBLE PRECISION X                                        DECK14    34
000004        DOUBLE PRECISION Y                                        DECK14    35
000004        DOUBLE PRECISION YV                                       DECK14    36
      C                                                                 DECK14    37
      C     SET DOUBLE PRECISION ONE                                    DECK14    38
000004        DONE = 1.000D+00                                          DECK14    39
      C                                                                 DECK14    40
000006        DO 160 I=1,NDATA                                          DECK14    41
000020        TEMP1 = PARAM(1)*X(I) + PARAM(2)                          DECK14    42
000032        TEMP2 = PARAM(3)*X(I) + PARAM(4)                          DECK14    43
000044        TEMP3 = TEMP1 + TEMP2                                     DECK14    44
000053        TEMP4 = TEMP3 * TEMP3                                     DECK14    45
000061        RDSQ  = DONE / TEMP4                                      DECK14    46
000073        A(I,2) = TEMP2 * TEMP2 * RDSQ                             DECK14    47
000104        A(I,1) = A(I,2) * X(I)                                    DECK14    48
000112        A(I,4) = TEMP1 * TEMP1 * RDSQ                             DECK14    49
000122        A(I,3) = A(I,4) * X(I)                                    DECK14    50
000130        TEMP5 = (TEMP1*TEMP2)/TEMP3                               DECK14    51
000151        YV(I) = Y(I) - TEMP5                                      DECK14    52
000157      160 CONTINUE                                                DECK14    53
      C                                                                 DECK14    54
      C                                                                 DECK14    55
000167        RETURN                                                    DECK14    56
000167        END                                                       DECK14    57
      C                                                                 DECK16     2
```

UNUSED COMPILER SPACE
017500

```
                SUBROUTINE ASIX( NPARAM, NDATA )                                        DECK16     3
      C                                                                                 DECK16     4
      C*************************************************************************      DECK16     5
      C**********                                                          **********   DECK16     6
      C**********                VERSION  15  MAY  1970                    **********   DECK16     7
      C**********                                                          **********   DECK16     8
      C*************************************************************************      DECK16     9
      C                                                                                 DECK16    10
      C                                                                                 DECK16    11
      C       ASIX CALCULATES A MATRIX WHICH IS RECTANGULAR (N*6)                       DECK16    12
      C       ASIX ALSO CALCULATEA Y VECTOR                                             DECK16    13
      C       RDSQ   IS RECIPROCAL OF DENOMINATOR SQUARED                               DECK16    14
      C                                                                                 DECK16    15
      C       LABELLED COMMON DECLARATIONS                                              DECK16    16
000004          COMMON                                                                  DECK16    17
               A/BLOCKA/ A(200,  6)                                                     DECK16    18
               P/BLOCKP/ PARAM( 6)                                                      DECK16    19
               X/BLOCKX/ X(200)                                                         DECK16    20
               Y/BLOCKY/ Y(200)                                                         DECK16    21
               V/BLOCKV/ YV(200)                                                        DECK16    22
      C                                                                                 DECK16    23
000004          DOUBLE PRECISION A                                                      DECK16    24
000004          DOUBLE PRECISION DONE                                                   DECK16    25
000004          DOUBLE PRECISION PARAM                                                  DECK16    26
000004          DOUBLE PRECISION RDEM                                                   DECK16    27
000004          DOUBLE PRECISION RDSQ                                                   DECK16    28
000004          DOUBLE PRECISION TEMP1                                                  DECK16    29
000004          DOUBLE PRECISION TEMP2                                                  DECK16    30
000004          DOUBLE PRECISION TEMP3                                                  DECK16    31
000004          DOUBLE PRECISION TEMP4                                                  DECK16    32
000004          DOUBLE PRECISION TEMP5                                                  DECK16    33
000004          DOUBLE PRECISION TEMP6                                                  DECK16    34
000004          DOUBLE PRECISION TEMP7                                                  DECK16    35
000004          DOUBLE PRECISION TEMP8                                                  DECK16    36
000004          DOUBLE PRECISION TEMP9                                                  DECK16    37
000004          DOUBLE PRECISION X                                                      DECK16    38
000004          DOUBLE PRECISION Y                                                      DECK16    39
000004          DOUBLE PRECISION YV                                                     DECK16    40
      C                                                                                 DECK16    41
      C       SET DOUBLE PRECISION CONSTANT EQUAL TO UNITY                              DECK16    42
000004          DONE = 1.000D+00                                                        DECK16    43
      C                                                                                 DECK16    44
000006          DO 160 I=1,NDATA                                                        DECK16    45
000023          TEMP1 = PARAM(1)*X(I) + PARAM(2)                                        DECK16    46
000035          TEMP2 = PARAM(3)*X(I) + PARAM(4)                                        DECK16    47
000047          TEMP3 = PARAM(5)*X(I) + PARAM(6)                                        DECK16    48
000061          TEMP4 = TEMP1 * TEMP1                                                   DECK16    49
000067          TEMP5 = TEMP2 * TEMP2                                                   DECK16    50
000075          TEMP6 = TEMP3 * TEMP3                                                   DECK16    51
000103          TEMP7 = TEMP2 * TEMP3 + TEMP1*TEMP3 + TEMP1*TEMP2                       DECK16    52
000130          TEMP8 = TEMP7 * TEMP7                                                   DECK16    53
000136          RDSQ  = DONE/TEMP8                                                      DECK16    54
000150          RDEM  = DONE/TEMP7                                                      DECK16    55
      C                                                                                 DECK16    56
000163          A(I,2) = TEMP5 * TEMP6 * RDSQ                                           DECK16    57
000175          A(I,4) = TEMP4 * TEMP6 * RDSQ                                           DECK16    58
000206          A(I,6) = TEMP4 * TEMP2 * RDSQ                                           DECK16    59
```

```
000217          A(I,1) = A(I,2) * X(I)                                          DECK16     60
000225          A(I,3) = A(I,4) * X(I)                                          DECK16     61
000233          A(I,5) = A(I,6) * X(I)                                          DECK16     62
000240          TEMP9  = TEMP1 * TEMP2 * TEMP3 * RDEM                           DECK16     63
000254          YV(I)  = Y(I) - TEMP9                                           DECK16     64
000262      160 CONTINUE                                                        DECK16     65
          C                                                                     DECK16     66
          C                                                                     DECK16     67
000275          RETURN                                                          DECK16     68
000275          END                                                             DECK16     69

UNUSED COMPILER SPACE
017100


                SUBROUTINE PQIN(NPARAM,NDATA)                                   DECK17      2
          C     SUBROUTINE PQIN READS IN VALUES OF P AND Q ALREADY CALCULATED   DECK17      3
          C     FROM EXPERIMENTAL DATA                                          DECK17      4
          C                                                                     DECK17      5
          C     LABELLED COMMON DECLARATIONS                                    DECK17      6
000004          COMMON                                                          DECK17      7
               P/BLOCKP/ PARAM( 6)                                              DECK17      8
               X/BLOCKX/ X(200)                                                 DECK17      9
               Y/BLOCKY/ Y(200)                                                 DECK17     10
          C                                                                     DECK17     11
000004          DOUBLE PRECISION PARAM                                          DECK17     12
000004          DOUBLE PRECISION X                                              DECK17     13
000004          DOUBLE PRECISION Y                                              DECK17     14
          C                                                                     DECK17     15
000004          WRITE(6,600)                                                    FEB01A      3
000007      600 FORMAT( 8H WARNING,//,                                          FEB01A      4
               1 25H SUBROUTINE PQ ENTERED,//                                   FEB01A      5
               2  37H VALUES OF P AND Q ALREADY CALCULATED,//  )                FEB01A      6
000011          DO 130 I=1,NPARAM                                               DECK17     16
000016          PARAM(I) = 0.0000D+00                                           DECK17     17
000020      130 CONTINUE                                                        DECK17     18
          C     READ VALUES OF PARAMETERS (PARAM(I))                            DECK17     19
000021          READ(5,550) (PARAM(I),I=1,NPARAM)                               DECK17     20
          C     DETAIL OF FORMAT FOR READING CONSTANTS   D20.5                  DECK17     21
          C     DECIMAL POINT IN COLUMN 11                                      DECK17     22
          C     D IN COLUMN 17                                                  DECK17     23
          C     SIGN OF EXPONENT IN COLUMN 18                                   DECK17     24
          C     EXPONENT IN COLUMNS 19 AND 20, RIGHT JUSTIFIED                  DECK17     25
000032      550 FORMAT (D20.5)                                                  DECK17     26
                                                                              DECK17     27
          C                                                                     DECK17     28
000034          DO 100 I=1,NDATA                                                JUL20A      1
000035          READ(5,500) X(I),Y(I)                                           DECK17     30
000046      500 FORMAT (2D20.8)                                                 DECK17     31
000050      100 CONTINUE                                                        DECK17     32
000052          RETURN                                                          DECK17     33
000052          END

UNUSED COMPILER SPACE
020100
```

LOAD MAP. 74/11/11. 20.21.57.

FL REQUIRED TO LOAD 50100
FL REQUIRED TO RUN 41200
INITIAL TRANSFER TO BARTTWO - 15321

BLOCK ASSIGNMENTS.

BLOCK	ADDRESS	LENGTH	FILE
/BLOCKA/	100	4540	
/BLOCKC/	4640	110	
/BLOCKD/	4750	14	
/BLOCKS/	4764	620	
/BLOCKM/	5604	1400	
/BLOCKP/	7204	14	
/BLOCKT/	7220	3000	
/BLOCKX/	12220	620	
/BLOCKY/	13040	620	
/BLOCKV/	13660	620	
/BLOCKZ/	14500	620	
BARTTWO	15320	5244	LGO
DATAGN	22564	565	LGO
GENSIX	23351	436	LGO
DGELG	24007	723	LGO
DATAIN	24732	2723	LGO
CHECK	27655	272	LGO
OPTALP	30147	1151	LGO
SUMARY	31320	226	LGO
AFOUR	31546	253	LGO
ASIX	32021	402	LGO
PQIN	32423	121	LGO
/GENVAR./	32544	0	
SYSTEM	32544	1532	RUNLIB
CPUCPR	34276	171	RUNLIB
DABS	34467	15	RUNLIB
DSQRT	34504	60	RUNLIB
GETBA	34564	17	RUNLIB
INPUTC	34603	130	RUNLIB
KODER	34733	1303	RUNLIB
KRAKER	36236	1055	RUNLIB
OUTPTC	37313	72	RUNLIB
REWINM	37405	63	RUNLIB
SIO£	37470	1440	RUNLIB
CPUSYS	41130	32	RUNLIB
CPUCPM	41162	4	RUNLIB

ENTRY POINTS.

ENTRY	ADDRESS	REFERENCES
BARTTWO		
BARTTWO	15321	
DATAGN		

```
  DATAGN          22565   BARTTWO         15351
GENSIX
  GENSIX          23352   BARTTWO         15365
DGELG
  DGELG           24010   BARTTWO         16021
DATAIN
  DATAIN          24733   BARTTWO         15376
CHECK
  CHECK           27656   BARTTWO         16072
OPTALP
  OPTALP          30150   BARTTWO         15537       15554
SUMARY
  SUMARY          31321   BARTTWO         16042
AFOUR
  AFOUR           31547   BARTTWO         15646
ASIX
  ASIX            32022   BARTTWO         15652
PQIN
  PQIN            32424   BARTTWO         15373
SYSTEM
  Q8NTRY          32566   BARTTWO         15322
  END             32670   BARTTWO         16077
                          DATAGN          23111
                          GENSIX          23627
                          DGELG           24540
                          DATAIN          25231
                          CHECK           30071
                          OPTALP          30406
                          SUMARY          31417
                          AFOUR           31737
                          ASIX            32320
                          PQIN            32477
  EXIT            32712
  STOP            32720   BARTTWO         16075
  ABNORML         32730   INPUTC          34663
                          KODER           36043
                          KRAKER          37076
                          OUTPTC          37373
                          REWINM          37455
  SYSTEMC         32745
  SYSTEMP         32774
  ONTRAP          33007
  SYSTEM          33233   DABS            34476
                          DSQRT           34545
                          INPUTC          34662
                          KODER           36042
                          KRAKER          37046       37053       37075
                          OUTPTC          37372
                          REWINM          37454
  LOT             34250
  COUNTA.         34254
CPUCPR
  RECOVR          34276
  CPR=            34313   SYSTEM          32607
  SETUP.          34313
DABS
  DABS            34470   DGELG           24060       24345
DSQRT
  DSQRT           34505   BARTTWO         16001
GETBA
  GETBA           34565   INPUTC          34623
                          REWINM          37413
```

		SIO£	37753							
INPUTC										
INPUTC	34605	BARTTWO	15325	15327	15331	15332	15357	15361	15362	
		GENSIX	23366	23371	23412	23617	23624			
			23370	23407	23413	23623				
		DATAIN	24752	24756	24757	24765	24770	24773	24776	247
		PQIN	32450	32454	32455	32462	32465	32470	32471	
KODER										
KODER	34734	OUTPTC	37317	37334						
KRAKER										
KRAKER	36237	INPUTC	34611	34647						
OUTPTC										
OUTPTC	37315	BARTTWO	15337	15403	15417	15434	15451	15527	16055	
			15341	15405	15424	15440	15516	15530	16062	
			15343	15406	15427	15442	15520	16047	16064	
			15344	15413	15430	15445	15521	16051	16067	
			15401	15416	15433	15450	15525	16054	16070	
		DATAGN	22573	22621	22626	22640	22675	23047	23054	230
			22574	22625	22634	22641	22676	23051	23057	
		GENSIX	23360	23376	23401	23423	23456	23577	23604	236
			23361	23400	23420	23424	23457	23601	23607	
		DGELG	24527	24531	24532					
		DATAIN	25016	25022	25172	25200	25205	25213	25221	
			25020	25023	25173	25202	25210	25216	25222	
		CHECK	27663	27670	30046	30053	30060	30063		
			27664	27671	30050	30056	30062			
		SUMARY	31327	31332	31340	31353	31365	31402		
			31331	31337	31351	31360	31372	31410		
		PQIN	32431	32432						
REWINM										
REWINM	37406	INPUTC	34630							
SIO£										
DAT.	37472	INPUTC	34644	34672	34677					
		KRAKER	37045	37052	37100	37106	37110	37110	37115	
		OUTPTC	37331	37344	37352					
SIO.CTL	37720	SYSTEM	33516							
		REWINM	37424	37431						
INITL.	37751	SYSTEM	33457	33514						
		INPUTC	34634							
		OUTPTC	37324							
		REWINM	37417							
SIO.	40021	SYSTEM	33461							
		INPUTC	34673							
		OUTPTC	37351							
SIO.END	40540	SYSTEM	33525							
		REWINM	37433							
CIO1.	40565	REWINM	37442	37444						
RCL1.	40575	SYSTEM	33530							
		REWINM	37435							
OPEN.	40603	SYSTEM	33701							
RDPRU.	40663									
BKSPRU.	40703									
ADVIN.	40713	REWINM	37430							
POSFI.	40741									
MVWDS.	41100									
SYSERR.	41111	INPUTC	34617							
CPUSYS										
SYS=	41133	SYSTEM	32571	32603	32710	32725	32742	33424	33543	337
			32577	32705	32715	32741	33376	33536	33740	
		CPUCPR	34327	34345	34422	34424				
		SIO£	40572	40601	40607	40645	41117			
		CPUCPM	41162							

```
      RCL=      41145
      WNB=      41152
      MSG=      41157   CPUCPR      34325     34334     34412
CPUCPM
      CPM=      41163   SYSTEM      33411
```

FLUID MECHANICS OF TIMBERS, DATA SET NUMBER 0

NUMBER OF BITS OF DATA IN THIS SET 10

PROGRAM IN TEST MODE

INPUT DATA

A1 = 1.0000000D+00
B1 = 5.0000000D-01
A2 = 2.0000000D+00
B2 = 1.5000000D+00

Y VALUES

I	X	Y
1	0.D+00	3.750000D-01
2	2.222222D-01	5.266204D-01
3	4.444444D-01	6.768519D-01
4	6.666667D-01	8.263889D-01
5	8.888889D-01	9.755291D-01
6	1.111111D+00	1.124421D+00
7	1.333333D+00	1.273148D+00
8	1.555556D+00	1.421759D+00
9	1.777778D+00	1.570286D+00
10	2.000000D+00	1.718750D+00

FLUID MECHANICS OF TIMBERS, DATA SET NUMBER 0

NUMBER OF BITS OF DATA IN THIS SET 10

INPUT DATA

A1	=	2.00000000D+00
B1	=	1.00000000D+00
A2	=	4.00000000D+00
B2	=	3.00000000D+00

I	PBAR	Q
1	0.D+00	3.75000000D-01
2	2.22222222D-01	5.26620370D-01
3	4.44444444D-01	6.76851852D-01
4	6.66666667D-01	8.26388889D-01
5	8.88888889D-01	9.75529101D-01
6	1.11111111D+00	1.12442130D+00
7	1.33333333D+00	1.27314815D+00
8	1.55555556D+00	1.42175926D+00
9	1.77777778D+00	1.57028620D+00
10	2.00000000D+00	1.71875000D+00

CONVERGENCE VALUE FOR ITERATION IS 1.0000000D-10

MAXIMUM NUMBER OF ITERATIONS IS 127

SUMMARY OF ITERATIONS FOR DATA SET NUMBER 0

I	ALPHA	COST FUNCTION	GRADIENT	A1	B1	A2	B2	A3	B3
0	0.D+00	1.2837187213100+01	8.3209D+00	2.00000D+00	1.00000D+00	4.00000D+00	3.00000D+00		
1	1.0000D+00	8.558438834462D-49	5.8854D-28	1.00000D+00	5.00000D-01	2.00000D+00	1.50000D+00		

VALUES OF CONSTANTS AFTER 1 ITERATIONS

A1 = 1.00000000D+00
B1 = , 5.00000000D-01
A2 = , 2.00000000D+00
B2 = , 1.50000000D+00

SUBROUTINE CHECK ENTERED

I	PBAR	Q	NEW Q	DIFFERENCE
1	0.D+00	3.750000D-01	3.750000D-01	3.809883D-25
2	2.222222D-01	5.266204D-01	5.266204D-01	-5.192472D-25
3	4.444444D-01	6.768519D-01	6.768519D-01	-3.300594D-25
4	6.666667D-01	8.263889D-01	8.263889D-01	-2.279492D-26
5	8.888889D-01	9.755291D-01	9.755291D-01	1.951074D-25
6	1.111111D+00	1.124421D+00	1.124421D+00	2.887862D-25
7	1.333333D+00	1.273148D+00	1.273148D+00	2.656126D-25
8	1.555556D+00	1.421759D+00	1.421759D+00	1.425756D-25
9	1.777778D+00	1.570286D+00	1.570286D+00	-6.401764D-26
10	2.000000D+00	1.718750D+00	1.718750D+00	-3.393743D-25

FLUID MECHANICS OF TIMBERS, DATA SET NUMBER 47002

NUMBER OF BITS OF DATA IN THIS SET 16

EXPERIMENTAL DATA

MANOMETER FACTOR F1 = 0.79570000D-01
MANOMETER FACTOR F2 = 0.79180000D-02

I	OUTLET PRESSURE	SPECIMEN DELTA P	FLOWMETER DELTA P	PBAR	Q
1	0.14250000D+04	0.24200000D+03	0.21000000D+02	0.19040982D+07	0.12478586D+02
2	0.12950000D+04	0.23500000D+03	0.21500000D+02	0.17311872D+07	0.11967826D+02
3	0.11870000D+04	0.23500000D+03	0.22000000D+02	0.15878451D+07	0.11240225D+02
4	0.10650000D+04	0.23400000D+03	0.22500000D+02	0.14258687D+07	0.10376913D+02
5	0.95000000D+03	0.25500000D+03	0.25500000D+02	0.12743448D+07	0.96654417D+01
6	0.81200000D+03	0.20000000D+03	0.21500000D+02	0.10882812D+07	0.88656034D+01
7	0.68100000D+03	0.24000000D+03	0.27000000D+02	0.91652471D+06	0.78495110D+01
8	0.51900000D+03	0.21800000D+03	0.28000000D+02	0.70034984D+06	0.68693243D+01
9	0.40500000D+03	0.17350000D+03	0.26000000D+02	0.54669448D+06	0.62607105D+01
10	0.37500000D+03	0.21400000D+03	0.33000000D+02	0.50901581D+06	0.60358077D+01
11	0.23900000D+03	0.15800000D+03	0.31000000D+02	0.32555388D+06	0.49357947D+01
12	0.13900000D+03	0.18450000D+03	0.49000000D+02	0.19422901D+06	0.41130078D+01
13	0.67000000D+02	0.17800000D+03	0.72000000D+02	0.98324370D+05	0.33822255D+01
14	0.59000000D+02	0.20200000D+03	0.86000000D+02	0.88973739D+05	0.33254719D+01
15	0.17000000D+02	0.17200000D+03	0.12600000D+03	0.31645453D+05	0.26023379D+01
16	0.20000000D+01	0.71000000D+02	0.12400000D+03	0.64035901D+04	0.21867902D+01

FLUID MECHANICS OF TIMBERS, DATA SET NUMBER 47002

NUMBER OF BITS OF DATA IN THIS SET 16

INPUT DATA

A1	=	5.00000000D-05
B1	=	4.00000000D+00
A2	=	5.00000000D-06
B2	=	5.00000000D+00

I	PBAR	Q
1	1.90409823D+06	1.24785865D+01
2	1.73118717D+06	1.19678263D+01
3	1.58784505D+06	1.12402249D+01
4	1.42586875D+06	1.03769131D+01
5	1.27434483D+06	9.66544168D+00
6	1.08828122D+06	8.86560340D+00
7	9.16524714D+05	7.84951104D+00
8	7.00349844D+05	6.86932428D+00
9	5.46694485D+05	6.26071047D+00
10	5.09015805D+05	6.03580772D+00
11	3.25553876D+05	4.93579466D+00
12	1.94229009D+05	4.11300776D+00
13	9.83243700D+04	3.38222548D+00
14	8.89737390D+04	3.32547187D+00
15	3.16454532D+04	2.60233786D+00
16	6.40359005D+03	2.18679018D+00

CONVERGENCE VALUE FOR ITERATION IS 1.000000D-10

MAXIMUM NUMBER OF ITERATIONS IS 127

SUMMARY OF ITERATIONS FOR DATA SET NUMBER 47002

I	ALPHA	COST FUNCTION	GRADIENT	A1	B1	A2	B2	A3	B3
0	1.0000D+00	1.4015468531990-01	3.8772D+05	5.00000D-05	4.00000D+00	5.00000D-06	5.00000D+00		
1	5.5000D-01	1.0083650659210-01	7.4998D+04	5.72161D-05	3.88034D+00	4.96057D-06	4.75629D+00		
2	7.5000D-01	9.6650397599370-02	9.1773D+04	6.19333D-05	3.76238D+00	4.94520D-06	4.65867D+00		
3	1.0600D+00	9.5383234526530-02	1.5478D+03	6.36172D-05	3.70766D+00	4.94285D-06	4.63735D+00		
4	1.0100D+00	9.5382041309530-02	9.9489D-01	6.35433D-05	3.71013D+00	4.94316D-06	4.63871D+00		
5	1.0000D+00	9.5382041220140-02	2.1938D-03	6.35423D-05	3.71011D+00	4.94316D-06	4.63874D+00		
6	7.8000D-01	9.5382041220140-02	4.7877D-04	6.35423D-05	3.71011D+00	4.94316D-06	4.63874D+00		
7	7.8000D-01	9.5382041220140-02	1.0438D-04	6.35423D-05	3.71011D+00	4.94316D-06	4.63874D+00		
8	7.8000D-01	9.5382041220140-02	2.2743D-05	6.35423D-05	3.71011D+00	4.94316D-06	4.63874D+00		
9	7.8000D-01	9.5382041220140-02	4.9525D-06	6.35423D-05	3.71011D+00	4.94316D-06	4.63874D+00		
10	7.8000D-01	9.5382041220140-02	1.0778D-06	6.35423D-05	3.71011D+00	4.94316D-06	4.63874D+00		
11	7.8000D-01	9.5382041220140-02	2.3445D-07	6.35423D-05	3.71011D+00	4.94316D-06	4.63874D+00		
12	7.8000D-01	9.5382041220140-02	5.0971D-08	6.35423D-05	3.71011D+00	4.94316D-06	4.63874D+00		
13	7.8000D-01	9.5382041220140-02	1.1076D-08	6.35423D-05	3.71011D+00	4.94316D-06	4.63874D+00		
14	7.8000D-01	9.5382041220140-02	2.4055D-09	6.35423D-05	3.71011D+00	4.94316D-06	4.63874D+00		
15	7.8000D-01	9.5382041220140-02	5.2221D-10	6.35423D-05	3.71011D+00	4.94316D-06	4.63874D+00		
16	7.8000D-01	9.5382041220140-02	1.1333D-10	6.35423D-05	3.71011D+00	4.94316D-06	4.63874D+00		
17	7.8000D-01	9.5382041220140-02	2.4587D-11	6.35423D-05	3.71011D+00	4.94316D-06	4.63874D+00		

VALUES OF CONSTANTS AFTER 17 ITERATIONS

A1 = 6.35423050D-05
B1 = , 3.71010652D+00
A2 = , 4.94315998D-06
B2 = , 4.63873555D+00

SUBROUTINE CHECK ENTERED

I	PBAR	Q	NEW Q	DIFFERENCE
1	1.904098D+06	1.247859D+01	1.262809D+01	-1.495079D-01
2	1.731187D+06	1.196783D+01	1.182410D+01	1.437214D-01
3	1.587845D+06	1.124022D+01	1.115592D+01	8.430173D-02
4	1.425869D+06	1.037691D+01	1.039848D+01	-2.156717D-02
5	1.274345D+06	9.665442D+00	9.686857D+00	-2.141572D-02
6	1.088281D+06	8.865603D+00	8.807308D+00	5.829532D-02
7	9.165247D+05	7.849511D+00	7.987059D+00	-1.375481D-01
8	7.003498D+05	6.869324D+00	6.935379D+00	-6.605504D-02
9	5.466945D+05	6.260710D+00	6.164177D+00	9.653386D-02
10	5.090158D+05	6.035808D+00	5.970122D+00	6.568590D-02
11	3.255539D+05	4.935795D+00	4.974119D+00	-3.832482D-02
12	1.942290D+05	4.113008D+00	4.150989D+00	-3.798094D-02
13	9.832437D+04	3.382225D+00	3.383478D+00	-1.252041D-03
14	8.897374D+04	3.325472D+00	3.292701D+00	3.277125D-02
15	3.164545D+04	2.602338D+00	2.608649D+00	-6.311441D-03
16	6.403590D+03	2.186790D+00	2.188136D+00	-1.346241D-03